



#### **DISCLAIMER**

This report was prepared as an account of work sponsored by an agency of the United States Government. Neither the United States Government nor any agency thereof, nor any of their employees, makes any warranty, expressed or implied, or assumes any legal liability or responsibility for the accuracy, completeness, or usefulness of any information, apparatus, product, or process disclosed, or represents that its use would not infringe privately owned rights. Reference herein to any specific commercial product, process, or service by trade name, trademark, manufacturer, or otherwise does not necessarily constitute or imply its endorsement, recommendation, or favoring by the United States Government or any agency thereof. The views and opinions of authors expressed herein do not necessarily state or reflect those of the United States Government.

This report has been reproduced directly from the best available copy.

INVESTIGATIONS OF ENHANCED OIL RECOVERY  
THROUGH USE OF CARBON DIOXIDE

Final Report for Period  
October 1, 1980 - December 31, 1984

Volume I: Phase Behavior Studies

By

Teresa G. Monger, Principal Investigator

and

Oscar K. Kimbler, David W. Bryant,  
Josh C. Fu & Russell Saragusa, Contributors

August 1985

Work Performed Under Contract No. AS19-80BC10344

Fred W. Burtch, Technical Project Officer  
Bartlesville Project Office  
P.O. Box 1398  
Bartlesville, Oklahoma 74005

Prepared for  
U.S. Department of Energy  
Assistant Secretary for Fossil Energy

Prepared by  
Louisiana State University  
Department of Petroleum Engineering  
Baton Rouge, Louisiana 70803

TABLE OF CONTENTS

	<u>Page</u>
TABLE OF CONTENTS . . . . .	ii
LIST OF TABLES . . . . .	iv
LIST OF FIGURES . . . . .	vi
ABSTRACT . . . . .	ix
WORK STATEMENT . . . . .	x
PART I - PHASE BEHAVIOR STUDIES WITH CARBON DIOXIDE IN SYNTHETIC OIL SYSTEMS . . . . .	1
INTRODUCTION . . . . .	1
EXPERIMENTAL SECTION . . . . .	1
RESULTS AND DISCUSSION . . . . .	3
CONCLUSIONS . . . . .	22
PART II - MULTIPLE CONTACT PHASE EQUILIBRIA EXPERIMENTS WITH MIXTURES OF CARBON DIOXIDE AND BROOK- HAVEN RESERVOIR OIL . . . . .	24
INTRODUCTION . . . . .	24
EXPERIMENTAL SECTION . . . . .	29
Flashing The Oil . . . . .	29
PVT Apparatus and Procedure . . . . .	30
Apparatus . . . . .	30
Procedure . . . . .	33
Sampling . . . . .	34
High Pressure Equipment . . . . .	35
High Pressure Procedure . . . . .	35
Low Pressure Equipment . . . . .	35
Low Pressure Procedure . . . . .	39
Compositional Analyses . . . . .	39
Chromatographic Analyses . . . . .	39
Time/Temperature Program . . . . .	40
Hydrocarbon Type Analyses . . . . .	40
RESULTS AND DISCUSSION . . . . .	41
BF Oil and Carbon Dioxide . . . . .	41

TABLE OF CONTENTS (Continued)

	<u>Page</u>
Single-Contact Experiments . . . . .	41
Analysis of Data . . . . .	41
Results and Discussion of the Single-Contacts . . . . .	46
Multiple-Contact Experiments . . . . .	66
Analysis of PVT Data . . . . .	66
Analysis of Density and Flash Data . . . . .	66
Analysis of Compositional Data . . . . .	67
Results and Discussion of the Forward Contacts . . . . .	68
Results and Discussion of the Swept Zone Contacts . . . . .	99
General Discussion . . . . .	123
CONCLUSIONS . . . . .	126
BIBLIOGRAPHY . . . . .	129
APPENDIX . . . . .	132

LIST OF TABLES

No.	Title	Page
1	Synthetic Oil Compositions (Mole Percent) . . . . .	4
2	Properties of Synthetic Oils . . . . .	5
3	Measured Values of Pressure and Volume For Isotherms of CO <sub>2</sub> -Oil 1 Mixtures . . . . .	7
4	Measured Values of Pressure and Volume For Isotherms of CO <sub>2</sub> -Oil 2 Mixtures . . . . .	11
5	Measured Values of Pressure and Volume For Isotherms of CO <sub>2</sub> -Oil 3 Mixtures . . . . .	15
6	Properties of Liquid Phases . . . . .	19
7	Liquid Phase Compositions (Mole Percent) . . . . .	20
8	Liquid-Liquid Equilibrium Ratios . . . . .	21
9	Liquid-Liquid Selectivities . . . . .	23
10	BF Oil Physical Properties . . . . .	42
11	Oil Composition Comparison . . . . .	43
12	Comparison of Reconstituted Reservoir Oil Flashes . . . . .	44
13	CO <sub>2</sub> -Rich Phase in the Forward Contacts - Physical Properties . . . . .	79
14	Oil-Rich Phase in the Forward Contacts - Physical Properties . . . . .	80
15	CO <sub>2</sub> -Rich Phase in the Forward Contacts - Molecular Weight . . . . .	82
16	Composition of the CO <sub>2</sub> -Rich Phase in the Forward Contacts . . . . .	83
17	Composition of the Liquid Collected from Flashing the CO <sub>2</sub> -Rich Phase in the Forward Contacts . . . . .	85
18	Oil-Rich Phase in the Forward Contacts - Molecular Weight . . . . .	87
19	Composition of the Oil-Rich Phase in the Forward Contacts . . . . .	88

LIST OF TABLES (Continued)

No.	Title	Page
20	Composition of the Liquid Collected from Flashing the Oil-Rich Phase in the Forward Contacts . . . . .	90
21	Best Estimate of Phase Compositions in the Forward Contacts . . . . .	94
22	Phase Compositions in the Forward Contacts . . . . .	96
23	<sup>13</sup> C NMR Results in the Forward Contacts . . . . .	97
24	CO <sub>2</sub> -Rich Phase in the Swept Zone Contacts - Physical Properties . . . . .	107
25	Oil-Rich Phase in the Swept Zone Contacts - Physical Properties . . . . .	108
26	CO <sub>2</sub> -Rich Phase in the Swept Zone Contacts - Molecular Weight . . . . .	109
27	Composition of the CO <sub>2</sub> -Rich Phase in the Swept Zone Contacts . . . . .	110
28	Composition of the Liquid Collected from Flashing the CO <sub>2</sub> -Rich Phase in the Swept Zone Contacts . . . . .	112
29	Oil-Rich Phase in the Swept Zone Contacts - Molecular Weight . . . . .	115
30	Composition of the Oil-Rich Phase in the Swept Zone Contacts . . . . .	116
31	Composition of the Liquid Collected from Flashing the Oil-Rich Phase in the Swept Zone Contacts . . . . .	118
32	Cumulative Oil Production in the Swept Zone Contacts . . . . .	120
33	Results of Aromatic Carbon Mass Balance . . . . .	122
34	Weight Percent Compositions of All Multiple-Contact Phases . . . . .	125

## LIST OF FIGURES

No.	Title	Page
1	Schematic of Experimental Apparatus . . . . .	2
2	Phase Equilibria for Mixtures of CO <sub>2</sub> and Oil 1 at 39.1°C . . . . .	10
3	Phase Equilibria for Mixtures of CO <sub>2</sub> and Oil 2 at 40.1°C . . . . .	14
4	Phase Equilibria for Mixtures of CO <sub>2</sub> and Oil 3 at 38.2°C . . . . .	18
5	Condensing - Gas Drive Process . . . . .	26
6	Vaporizing - Gas Drive Process . . . . .	27
7	Transfer Vessel . . . . .	31
8	Schematic of Phase Behavior Equipment . . . . .	32
9	High Pressure/Temperature Sampling Yoke . . . . .	36
10	High Pressure/Temperature Sampling Syringe . . . . .	37
11	Schematic of Low Pressure Sampling System . . . . .	38
12	P-X Diagram of BF Oil @ 141.4°F . . . . .	47
13	P-X Diagram of BF Oil @ 111°F . . . . .	48
14	Pressure-Volume Isotherms: 89.3% CO <sub>2</sub> - 10.7% BF Oil 79.8°F . . . . .	49
15	Swelling Index: 23.7% CO <sub>2</sub> - 76.3% BF @ 142.5°F . . . . .	51
16	Swelling Index: 48.2% CO <sub>2</sub> - 51.8% BF @ 142.3°F . . . . .	52
17	Swelling Index: 68.5% CO <sub>2</sub> - 31.5% BF @ 141.1°F . . . . .	53
18	Swelling Index: 78.8% CO <sub>2</sub> - 21.2% BF @ 140.0°F . . . . .	54
19	Swelling Index: 87.2% CO <sub>2</sub> - 12.8% BF @ 141.3°F . . . . .	55
20	Maximum Swelling vs Pressure for the Single- Contacts @ 141.4°F . . . . .	56
21	Swelling Index: 23.7% CO <sub>2</sub> - 76.3% BF @ 111.3°F . . . . .	57
22	Swelling Index: 48.2% CO <sub>2</sub> - 51.8% BF @ 111.2°F . . . . .	58
23	Swelling Index: 68.5% CO <sub>2</sub> - 31.5% BF @ 111.0°F . . . . .	59
24	Swelling Index: 78.8% CO <sub>2</sub> - 21.2% BF @ 110.6°F . . . . .	60

LIST OF FIGURES (Continued)

No.	Title	Page
25	Swelling Index: 87.2% CO <sub>2</sub> - 12.8% BF @ 110.3°F . . . . .	61
26	Swelling Index: 89.3% CO <sub>2</sub> - 10.7% BF @ 111.5°F . . . . .	62
27	Swelling Index: 94.6% CO <sub>2</sub> - 5.4% BF @ 111.3°F . . . . .	63
28	Maximum Swelling vs Pressure for the Single- Contacts @ 111.0°F . . . . .	64
29	CO <sub>2</sub> Density at Run Temperatures . . . . .	65
30	Summary of Forward Contacts . . . . .	69
31	Pressure-Volume Isotherms: First Forward Contact 112.6°F #2 . . . . .	72
32	Pressure-Volume Isotherms: Second Forward Contact 111.8°F . . . . .	73
33	Pressure-Volume Isotherms: Third Forward Contact 111.9°F . . . . .	74
34	Swelling Index: First Forward Contact @ 112.8°F . . . . .	75
35	Swelling Index: Second Forward Contact @ 111.8°F . . . . .	76
36	Swelling Index: Third Forward Contact @ 111.9°F . . . . .	77
37	Swelling Indexes Forward Contacts . . . . .	78
38	Composition of the CO <sub>2</sub> -Rich Phase of the Forward Contacts . . . . .	84
39	Liquid Composition from Flash of CO <sub>2</sub> -Rich Phase in Forward Contacts . . . . .	86
40	Composition of the Oil-Rich Phase of the Forward Contacts . . . . .	89
41	Liquid Composition from Flash of Oil-Rich Phase in Forward Contacts . . . . .	91
42	Best Estimate Pseudoternary Representation of the Mole Percent Composition of the CO <sub>2</sub> -Rich Phase in the Forward Contacts at approximately 1809 psia and 111.9°F . . . . .	93

LIST OF FIGURES (Continued)

No.	Title	Page
43	Pseudoternary Representation of the Mole Percent Compositions of the CO <sub>2</sub> -Rich and Oil-Rich Phases in the Forward Contacts at approximately 1809 psia and 111.9°F . . . . .	95
44	Percent Error in Mass Balances of Forward Contacts . . . . .	98
45	Summary of Swept Zone Contacts . . . . .	100
46	Pressure-Volume Isotherms: First Swept Zone Contact 111.7°F #2 . . . . .	101
47	Pressure-Volume Isotherms: Second Swept Zone Contact 111.7°F . . . . .	102
48	Swelling Index: First Swept Zone Contact @ 111.7°F . . . . .	104
49	Swelling Index: Second Swept Zone Contact @ 111.7°F . . . . .	105
50	Swelling Indexes Swept Zone Contacts . . . . .	106
51	Composition of the CO <sub>2</sub> -Rich Phase of the Swept Zone Contacts . . . . .	111
52	Liquid Composition from Flash of CO <sub>2</sub> -Rich Phase in Swept Zone Contacts . . . . .	113
53	Composition of the Oil-Rich Phase of the Swept Zone Contacts . . . . .	117
54	Liquid Composition from Flash of Oil-Rich Phase in Swept Zone Contacts . . . . .	119
55	Cumulative Percents of OOIP Produced . . . . .	121
56	Pseudoternary Representation of the Weight Percent Compositions of the CO <sub>2</sub> -Rich and Oil-Rich Phases in the Multiple-Contact Experiments at approximately 1812 psia and 111.8°F . . . . .	124
57	Pseudoternary Representation, Comparison of Forward Contacts Using BF Oil and of Sandpack Displacements of RR Oil on a Mole Percent Basis . . . . .	127

## ABSTRACT

The literature contains a large number of reports which use oil displacement results from dynamic systems to infer the CO<sub>2</sub>-oil phase behavior relevant to the multiple-contact miscible (MCM) process in CO<sub>2</sub> flooding. However, reports with direct measurements of pertinent phase-equilibria data are less available, especially for mixtures containing heavy hydrocarbons. For example, just a few papers in the literature use static, multiple-contact PVT measurements to directly address the phase behavior in the MCM process, and none of these examines a highly asphaltic crude oil. A quantitative understanding of the MCM phase behavior, including the effects of heavy components, is needed to calibrate equations of state in reservoir simulators used to predict CO<sub>2</sub> flood performance. This study provides direct experimental data for several CO<sub>2</sub>-oil systems containing heavy hydrocarbons.

In Part I of this study, compositional effects due to the chemical nature of the heavy hydrocarbons are explored using synthetic oils which model the phase behavior observed for natural reservoir fluids. The phase behavior of three CO<sub>2</sub>-synthetic oil systems are reported at temperatures near 40°C and pressures up to 240 atm. The three synthetic oils were made using selected aromatic and/or paraffinic components, and include thirty mole percent heavy hydrocarbons. The two-phase liquid-liquid region present at high CO<sub>2</sub> levels is examined, and the compositions and densities of both liquid phases are determined. The results show that heavy paraffins are more readily extracted into the CO<sub>2</sub>-rich liquid phase in the presence of aromatics. As a consequence of the enhanced extraction, aromatics impair CO<sub>2</sub>'s ability to selectively solubilize lighter components from a mixture of hydrocarbons.

Part II of this study focuses on multiple-contact CO<sub>2</sub>-oil phase behavior for mixtures of a highly asphaltic crude oil. The oil was Brookhaven reservoir oil modified to resemble oil contacted by CO<sub>2</sub> during a typical flood. Single-contact experiments were performed to construct a P-X diagram. Forward multiple-contacts were performed to determine the phase behavior at the flood front in the MCM process, while swept zone multiple-contacts were performed to determine the phase behavior near the well-bore and perhaps relevant to the vaporization huf-n-puf process. Compositional, density, gas-liquid ratio, and percent phase volume data were measured for both a CO<sub>2</sub>-rich and an oil-rich phase in each multiple-contact. Swelling indexes are presented for all contacts.

The single-contact results show no liquid-liquid-vapor three phase region or liquid-liquid critical point at temperatures greater than 111 °F. A critical CO<sub>2</sub> level must be reached before substantial hydrocarbon extraction occurs. The forward multiple-contacts show that CO<sub>2</sub> is multiple-contact miscible with the oil by the vaporizing-gas drive mechanism at about 1809 psia and 111.9°F. Precipitation of a tar-like, highly aromatic solid is associated with the development of miscibility. The swept zone multiple-contacts show a cumulative liquid volume production of about 35% OOIP after the second CO<sub>2</sub> contact, with further contacts recovering essentially no additional oil. The residual oil is composed of very heavy, highly aromatic hydrocarbon.

## WORK STATEMENT

The contract with the U.S. Department of Energy required the performance of five tasks. Three of these tasks relate to displacement studies and are addressed in Volume II of this Final Report. The remaining two tasks relate to phase behavior studies as summarized below:

### TASK III

To perform basic phase equilibria measurements for single contact mixtures of carbon dioxide and oil which will broaden the study of miscibility mechanism(s) associated with CO<sub>2</sub> displacement.

- (a) Measurements of the swelling index and saturation pressure will be made for mixtures of CO<sub>2</sub> and two Appalachian crude oils over the entire CO<sub>2</sub> compositional range. Variations of temperature and pressure which are typical of Appalachian reservoir conditions and which extend above and below the critical locus for CO<sub>2</sub> will be examined.
- (b) Measurements of the swelling index, saturation pressure, phase compositions, and phase densities will be made for mixtures of CO<sub>2</sub> and several synthetic crude oils over the entire CO<sub>2</sub> compositional range. The synthetic oils will be composed of selected paraffinic, aromatic, and naphthenic hydrocarbons. Temperatures and pressures which extend above and below the critical locus for CO<sub>2</sub> will be examined.
- (c) Measurements of the swelling index, saturation pressure, phase compositions, and phase densities will be made for mixtures of CO<sub>2</sub> and Brookhaven reservoir oil. The entire CO<sub>2</sub> compositional range will be examined. Temperatures and pressures which extend above and below the critical locus for CO<sub>2</sub> will be examined. Lower molecular weight hydrocarbons will be reconstituted with dead Brookhaven oil to study compositional effects. Conditions which lead to the development of multiple liquid phases or the precipitation of a solid phase will be probed.

### TASK IV

To perform basic phase equilibria measurements for multiple contact mixtures of carbon dioxide and oil which will probe the role of phase behavior in the CO<sub>2</sub> displacement process.

- (a) Phase behavior studies will be made with mixtures of fresh crude oil and an "enriched" CO<sub>2</sub> phase which has been extracted from a single contact mixing of CO<sub>2</sub> with crude oil.
- (b) Phase behavior studies will be made with mixtures of fresh CO<sub>2</sub> and a "striped" crude oil which has been extracted from a single contact mixing of CO<sub>2</sub> with crude oil.
- (c) Phase compositional and/or density effects will be examined as pertain to the study of miscibility mechanism(s) associated with CO<sub>2</sub> displacement.

Full details of these completed contract requirements are presented in Volume I of this Final Report, with two exceptions: (1) work performed in support of subtask IIIa has been previously reported (Monger and Khakoo, 1981), and (2) some of the work performed in support of subtask IIIb, specifically results for synthetic oils containing haphthenic hydrocarbons, have been previously reported (Monger and McMullan, 1983).



## PART I - PHASE BEHAVIOR STUDIES WITH CARBON DIOXIDE IN SYNTHETIC OIL SYSTEMS

### INTRODUCTION

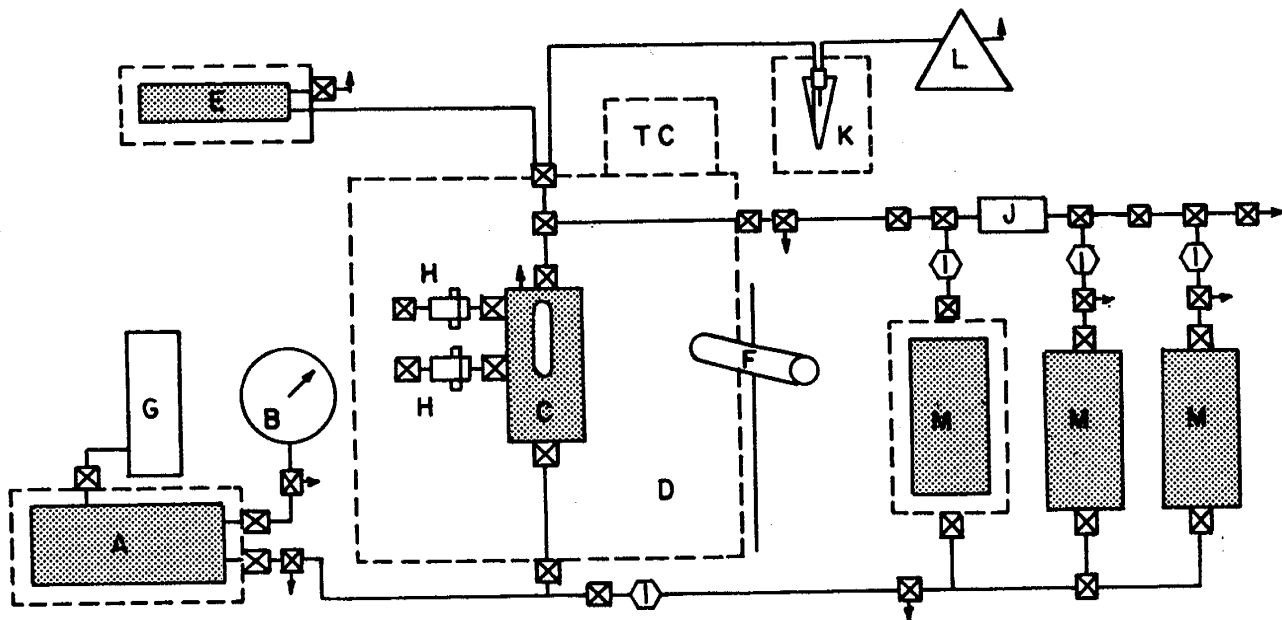
Carbon dioxide is gaining popularity as an enhanced oil recovery fluid (Holm, 1982), and as the preferred solvent for several industrial extraction processes. Use of CO<sub>2</sub> is usually attractive because it is relatively available, inexpensive, and environmentally safe. In enhanced oil recovery applications specifically, the CO<sub>2</sub> property most germane to the oil displacement mechanism is its ability to become miscible with reservoir oil through in situ multiple contacts. Two types of mass transfer occur. Carbon dioxide dissolves in and subsequently swells the oil, and in some cases, the composition of the displacing CO<sub>2</sub>-rich phase is altered by hydrocarbon enrichment to the point that it is first-contact miscible with the original in place oil. Considerable research efforts continue to delineate the phase equilibria which pertain to the development of multiple contact miscibility between CO<sub>2</sub> and oil (Gardner, et al., 1981). One variable which appears to affect the phase behavior is the aromatic content of the oil (Monger and Khakoo, 1981).

Advances in computer implemented equations of state are making the prediction of CO<sub>2</sub>-hydrocarbon phase behavior easier and more reliable. An important consideration in using an equation of state with CO<sub>2</sub>-reservoir oil mixtures, is the characterization of the heavy hydrocarbon components. One characterization method which appears to accurately match experimental data in the critical point region for rich gas-reservoir oil mixtures, is based upon assigning separate paraffinic, aromatic, and naphthenic cuts (Williams, et al., 1980). One of the aims of this study is to provide experimental data to assist similar modelling efforts for CO<sub>2</sub>-reservoir oil mixtures. Experimental phase equilibrium data for mixtures containing CO<sub>2</sub> and heavy hydrocarbons, particularly aromatics, are scarce, and the behavior of multi-component CO<sub>2</sub>-hydrocarbon systems is not readily deduced from the phase equilibria of binary or ternary systems.

### EXPERIMENTAL SECTION

The apparatus used in this study is schematized in Figure 1. The Ruska P-V-T set-up incorporated a viewable 192 cc through windowed equilibrium cell (Model 2329-800-16800), housed in a temperature controlled air bath (Model 2320-801-00), and manifolded to a temperature controlled 1000 cc positive displacement pump (Model 2236-WIII) filled with mercury. The cell and pump were also manifolded to storage reservoirs. Temperature was maintained to  $\pm 0.3^\circ\text{C}$  with an Omega Model 157-713 J temperature controller. Temperature was monitored to  $\pm 0.05^\circ\text{C}$  using an Omega Model 199 digital thermometer employing numerous Pt - resistance probes. Pressure was measured with a Heise Bourdon tube gage to  $\pm 0.5$  atm at the maximum pressure tested, based upon calibration versus an accurate dead weight tester. Volumes were calculated from pump displacements measured to 0.01 cc and cathetometer readings measured to  $\pm 0.1$  mm. The overall performance of the P-V-T apparatus was checked versus the reported pressure-volume isotherm for the binary system n-decane-CO<sub>2</sub> at 160°F, and was found to agree within 1% of the reported data (Reamer and Sage, 1963).

A Mettler - Paar DMA 45 digital density meter with a DMA 512 remote cell for high pressure/temperature measurement was also connected to the P-V-T cell. In addition, side ports on the cell incorporated Precision Sampling high pressure/temperature sampling yokes which permitted syringe collection of microliter size



- |                                      |                             |
|--------------------------------------|-----------------------------|
| A - Positive Displacement Pump       | G - Mercury Reservoir       |
| B - Pressure Gage                    | H - Sampling Yokes          |
| C - P-V-T Cell                       | I - Mercury Level Indicator |
| D - Air Bath                         | J - Line Filter             |
| E - Densitometer                     | K - Flash Separator         |
| F - Cathetometer                     | L - Wet Test Meter          |
| TC - Temperature Controller          | M - Storage Reservoirs      |
| → To Vent, Vacuum, or Compressed Gas |                             |

Figure 1. Schematic of experimental apparatus.

samples of equilibrated phases for direct chromatographic analysis using a Hewlett-Packard 5880 gas chromatograph (see Part II). Correlating analyses of equilibrated phases were made by flash liberation and recombination methods. The high pressure syringe sampling technique provided the more reliable estimate of CO<sub>2</sub> and pentane content, with minor disturbance of the sample mixture. The analyses of flashed oil samples gave more accurate results for the heaviest hydrocarbons, but the sample mixture was consequently sacrificed. Pressure control was generally better than  $\pm 1$  atm during either type of phase sampling, as well as during phase density determinations.

In a typical experiment, synthetic oil and CO<sub>2</sub> were volumetrically charged at constant temperature and pressure from pressurized storage reservoirs into the P-V-T cell. The cell was then brought to run temperature and equilibrated overnight. The cell's contents were mechanically mixed and P-V-T measurements were recorded as a function of increasing pressure by injecting mercury into the cell. Additional steps were also taken to minimize the contamination of manifold mercury. The mixing plus equilibration time required to obtain stable readings for each data point was usually less than 45 minutes. Although temperature was accurately known, the day to day repeatability was somewhat impaired by changes in room temperature, despite cold junction compensation in the temperature controller. To avoid adverse effects on temperature equilibration during a run, no adjustments were made to improve temperature repeatability. All but 6 cc of the cell volume could be observed with an external cathetometer view site calibrated to 0.1 cc. Because the upper 6 cc of the cell was not visible through the cell windows, data were not collected at saturation conditions. The bubble-point and dew-point pressures used to construct phase envelopes were determined from least squares analyses of the pressure dependence of the volume percent of vapor or liquid phase. The least squares method was simple and highly reproducible; however, the predicted bubble-points were usually about 2% higher than values suggested by other curve fitting relations such as the "Y" correlation.

The CO<sub>2</sub> and the various hydrocarbons examined in this study were the highest purity provided by the manufacturer, and were used without further purification, except for flashing the CO<sub>2</sub> from the main storage cylinder prior to liquefaction, and some filtering of hydrocarbons. The CO<sub>2</sub> used in this study had a stated minimum mole purity of 99.5%. The hydrocarbons used were obtained from various vendors and were typically 99% pure.

## RESULTS AND DISCUSSION

To overcome the inherent difficulties in measuring or modelling how hydrocarbons distribute between phases in the myriad system of a natural oil, synthetic oils were created using selected aromatic and/or paraffinic compounds. Analogous components were not chosen on the basis of equivalent carbon number. Selections were instead based upon a match of physical properties (density, melting point, normal boiling point), and whether phase equilibria data for binary and ternary systems were available (Zarah, et al., 1974; Yang, et al., 1976). Table 1 shows the compositions of the three oils that were examined, and Table 2 contrasts various properties of the oils. The low molecular weight portions of the oils were similar in that each oil contained 20 mole percent pentane and at least 30 mole percent decane. Analogous component substitutions largely appear in the high molecular weight portions of the oils. For example, the squalane content of the paraffinic oil (oil 1) is replaced with biphenyl in the paraffinic-aromatic oil (oil 2). The seven component oil (oil 3) is a 50-50 blend of oil 1 and oil 2.

Table 1

SYNTHETIC OIL COMPOSITIONS (MOLE PERCENT)

<u>OIL 1</u>	<u>OIL 2</u>	<u>OIL 3</u>
20% Pentane	20% Pentane	20% Pentane
50% Decane	30% Decane 20% n-Butylbenzene	40% Decane 10% n-Butylbenzene
20% Eicosane	20% 2-Methylnaphthalene	10% Eicosane 10% 2-Methylnaphthalene
10% Squalane	10% Biphenyl	5% Squalane 5% Biphenyl

Table 2

PROPERTIES OF SYNTHETIC OILS

	<u>OIL 1</u>	<u>OIL 2</u>	<u>OIL 3</u>
<u>Molecular Weight (g/g-mol)</u>	183	128	156
<u>Density (g/cc)</u>			
(21.1°C, 1 atm)	0.756	0.823	0.780
(21.1°C, 102 atm)	0.763	0.830	0.787
(37.8°C, 102 atm)	0.752	0.819	0.776
<u>Viscosity (cp)</u>			
(21.1°C, 1 atm)	2.27	1.13	1.54
<u>Carbon Content (%)</u>			
(saturated)	100	53	80
(unsaturated)	0	47	20

The raw experimental values of pressure and volume from the isotherms examined for CO<sub>2</sub> - oil 1 mixtures are presented in Table 3. Figure 2 shows the complete phase envelope at 39.1 °C generated from least squares analyses of the data in Table 3 corrected to 39.1°C using room temperature data reported for the same CO<sub>2</sub> - oil 1 mixtures (Monger and McMullan, 1983). Several features of this phase envelope are common with those reported for CO<sub>2</sub>-crude oil mixtures, exhibiting Type II phase behavior (Stalkup, 1983a). These are simple bubble-point behavior for mixtures with moderate amounts of CO<sub>2</sub>, a region of liquid-liquid immiscibility for mixtures with high amounts of CO<sub>2</sub>, and a three phase liquid-liquid-vapor region which is small on a pressure scale but easily observed on a volume scale. Two additional features of the synthetic oil phase behavior contrast with what is routinely reported for natural crudes (Stalkup, 1983a). No solid phase was observed and the size of the liquid-liquid phase region is notably smaller. Both of these distinctions are likely due to the absence of C<sub>30+</sub> components in the synthetic oil (Orr, et al., 1981). Figure 3 shows the complete phase envelope at 40.1°C generated for mixtures of CO<sub>2</sub> with oil 2. The raw experimental values of pressure and volume which were analyzed by least squares to construct Figure 3 are presented in Table 4. The data were again smoothed to the same temperature using room temperature data reported for the same CO<sub>2</sub> - oil 2 mixtures (Monger and McMullan, 1983). In contrast to what is observed for oil 1, complete miscibility between CO<sub>2</sub> and oil 2 is achieved above a measured bubble-point pressure of 85 atm. Figure 4 shows the complete phase envelope at 38.2°C generated for mixtures of CO<sub>2</sub> with oil 3. The raw experimental values of pressure and volume which were analyzed by least squares to construct Figure 4 are presented in Table 5. Type II phase behavior is exhibited with the size of the liquid-liquid phase region greatly reduced. The open circle at 100% CO<sub>2</sub> in Figures 2, 3 and 4 is the extrapolated vapor pressure of pure CO<sub>2</sub> (Newitt, et al., 1956). This is a hypothetical vapor pressure since CO<sub>2</sub> is supercritical.

The asterisks in Figure 2 for oil 1 and Figure 4 for oil 3 indicate the conditions at which samples of both CO<sub>2</sub>-rich liquid and oil-rich liquid were taken for phase analyses. Oil 2 is single phase at these conditions. For oil 1, at 38.5°C and 96.5 atm, the total 90.0 mole percent CO<sub>2</sub> sample mixture exhibited a density of 0.768 g/cc and a molar volume of 75.4 cc/g-mol. For oil 3, at 38.7°C and 95.3 atm, the total 90.0 mole percent CO<sub>2</sub> sample mixture exhibited a density of 0.791 g/cc and a molar volume of 69.8 cc/g-mol. The results of the liquid-liquid phase analyses are presented in Tables 6 and 7. The density and volume percent values listed in Table 6 represent raw experimental data. Other data listed in Tables 6 and 7 are smoothed by material balance calculations. The data show that for both sample mixtures the phase which predominates on a mass and volume basis is the less dense, CO<sub>2</sub>-rich liquid phase. For oil 1, the CO<sub>2</sub>-rich liquid phase extracts 38.2 mole percent or 31.7 weight percent of the oil. For oil 3, hydrocarbon extracted by the CO<sub>2</sub>-rich liquid phase is significantly improved to 78.2 mole percent or 76.4 weight percent of the oil.

Table 8 presents liquid-liquid equilibrium ratios calculated from the liquid phase compositions listed in Table 7. The results in Table 8 show that for both oil 1 and oil 3, CO<sub>2</sub> is the only component that preferentially partitions into the CO<sub>2</sub>-rich liquid phase. All of the hydrocarbon components concentrate in the oil-rich liquid phase. This is perhaps surprising for the aromatic components, since the oil 2 phase envelope (Figure 3) shows that CO<sub>2</sub> and the aromatics are completely miscible at the sampling conditions. The results in Table 8 also show that the aromatic components in oil 3 greatly enhance the ability of the CO<sub>2</sub>-rich liquid

Table 3

MEASURED VALUES OF PRESSURE AND VOLUME FOR ISOTHERMS OF CO<sub>2</sub> - OIL 1 MIXTURES

<u>PRESSURE</u> (atm)	<u>PHASE</u> <u>REGION</u>	<u>TOTAL MOLAR</u> <u>VOLUME (cc/g-mol)</u>	<u>VAPOR</u> <u>(volume %)</u>	<u>L<sub>CO2</sub></u> <u>(volume %)</u>	<u>L<sub>OIL</sub></u> <u>(volume %)</u>
28.5 MOLE PERCENT CO <sub>2</sub> , 40.0°C					
12.2	L <sub>OIL</sub> + V	545.5	66.74	0	33.26
13.5	L <sub>OIL</sub> + V	488.3	62.43	0	37.57
14.4	L <sub>OIL</sub> + V	451.6	59.59	0	40.41
16.1	L <sub>OIL</sub> + V	390.5	53.02	0	46.98
24.7	L <sub>OIL</sub> + V	227.7	16.31	0	83.69
28.7	L <sub>OIL</sub> <sub>a</sub>	196.9	a	0	a
50.0	L <sub>OIL</sub>	191.3	0	0	100
97.8	L <sub>OIL</sub>	189.7	0	0	100
149.1	L <sub>OIL</sub>	188.6	0	0	100
196.6	L <sub>OIL</sub>	187.7	0	0	100
240.0	L <sub>OIL</sub>	186.9	0	0	100
51.9 MOLE PERCENT CO <sub>2</sub> , 42.1°C					
36.5	L <sub>OIL</sub> + V	276.3	52.52	0	47.48
43.4	L <sub>OIL</sub> + V	217.1	37.57	0	62.43
52.3	L <sub>OIL</sub> + V	166.3	15.07	0	84.93
63.7	L <sub>OIL</sub>	145.7	0	0	100
93.6	L <sub>OIL</sub>	143.8	0	0	100
141.1	L <sub>OIL</sub>	142.8	0	0	100
190.2	L <sub>OIL</sub>	141.9	0	0	100
237.4	L <sub>OIL</sub>	141.1	0	0	100
76.5 MOLE PERCENT CO <sub>2</sub> , 40.4°C					
70.7	L <sub>OIL</sub> + V	144.6	44.65	0	55.35
75.3	L <sub>OIL</sub> + V	124.1	31.60	0	68.40
80.8	L <sub>OIL</sub> + V	101.3	7.74	0	92.26
82.9	L <sub>OIL</sub> + V	99.4	6.80	0	93.20
93.2	L <sub>OIL</sub>	97.0	0	0	100
131.9	L <sub>OIL</sub>	95.9	0	0	100
161.7	L <sub>OIL</sub>	95.1	0	0	100
189.2	L <sub>OIL</sub>	94.5	0	0	100
217.1	L <sub>OIL</sub>	94.0	0	0	100

Table 3 (cont.)

84.3 MOLE PERCENT CO<sub>2</sub>, 40.7°C

69.5	L <sub>OIL</sub> + V	175.8	70.42	0	29.58
76.3	L <sub>OIL</sub> + V	139.8	59.05	0	40.95
81.4	L <sub>OIL</sub> + V	112.3	42.94	0	57.06
84.0	L <sub>OIL</sub> + L <sub>CO2</sub> + V	97.6	28.02	2.92	69.06
84.8	L <sub>OIL</sub> + L <sub>CO2</sub> + V	92.3	12.27	17.07	70.66
93.2	L <sub>OIL</sub> + L <sub>CO2</sub>	85.8	0	23.67	76.33
120.2	L <sub>OIL</sub>	82.9	0	0	100
155.4	L <sub>OIL</sub>	81.7	0	0	100
190.3	L <sub>OIL</sub>	80.8	0	0	100
231.4	L <sub>OIL</sub>	79.8	0	0	100

89.7 MOLE PERCENT CO<sub>2</sub>, 39.1°C

79.1	L <sub>OIL</sub> + L <sub>CO2</sub> + V	106.0	52.42	10.29	37.56
79.0	L <sub>OIL</sub> + L <sub>CO2</sub> + V	100.3	43.26	17.96	38.78
79.6	L <sub>OIL</sub> + L <sub>CO2</sub> + V	94.4	33.02	27.16	39.82
80.2	L <sub>OIL</sub> + L <sub>CO2</sub> + V	88.3	19.40	39.29	41.31
80.8	a	82.4	a	a	43.03
93.8	L <sub>OIL</sub> + L <sub>CO2</sub>	76.8	0	56.95	43.05
119.8	L <sub>OIL</sub> + L <sub>CO2</sub>	73.6	0	57.45	42.55
157.0	L <sub>OIL</sub>	71.6	0	100	0
194.3	L <sub>OIL</sub>	70.3	0	100	0
237.7	L <sub>OIL</sub>	69.1	0	100	0

90.0 MOLE PERCENT CO<sub>2</sub>, 39.1°C<sup>b</sup>

95.4	L <sub>OIL</sub> + L <sub>CO2</sub>	75.9	0	59.26	40.74
102.0	L <sub>OIL</sub> + L <sub>CO2</sub>	75.0	0	59.21	40.79
108.0	L <sub>OIL</sub> + L <sub>CO2</sub>	74.2	0	59.36	40.64
115.0	L <sub>OIL</sub> + L <sub>CO2</sub>	73.6	0	60.08	39.92
123.1	L <sub>OIL</sub> + L <sub>CO2</sub>	72.9	0	61.03	38.97
130.2	L <sub>OIL</sub> + L <sub>CO2</sub>	72.4	0	67.06	32.94
138.8	L <sub>CO2</sub>	71.9	0	100	0
154.2	L <sub>CO2</sub>	71.2	0	100	0
174.2	L <sub>CO2</sub>	70.5	0	100	0
196.0	L <sub>CO2</sub>	69.8	0	100	0
229.2	L <sub>CO2</sub>	68.9	0	100	0

Table 3 (cont.)

93.9 MOLE PERCENT CO<sub>2</sub>, 42.1°C

88.4	L <sub>OIL</sub> + L <sub>CO2</sub>	88.8	0	77.34	22.66
89.2	L <sub>OIL</sub> + L <sub>CO2</sub>	83.8	0	77.32	22.68
90.3	L <sub>OIL</sub> + L <sub>CO2</sub>	83.7	0	77.21	22.79
105.7	L <sub>OIL</sub> + L <sub>CO2</sub>	72.2	0	78.48	21.52
130.6	L <sub>OIL</sub> + L <sub>CO2</sub>	67.5	0	86.33	13.67
160.6	L <sub>OIL</sub> + L <sub>CO2</sub>	64.7	0	93.18	6.82
195.5	L <sub>CO2</sub>	63.0	0	100	0
232.6	L <sub>CO2</sub>	61.8	0	100	0

<sup>a</sup>Near bubble-point. Possible L/V interface in cell's dead volume.

<sup>b</sup>Duplicate run.

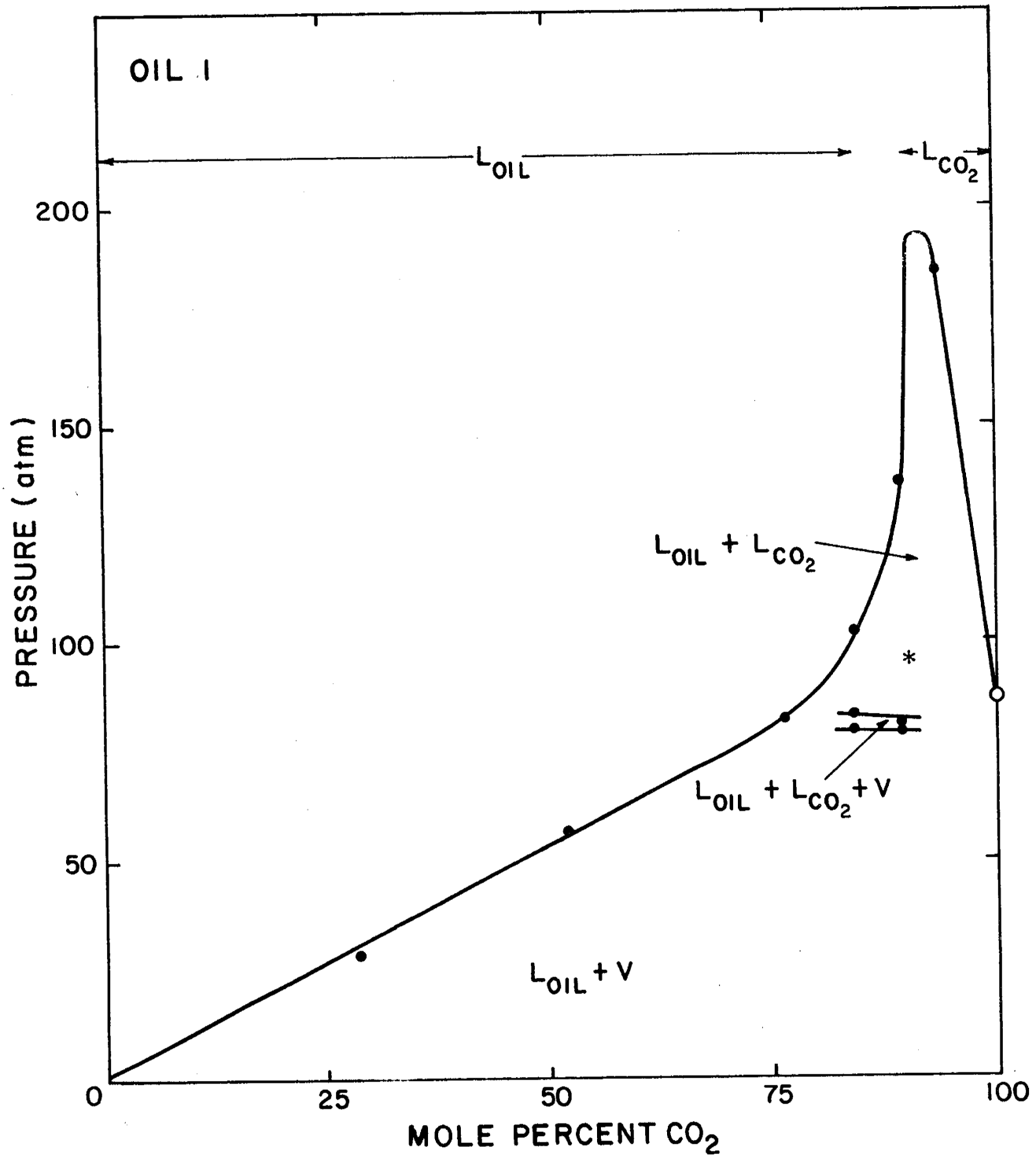


Figure 2. Phase equilibria for mixtures of CO<sub>2</sub> and oil 1 at 39.1°C. Closed circles are data points; open circle is extrapolated CO<sub>2</sub> vapor pressure; asterisk indicates liquid-liquid sampling condition.

Table 4

MEASURED VALUES OF PRESSURE AND VOLUME FOR ISOTHERMS OF CO<sub>2</sub> - OIL 2 MIXTURES

<u>PRESSURE</u> (atm)	<u>PHASE</u> <u>REGION</u>	<u>TOTAL MOLAR</u> <u>VOLUME (cc/g-mol)</u>	<u>VAPOR</u> (volume %)	<u>LIQUID</u> (volume %)
24.7 MOLE PERCENT CO <sub>2</sub> , 41.2°C				
20.8	L <sub>OIL</sub> + V	223.3	42.63	57.37
23.5	L <sub>OIL</sub> + V	187.4	30.84	69.16
29.0	L <sub>OIL</sub> + V	144.9	8.76	91.24
31.4	L <sub>OIL</sub> <sub>a</sub>	135.3	a	a
66.4	L <sub>OIL</sub>	131.3	0	100
110.0	L <sub>OIL</sub>	130.4	0	100
160.1	L <sub>OIL</sub>	129.4	0	100
216.2	L <sub>OIL</sub>	128.9	0	100
49.7 MOLE PERCENT CO <sub>2</sub> , 39.9°C				
47.6	L <sub>OIL</sub> + V	152.6	36.13	63.87
50.5	L <sub>OIL</sub> + V	134.2	25.69	74.31
56.4	L <sub>OIL</sub> + V	109.8	6.08	93.92
69.1	L <sub>OIL</sub>	104.4	0	100
94.0	L <sub>OIL</sub>	103.7	0	100
141.7	L <sub>OIL</sub>	103.0	0	100
178.6	L <sub>OIL</sub>	102.4	0	100
223.2	L <sub>OIL</sub>	101.8	0	100
74.9 MOLE PERCENT CO <sub>2</sub> , 39.9°C				
75.2	L <sub>OIL</sub> + V	83.2	8.81	91.19
76.3	L <sub>OIL</sub> + V	80.3	4.10	95.90
108.1	L <sub>OIL</sub>	77.5	0	100
132.3	L <sub>OIL</sub>	76.8	0	100
147.1	L <sub>OIL</sub>	75.7	0	100
212.2	L <sub>OIL</sub>	75.2	0	100

Table 4 (cont.)

81.5 MOLE PERCENT CO<sub>2</sub>, 40.6°C

61.8	L <sub>OIL</sub> + V	199.9	79.74	20.26
67.1	L <sub>OIL</sub> + V	166.7	74.18	25.82
71.2	L <sub>OIL</sub> + V	138.6	65.59	34.41
75.6	L <sub>OIL</sub> + V	109.9	49.89	50.11
80.0	L <sub>OIL</sub> + V	84.4	23.39	76.61
99.5	L <sub>OIL</sub>	71.9	0	100
145.6	L <sub>OIL</sub>	70.3	0	100
187.9	L <sub>OIL</sub>	69.3	0	100
229.0	L <sub>OIL</sub>	68.4	0	100

81.8 MOLE PERCENT CO<sub>2</sub>, 40.7°C<sup>b</sup>

58.2	L <sub>OIL</sub> + V	230.0	83.82	16.18
66.4	L <sub>OIL</sub> + V	173.0	75.78	24.22
77.4	L <sub>OIL</sub> + V	95.6	36.43	63.57
79.3	L <sub>OIL</sub> + V	80.5	15.96	84.04
92.9	L <sub>OIL</sub>	72.3	0	100
124.9	L <sub>OIL</sub>	71.1	0	100
163.0	L <sub>OIL</sub>	70.0	0	100
199.3	L <sub>OIL</sub>	69.0	0	100
235.4	L <sub>OIL</sub>	68.2	0	100

88.9 MOLE PERCENT CO<sub>2</sub>, 38.9°C

73.3	L <sub>OIL</sub> + V	145.0	78.62	21.38
75.4	L <sub>OIL</sub> + V	112.3	63.02	36.98
76.8	L <sub>OIL</sub> + V	91.2	43.76	56.24
79.3	L <sub>OIL</sub> <sub>a</sub>	68.3	a	a
107.8	L <sub>OIL</sub>	65.0	0	100
144.7	L <sub>OIL</sub>	63.2	0	100
189.1	L <sub>OIL</sub>	61.7	0	100
230.4	L <sub>OIL</sub>	60.6	0	100

92.8 MOLE PERCENT CO<sub>2</sub>, 40.0°C

78.9	L <sub>OIL</sub> + V	83.4	37.97	62.03
81.6	L <sub>OIL</sub> + V	74.9	22.98	77.02
82.2	L <sub>OIL</sub> + V	70.3	12.07	87.93
108.0	L <sub>OIL</sub>	63.2	0	100
148.5	L <sub>OIL</sub>	60.5	0	100
185.8	L <sub>OIL</sub>	58.9	0	100
225.6	L <sub>OIL</sub>	57.7	0	100

Table 4 (cont.)

94.8 MOLE PERCENT CO<sub>2</sub>, 39.8°C

82.1	L <sub>OIL</sub> + V	69.2	9.49	90.51
83.8	<sup>a</sup>	66.3	a	a
100.3	L <sub>OIL</sub>	62.4	0	100
149.6	L <sub>OIL</sub>	58.5	0	100
188.3	L <sub>OIL</sub>	56.7	0	100
232.0	L <sub>OIL</sub>	55.1	0	100

<sup>a</sup>Near bubble-point. Possible L/V interface in cell's dead volume.  
<sup>b</sup>Duplicate run.

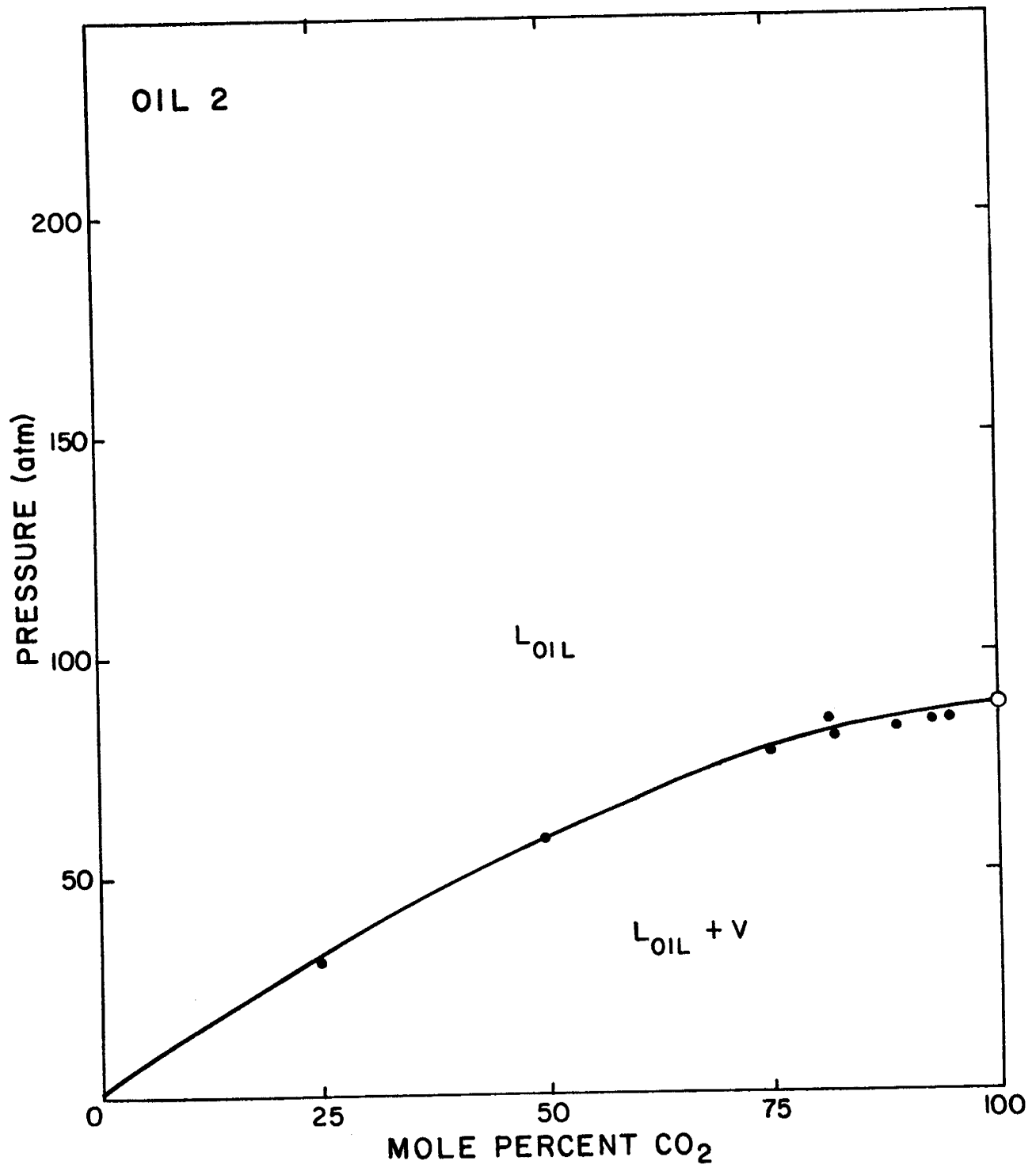


Figure 3. Phase equilibria for mixtures of CO<sub>2</sub> and oil 2 at 40.1°C. Closed circles are data points; open circle is extrapolated CO<sub>2</sub> vapor pressure.

Table 5

MEASURED VALUES OF PRESSURE AND VOLUME FOR ISOTHERMS OF CO<sub>2</sub> - OIL 3 MIXTURES

<u>PRESSURE</u> (atm)	<u>PHASE</u> <u>REGION</u>	<u>TOTAL MOLAR</u> <u>VOLUME (cc/g-mol)</u>	<u>VAPOR</u> <u>(volume %)</u>	<u>L<sub>CO2</sub></u> <u>(volume %)</u>	<u>L<sub>OIL</sub></u> <u>(volume %)</u>
31.9 MOLE PERCENT CO <sub>2</sub> , 38.0°C					
15.3	L <sub>OIL</sub> + V	435.5	67.45	0	32.55
18.3	L <sub>OIL</sub> + V	344.4	57.59	0	42.41
23.0	L <sub>OIL</sub> + V	253.4	40.85	0	59.15
27.4	L <sub>OIL</sub> + V	197.0	22.95	0	77.05
30.9	L <sub>OIL</sub> <sub>a</sub>	163.3	a	0	a
64.9	L <sub>OIL</sub>	156.2	0	0	100
114.0	L <sub>OIL</sub>	155.4	0	0	100
163.8	L <sub>OIL</sub>	154.5	0	0	100
212.1	L <sub>OIL</sub>	153.8	0	0	100
245.4	L <sub>OIL</sub>	153.2	0	0	100
50.7 MOLE PERCENT CO <sub>2</sub> , 38.2°C					
29.1	L <sub>OIL</sub> + V	343.0	68.16	0	31.84
34.1	L <sub>OIL</sub> + V	271.1	58.65	0	41.35
41.2	L <sub>OIL</sub> + V	199.4	41.41	0	58.59
48.3	L <sub>OIL</sub> + V	148.3	17.64	0	82.36
55.9	L <sub>OIL</sub> <sub>a</sub>	128.0	a	0	a
58.2	L <sub>OIL</sub>	127.9	0	0	100
102.6	L <sub>OIL</sub>	126.9	0	0	100
144.1	L <sub>OIL</sub>	126.2	0	0	100
191.0	L <sub>OIL</sub>	125.4	0	0	100
238.8	L <sub>OIL</sub>	124.7	0	0	100
70.0 MOLE PERCENT CO <sub>2</sub> , 38.5°C					
53.6	L <sub>OIL</sub> + V	175.2	56.62	0	43.38
55.9	L <sub>OIL</sub> + V	158.9	50.65	0	49.35
58.4	L <sub>OIL</sub> + V	142.6	43.38	0	56.62
61.2	L <sub>OIL</sub> + V	126.4	34.51	0	65.49
63.1	L <sub>OIL</sub> + V	115.5	25.86	0	74.14
66.1	L <sub>OIL</sub> <sub>a</sub>	99.2	a	0	a
96.8	L <sub>OIL</sub>	93.2	0	0	100
134.4	L <sub>OIL</sub>	92.5	0	0	100
184.2	L <sub>OIL</sub>	91.7	0	0	100
232.0	L <sub>OIL</sub>	90.9	0	0	100

Table 5 (cont.)

82.6 MOLE PERCENT CO<sub>2</sub>, 38.0°C

73.8	L <sub>OIL</sub> + V	103.4	40.19	0	59.81
74.4	L <sub>OIL</sub> + V	97.1	33.84	0	66.16
74.8	L <sub>OIL</sub> + V	90.7	25.72	0	74.28
75.5	L <sub>OIL</sub> + V	84.4	16.30	0	83.70
75.5	L <sub>OIL</sub> <sup>a</sup>	78.1	a	0	a
106.9	L <sub>OIL</sub>	75.3	0	0	100
129.6	L <sub>OIL</sub>	74.4	0	0	100
162.6	L <sub>OIL</sub>	73.4	0	0	100
197.3	L <sub>OIL</sub>	72.5	0	0	100
233.3	L <sub>OIL</sub>	71.7	0	0	100

89.7 MOLE PERCENT CO<sub>2</sub>, 38.4°C

77.5	L <sub>OIL</sub> + L <sub>CO2</sub> + V	83.6	31.02	45.95	23.02
77.7	L <sub>OIL</sub> + L <sub>CO2</sub> + V	81.2	26.48	50.42	23.09
77.7	L <sub>OIL</sub> + L <sub>CO2</sub> + V	78.9	21.80	55.22	22.98
77.8	L <sub>OIL</sub> + L <sub>CO2</sub> + V	76.5	16.06	60.85	23.09
77.9	L <sub>OIL</sub> + L <sub>CO2</sub> + V	74.1	10.35	66.42	23.23
77.9	L <sub>OIL</sub> <sup>a</sup>	71.7	a	a	23.36
85.7	L <sub>OIL</sub> + L <sub>CO2</sub>	68.5	0	82.00	18.00
110.2	L <sub>CO2</sub>	65.5	0	100	0
146.3	L <sub>CO2</sub>	63.6	0	100	0
194.5	L <sub>CO2</sub>	61.8	0	100	0
232.2	L <sub>CO2</sub>	60.7	0	100	0

90.0 MOLE PERCENT CO<sub>2</sub>, 38.7°C<sup>b</sup>

85.0	L <sub>OIL</sub> + L <sub>CO2</sub>	71.3	0	63.89	36.11
91.2	L <sub>OIL</sub> + L <sub>CO2</sub>	70.2	0	81.23	18.77
99.3	L <sub>CO2</sub>	69.4	0	100	0
129.9	L <sub>CO2</sub>	67.7	0	100	0
157.9	L <sub>CO2</sub>	66.6	0	100	0
188.3	L <sub>CO2</sub>	65.6	0	100	0
215.4	L <sub>CO2</sub>	64.8	0	100	0
226.2	L <sub>CO2</sub>	64.3	0	100	0

Table 5 (cont.)

90.3 MOLE PERCENT CO<sub>2</sub>, 38.0°C

73.4	L <sub>OIL</sub> + V	154.0	90.66	0	9.34
76.5	L <sub>OIL</sub> + V	124.1	84.63	0	15.37
77.4	L <sub>OIL</sub> + L <sub>CO2</sub> + V	104.2	69.59	20.26	10.15
78.0	L <sub>OIL</sub> + L <sub>CO2</sub> + V	84.2	41.76	48.51	9.72
78.7	<sup>a</sup> L <sub>OIL</sub> + L <sub>CO2</sub>	69.1	<sup>a</sup>	<sup>a</sup>	9.05
92.7	L <sub>OIL</sub> + L <sub>CO2</sub>	63.6	0	96.03	3.97
135.6	L <sub>CO2</sub>	59.2	0	100	0
174.7	L <sub>CO2</sub>	57.3	0	100	0
198.6	L <sub>CO2</sub>	56.4	0	100	0
235.0	L <sub>CO2</sub>	55.3	0	100	0

95.2 MOLE PERCENT CO<sub>2</sub>, 38.2°C

79.7	L <sub>OIL</sub> + L <sub>CO2</sub> + V	84.3	39.04	58.35	2.62
80.4	<sup>a</sup> L <sub>OIL</sub> + L <sub>CO2</sub>	74.3	<sup>a</sup>	<sup>a</sup>	2.66
83.5	L <sub>OIL</sub> + L <sub>CO2</sub>	69.4	0	98.21	1.79
92.5	L <sub>OIL</sub> + L <sub>CO2</sub>	64.4	0	99.43	0.57
117.5	L <sub>CO2</sub>	59.6	0	100	0
160.5	L <sub>CO2</sub>	56.1	0	100	0
203.4	L <sub>CO2</sub>	54.0	0	100	0
235.8	L <sub>CO2</sub>	52.8	0	100	0

<sup>a</sup>Near bubble-point. Possible L/V interface in cell's dead volume.

<sup>b</sup>Duplicate run.

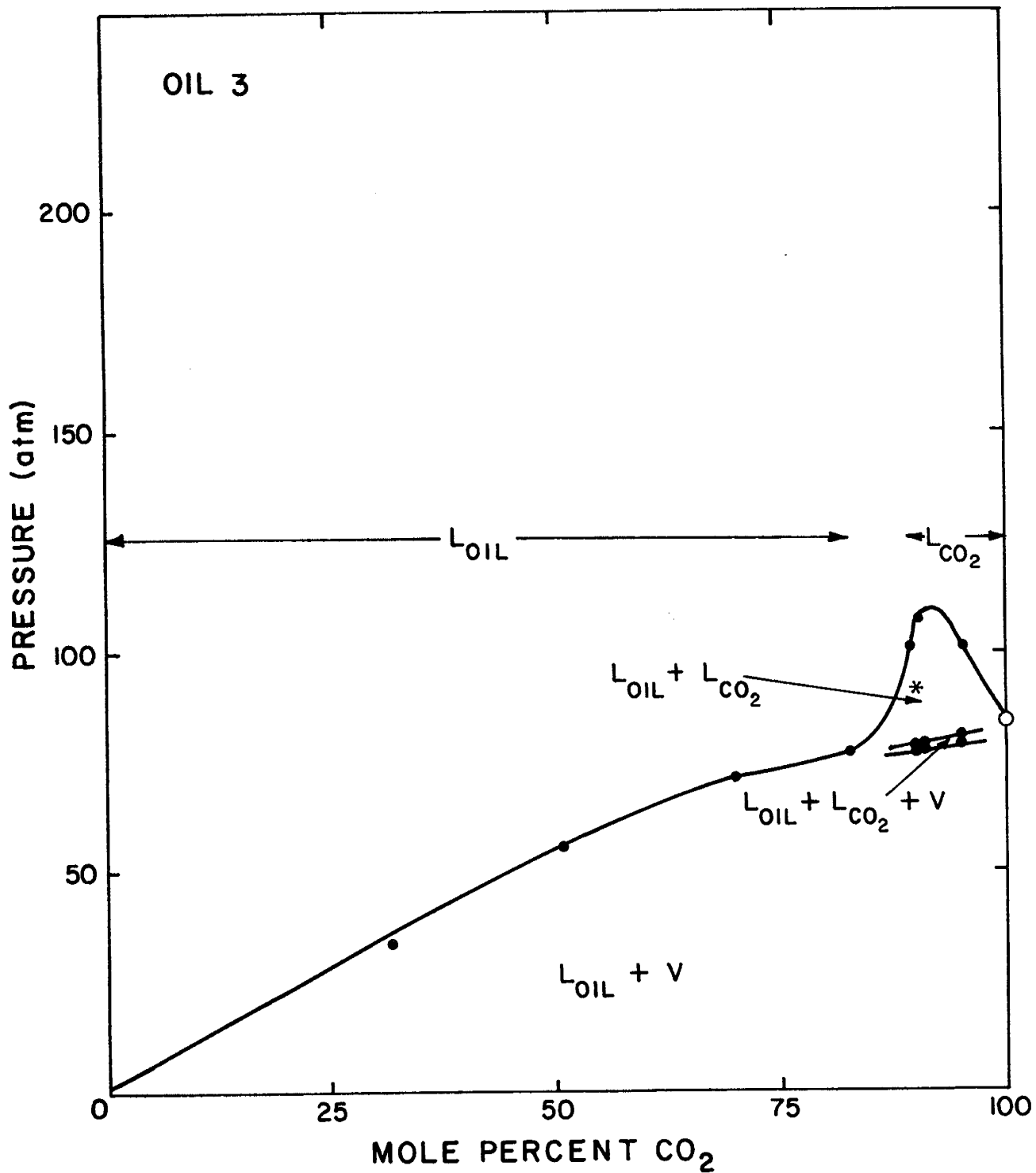


Figure 4. Phase equilibria for mixtures of CO<sub>2</sub> and oil 3 at 38.2°C. Closed circles are data points; open circle is extrapolated CO<sub>2</sub> vapor pressure; asterisk indicates liquid-liquid sampling condition.

Table 6

PROPERTIES OF LIQUID PHASES

	<u>OIL 1</u>		<u>OIL 3</u>	
	<u>L<sub>CO<sub>2</sub></sub></u>	<u>L<sub>OIL</sub></u>	<u>L<sub>CO<sub>2</sub></sub></u>	<u>L<sub>OIL</sub></u>
<u>Density (g/cc)</u>				
(38.6°C, 97.1 atm)	0.749	0.779		
(37.4°C, 95.2 atm)			0.785	a
<u>Volume (%)</u>				
(38.5°C, 96.5 atm)	60.7	39.3		
(38.7°C, 91.2 atm)			83.9	16.1
<u>Molar Volume (cc/g-mol)</u>				
(38.5°C, 96.5 atm)	66.4	95.6		
(38.7°C, 91.2 atm)			68.7	79.1

- a. Insufficient sample for direct measurement; density by material balance = 0.797 g/cc.

Table 7

LIQUID PHASE COMPOSITIONS (MOLE PERCENT)

<u>COMPONENT</u>	<u>OIL 1</u>		<u>OIL 3</u>	
	<u>L<sub>CO<sub>2</sub></sub></u>	<u>L<sub>OIL</sub></u>	<u>L<sub>CO<sub>2</sub></sub></u>	<u>L<sub>OIL</sub></u>
CO <sub>2</sub>	94.44	80.32	90.87	84.82
Pentane	1.53	3.01	1.95	2.25
Decane	3.15	9.02	3.68	5.90
n-Butylbenzene	—	—	0.92	1.47
Eicosane	0.65	4.96	0.84	1.96
2-Methylnaphthalene	—	—	0.89	1.66
Squalane	0.23	2.69	0.41	1.05
Biphenyl	—	—	0.44	0.86

Table 8

LIQUID-LIQUID EQUILIBRIUM RATIOS<sup>a</sup>

<u>COMPONENT</u>	<u>OIL 1</u>	<u>OIL 3</u>
CO <sub>2</sub>	1.176	1.071
Pentane	0.508	0.867
n-Butylbenzene	—	0.626
Decane	0.349	0.624
2-Methylnaphthalene	—	0.536
Biphenyl	—	0.512
Eicosane	0.131	0.429
Squalane	0.086	0.390

a. 
$$\frac{\text{Mole fraction of component in CO}_2\text{-rich liquid phase}}{\text{Mole fraction of component in oil-rich liquid phase}}$$

phase to extract paraffinic hydrocarbons. This dramatic result is evident from a comparison of the oil 1 and oil 3 data for any of the paraffins, but is most pronounced for eicosane and squalane.

The expected relationship between a hydrocarbon's molecular weight and its solubility in the CO<sub>2</sub>-rich liquid phase is also illustrated by the data in Table 8 (Zarah, et al., 1974; Yang, et al., 1976). Table 8 lists components in order of increasing molecular weight. For both oil 1 and oil 3, the liquid-liquid equilibrium ratio decreases with increasing hydrocarbon molecular weight. Thus CO<sub>2</sub> exhibits the ability to selectively extract lighter components from a mixture of hydrocarbons. Table 9 presents liquid-liquid selectivities calculated from the liquid phase compositions listed in Table 7. The results in Table 9 show that selective extraction by CO<sub>2</sub> is significantly impaired by the presence of aromatic components.

### CONCLUSIONS

1. Several features of the phase behavior exhibited by mixtures of CO<sub>2</sub> with complex reservoir fluids can be modelled using synthetic oils created from a small number of hydrocarbon components. This facilitates studies of oil compositional effects in CO<sub>2</sub> flooding, because experimental data can be more easily verified by material balance.
2. No solid phase was observed for CO<sub>2</sub>-synthetic oil mixtures, and the liquid-liquid phase regions which were observed were notably smaller. Both of these distinctions are likely due to the absence of C<sub>30+</sub> components.
3. The ability of supercritical CO<sub>2</sub> to extract hydrocarbons is influenced by the presence of aromatic components. Phase equilibria results suggest that both heavy paraffinic and heavy aromatic hydrocarbons must be present to demonstrate this compositional effect. This improves our understanding of the CO<sub>2</sub> multiple-contact miscible displacement process, because natural reservoir fluids contain heavy hydrocarbons of both chemical types.
4. Paraffins, especially heavy paraffins, are more readily extracted into the CO<sub>2</sub>-rich liquid phase in the presence of heavy aromatics. As a consequence of the improved extraction, aromatics impair CO<sub>2</sub>'s ability to selectively solubilize lighter hydrocarbon components. Both effects are beneficial in enhanced oil recovery operations using CO<sub>2</sub>, because an efficient CO<sub>2</sub> flood depends upon extensive hydrocarbon extraction into a CO<sub>2</sub>-rich phase, with no selectivity requirements.
5. The phase behavior results provide an explanation for laboratory displacement experiments which showed that when a highly paraffinic crude oil was enriched with heavy aromatics, the CO<sub>2</sub> miscibility pressure was lowered and oil recovery was improved (Holm and Josendal, 1982).

TABLE 9  
LIQUID-LIQUID SELECTIVITIES<sup>a</sup>

<u>Lighter Component</u>	<u>Heavier Component</u>	<u>OIL 1</u>	<u>OIL 3</u>
Decane	Eicosane	2.66	1.46
Decane	2-Methylnaphthalene	—	1.16
n-Butylbenzene	Eicosane	—	1.46
n-Butylbenzene	2-Methylnaphthalene	—	1.17
Decane	Squalene	4.08	1.60
Decane	Biphenyl	—	1.22
n-Butylbenzene	Squalene	—	1.60
n-Butylbenzene	Biphenyl	—	1.22

a.  $\frac{\text{Mole fraction lighter component}}{\text{Mole fraction heavier component}}$  CO<sub>2</sub>-rich liquid Phase

$\frac{\text{Mole fraction lighter component}}{\text{Mole fraction heavier component}}$  oil-rich liquid phase

## PART II - MULTIPLE CONTACT PHASE EQUILIBRIA EXPERIMENTS WITH MIXTURES OF CARBON DIOXIDE AND BROOKHAVEN RESERVOIR OIL

### INTRODUCTION

The ultimate oil recovery resulting from both primary and secondary immiscible flooding processes is generally within the range of 20 to 40% of the original oil in place. The ultimate recovery achievable by immiscible flooding is a function of three factors:

- (1) volumetric sweepout of the reservoir by the injection fluid,
- (2) capture of the displaced oil at producing wells, and
- (3) displacement efficiency of the injection fluid in the reservoir portion that is swept (Stalkup, 1983a).

Of these three factors miscible flooding greatly improves the third. The displacement efficiency of immiscible floods is a function of the rock wettability and the interfacial tension (IFT) at the oil/ water or oil/gas interface (Stalkup, 1983a). Of the two, miscible displacement affects the IFT more significantly; although, it has been reported in the literature that in certain miscible processes the rock wettability is also affected (Ehrlich, et al., 1983). Two fluids are miscible when they mix together in all proportions and the mixture remains single phase. Since only one phase results from the mixing, there are no interfaces and consequently no IFT between the fluids (Stalkup, 1983a). Because of no IFT between the fluids, 100% recovery of the oil contacted can be obtained in miscible floods.

There are two classifications of fluids used in miscible displacements:

- (1) first-contact miscible (FCM), and
- (2) dynamic or multiple-contact miscible (MCM).

The FCM solvents mix directly with reservoir oils in all proportions and their mixtures always remain single phase. Propane and liquid petroleum gas (LPG) are the solvents most commonly used in the FCM process. The MCM solvents develop miscibility in-situ by mass transfer of oil and solvent components through repeated contacts with the reservoir oil. The fluids most commonly used in the MCM process are enriched natural gas, high pressure natural gas, flue gas, nitrogen, and carbon dioxide ( $\text{CO}_2$ ) (Stalkup, 1983b).

There are two main mechanisms in the MCM spectrum. One is the condensing-gas drive process which develops miscibility by the transfer of intermediate-molecular-weight hydrocarbons ( $\text{C}_2 - \text{C}_6$ ) from the injected gas into the reservoir oil. Natural gas with appreciable concentrations of  $\text{C}_2 - \text{C}_6$  hydrocarbons is normally the injection fluid. The other is the vaporizing-gas drive process which develops miscibility by the transfer of intermediate-molecular-weight hydrocarbons from the reservoir oil into the injected gas. High pressure natural gas, flue gas, and nitrogen are normally the injection fluids (Stalkup, 1983b). The mechanism which best describes the use of  $\text{CO}_2$  is not completely understood.

Through the use of pseudoternary diagrams, Hutchinson and Braun (1961) discuss the mass transfer mechanisms by which MCM operates. In the condensing-gas drive process (Figure 5), the oil is enriched with the intermediate-molecular-weight hydrocarbons from the injection gas causing the oil's composition to move along the bubble-point curve to the plait point. In the vaporizing-gas drive process (Figure 6), the injection gas is enriched with intermediate-molecular-weight hydrocarbons from the oil causing the gas's composition to move along the dew-point curve to the plait point. Miscibility is developed once the composition of the oil or injection gas reaches the plait point. Significant IFT reduction is obtained for compositions which approach but do not reach the plait point, thus the MCM process is effective despite the adverse affects of dispersion or viscous fingering.

The mechanism by which CO<sub>2</sub> develops miscibility is not completely understood. At reservoir temperatures greater than 120°F, CO<sub>2</sub> appears to develop miscibility by the vaporizing-gas drive mechanism. This is referred to as Type I phase behavior (Stalkup, 1983a). In Type I phase behavior, only vapor and liquid phases coexist on the P-X diagram. At reservoir temperatures less than 120°F, CO<sub>2</sub> appears to develop miscibility by a combination of the vaporizing-gas and condensing-gas drive mechanisms. This is referred to as Type II phase behavior (Stalkup, 1983a). In Type II phase behavior, a three phase region is found on the P-X diagram. In this region there are two distinct liquid phases and a vapor phase (Stalkup, 1983a). It is reported in the literature that a solid asphaltic phase has been seen in both types of phase behavior (Monger, 1984; Shelton and Yarborough, 1976). Carbon dioxide has a distinct advantage over natural gas, flue gas, or nitrogen, because it can achieve miscibility at substantially lower pressures making CO<sub>2</sub> flooding amenable to a broader spectrum of reservoirs (Stalkup, 1983a). This ability comes from the fact that the vaporizing-gas drive gases extract mainly C<sub>2</sub> - C<sub>6</sub> while CO<sub>2</sub> extracts hydrocarbons as deep as C<sub>30</sub> (Holm and Josendal, 1974).

There are many papers in the literature that report the phase equilibria observed in static, single-contact pressure-volume-temperature (PVT) measurements of CO<sub>2</sub>-oil systems. Also, a large number of papers use oil displacement results from dynamic systems to infer the CO<sub>2</sub> and oil phase behavior relevant to the MCM process. There are, however, just a few papers in the literature which use static, multiple-contact PVT measurements to directly address the phase behavior in the MCM process. These papers are briefly discussed in the next paragraph. A good understanding of the multiple-contact phase behavior is needed to calibrate the equation of state (EOS) used in reservoir simulators to predict CO<sub>2</sub> flood performance.

Coats and Smart (1982) examined the compositions that resulted from multiple-contact vaporization of a crude oil with a predominately methane gas. In their experiment, they contacted the oil with the gas, allowed the system to equilibrate, then sampled and removed the vapor phase at constant pressure. The compositional data from their experiment were used to calibrate an EOS. Shelton and Yarborough (1976) did multiple-contact work using rich gas which behaves somewhat like CO<sub>2</sub>. The results from their vaporization experiments showed that the oil-rich phase was stripped of its C<sub>4+</sub> fraction. In their single-contact work, they reported the precipitation of a tar-like solid for both CO<sub>2</sub> and the rich gas. There was no multiple-contact work done with CO<sub>2</sub>. Menzie and Nielsen (1963) did multiple-contact work in determining the success of oil recovery by CO<sub>2</sub> vaporization. They contacted oil with CO<sub>2</sub> at a 1:1 volume ratio at run conditions. The contents in the cell were agitated and allowed to come to equilibrium. The vapor phase was then removed from the cell at constant pressure. The amount of hydrocarbons produced from the vapor phase was measured. Menzie and Nielsen found that the higher

# CONDENSING-GAS DRIVE PROCESS

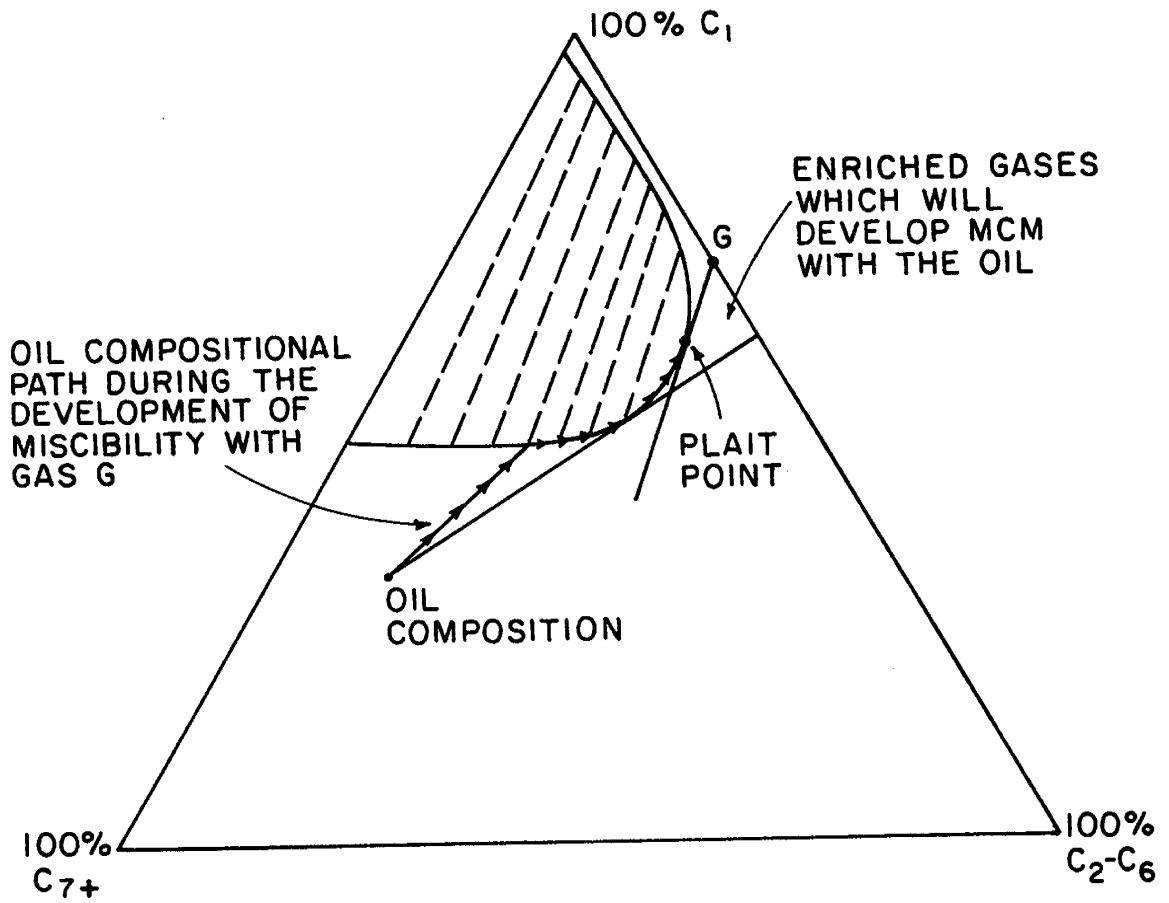


Figure 5.

# VAPORIZING-GAS DRIVE PROCESS

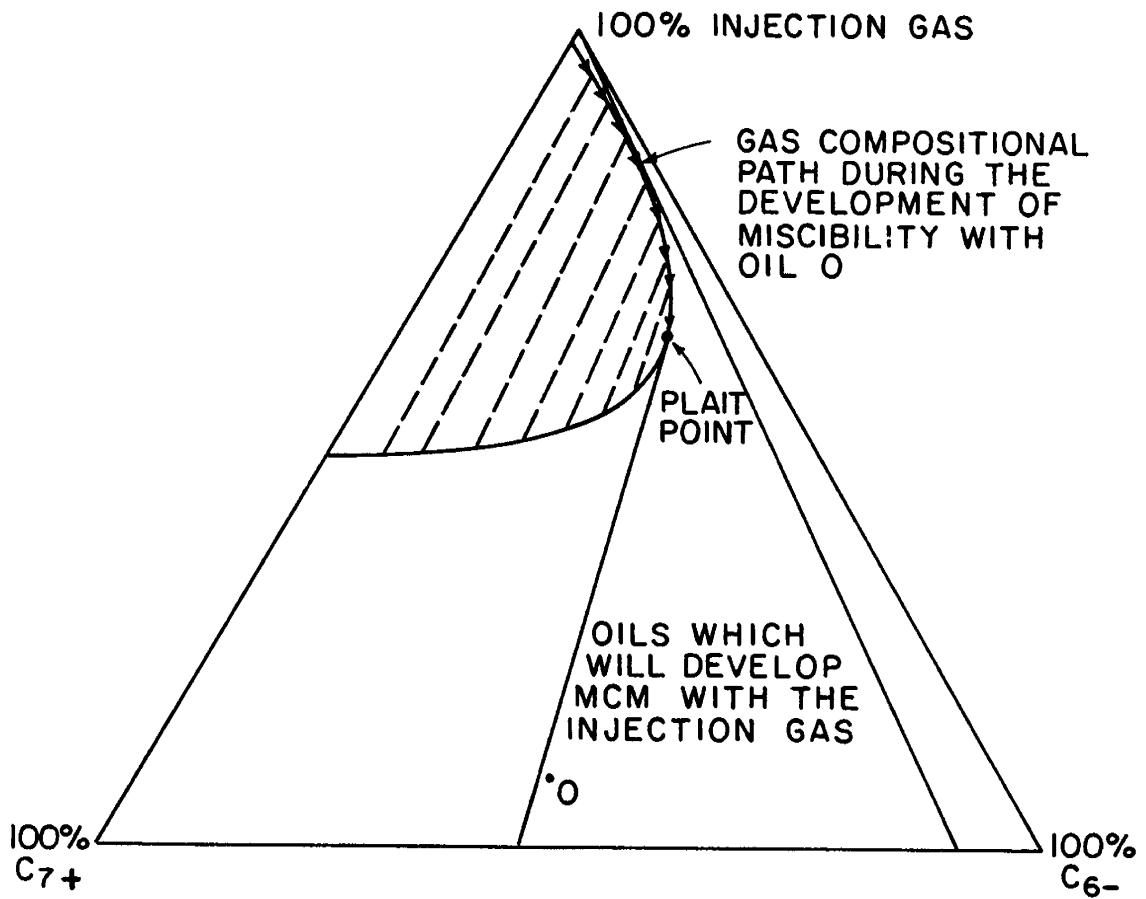


Figure 6.

the pressure the greater the amount of hydrocarbons produced. They also measured the density of the produced liquid and the liquid left in the cell after each contact. Their results showed that the density of both liquids increased after each contact. Gardner, et. al., (1979) did forward and swept zone multiple-contact work using CO<sub>2</sub>. Forward contacts consist of contacting the CO<sub>2</sub>-rich phase, which results from a previous mixing, with fresh reservoir oil. Forward contacts represent what is happening at the flood front where miscibility is developed. Swept zone contacts consist of contacting the oil-rich phase, which results from a previous mixing, with pure CO<sub>2</sub>. The swept zone contacts represent what is happening in the near wellbore vicinity where the residual oil is being stripped by fresh CO<sub>2</sub>. Their work was done with Wasson crude at 105°F which exhibited Type II phase behavior. They performed multiple-contact experiments at 2000 psia and 1350 psia using a 2:1 volume mixture of CO<sub>2</sub> or the predominant CO<sub>2</sub>-rich phase to the oil at run conditions. Single-contact results show that at 2000 psia and high CO<sub>2</sub> concentrations only two liquid phases appear plus a small amount of precipitate. Certain overall cell compositions at 1350 psia produced a lower liquid, upper liquid, and vapor plus a small amount of precipitate. The results of their forward contacts at 2000 psia indicate that miscibility was obtained after the second forward contact with the cell being completely filled with the upper liquid phase plus a small amount of precipitate. Gardner, et al. warn against interpreting the phase behavior results as what is happening at the flood front because the effects of dispersion had not been taken into account. The forward contact results showed that miscibility appeared to be developed by the vaporizing-gas drive mechanism involving two liquid phases, while swept zone contacts showed the CO<sub>2</sub> stripping away at the residual oil phase. Significant precipitation was noted in the forward contacts, and the precipitate had a high affinity for the glass window of the PVT cell. No such precipitate was seen in the swept zone contacts. The multiple-contact experiments at 1350 psia were similar to those at 2000 psia. The forward contacts were different in two ways. The upper phase which was a vapor decreased with successive contacts, and the amount of precipitate increased from contact to contact. It was noted that the precipitate still had a high affinity for glass. Very little compositional data was taken in either set of experiments. Turek, et al., (1984) presented data from both single- and multiple-contacts using CO<sub>2</sub> and several West Texas reservoir oils. In their single-contact work, they found the absence of a liquid-liquid critical point and no liquid-liquid-vapor region at temperatures above 110°F. The forward contacts were done by filling the PVT cell with CO<sub>2</sub> and recombined reservoir oil to give an overall composition of 90 mole% CO<sub>2</sub>. The system was allowed to come to equilibrium and the phases were sampled. The oil-rich liquid phase was then removed at constant pressure, and a second recombined oil volume equal to the first was charged into the cell. Additional contacts were conducted in the same manner. The sampling consisted of measuring the density, viscosity, and composition of each phase. The swept zone contacts were conducted by filling the cell with recombined reservoir oil and adding CO<sub>2</sub> incrementally until the overall composition was in the liquid-liquid region. After equilibration at a fixed pressure and sampling, the CO<sub>2</sub>-rich liquid phase was removed from the cell at constant pressure. Carbon dioxide was then added to the cell to create the second swept zone contact. The sampling consisted of measuring the density, viscosity, and composition of each phase. The results of the forward contacts show that the amount of C<sub>1</sub> - C<sub>6</sub> in the CO<sub>2</sub>-rich phase increases from contact to contact. Also, there is an increase in the C<sub>7+</sub> fraction in the CO<sub>2</sub>-rich phase from contact to contact. Unfortunately, there is no detailed composition of the C<sub>7+</sub> fraction to determine which hydrocarbons are in the CO<sub>2</sub>-rich phase. The results of the swept zone contacts show that the residual oil-rich phase will have a high viscosity and a composition of approximately 80 mole% CO<sub>2</sub> with the remainder

being heavy hydrocarbons. Miscibility was not obtained in the forward contacts which were carried out to five contacts. Also, there was no mention of a solid precipitate in the forward contacts.

Most of the previous work performed to infer MCM phase behavior used oil displacement results and effluent compositions. Only two papers report the use of static, multiple-contact PVT measurements to directly address the MCM phase behavior. Of the two papers, only one presents compositional data. There are no papers in the literature in which a highly asphaltic crude oil was used in the MCM experiments. This study was undertaken to contribute additional static, multiple-contact PVT measurements and compositional data to the literature and to investigate the MCM phase behavior for a highly asphaltic crude oil. Another unique feature of this study is that the oil used was modified to resemble the composition of the reservoir oil that would be contacted by the CO<sub>2</sub> during a flood. This modification consisted of flashing the oil at 60 psia and 32°F. This was done because when CO<sub>2</sub> first contacts the oil, it vaporizes and/or exchanges place with the methane and to a lesser extent C<sub>2</sub> - C<sub>4</sub> (Holm and Josendal, 1974). It has been reported by different investigators that in non-gravity-stable floods the methane and to a lesser extent C<sub>2</sub> - C<sub>6</sub> bank ahead of the flood front (Tiffin and Yellig, 1982; Leach and Yellig, 1979; Holm and Josendal, 1982). This is because the methane is more mobile than the CO<sub>2</sub>. Also, it has been reported via personal correspondence that the methane banks behind the flood front in gravity-stable displacements. This is because the density of the methane is less than that of the CO<sub>2</sub> at reservoir conditions. Single- and multiple-contact constant-composition, pressure traverses were performed in a Ruska through window PVT cell. Swelling indexes were calculated for each of the pressure traverses in order to determine the maximum swelling of the oil-rich phase and to determine the maximum extraction by the CO<sub>2</sub>-rich phase. Detailed compositional analyses of the resulting phases were made for forward contacts to give some insight into how CO<sub>2</sub> develops miscibility. The compositional analyses were used to conclude how deep the CO<sub>2</sub>-rich phase would extract hydrocarbons and to what extent those hydrocarbons would be extracted. Also, detailed compositional analyses of the resulting phases were made for the swept zone contact to determine the composition and the amount of the residual oil left in the reservoir during the development of miscibility and in immiscible floods. Immiscible flooding behavior is likely to describe the huff-n-puff method of oil recovery (Patton, 1979). To some extent this study also addresses the precipitate that results during the development of miscibility.

## EXPERIMENTAL SECTION

### Flashing The Oil

The oil used in this study came from the Brookhaven field located in South Central Mississippi. Brookhaven oil is a highly asphaltic, black crude. This oil was selected because phase behavior data is lacking on crudes of this nature, and the phase behavior results could be compared to a wealth of oil displacement data already available (Whitehead, et. al., 1981). In addition, an ample supply of the oil was available. The stock tank oil has a gravity of 34.3° API and a molecular weight by freezing point depression of 246 g/g-mole. The reconstituted reservoir oil has a GOR of 276 SCF/STB at 83°F. The reservoir oil was reconstituted by Whitehead, et. al. (1981) and stored in a spherical transfer vessel at 1500 psia which is well above the bubble point pressure of 1000 psia.

The oil used in the PVT experiments was modified to resemble the composition of the reservoir oil that would be contacted by CO<sub>2</sub> during a flood. The modification consisted of performing a flash vaporization of the reconstituted reservoir oil at approximately 60 psia and 32°F. The flash vaporization was accomplished through the use of a 2400 cc transfer vessel (Figure 7).

The following procedure was used in flashing the oil. The transfer vessel was cleaned using toluene and hexane. The piston was pushed to the top of the vessel, and the vessel was filled with hydraulic fluid. A Ruska double barrel, positive displacement pump was connected to the bottom of the vessel while the top of the vessel was connected to the spherical transfer vessel which contained the reconstituted reservoir (RR) oil. The hydraulic fluid was pressurized to a pressure slightly greater than that of the RR oil to ensure that the piston was at the top of the transfer vessel. RR oil was then allowed to flow through the top of the transfer vessel to flush out any air or impurities trapped in the flow lines. After about 10 cc of oil were caught in a beaker on the downstream side of the transfer vessel, a reference volume of 250 cc of RR oil at 1500 psia and room temperature was drawn into the transfer vessel. The transfer vessel was disconnected and then put into an ice-water bath. It remained in the ice-water bath from four to six hours to obtain temperature equilibrium. A pressure drop of approximately 1100 psi was observed due to the cooling of the vessel's contents. Once temperature equilibrium was obtained, the vessel was extracted from the ice-water bath, and all the hydraulic fluid was removed from the vessel. Ice was packed around the top of the transfer vessel to counteract room temperature effects. The transfer vessel was rocked while the hydraulic fluid was withdrawn so phase equilibrium could be obtained. The pressure on the vessel was about 60 psia after the hydraulic fluid was removed and phase equilibrium was obtained. The transfer vessel was then connected to the double barrel Ruska pump and the gas resulting from the flash vaporization was removed at constant pressure. The modified oil was then transferred into the oil reservoir on the back of the PVT apparatus. Approximately 200 cc of Brookhaven "Flashed" (BF) oil at 1000 psia and room temperature were obtained from the flash. This procedure was repeated several times during the course of the experimental work with good reproducibility, as confirmed by gas chromatographic analyses of the BF oil. Oil compositions will be presented in "Results and Discussion".

## PVT Apparatus and Procedure

### Apparatus

The existing PVT apparatus used in this study is shown in Figure 8. The Ruska PVT set-up housed two viewable 191 cc through window equilibrium cells in a temperature controlled air bath. The cells were manifolded to two temperature controlled 1000 cc positive displacement Ruska pumps. The cells and pumps were also manifolded to storage reservoirs. The air bath temperature was maintained to  $\pm 0.5^\circ\text{F}$  of run temperature with an Omega Model 157-713 J temperature controller. Ruska pump temperatures were maintained using a Neslab Exacal 100 glycol bath circulator with an Endocal 150 flow through cooler. The temperature of the pumps, cells, air bath, and other PVT equipment was monitored to  $\pm 0.1^\circ\text{F}$  using an Omega Model 199 digital thermometer employing numerous Pt-resistance probes. Pressure was measured with an analog or digital Heise Bourdon tube gauge to  $\pm 5$  psi at the maximum pressure tested of 5000 psia, based upon calibration versus an accurate dead weight tester. Volumes were calculated from pump displacements measured to  $\pm 0.01$  cc and

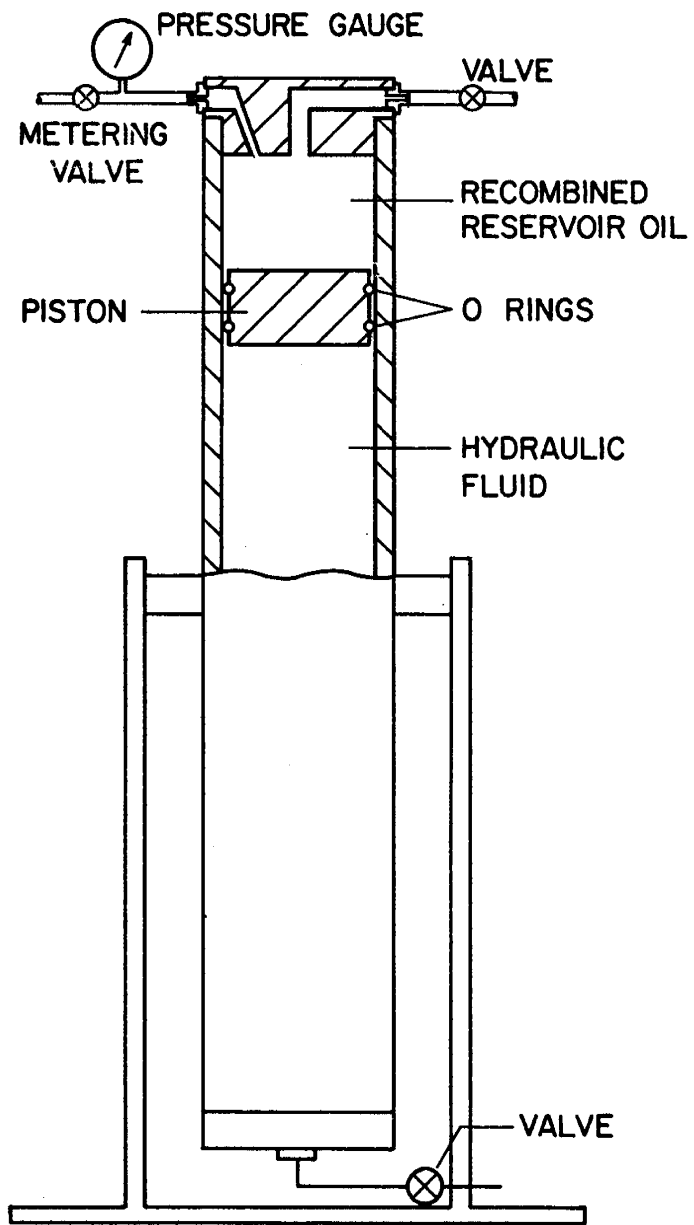
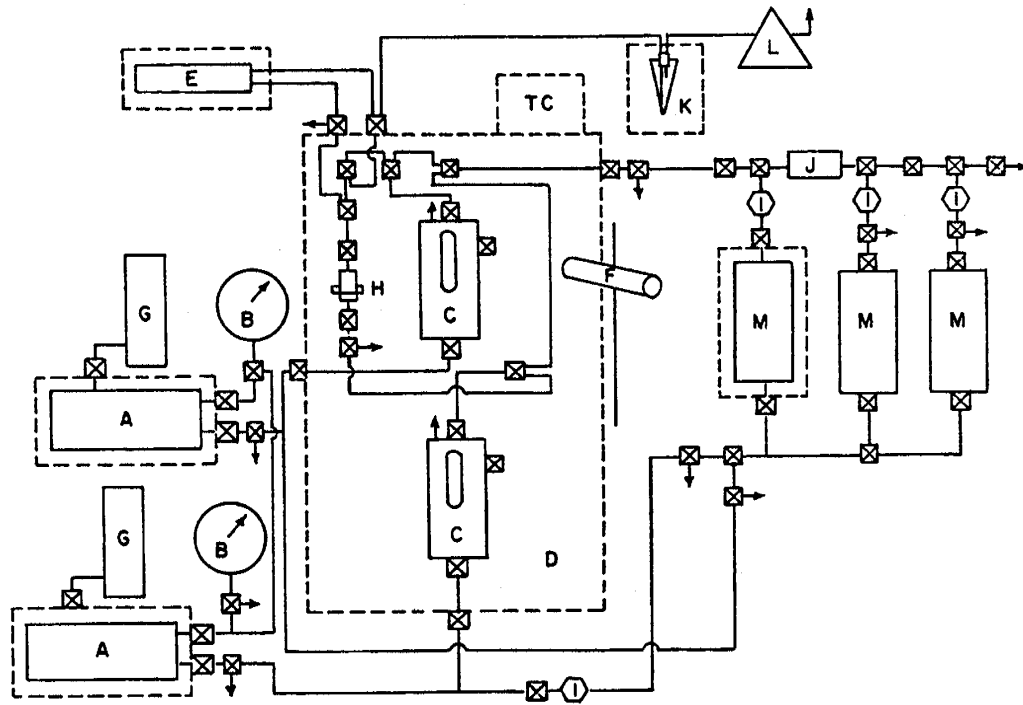


Figure 7. Transfer Vessel



- |                                      |                             |
|--------------------------------------|-----------------------------|
| A - Positive Displacement Pump       | G - Mercury Reservoir       |
| B - Pressure Gage                    | H - Sampling Yoke           |
| C - P-V-T Cell                       | I - Mercury Level Indicator |
| D - Air Bath                         | J - Line Filter             |
| E - Densitometer                     | K - Flash Separator         |
| F - Cathetometer                     | L - Wet Test Meter          |
| TC - Temperature Controller          | M - Storage Reservoirs      |
| → To Vent, Vacuum, or Compressed Gas |                             |

Figure 8. Schematic of Phase Behavior Equipment

cathetometer readings measured to 0.1 mm. The maximum working pressure of the PVT apparatus was 4000 psia. The overall performance of the PVT apparatus was checked versus the reported pressure-volume isotherm for the binary system n-decane-CO<sub>2</sub> at 160°F, and was found to agree within 1% of the data reported by Reamer and Sage (1963).

### Procedure

The PVT experiments were done for single- and multiple-contacts. Single-contact experiments for mixtures covering the entire CO<sub>2</sub> compositional range were performed at approximately 111°F and 141°F. These two temperatures permitted the investigation of both Type I and Type II phase behavior (Stalkup, 1983a). Also, these temperatures coincide with preexisting sandpack displacement data (Whitehead, et. al., 1981). In addition one CO<sub>2</sub>-BF oil mixture was examined at room temperature. All single-contact experiments employed the following procedure. The clean respective flow lines and cell were first evacuated using a vacuum pump. A vacuum of approximately 100 - 150 μm as measured by a McLeod vacuum gauge was obtained. The cell was then volumetrically charged with BF oil from the oil reservoir at known pressure and temperature. The flow lines were again cleaned using toluene and hexane and evacuated. Carbon dioxide was then volumetrically charged into the cell from the CO<sub>2</sub> reservoir at known pressure and temperature to make the desired total composition. The mole percents of CO<sub>2</sub> and BF oil were calculated using the appropriate molecular weight and density at the pressure and temperature of the charge. The air bath was turned on at least 12 hours before the start of a constant-composition, pressure traverse (run) to ensure temperature equilibrium in the PVT cell. A run was then performed as described below to a maximum pressure of about 3500 psia. The system was then allowed to settle overnight to let the mercury precipitate out of the oil-rich phase. All but approximately 50 cc of the mercury was withdrawn at about 1 cc/min from the cell into the pump the following day. The slow withdrawal rate minimized contamination of the manifold mercury with sample which would then be lost from the cell. Stable pressure and volume readings were taken after mercury withdrawal. This was done to keep track of the mercury balance in the cell. Additional CO<sub>2</sub> was then charged into the cell, thus making a new total composition in the cell. After three runs, the contents of the cell were removed to terminate the growing carry over error in the cell's mercury balance. The cell was cleaned with toluene and hexane and dried with compressed air or nitrogen. This entire process was repeated several times to complete the single-contact PVT experiments.

The following procedure was used for completing each run. A manifold compressibility check was done to account for pressure effects on the mercury outside the cell and to check for leaks in the flow lines. The bottom of the cell was opened and mercury was injected into the cell until the pressure increased by 50 to 70 psi. The indicated pump volume was then recorded. To obtain phase equilibrium in a reasonably short time, the bottom of the cell was closed, and the contents of the cell were thoroughly mixed by rocking the cell in a horizontal position. Rotating the cell to a horizontal position increases the surface area available for mass transfer and the rocking increases it even more by creating waves. The mercury in the cell also enhanced the mixing, so that phase equilibrium was obtained with 10 min of cell rocking. The system was then completely inverted and then turned right-side-up. The bottom of the cell was then opened so pressure measurements could be taken. Pressure, pump temperature, and cell temperature were recorded every 5 min. until a stable reading was obtained. The interface was then measured using the cathetometer. This procedure was repeated until the pressure was near

2000 psia, and then pressure increments of 500 psi were employed until a maximum pressure of approximately 3500 psia was obtained.

The multiple-contact experiments were done at approximately 112°F. This temperature was selected because available oil displacement results at this temperature did not show an atypical "S" appearance in the oil recovery versus pressure curve (Monger, 1984). The procedure was similar to the single-contacts, except that sample mixtures were created on a phase volume basis at a prescribed pressure and temperature instead of a mole CO<sub>2</sub> and BF oil basis. The forward and swept zone contacts were performed at approximately 2:1 volume mixture of the CO<sub>2</sub>-rich phase to the BF oil or the CO<sub>2</sub> to the oil-rich phase, respectively. A 2:1 volume mixture was chosen to reflect that the CO<sub>2</sub> or the CO<sub>2</sub>-rich phase is at least twice as mobile as the oil or oil-rich phase. The conditions at which the 2:1 volume mixtures were made were approximately 1800 psia and 111°F. Sandpack displacements (Monger and McMullan, 1983) and the minimum miscibility pressure correlations of Yelling and Metcalf (1980), and Holm and Josendal (1982) predicted that 1800 psia is at or above the minimum miscibility pressure of the oil at 112°F. Also, 1800 psia is approaching the upper limit of the high pressure/temperature compositional sampling equipment.

The multiple-contacts were started with an initial mixture of 94.6 mole% CO<sub>2</sub> and 5.4 mole% BF oil because this mixture was in the two phase region of the P-X diagram. In the forward contacts, the CO<sub>2</sub>-rich phase was sampled and metered into an evacuated cell at constant pressure. After the CO<sub>2</sub>-rich phase was charged into the evacuated cell, the oil-rich phase was sampled. The CO<sub>2</sub>-rich phase was then contacted with fresh BF oil. A pressure traverse was conducted as described above to a maximum pressure of about 3500 psia. The system was then allowed to sit at high pressure and run temperature for at least 12 hours to let the mercury settle out of the oil-rich phase. By withdrawing mercury from the cell at 0.5 to 1.0 cc/min, the pressure was lowered to approximately 1800 psia for sampling and charging an evacuated cell with the CO<sub>2</sub>-rich phase for the second forward contact. Three forward contacts were done in this manner. In the swept zone contacts, the CO<sub>2</sub>-rich phase of the initial mixture was sampled and removed at constant pressure and the oil-rich phase was trapped in the cell. The mercury was then removed from the cell at about 1 cc/min. until approximately 50 cc remained in the cell. The oil-rich phase was then contacted with pure CO<sub>2</sub> and a run was conducted as described above to a maximum pressure of approximately 3500 psia. The system was allowed to sit at high pressure and run temperature for at least 12 hours so the mercury could settle out of the oil-rich phase. Following sampling and removal of the CO<sub>2</sub>-rich phase at constant pressure, the mercury was withdrawn from the cell leaving approximately 50 cc in the cell. The cell was then charged with pure CO<sub>2</sub> for the second swept zone contact. Two swept zone contacts were completed in this manner.

### Sampling

Sampling consisted of measuring the density and composition of each phase. High pressure and low pressure sampling were performed for all of the multiple-contact PVT experiments.

### High Pressure Equipment

High pressure density measurements were made with a Mettler - Paar DMA 45 digital density meter with a DMA 512 high pressure/temperature remote cell. The DMA 512 cell was manifolded to the PVT cells and the temperature on the DMA 512 cell was maintained by a second Neslab Exacal 100 glycol bath circulator with an Endocal 150 flow through cooler. The high pressure compositional sampling was performed using a modified Precision Sampling high pressure/temperature sampling yoke and syringe (Figures 9 and 10). The yoke was inside the air bath and connected to both PVT cells (Figure 8). The plumbing was arranged such that the phases could flow through the DMA 512 cell and the sampling yoke, thus minimizing the amount of phase lost by sampling multiple-contact mixtures.

### High Pressure Procedure

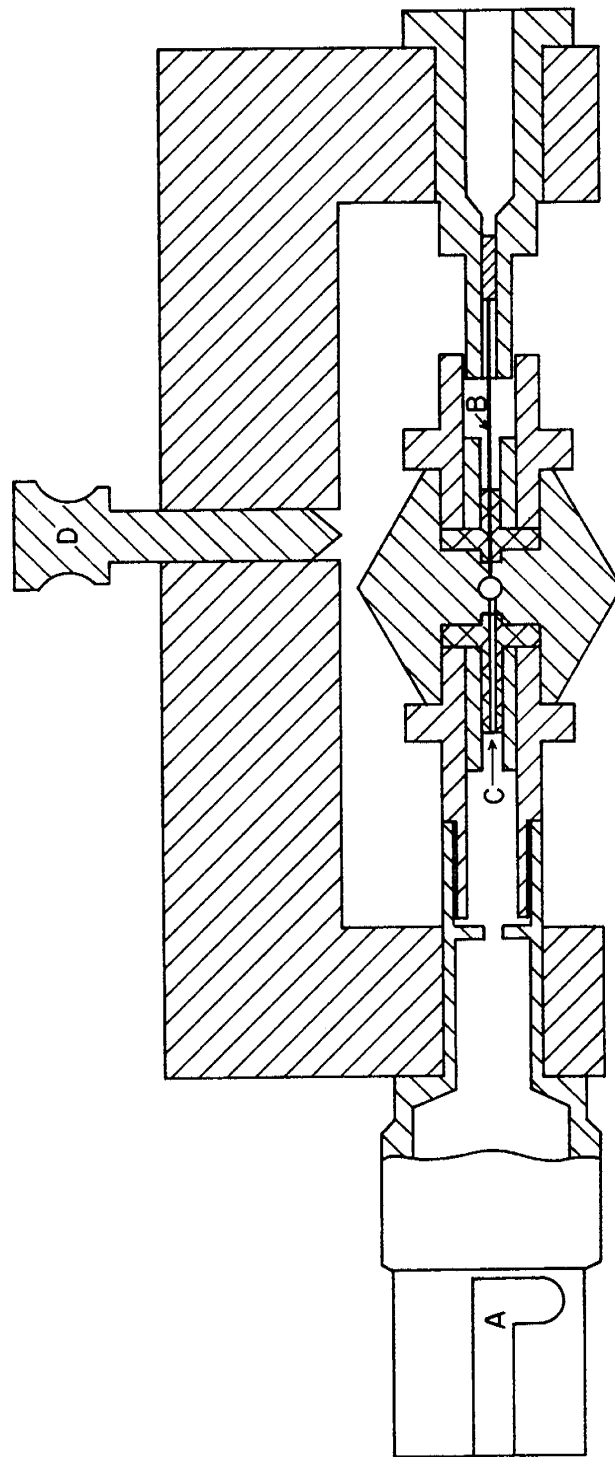
Before the phases were sampled and/or metered into an evacuated cell, the flow lines that contained the DMA 512 cell and the sampling yoke were evacuated. The DMA 512 cell and the sampling yoke were then filled with the phase. Approximately 2 cc of the phase were bled out of the flow line downstream of the sampling yoke to ensure that a representative sample of the phase was in each apparatus.

The following procedure was used to obtain high pressure/temperature compositional samples. The syringe was inserted into the yoke and locked in place. The yoke was then opened by releasing the set screw and pushing back on it causing the yoke needle to unseat from the forward packing. The syringe was then opened by unlocking and pulling back on the barrel assembly unseating the needle from the needle packing. The sample flowed into the syringe barrel pushing the plunger back. To ensure that a good sample was taken, the plunger was pushed in several times and then allowed to remain back for several seconds. The syringe and yoke were then closed. The sample was visually observed to ensure single phase quality and then injected into a Hewlett Packard 5880 gas chromatograph. Several samples of each phase were analyzed to increase the quality of the data. The working life of the syringe and the yoke was limited. The yoke required rebuilding after about every fourth sampling session, while the syringe required rebuilding after and sometimes during each sampling session. A sampling session consisted of sampling both phases that resulted from a run.

The gas chromatograph took approximately 90 min to completely analyze a sample. Cell sampling conditions were reestablished during this time with pressure adjustments every 10 - 15 min. The frequency readout of the density meter and the temperature of the DMA 512 cell were also recorded. The frequency, pressure, and temperature were used to calculate the high pressure/temperature density of the phase.

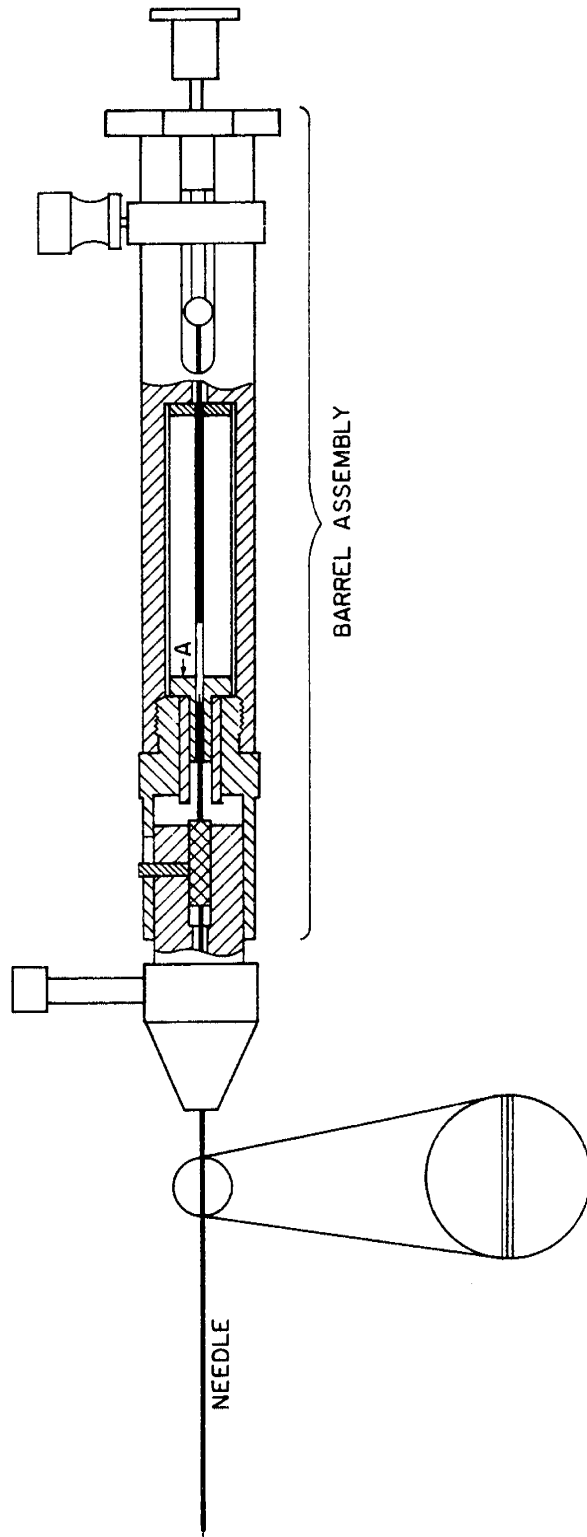
### Low Pressure Equipment

Low pressure sampling of the phases was performed using a low pressure separator system constructed for this study (Figure 11). Gas resulting from a phase flash was measured to  $\pm 0.01$  liters with a GCA/Precision Scientific wet test meter calibrated within the manufacture's specifications. The accuracy of the wet test meter was within  $\pm 0.5\%$  of the total volume. A metering valve was used to regulate the flow rate of the phase. The liquid was measured to  $\pm 0.5$  cc with a graduated-conical tube. The liquid was then transferred into a vial with septum cap and



- A- SYRINGE LOCK
- B- YOKE NEEDLE
- C- FORWARD PACKING
- D- SET SCREW

Figure 9. High Pressure/Temperature Sampling Yoke



A - NEEDLE PACKING

Figure 10. High Pressure/Temperature Sampling Syringe

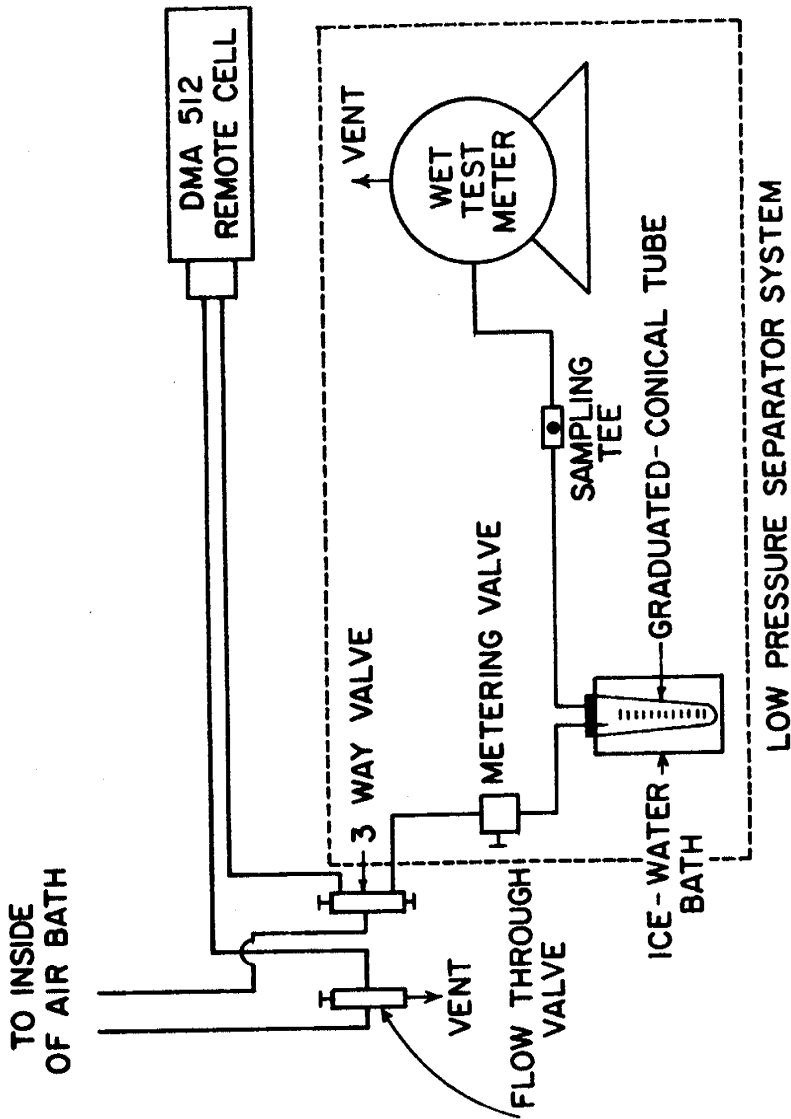


Figure 11. Schematic of Low Pressure Sampling System

placed in a refrigerator for later compositional analysis. The gas was sampled during the flash process using a low pressure tee and a 10 cc, low pressure Precision Sampling Pressure-Lok syringe. The low pressure sampling tee was composed of a 1/4 in. stainless steel Swage-Lock tee with a HP 5880-8754 septum on the perpendicular section of the tee. Low pressure density measurements were conducted using a 0.25 cc Precision Sampling Pressure-Lok syringe, a sample vial with a septum cap, and a Mettler Analytical balance.

#### Low Pressure Procedure

The following procedure was used to obtain low pressure samples. A stable pressure reading was obtained before starting the controlled flash. The metering valve was then opened letting the phase flash into the graduated-conical tube. After about 0.2 liters of gas had passed through the wet test meter, approximately 10 cc of the low pressure gas was collected. Approximately 5 cc were pushed out of the syringe to ensure that a good sample would be shot into the gas chromatograph. The rest of the low pressure gas sample was injected into the gas chromatograph at a fast rate so that the concentration of the gas molecules would be great enough to give reliable results. Two low pressure gas samples were usually obtained during a flash. The pressure was stabilized at the end of the controlled flash so that the amount of phase flashed could be calculated.

All low pressure liquid compositional sampling was done using a 10 microliter Hamilton syringe. The sample was removed from the refrigerator and warmed to room conditions. A two microliter sample was then injected into the gas chromatograph.

The following procedure was used in measuring the low pressure density of the liquid samples obtained from flashing the phases. The sample vial with a septum cap was weighed. The syringe was then filled with 0.25 cc of sample and weighed. The sample was then injected into the sample vial, and the empty syringe was weighed. This was usually repeated four times until the desired volume was obtained in the sample vial. The sample vial was then weighed, and the density was calculated from the recorded volumes and weights. The results of this method agreed well with those obtained from the DMA 45 density meter. The advantage of this method was that none of the sample was lost.

### Compositional Analysis

#### Chromatographic Analysis

The chromatographic analysis was done with a Hewlett-Packard 5880 gas chromatograph equipped with two thermal conductivity detectors (TCD). The cryogenic gas used by the 5880 was liquefied carbon dioxide. The columns used in the gas chromatograph consisted of 9 ft. long, 1/4 in. outside diameter stainless steel high performance columns packed with 80/100 mesh, Chromosorb-w beads coated with 10% OV-101. The columns were conditioned by heating them from room temperature to 350°C at a rate of 50°C/half-hour and then cooling them to room temperature at the same rate with the carrier gas off. Once at room temperature, carrier gas flow was resumed and the same heating and cooling procedure was repeated. The columns were disconnected from the detectors at all times during their conditioning. Once the conditioning was finished, the columns were connected to the detectors, and the carrier gas flow rate through each column was adjusted to 30 cc/min. The carrier

gas used was 99.995% pure Helium equipped with a moisture trap.

### Time/Temperature Program

Several time/temperature programs were used during the course of this study in an effort to breakout the methane, carbon dioxide, and ethane fractions. The time/temperature program, which gave the best results without operating outside the instruments cryogenic limits, is presented below.

Initial Value = -45°C  
Initial Time = 1.00 min.

#### Level 1

Program Rate = 0.25°C/min.  
Final Value = -43°C  
Final Time = 0.00 min.

#### Level 2

Program Rate = 10.00°C/min.  
Final Value = 350°C  
Final Time = 16.00 min.

Post Value = 350°C  
Post Time = 10.00 min.

A standard Matheson gas sample, which contained C<sub>1</sub> - C<sub>5</sub> and CO<sub>2</sub>, was injected into the gas chromatograph to obtain the retention times of the light components. Two microliters of Hewlett-Packard Boiling Point Calibration Sample #1 (5080-8716) was injected into the gas chromatograph to obtain the retention times of the C<sub>5</sub>-C<sub>36</sub> components. These retention times were used to analyze the gas chromatograph results. A new set of retention times were obtained every time new columns were installed or when the time/temperature program was changed. Also, the retention times were checked periodically to ensure that the gas chromatograph was operating properly.

### Hydrocarbon Type Analysis

The aromaticities of the liquid samples acquired from flashing the phases were obtained using natural abundance carbon-13 nuclear magnetic resonance spectrometry (<sup>13</sup>C NMR), as described in Method 3 of Shoolery and Budde (1976). If time did not allow delays between pulses, Method 2 was employed and a response factor determined from the results of a control sample was used to correct for reduced sensitivity. All <sup>13</sup>C NMR measurements were performed by the Chemistry Department at LSU. The procedure employed in making a sample for <sup>13</sup>C NMR differed somewhat from that described by Shoolery and Budde (1976) and is described below. Approximately 1.0 cc of the sample was mixed with 25 mg of chromium acetylacetonate (CrAcAc) and then diluted with 0.4 cc of deuteriochloroform solvent. If 1.0 cc of the sample could not be sacrificed, the CrAcAc and solvent were proportioned to the amount of sample available.

## RESULTS AND DISCUSSION

### BF Oil and Carbon Dioxide

The BF oil was modified by performing a flash vaporization of the reconstituted reservoir (RR) oil as described in the previous section. Several physical properties of the BF oil were measured and are shown in Table 10. The physical properties consisted of densities measured at different pressures and temperatures, the gas-liquid-ratio (GLR) measured above the bubble point, and the shrinkage factor measured at 1000 psia and 72°F. The method used to calculate these physical properties is described in a later section. Table 10 also shows the molecular weight and the aromatic carbon content of the BF oil.

Table 11 compares the composition of the RR oil (Whitehead, et. al., 1981) to that of the BF oil calculated from high pressure/ temperature samples and from recombining the BF oil flash liberation results. The compositional results in Table 11 show that methane was the main component lost in the modification of the RR oil. Also, the close agreement between the high pressure/temperature (HP/T) results and the recombination of BF oil flash liberation (RF) results is well within experimental error.

Through the course of this study the RR oil had to be flashed several times to obtain a sufficient volume of BF oil. Table 12 compares the compositional results obtained from two different flash vaporizations. The results illustrate that good reproducibility was obtained. The differences in component mole percents are largely due to inherent experimental errors of the gas chromatograph. The method used to analyze gas chromatographic measurements for the BF oil is presented in a later section.

The carbon dioxide used in the PVT experiments was supplied by LSU Plant Stores. Gas chromatographic analysis of the CO<sub>2</sub> gas showed that it was composed of 0.4 mole percent methane and 99.6 mole percent carbon dioxide. This methane content was neglected when calculating the amount of CO<sub>2</sub> metered into the PVT cell.

### Single-Contact Experiments

#### Analysis of Data

A modified Ruska computer program was used to calculate the total sample volume, the oil-rich phase volume, and the CO<sub>2</sub>-rich phase volume. A listing of the program can be found in the Appendix. The program required the following information:

1. PVT system calibration constants,
2. Initial cell pressure, cell temperature, and known volume of mercury in the cell,

Table 10: BF Oil Physical Properties

Temperature (°F) Pressure (psia)	100 Density (g/cc)	150 Density (g/cc)
2500	0.8414	0.8291
1800	0.8380	0.8259
1200	0.8351	0.8234
500	0.8318	0.8176

$$\text{GLR} = 29 \frac{\text{CF}}{\text{BBL}}$$

$$\text{Shrinkage Factor} = 0.995 \frac{\text{BBL}}{\text{RB}} @ 1000 \text{ psia} \ \& \ 72^\circ\text{F}$$

$$\text{Molecular Weight} = 186.4 \frac{\text{g}}{\text{g-mole}}$$

$$\text{Aromatic Carbon Content} = 11.9\%$$

Table 11: Oil Composition Comparison

Component	RR Oil	BF Oil (HP/T)	
		Mole %	BF Oil (RF)
C <sub>1</sub>	11.4	2.760	2.275
C <sub>2</sub>	4.1	4.150	3.007
C <sub>3</sub>	2.1	3.974	3.784
C <sub>4</sub>	3.5	7.821	7.919
C <sub>5</sub>	1.8	4.315	5.004
C <sub>6</sub>	2.8	5.322	6.961
C <sub>7</sub>	6.1	6.333	7.027
C <sub>8</sub>	6.7	8.207	8.038
C <sub>9</sub> , C <sub>10</sub>	6.9	11.618	10.695
C <sub>11</sub> , C <sub>12</sub>	7.1	8.697	8.779
C <sub>13</sub> , C <sub>14</sub>	8.6	6.790	7.279
C <sub>15</sub> , C <sub>16</sub>	9.8	5.068	5.507
C <sub>17</sub> , C <sub>18</sub>	9.7	4.387	4.546
C <sub>19</sub> , C <sub>20</sub> , C <sub>21</sub>	7.8	3.822	4.023
C <sub>22</sub> , C <sub>23</sub> , C <sub>24</sub> , C <sub>25</sub>	6.2	3.596	3.394
C <sub>26</sub> , C <sub>27</sub> , C <sub>28</sub>	3.0	1.730	1.556
C <sub>29</sub> , C <sub>30</sub> , C <sub>31</sub>	0.7	1.328	0.994
C <sub>32</sub>	.01	0.361	0.225
C <sub>33</sub>		0.370	0.170
C <sub>34</sub>		0.282	0.116
C <sub>35</sub>		0.297	0.079
C <sub>36+</sub>		8.773	8.621

HP/T - Results obtained from high pressure/temperature sample  
 RF - Results obtained from recombining the flash liberation data

Table 12: Comparison of Reconstituted Reservoir Oil Flashes

Component	Mole %	
	Flash 1	Flash 2
C <sub>1</sub>	2.687	3.099
C <sub>2</sub>	5.219	3.721
C <sub>3</sub>	4.659	3.444
C <sub>4</sub>	8.401	6.254
C <sub>5</sub>	4.324	4.673
C <sub>6</sub>	4.353	5.654
C <sub>7</sub>	5.795	7.076
C <sub>8</sub>	7.503	7.665
C <sub>9</sub>	5.622	5.560
C <sub>10</sub>	5.509	5.231
C <sub>11</sub>	4.954	4.497
C <sub>12</sub>	4.186	4.343
C <sub>13</sub>	3.886	3.826
C <sub>14</sub>	3.174	3.309
C <sub>15</sub>	2.827	2.786
C <sub>16</sub>	2.305	2.470
C <sub>17</sub>	2.451	2.520
C <sub>18</sub>	2.254	2.131
C <sub>19</sub>	1.085	1.305
C <sub>20</sub>	1.284	1.367
C <sub>21</sub>	1.112	1.206
C <sub>22</sub>	0.995	1.099
C <sub>23</sub>	1.147	1.323
C <sub>24</sub>	0.716	0.826
C <sub>25</sub>	0.624	0.584
C <sub>26</sub>	0.586	0.680
C <sub>27</sub>	0.529	0.553
C <sub>28</sub>	0.665	0.613
C <sub>29</sub>	0.490	0.530
C <sub>30</sub>	0.425	0.470
C <sub>31</sub>	0.392	0.465
C <sub>32</sub>	0.361	0.424
C <sub>33</sub>	0.318	0.411
C <sub>34</sub>	0.286	0.388
C <sub>35</sub>	0.272	0.410
C <sub>36</sub> <sup>+</sup>	8.603	9.093
Molecular Weight (g/g-mole)	184.3	192.1

3. Indicated pump volumes from a manifold compressibility check,
4. Run title,
5. Average pump and cell temperatures,
6. Cathetometer readings (at cell position upright or inverted), cell pressure, indicated pump displacement, and pump code (1=manifold compressibility, 2=opening the cell for the first time, 3=recording a run, and 4=changing the cell or pump temperature).

Briefly, the program calculated volumes as a function of pressure and temperature. The cell capacity was determined from the calibration constants. A material balance on the mercury was run to generate the volume of mercury in the cell. Total sample volume was computed as the difference between the cell capacity and the volume of mercury in the cell. Phase volumes were determined by converting cathetometer readings to cell volumes and subtracting the contribution(s) from the mercury plus any denser phase in the cell.

Graphs of total sample volume versus pressure and percent phase volumes versus pressure were prepared to determine simple bubble-point and apparent-critical pressures. Simple bubble-point pressures identify the phase boundary between the liquid-vapor and single liquid phase regions. The apparent-critical pressure is here defined as the pressure at which the total sample compressibility changes from the compressibility of a liquid-gas system to a liquid-liquid system. The apparent-critical pressure does not distinguish between distinct phase regions, but rather indicates changes in the chemical and physical properties of the CO<sub>2</sub>-rich phase which are believed to be related to oil displacement efficiency (Holm and Josendal, 1982). Graphs and tabulated values of volumetric data can be found in the Appendix. The simple bubble-point pressure was determined by drawing a smooth curve through the percent phase volume points and reading the pressure at 100% oil-rich phase volume and 0% CO<sub>2</sub>-rich phase volume from the extrapolated curves. The apparent-critical pressure was determined by drawing straight lines through the percent volume data points in the liquid-gas compressibility region and those in the liquid-liquid compressibility region. The apparent-critical pressure was taken as the pressure at which the lines of the oil-rich phase or the lines of the CO<sub>2</sub>-rich phase intersected. The pressure was then checked against the total sample volume versus pressure curve to ensure that the selected value was in the changing slope region of the curve. Attempts were made at calculating the simple bubble-point and apparent-critical pressures using various exponential curve fits to the total sample volume data. Good agreement between the graphical and calculated values was obtained for bubble point, but no agreement was obtained for apparent-critical pressures. Bubble-point and apparent-critical pressures were not confirmed by direct experimental observations because the upper 6 cc of the PVT cell are not visible through the cell windows. Indirect methods of determining bubble point pressure are common in the industry.

The swelling of the oil by CO<sub>2</sub> was also investigated. A dimensionless swelling index was derived, so results from different runs could be compared. The swelling index is similar to the formation volume factor and is calculated as

$$\text{swelling index} = \frac{\text{volume of oil-rich phase}}{\text{volume of BF oil}} @ P, T.$$

The oil-rich phase is analogous to CO<sub>2</sub>-saturated oil, while the BF oil is analogous to CO<sub>2</sub>-free oil. The swelling index calculation given above differs from that given by Holm and Josendal (1974). They calculate the swelling index as the volume of CO<sub>2</sub> saturated oil divided by the volume of stock tank oil charged into the cell. The swelling index calculation presented in this study is more representative of the volume effects of CO<sub>2</sub> on the oil because it takes into account pressure and temperature effects on the CO<sub>2</sub> free oil. The oil-rich phase volume at run pressure and temperature was calculated by the PVT program. The BF oil volume at the same pressure and temperature was calculated using the compressibility of the BF oil at the run temperature and the volume of BF oil that was charged into the cell. Compressibility functions for BF oil at the average run temperatures of 111.0°F and 141.4°F were calculated from second degree polynomial least squares curve fits of the total sample volume data determined from 100% BF oil runs at 111°F and 143°F. Swelling indexes were plotted against pressure and smooth curves were drawn through the data points. The curves were forced to intersect at the bubble-point pressure to follow the physical constraint that the point of maximum swelling should occur at the point where the first bubble of free gas appears as the pressure of the system is lowered.

### Results and Discussion of the Single-Contacts

Single-contact experiments were conducted at approximately 141.4°F and 111.0°F. Figures 12 and 13 show the phase envelopes generated at these average temperatures. For both temperatures, simple bubble-point behavior was observed for cell compositions less than 70 mole percent CO<sub>2</sub>. Examples of the pressure-volume behavior recorded for these moderate CO<sub>2</sub> concentration mixtures are included in the Appendix. Typically, a sharp break occurs in the pressure-volume relationship at the bubble point. At higher pressures, a single dark liquid phase was present in the PVT cell. At lower pressures, a colorless vapor phase appeared on top of the dark liquid phase. At cell compositions greater than 70 mole percent CO<sub>2</sub>, the system remained two phase with a change in the overall sample compressibility. The total sample compressibility changed from a gas-liquid type to a liquid-liquid type at pressures ranging between 2100 psia and 1900 psia for the 141.4°F runs and between 1440 psia and 1325 psia for the 111.0°F runs as can be seen in Figures 12 and 13. Visual observations during the runs at both temperatures indicated that a second liquid phase develops during mercury injection into the cell to increase the pressure, but upon equilibration the second liquid phase disappears. The formation of a black precipitate plus a small amount of a colorless granular precipitate was also noted. The colorless granular precipitate may have been cell window effects. Both of the above observations were noted in conjunction with the CO<sub>2</sub>-rich phase assuming a very dense appearance. The dense CO<sub>2</sub>-rich phase resembled fog and could not be distinguished as a liquid or gas, thus it was termed a fluid (F). As can be seen in the P-X diagrams (Figures 12 and 13), no liquid-liquid-vapor (L-L-V) region and no liquid-fluid critical point were observed. To determine if the CO<sub>2</sub>-BF oil system was capable of creating a three phase L-L-V region, a run of 89.3 mole percent CO<sub>2</sub> composition was performed at 79.8°F. The total sample volume versus pressure and percent phase volumes versus pressure graphs are shown in Figure 14. At pressures less than about 873 psia, a dark oil-rich liquid phase was observed in equilibrium with a colorless vapor phase. Above this pressure, and additional straw-colored CO<sub>2</sub>-rich liquid phase formed. The three phase L-L-V region was present over a small pressure range with the vapor phase vanishing at about 950 psia. The oil-rich and CO<sub>2</sub>-rich liquid phases persisted to the maximum pressure investigated. The second liquid phase was also observed at room temperature for a 94.6% CO<sub>2</sub> - 5.4% BF oil mixture, but disappeared at approximately 105°F

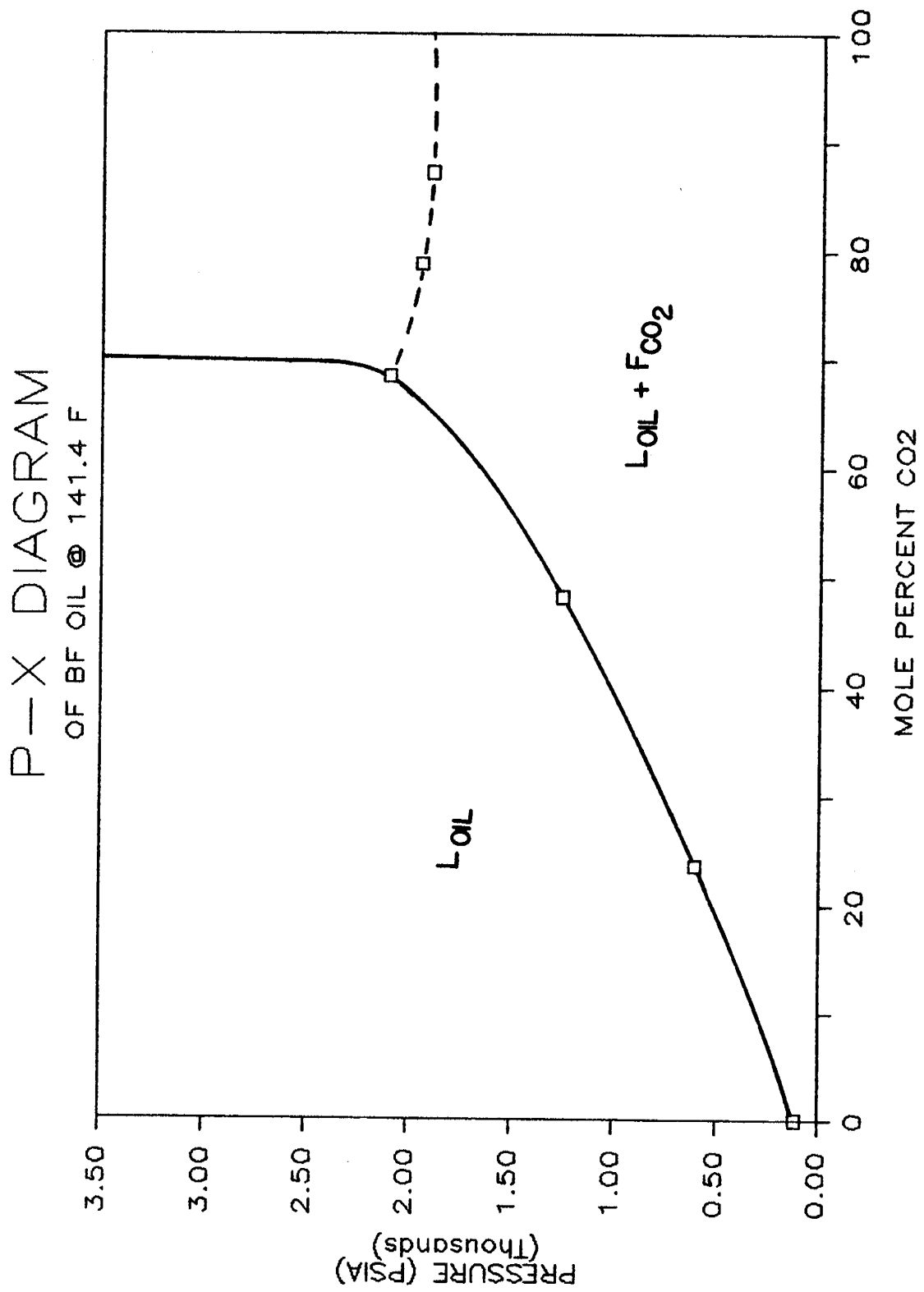


Figure 12.

P-X DIAGRAM  
BROOKHAVEN "FLASHED" AT 111°F

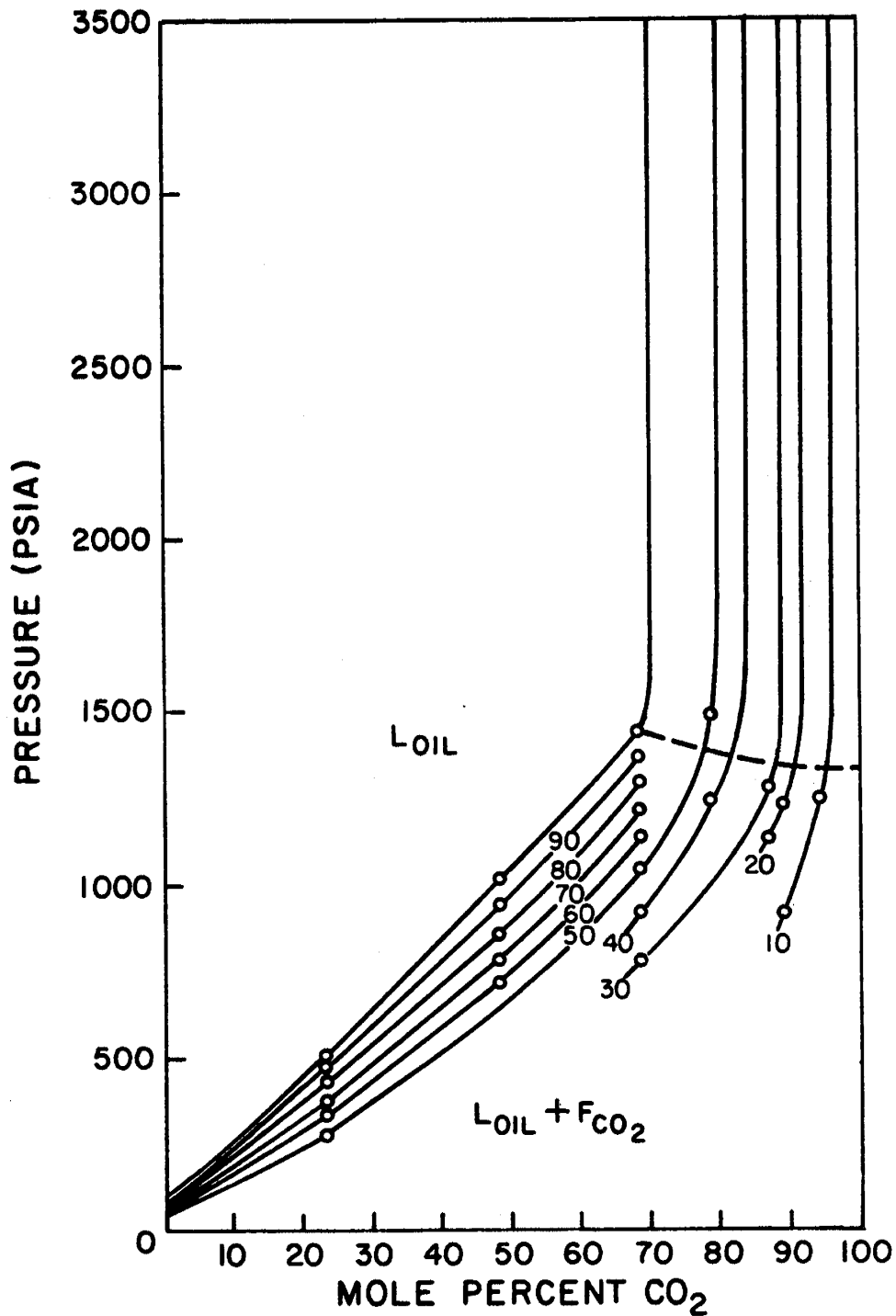


Figure 13.

# 89.3% CO<sub>2</sub> - 10.7% BF 79.8F

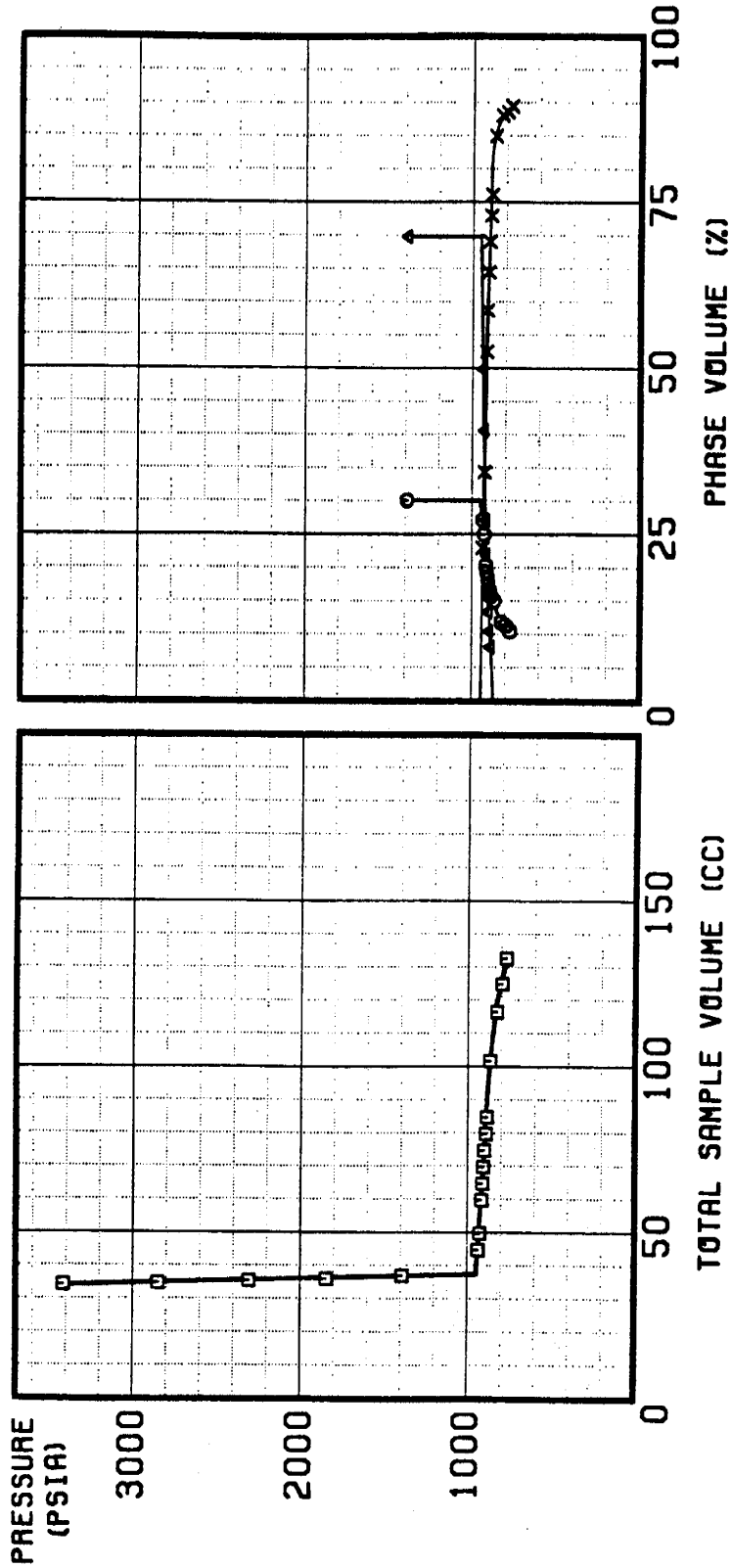


Figure 14. Pressure-Volume Isotherms (circles, oil-rich liquid phase; triangles, CO<sub>2</sub>-rich liquid phase; x's, vapor phase)

as the cell temperature was elevated to 111°F for a subsequent run. The above observations indicate that at run temperatures below approximately 105°F CO<sub>2</sub>-BF oil mixtures exhibit Type II phase behavior while at run temperatures above approximately 105°F Type I phase behavior is observed (Stalkup, 1983a).

The swelling index graphs for the 141.4°F runs appear in Figures 15 - 19. These plots illustrate that for cell compositions less than 70 mole percent CO<sub>2</sub> the oil was swollen to a maximum value at the bubble point. Slight decreases in the swelling index at higher pressures reflect the fact that CO<sub>2</sub> saturated BF oil is more compressible than the BF oil. For cell compositions greater than 70 mole percent CO<sub>2</sub>, the oil swells to a maximum value and then hydrocarbon extraction into the CO<sub>2</sub>-rich phase causes the swelling index to decrease at a much faster rate than expected from compressibility differences. Although, the pressures at which maximum swelling occurs for high CO<sub>2</sub> concentration mixtures do not numerically match the apparent critical pressures shown on the phase envelope (Figure 12), qualitative agreement is seen. Figure 20 compares the maximum swelling versus pressure for the 141.4° F runs. The curve shows that as the mole percent CO<sub>2</sub> increases, the maximum swelling pressure and swelling value increase until the cell composition reaches 68.5% CO<sub>2</sub>. A rapid decrease then occurs for the maximum swelling pressure and swelling value as the cell composition increases to 78.8% CO<sub>2</sub>. As the CO<sub>2</sub> concentration further increases, the maximum swelling value decreases, but the maximum swelling pressure remains approximately constant. The apparent-critical pressure is also approximately constant with increases in CO<sub>2</sub> concentration (Figure 12).

The swelling index graphs for the 111.0°F runs are presented in figures 21 - 27. The same trends are seen in these graphs as were discussed for the 141.4°F graphs. Figure 28 shows the maximum swelling versus pressure for the different CO<sub>2</sub> concentrations investigated at 111.0°F. The curve shows that the maximum swelling pressure and swelling value increase until the cell composition reaches 68.5% CO<sub>2</sub>. A decrease again occurs for the maximum swelling pressure and swelling value as the cell composition increases to 78.8% CO<sub>2</sub>. With further increases in the mole percent of CO<sub>2</sub>, the maximum swelling value decreases while the maximum swelling pressure changes only slightly. Similar qualitative agreement is seen between the apparent critical pressures (Figure 13) and the maximum swelling pressures for the 111.0°F runs as was observed for the 141.4°F runs within experimental error.

The reason the maximum swelling value and the pressure of maximum swelling start to decline after the CO<sub>2</sub> concentration exceeds 68.5% is that the CO<sub>2</sub> concentration is great enough for the vaporization process to become significant. For increasing CO<sub>2</sub> concentrations greater than 68.5%, the oil is swollen less and more hydrocarbon is extracted into the CO<sub>2</sub>-rich phase. This can be seen by comparing the swelling index graphs for each run temperature. Figure 29 is a plot of CO<sub>2</sub> density versus pressure for the run temperatures. The density of CO<sub>2</sub> at the maximum swelling pressures for CO<sub>2</sub> concentrations greater than 68.5% is approximately 0.35 g/cc for the 141.4°F runs and 0.32 g/cc for the 111.0°F runs. These density values are in agreement with the reported CO<sub>2</sub> density range of 0.25 to 0.35 g/cc required for the start of substantial hydrocarbon extraction (Holm and Josendal, 1982). Holm and Josendal (1982) state that hydrocarbon extraction increases as the pressure increases because the CO<sub>2</sub> solvency (density) also increases. This is reflected in the high CO<sub>2</sub> concentration results at both run temperatures. The maximum swelling value for each composition is approximately the same for both temperatures except at 68.5% CO<sub>2</sub>, where the maximum swelling value at

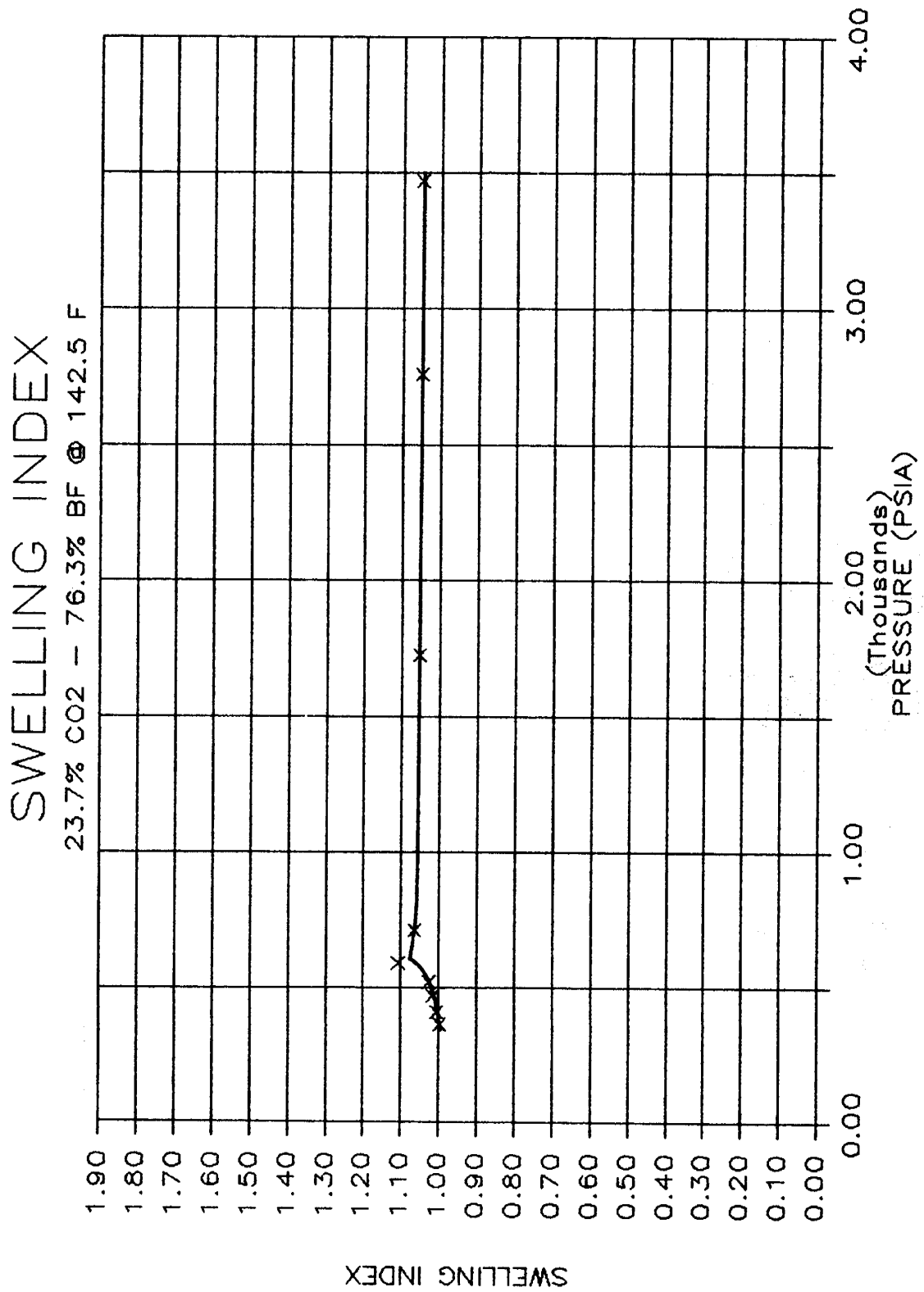


Figure 15.

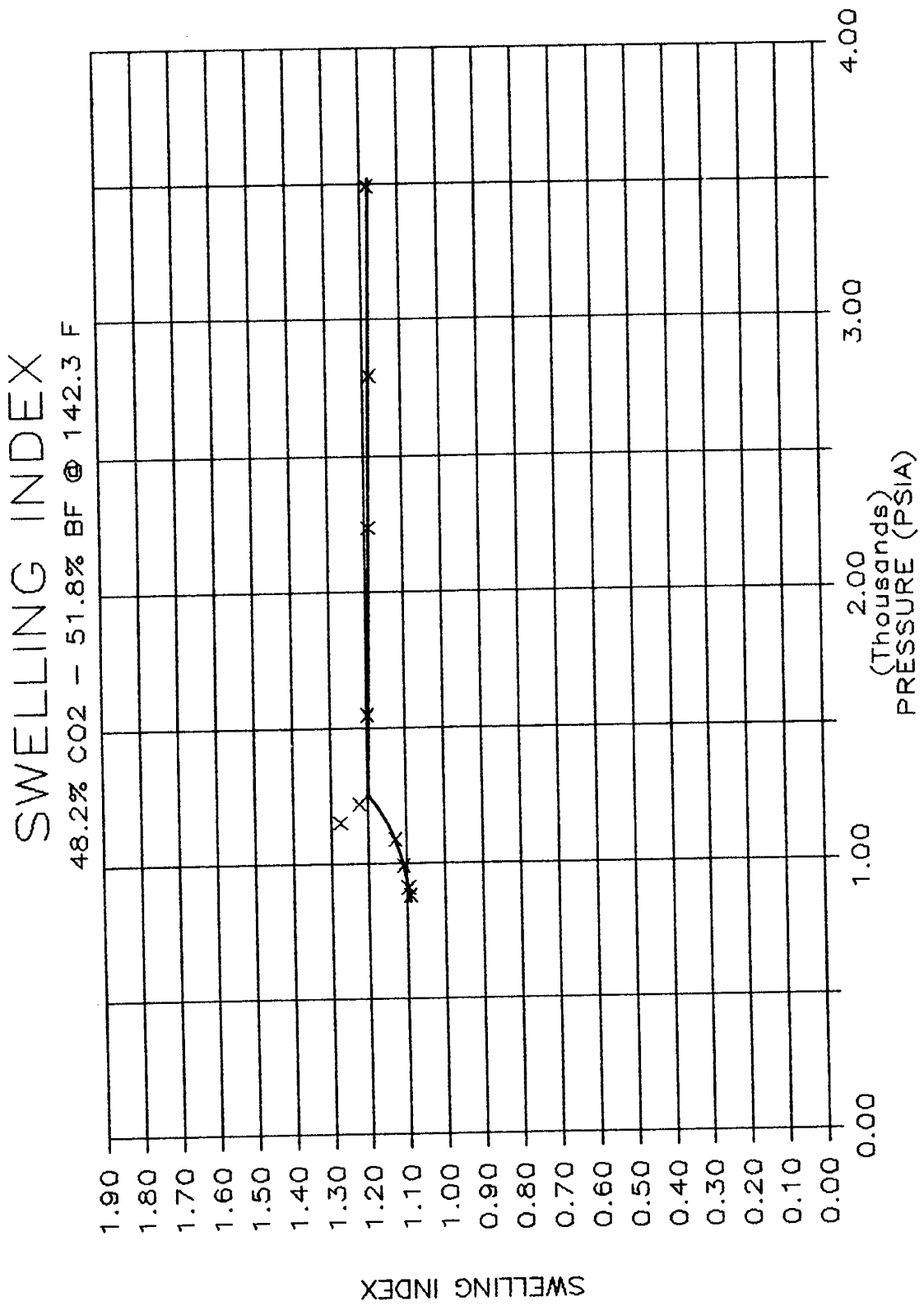


Figure 16.

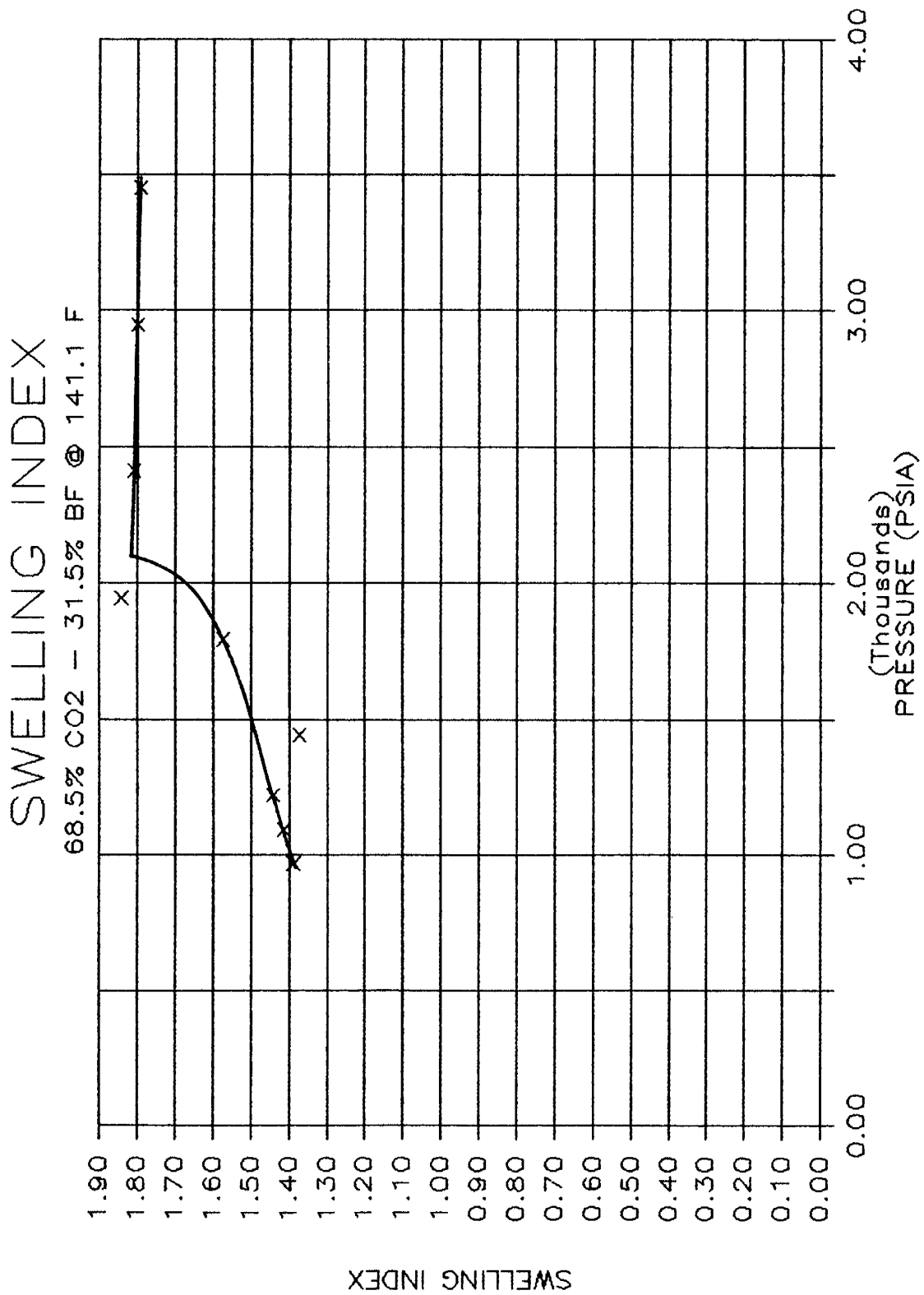


Figure 17.

SWELLING INDEX  
78.8% CO<sub>2</sub> - 21.2% BF @ 140.0 F

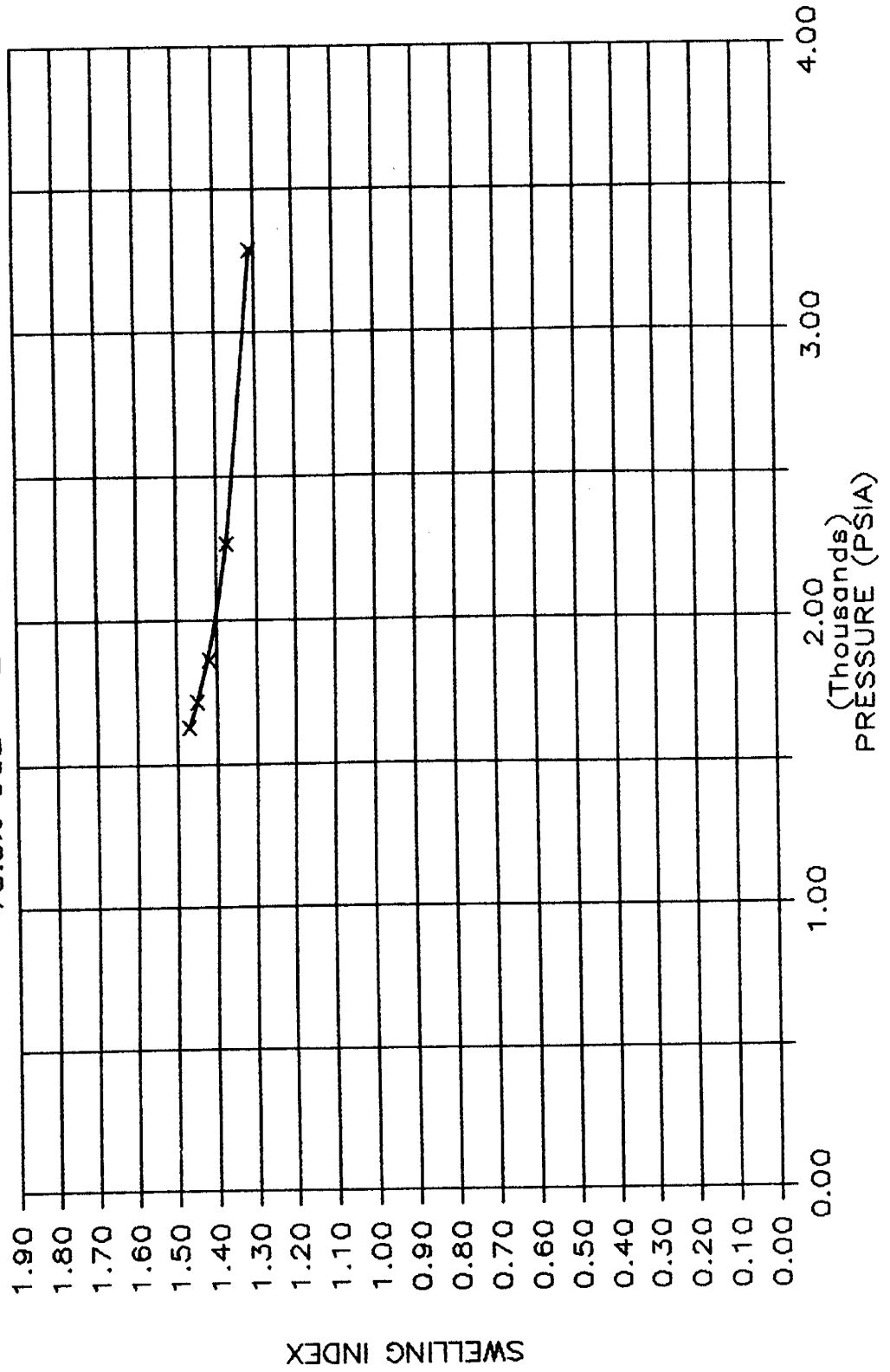


Figure 18.

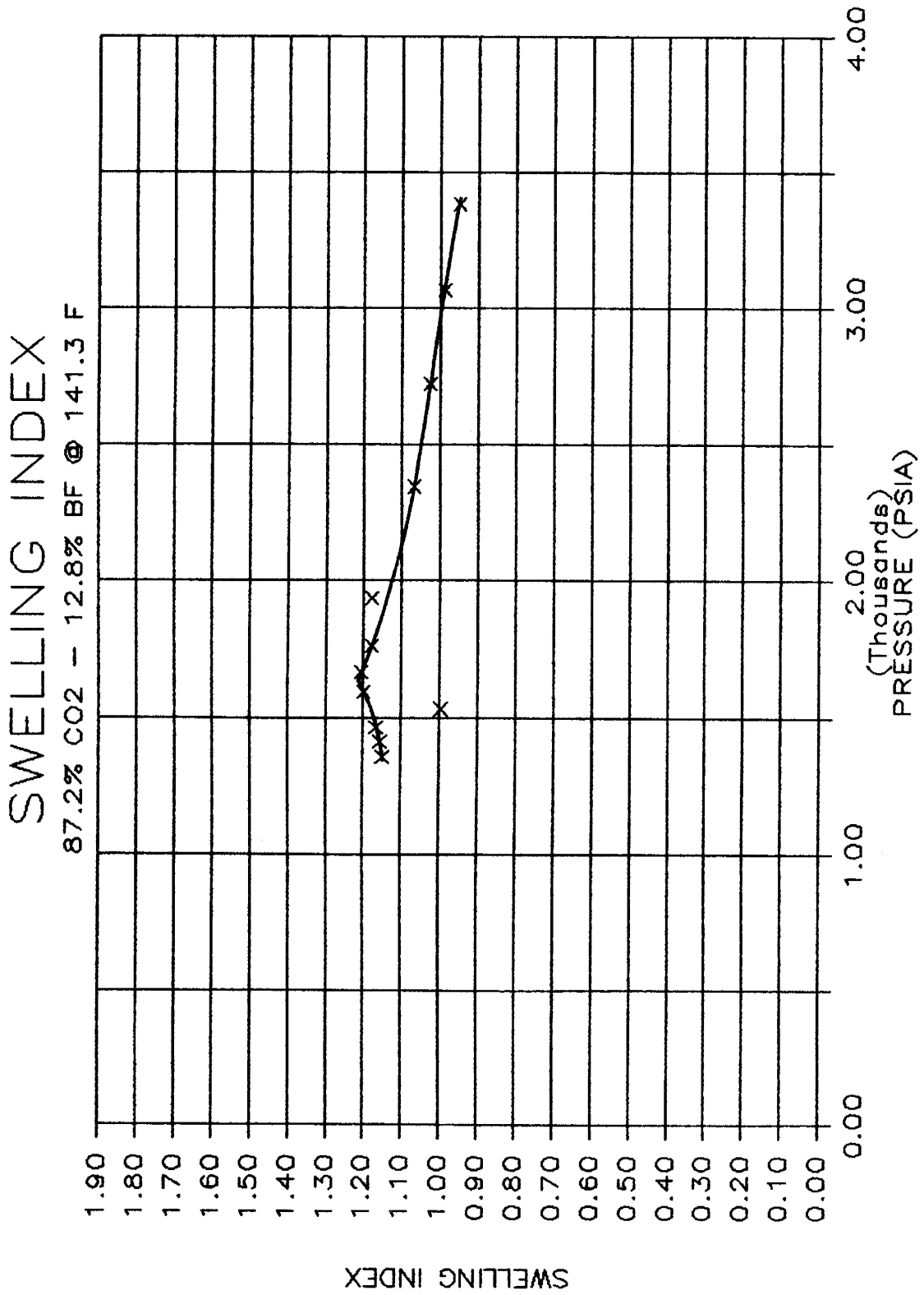


Figure 19.

MAXIMUM SWELLING VS PRESSURE  
 FOR THE SINGLE-CONTACTS @ 141.4 F

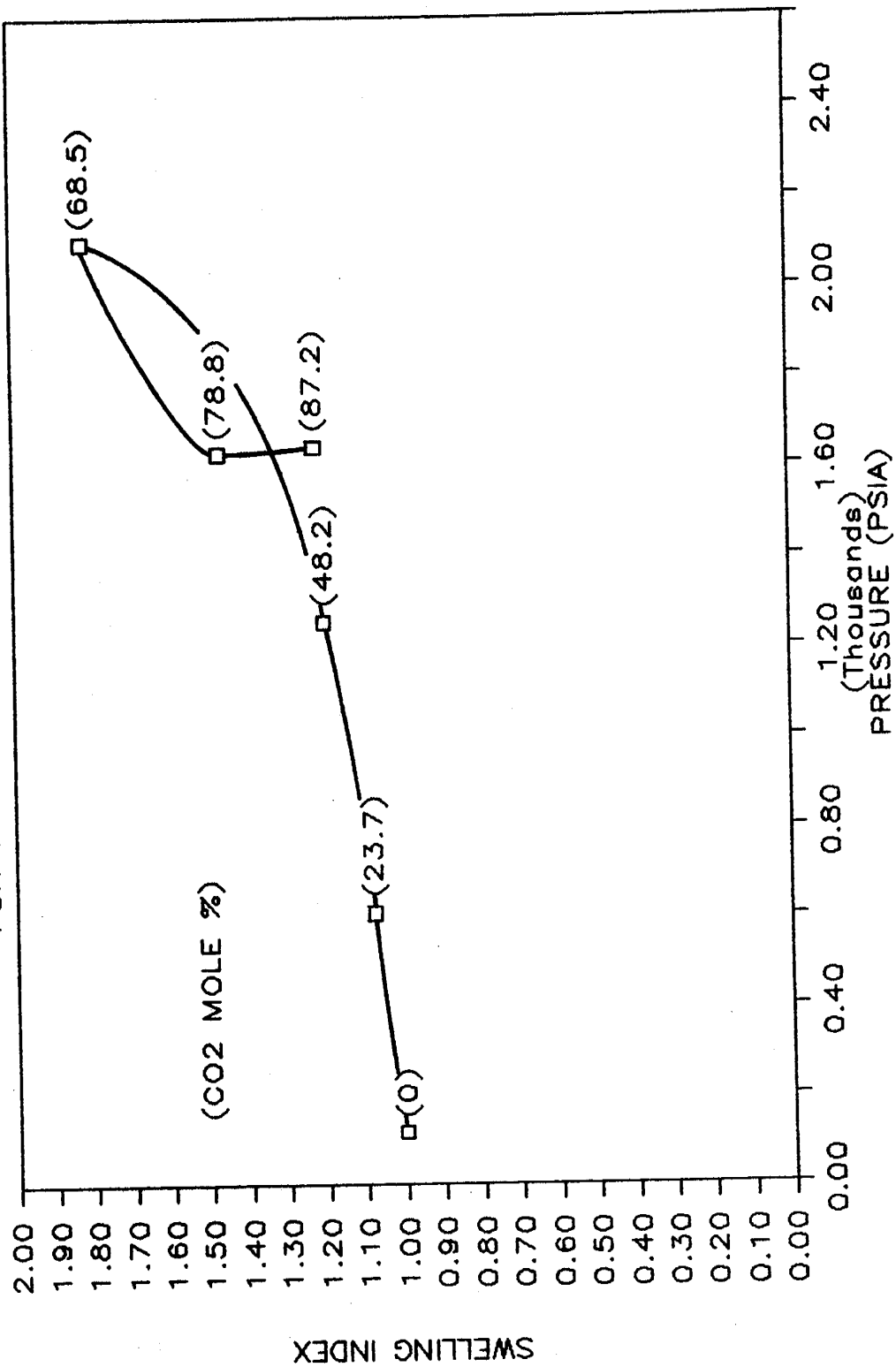


Figure 20.

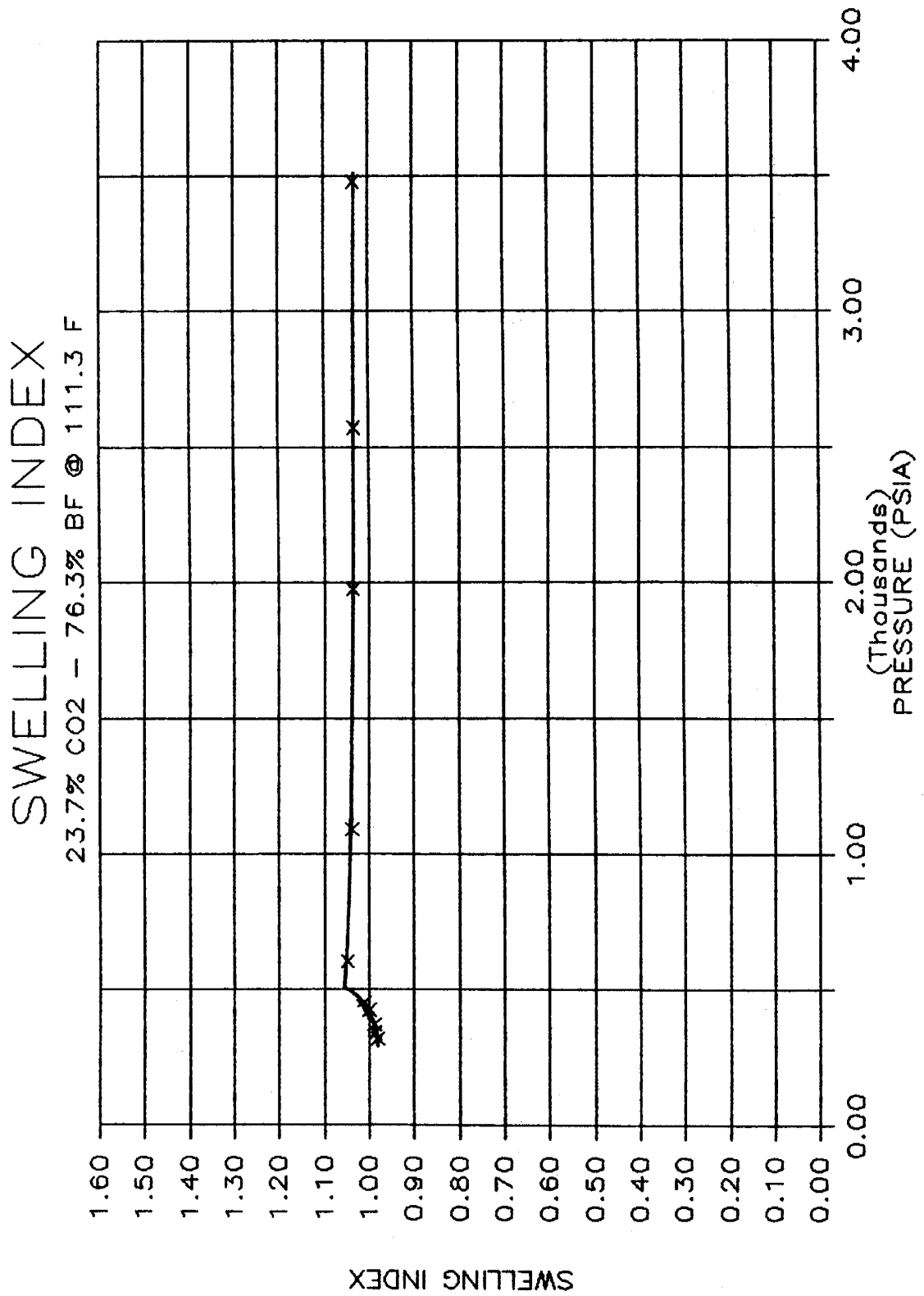


Figure 21.

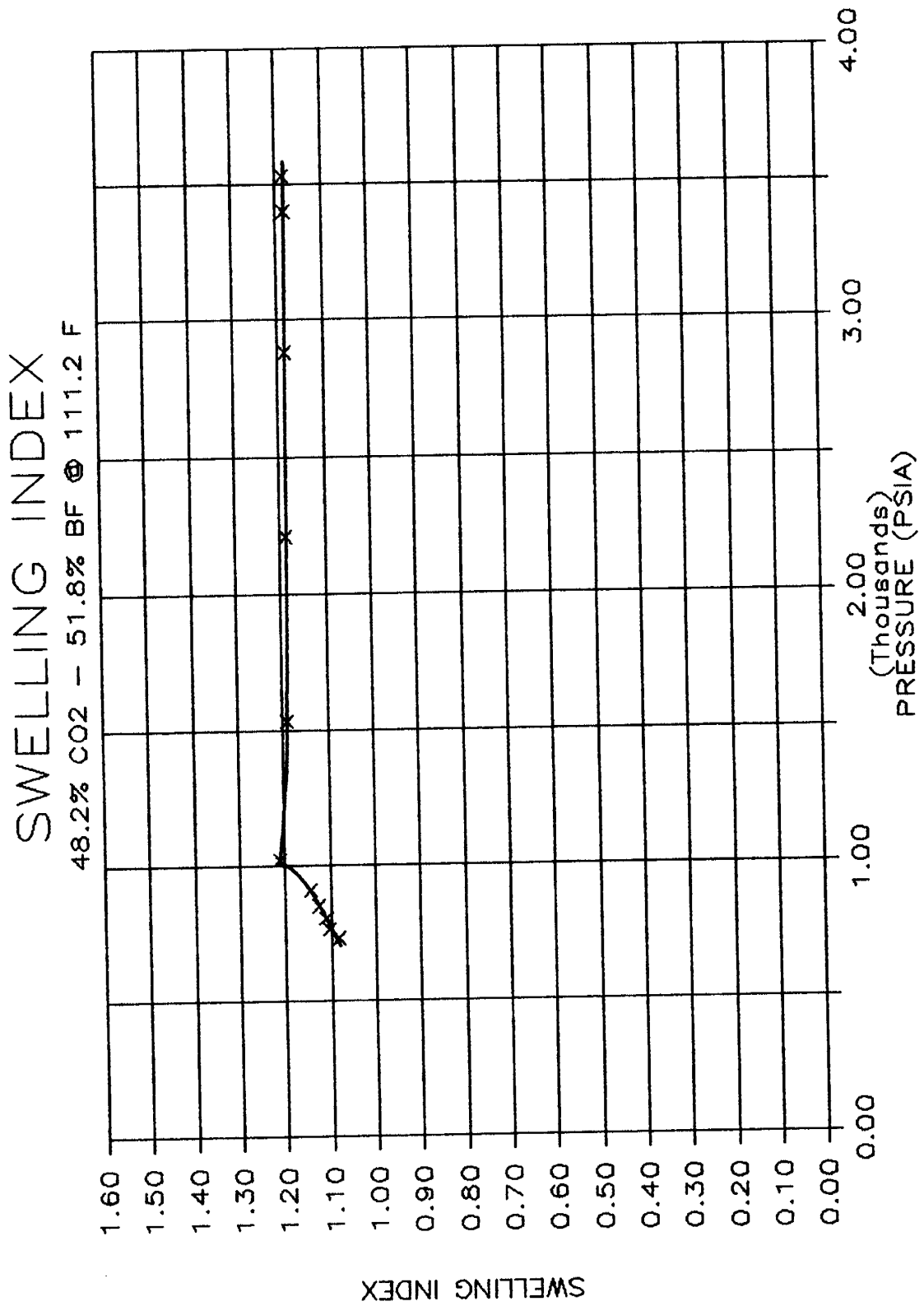


Figure 22.

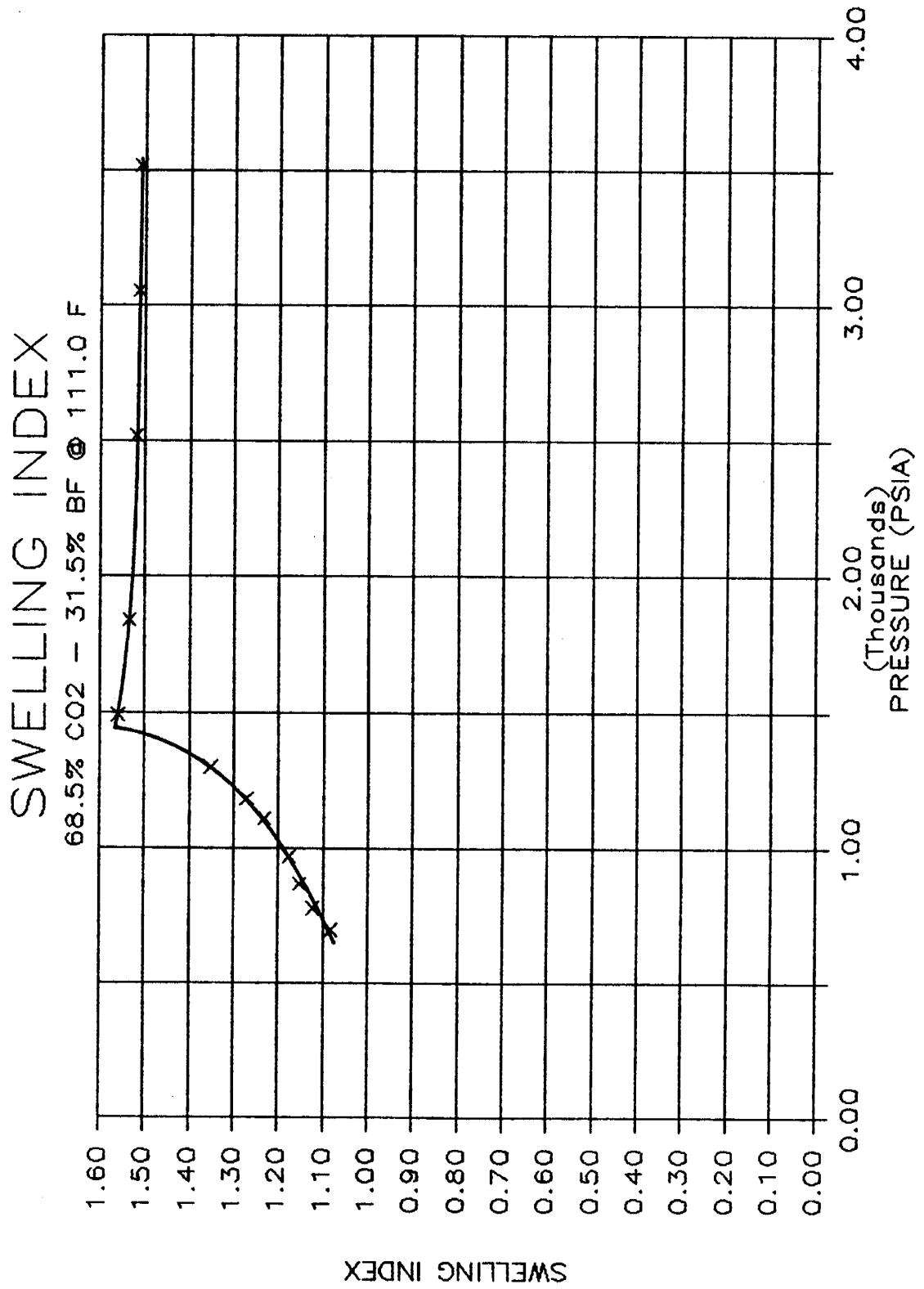


Figure 23.

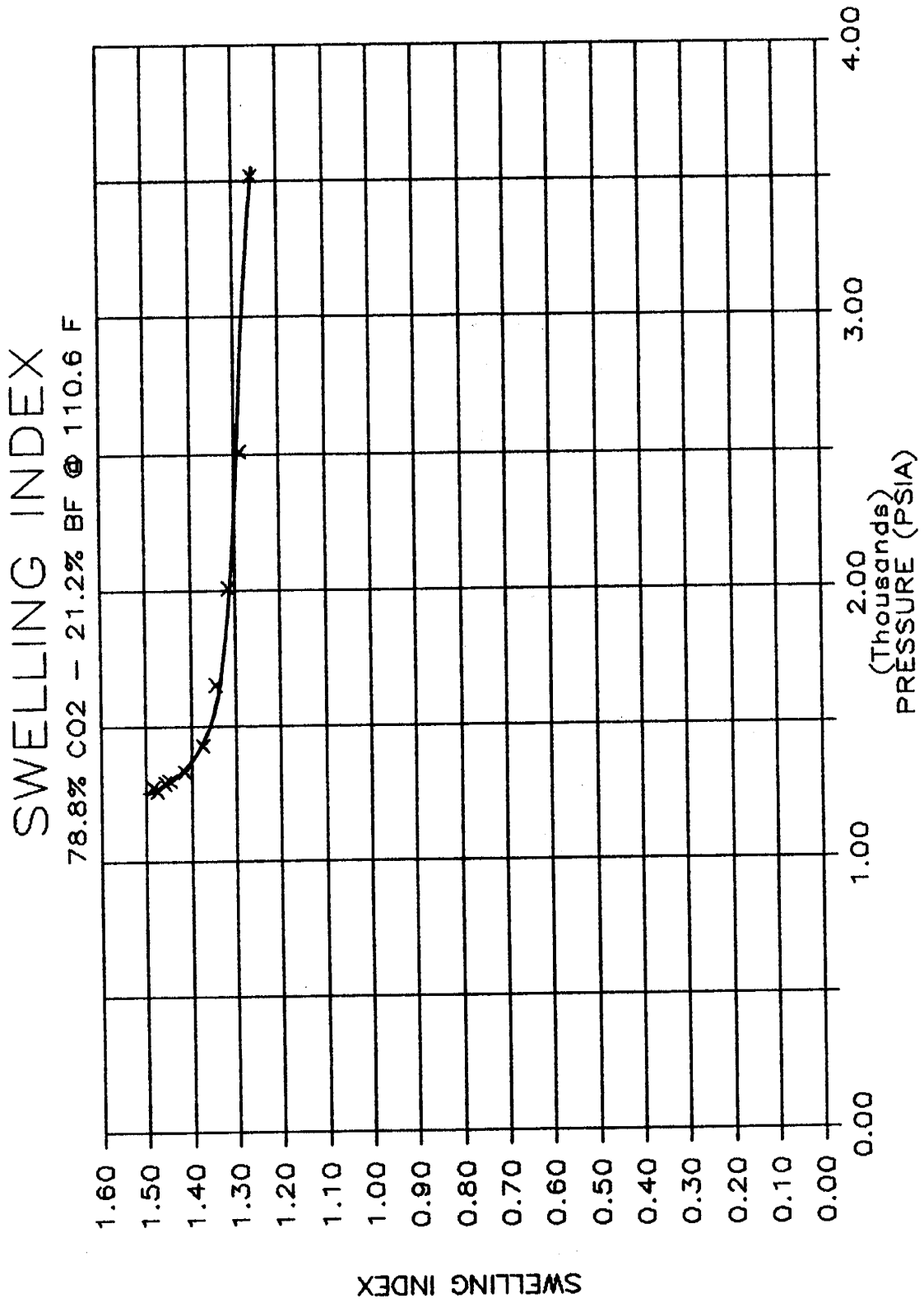


Figure 24.

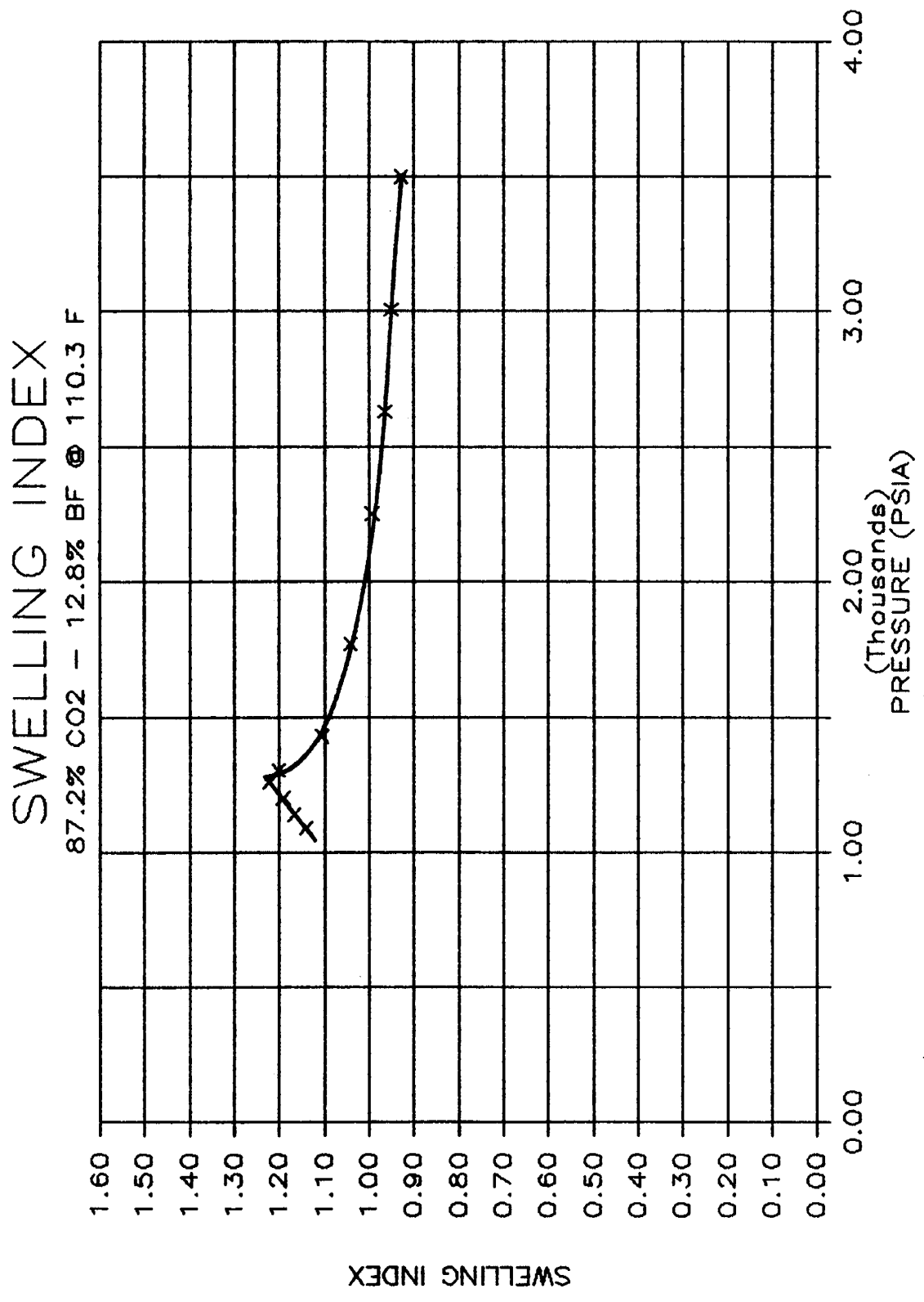


Figure 25.

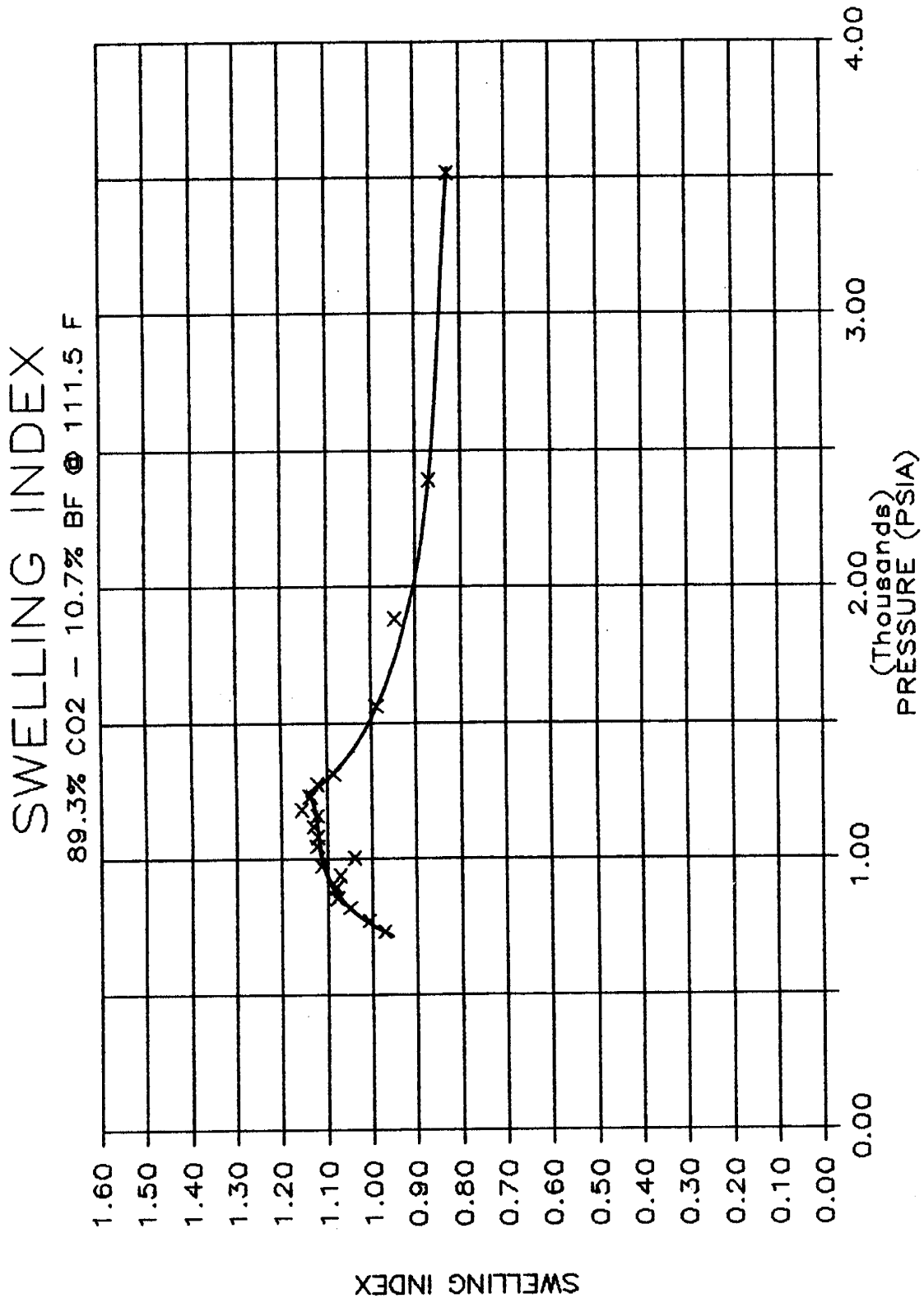


Figure 26.

SWELLING INDEX  
94.6% CO<sub>2</sub> - 5.4% BF @ 111.3 F

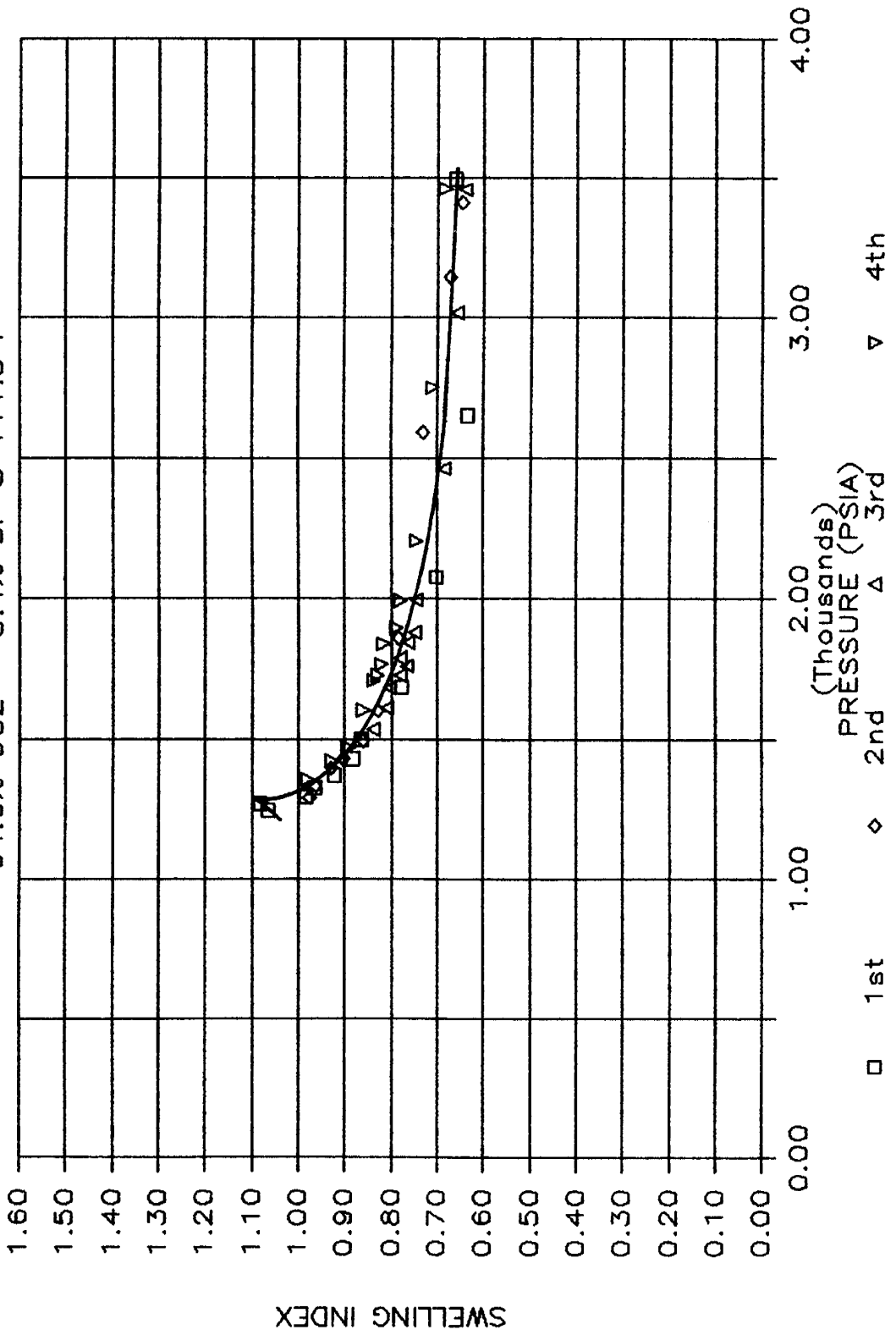


Figure 27.

MAXIMUM SWELLING VS PRESSURE  
 FOR THE SINGLE-CONTACTS @ 111.0 F

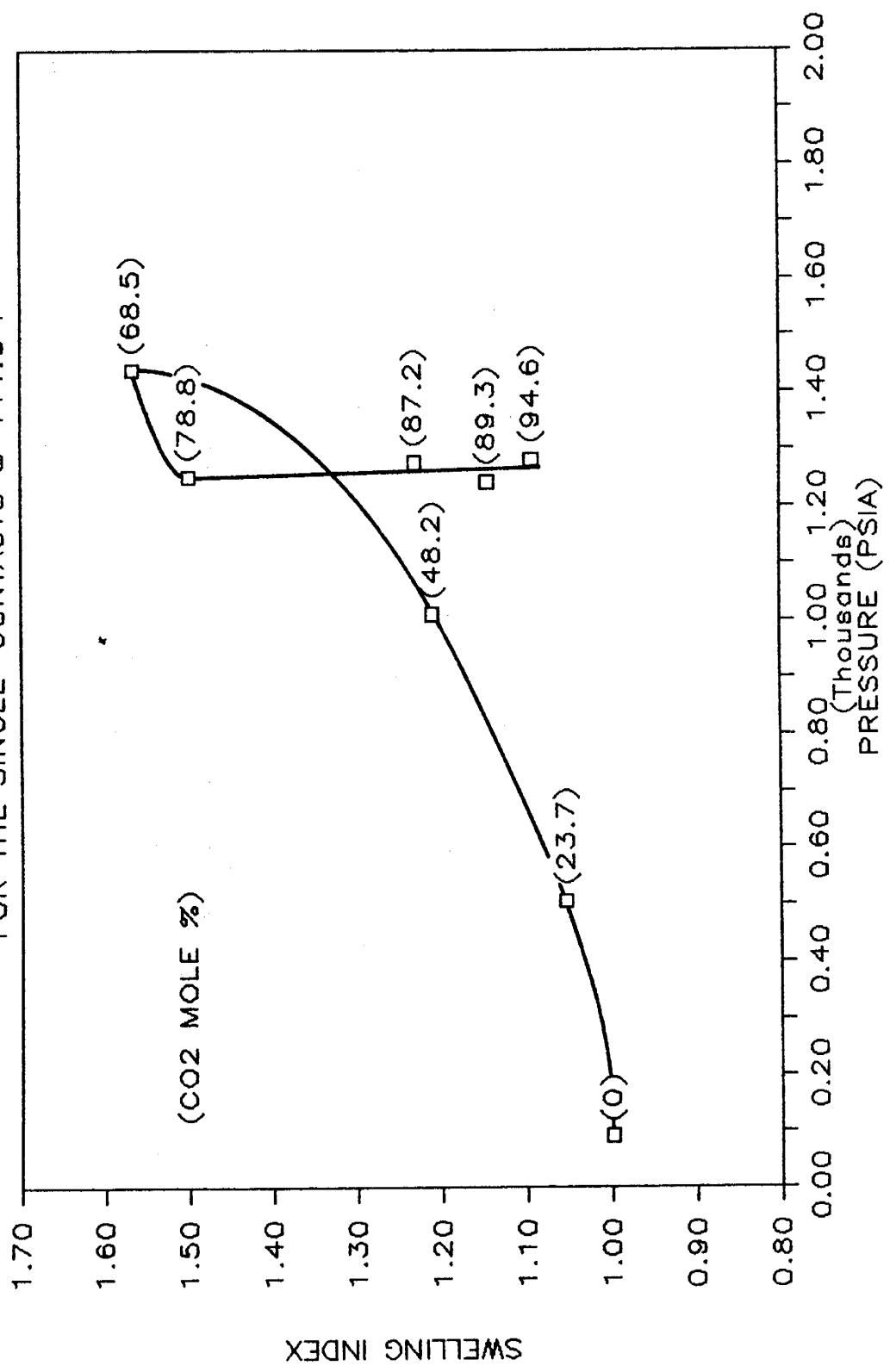


Figure 28.

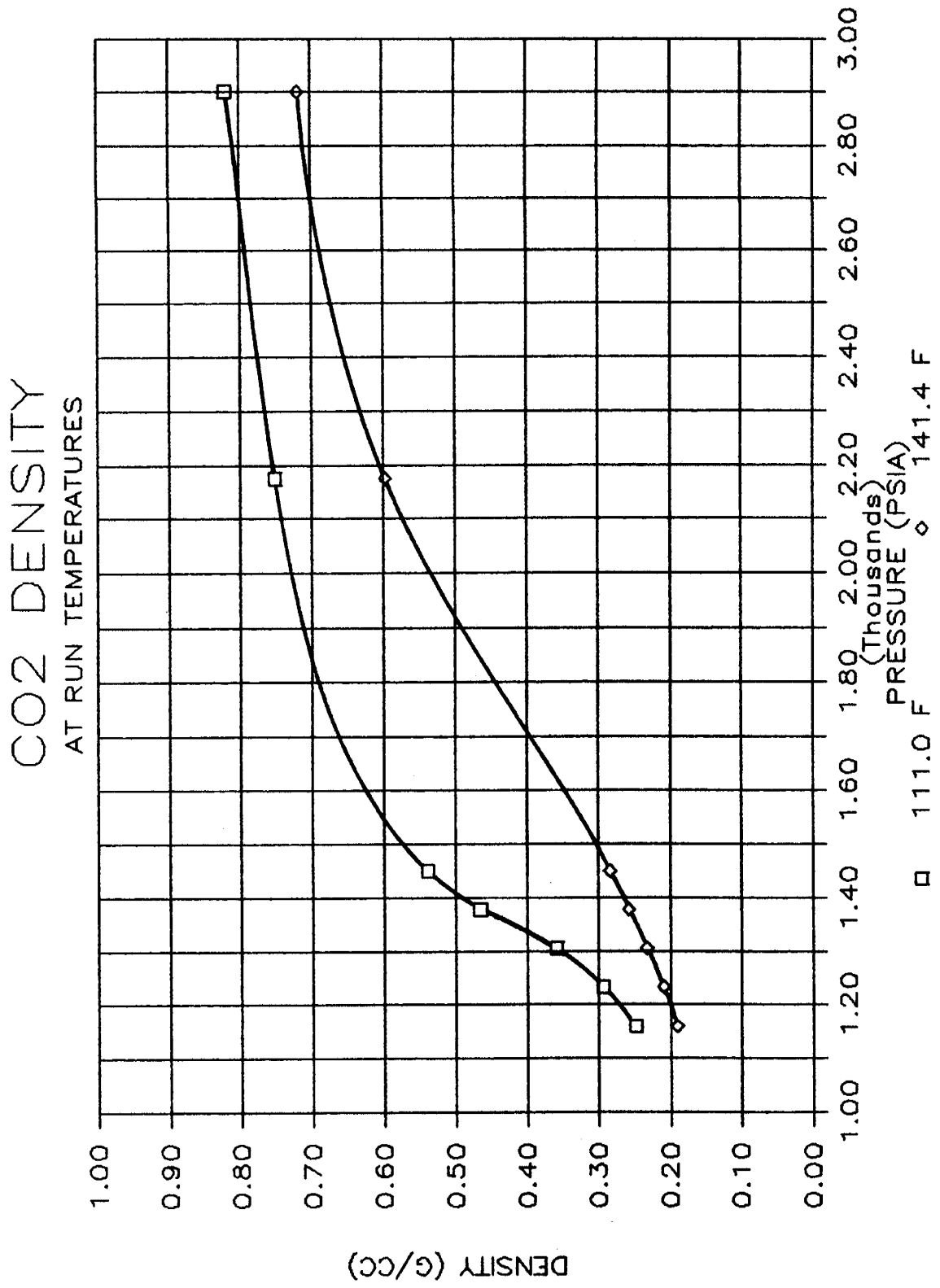


Figure 29.

141.4°F is greater than the value at 111.0°F. On the basis of swelling index definition, the maximum swelling values should be the same. It seems likely that the maximum swelling values at 68.5% CO<sub>2</sub> are different because the CO<sub>2</sub> concentration is very close to the turning point concentration necessary for substantial hydrocarbon extraction (Monger and Khakoo, 1981). The swelling index results are more applicable to immiscible CO<sub>2</sub> flooding processes like the huf-n-puf method of oil recovery. The data indicate that for maximum swelling of the BF oil, the CO<sub>2</sub> concentration in the reservoir should be approximately 68.5 mole percent. If oil vaporization is desired, the carbon dioxide concentration and the reservoir pressure should be as high as field operations will allow.

## Multiple-Contact Experiments

### Analysis of PVT Data

The computer program used to analyze the raw PVT data from the single-contact experiments was also used to analyze the data collected in the multiple-contact experiments. No apparent-critical pressure calculations were made for the multiple-contact experiments. Swelling indexes were calculated using the method described for the single-contact experiments. Since the multiple-contact experiments were conducted at an average run temperature of 111.8°F, only the compressibility function for 100% BF oil at 111°F was used. Swelling index calculations for the forward contacts were identical to the procedure outlined for the single-contact experiments because a known volume of BF oil was contacted with the CO<sub>2</sub>-rich phase of a previous mixing. In the swept zone contacts, the volume of BF oil was calculated from the volume and the swelling indexes of the oil-rich phase left in the cell upon removal of the CO<sub>2</sub>-rich phase. The volume of BF oil had to be calculated using the above method because a known volume of the oil-rich phase from a previous mixing was contacted with pure CO<sub>2</sub> in the swept zone contacts.

### Analysis of Density and Flash Data

The high pressure/temperature phase densities were calculated using the frequency readout of the DMA 45 density meter, the pressure and the temperature at which the readout occurred, and the following equations

$$\text{Density} = \frac{f - B}{A}$$

$$A = 3.1884 + 1.4269 \times 10^{-3} T + 1.029 \times 10^{-6} T^2$$

$$B = 14.9353 + 5.8257 \times 10^{-3} T + 4.4427 \times 10^{-6} T^2 + 4.53 \times 10^{-6} (P - 100)$$

where,

f - DMA Frequency

T - Temperature (°C)

P - Pressure (psia).

Density calculations for the liquid collected from a flash liberation of the phases were performed at room temperature and pressure as described previously. Briefly, these calculations were performed by weighing several known volumes of the sample, dividing the weight by the volume, and averaging the results. This method of measuring the sample density was as accurate as using the low pressure DMA 45 cell and had the added advantage that none of the sample was lost.

Low pressure density measurements required flash liberation of the phases. The phase's gas-liquid ratio (GLR) and shrinkage factor (SF) were calculated from the wet test meter gas volume, the measured liquid volume, and the volume of the phase flashed. The GLR was calculated by dividing the wet test meter gas volume by the measured liquid volume, and the SF was calculated by dividing the measured liquid volume by the volume of phase flashed.

### Analysis of Compositional Data

Two types of compositional data were taken. One type was the gas chromatographic data which characterized the hydrocarbon components of the phase on a molecular weight distribution basis. The other type characterized the hydrocarbon chemistry of the phase on the basis of aromatic carbon content.

Raw chromatographic data were collected from high pressure/temperature samples of the phases and from low pressure gas and low pressure liquid samples obtained from flash liberation of the phases. The analysis of the gas chromatograph (GC) results required that area counts be grouped into units corresponding to the retention time brackets established by the results of a qualitative standard. The methane through pentane and carbon dioxide areas were usually picked by peak recognition. The standard sample's retention times were used to pick  $C_6$ - $C_{36}$  areas. Sometimes the ethane's GC response was included in the carbon dioxide's  $C_6$ - $C_{36}$  response because of the large quantity of  $CO_2$  in the phases. To account for the ethane, the  $C_3$ ,  $C_4$ , and  $C_5$  areas were multiplied by the  $C_2$  to  $C_3$ ,  $C_2$  to  $C_4$ , and  $C_2$  to  $C_5$  area ratios, respectively. The area ratios were calculated from the BF oil's GC response. The three calculated  $C_2$  areas were averaged, and the average value was subtracted from the  $CO_2$ 's area. Methane was not used to calculate the ethane area because it is believed that the methane banks in the  $CO_2$ -rich phase. Propane through pentane were used because it is believed that they maintain approximately the same ratio in both phases. For every sample shot, all of the area counts for each of the components were totaled and entered into a computer data file.

The ASTM procedure for determining the percentage of hydrocarbons detected by the gas chromatograph was used to account for the heavy hydrocarbon components unseen by the GC (ASTM Book of Standards, 1976). The ASTM procedure treats area percents as weight percents. The concept that area percents are equal to weight percents is not precisely correct, but it is a fairly good approximation. This concept was used throughout the chromatographic analyses because time did not permit the calculation and utilization of response factors. The area corresponding to heavy components,  $C_{37+}$ , was calculated from the  $C_5$  to  $C_{36}$  area and the ASTM determined percentage of hydrocarbon detected. The  $C_5$  to  $C_{36}$  area was used as opposed to including gaseous components because the ASTM procedure requires a portion of the sample to be laced with an internal standard containing  $C_{14}$  -  $C_{17}$ . Since, the mixing of sample and internal standard could best be accomplished at room conditions, the ASTM percentage of hydrocarbons detected was necessarily based on the  $C_5$  to  $C_{36}$  area. The ASTM procedure was performed on flash liberated liquids from all of the oil-rich phases and the BF oil.

A Basic program was written to calculate the weight percent of each component, the moles of each component based on a 100 g mixture, the mole percent of each component, and the molecular weight of the sample. The program was written such that the run title, sample name, fraction of hydrocarbons detected, and up to 10 data files could be entered from the key board. The multiple data file entry utility proved to be an important feature of the program because it facilitated analysis of combinations of sample shots which generated averaged chromatographic results. The averaging was performed using results obtained for the same mixture and phase which had similar molecular weights and weight percents of carbon dioxide. The results were averaged to smooth the data to yield a more representative profile of the components in the phase. A listing of the computer program (GCA) can be found in the Appendix.

Another Basic computer program was written to calculate the phase chromatographic composition from the recombination of flash data. The weight percents of the gas's components and of the liquid's components were entered into a computer data file. The run title, data file name, gas density, liquid density, gas volume, and liquid volume were entered through the key board. The program was written such that new values of densities and volumes could be entered without reentering the run title and data file name. This facilitated sensitivity checks of the chromatographic compositional results over the accuracy range of the volume and density measurements. The results were then plotted on a pseudoternary diagram and the composition that mapped closest to the two phase envelope was chosen to be the most representative of the phase.

The hydrocarbon type analyses were performed by conducting an aromatic carbon mass balance on each phase from contact to contact. The weight of aromatic carbon in the phase was calculated by first multiplying the grams of phase by the C<sub>6+</sub> weight percent to restrict the mass balance to stock tank oil (STO) components, and then by the percent of aromatic carbon as determined by <sup>13</sup>C NMR. Percent error calculations were performed for both total STO and aromatic masses using the following equation

$$\text{Percent Error} = \frac{\text{Mass Charged} - \text{Mass Calculated}}{\text{Mass Charged}} * 100\%.$$

Percent errors between ±6% were considered to be within experimental error. Percent errors greater than 6% or less than -6% indicate that the aromatic carbons precipitated out of the phase or that the experimental results are incorrect. The percent of aromatic carbon was determined according to the procedure outlined by Shoolery and Budde (1976). Since the samples for <sup>13</sup>C NMR analysis were prepared at room conditions and the <sup>13</sup>C NMR test was conducted at room conditions, it was assumed that the C<sub>6+</sub> weight fraction was most representative of the sample's hydrocarbon content. It was also assumed that the weight of hydrogen and various trace elements could be neglected because the general formulas for hydrocarbons average about 10 g of carbon to 1 g of hydrogen.

#### Results and Discussion of the Forward Contacts

Starting with the initial mixture, Figure 30 illustrates volume percent compositions and resulting percent phase volumes at approximately 1809 psia and 111.9°F for each of the forward contacts.

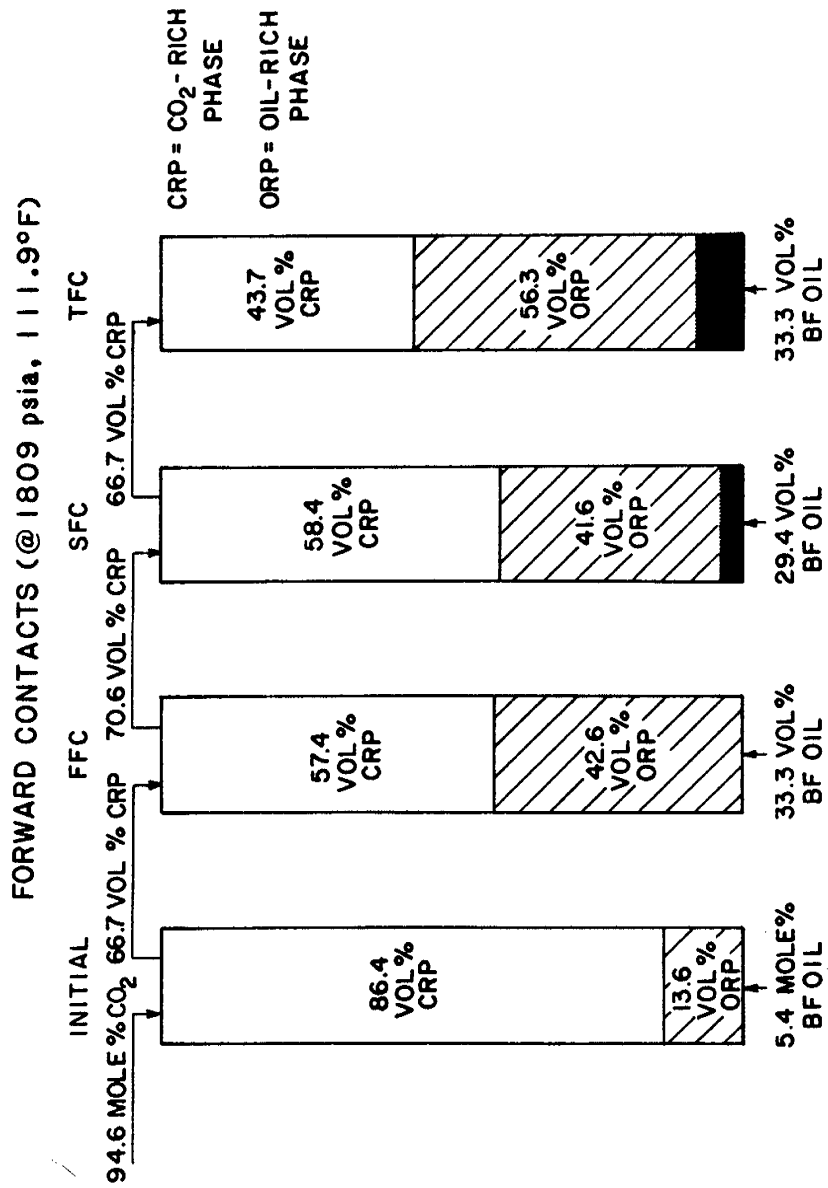


Figure 30. Summary of Forward Contacts (volume percent of oil-rich phase includes precipitate shown in black)

Visual observations during the first forward contact (FFC) resembled those seen in the high CO<sub>2</sub> concentration single-contact runs except there was a noticeable increase in the amount of black precipitate. The second liquid phase appeared to be condensing out of the CO<sub>2</sub>-rich phase as mercury was injected into the cell to increase the pressure, but upon equilibration the second liquid phase disappeared. The amount of precipitate appearing on the cell window increased as the pressure increased with the majority of precipitate coming out of solution after the cell pressure exceeded 2500 psia. The amount of precipitate became so great at high pressures (> 3000 psia) that the laboratory lights had to be turned off to view the interface. An increase in the surface tension was noticed at high pressures because small bubbles would appear on top of the oil-rich phase next to the cell window. It usually took 5-10 min. for these bubbles to burst.

Visual observations during the second forward contact (SFC) run were similar to those seen in the FFC, except that more of the black precipitate came out of solution. The precipitation of the solid phase completely covered the cell window at 3468 psia. The cell appeared to be completely filled with a single-phase, dark liquid. The cell was allowed to remain upright at high pressure and run temperature for 12 hours. With the laboratory lights off, the interface location could be estimated. The precipitate resembled tar balls, and mercury was unable to displace it during flash liberation of the oil-rich phase. During cleanup procedures, it was observed that large globs of a tar-like substance adhered to the cell windows. This indicated that the precipitate had a high affinity for glass. The precipitate was easily dissolved with toluene. The color of the oil-rich phase as viewed through the high pressure/temperature syringe was a dark red. The same dark red color was observed viewing the liquid collected from flash liberation of the oil-rich phase through a microliter syringe. In the initial and FFC mixtures, the oil-rich phase was black and did not transmit light when viewing the phase in the glass barrel of the high pressure/temperature syringe.

The amount of precipitate observed in the third forward contact (TFC) surpassed that in the SFC. The black, tar-like precipitate almost covered the cell window at 2463 psia. When the pressure was increased to 2760 psia, the cell window turned black, and the interface was completely lost. The cell was allowed to remain upright at high pressure and run temperature for about 30 hours. The cell window remained black. It is believed that miscibility was obtained, and that the black, tar-like precipitate was a byproduct. Even during compositional sampling, the precipitate completely covered the cell window. It was confirmed, however, that there were two phases at sampling conditions by viewing the high pressure/temperature samples through the syringe barrel. The color of the oil-rich phase was dark red, but lighter than that of the SFC. This was evident for samples in both the high pressure/temperature syringe and the low pressure microliter syringe. The precipitate had a high affinity for glass because mercury injected into the cell to keep cell pressure constant during flash liberation of the phases could not be seen. Upon lowering the pressure for compositional sampling, the phases seemed to occupy about the same volumes as they did before the precipitate came out of solution.

The bubbles that appeared on top of the oil-rich phase next to the cell window in the FFC also appeared in the SFC and TFC but at progressively lower pressures. This apparent increase in surface tension appeared to coincide with increased precipitation, thus reflecting the solid phase immiscibility. The bubbles are also related to the phase densities becoming almost identical. In all three forward contacts, the development of the non-equilibrium second liquid phase upon mercury

injection occurred at the pressure where the percent oil-rich phase volume was maximum.

Figures 31 - 33 show the total sample volume versus pressure and percent phase volumes versus pressure graphs for the forward contacts. The graphs of percent phase volumes show a break in the curve at approximately 1290 psia. The graphs also indicate that the percent volume of oil-rich phase is maximum at the break. The maximum value increases from 43% in the FFC to 44% in the SFC to 58% in the TFC. The break in the percent phase volume curves has a mechanistic explanation. Below the break, at lower pressures, the oil-rich phase volume is increased by CO<sub>2</sub> swelling and condensation of hydrocarbons from the CO<sub>2</sub>-rich phase. Carbon dioxide density at 1290 psia and 111.9°F is about 0.34 g/cc. This value is within the CO<sub>2</sub> density range required for the start of substantial hydrocarbon extraction as reported by Holm and Josendal (1982). Above the break, at higher pressures, the percent oil-rich phase volume decreases as a result of this substantial hydrocarbon extraction. The rate at which the oil-rich phase shrinks, increases from contact to contact because the hydrocarbons carried over with the CO<sub>2</sub>-rich phase of a previous contact assist the extraction process further to recover more extractable hydrocarbons. This explanation is confirmed in the chromatographic compositional analysis of the oil-rich and CO<sub>2</sub>-rich phases.

The same CO<sub>2</sub> swelling and hydrocarbon extraction trends can be seen in the swelling index graphs of the forward contacts (Figures 34 - 37). Figure 37 shows that maximum swelling increases with advancing contacts, and that the maximum swelling pressure is about 1236 psia for all three contacts. Carbon dioxide density at 1236 psia and 111.9°F is approximately 0.29 g/cc. This value is within the density range for hydrocarbon extraction to become significant (Holm and Josendal, 1982). The effects of CO<sub>2</sub> swelling and hydrocarbon condensation are better illustrated by the swelling index curves. The increase in the rate at which hydrocarbon extraction occurs as the pressure is increased for each contact is also indicated by the crossing of the FFC and SFC swelling index curves at approximately 2950 psia.

The physical properties of the CO<sub>2</sub>-rich phase in the forward contacts are shown in Table 13. The high pressure/temperature density, GLR, and SF were measured at approximately 1809 psia and 111.9°F. The density of the liquid from a flash liberation was measured at room conditions. The high pressure/temperature density increases from 0.7350 g/cc for the initial mixture to 0.7720 g/cc for the TFC, with the FFC and SFC densities falling between. There is also an increase in the flashed liquid densities. This increase occurs because more hydrocarbons of higher molecular weight are extracted into the CO<sub>2</sub>-rich phase. The GLR decreases and the SF increases as the contacts advance. This indicates that there are less gaseous components and more liquid components in the CO<sub>2</sub>-rich phase for each successive contact. This is to be expected because CO<sub>2</sub> is the major gaseous component in the mixture and a certain amount of it remains in the oil-rich phase of the previous contact.

Table 14 shows the physical properties of the oil-rich phase for the forward contacts. The trends observed for the oil-rich phase are the reverse of those seen for the CO<sub>2</sub>-rich phase. The high pressure/temperature density decreases as the contacts advance for two reasons. First, the oil-rich phase is increasingly enriched with intermediate molecular weight hydrocarbons and CO<sub>2</sub>. Second, very high molecular weight hydrocarbons are removed as the solid phase precipitates out.

# FIRST FORWARD CONTACT 112.6F #2

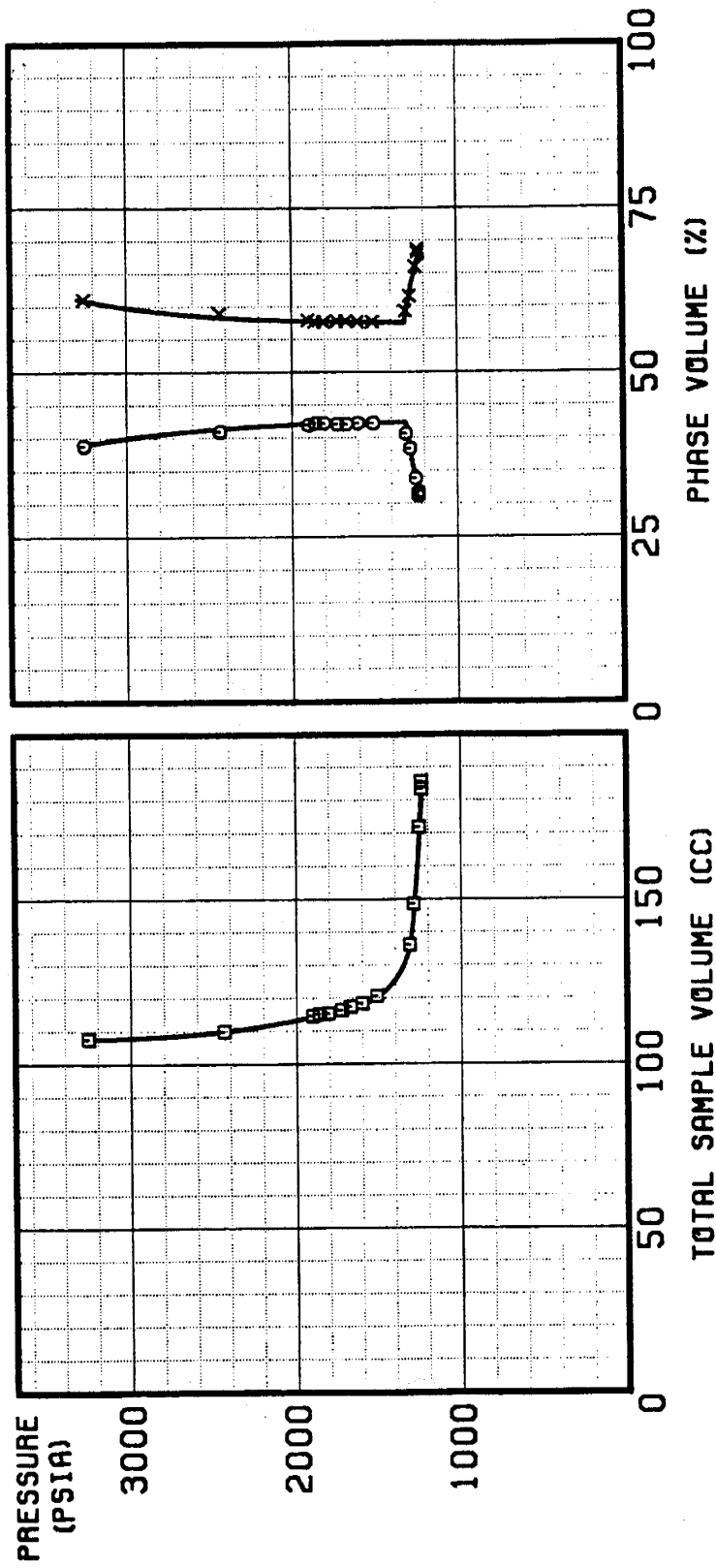


Figure 31. Pressure-Volume Isotherms (circles, oil-rich phase; x's, CO<sub>2</sub>-rich phase)

## SECOND FORWARD CONTACT 111.8F

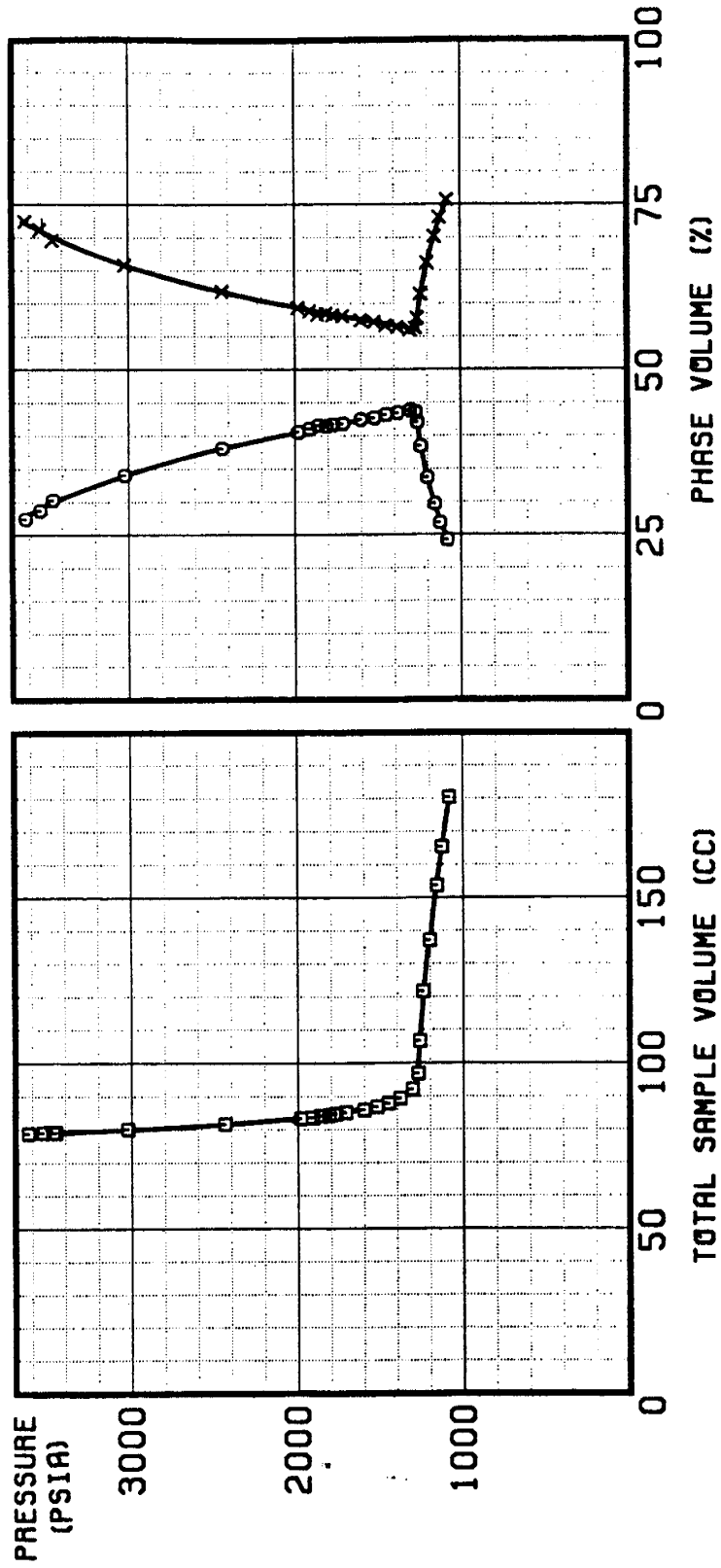


Figure 32. Pressure-Volume Isotherms (circles, oil-rich phase; x's, CO<sub>2</sub>-rich phase)

# THIRD FORWARD CONTACT 111.9F

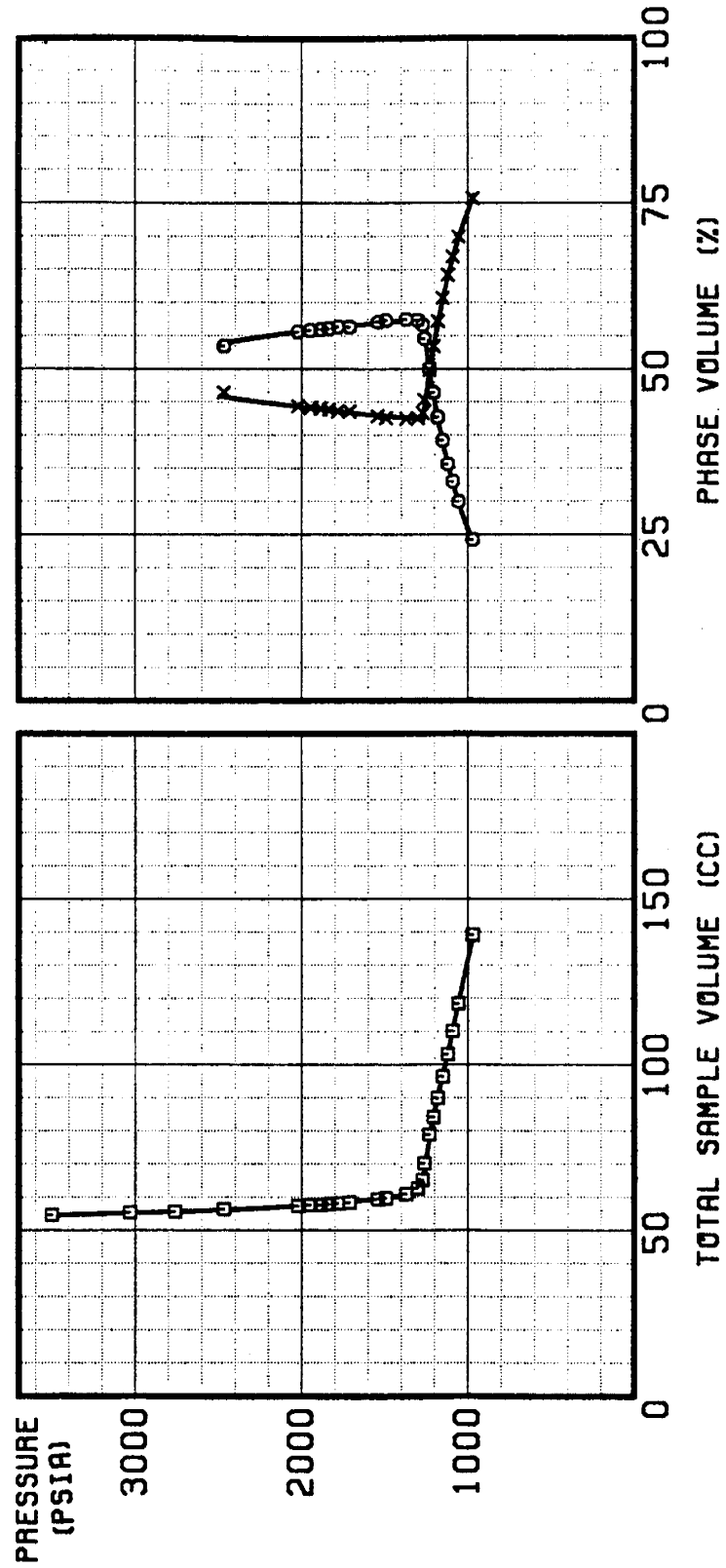


Figure 33. Pressure-Volume Isotherms (circles, oil-rich phase; x's, CO<sub>2</sub>-rich phase)

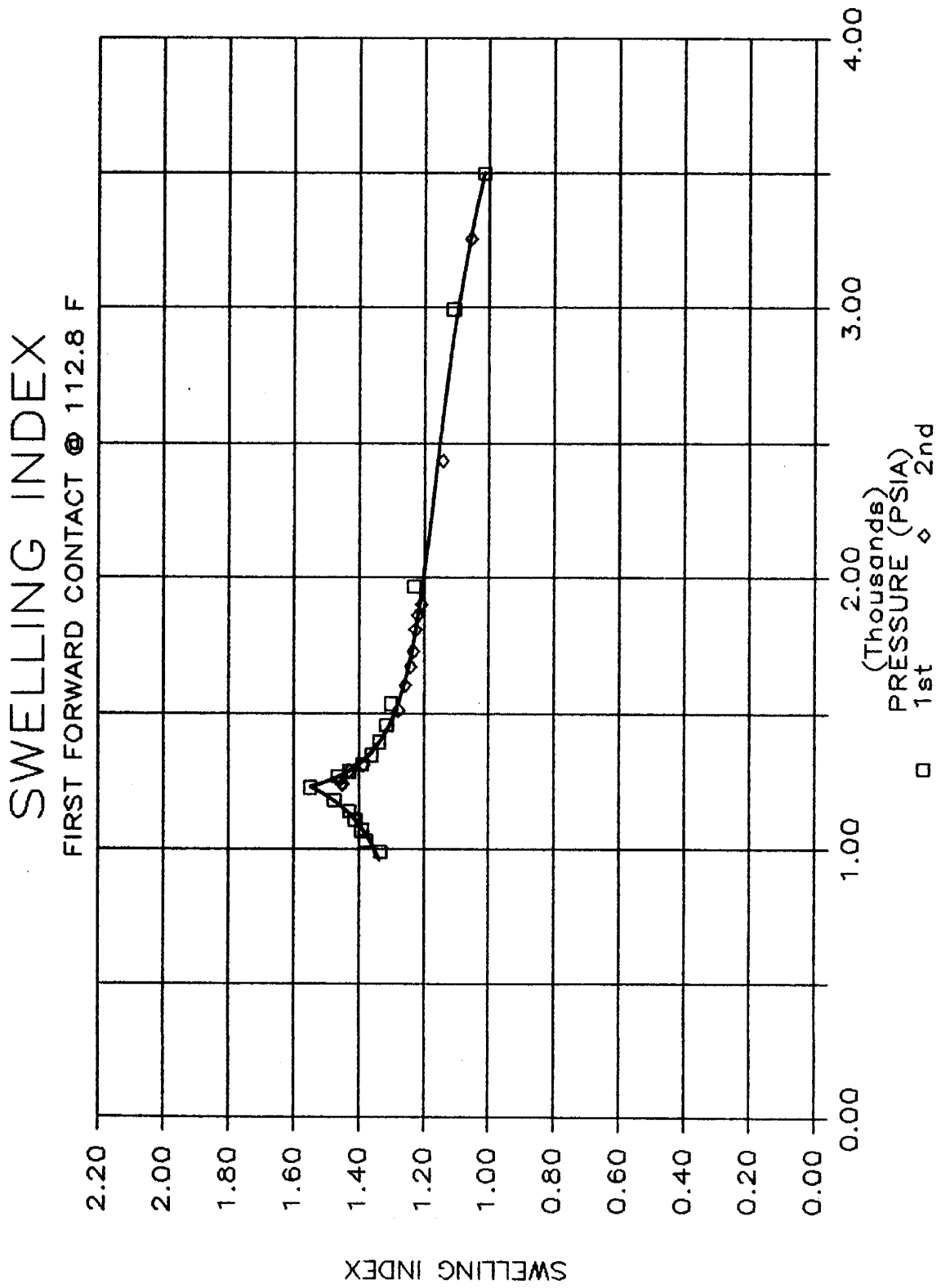


Figure 34.

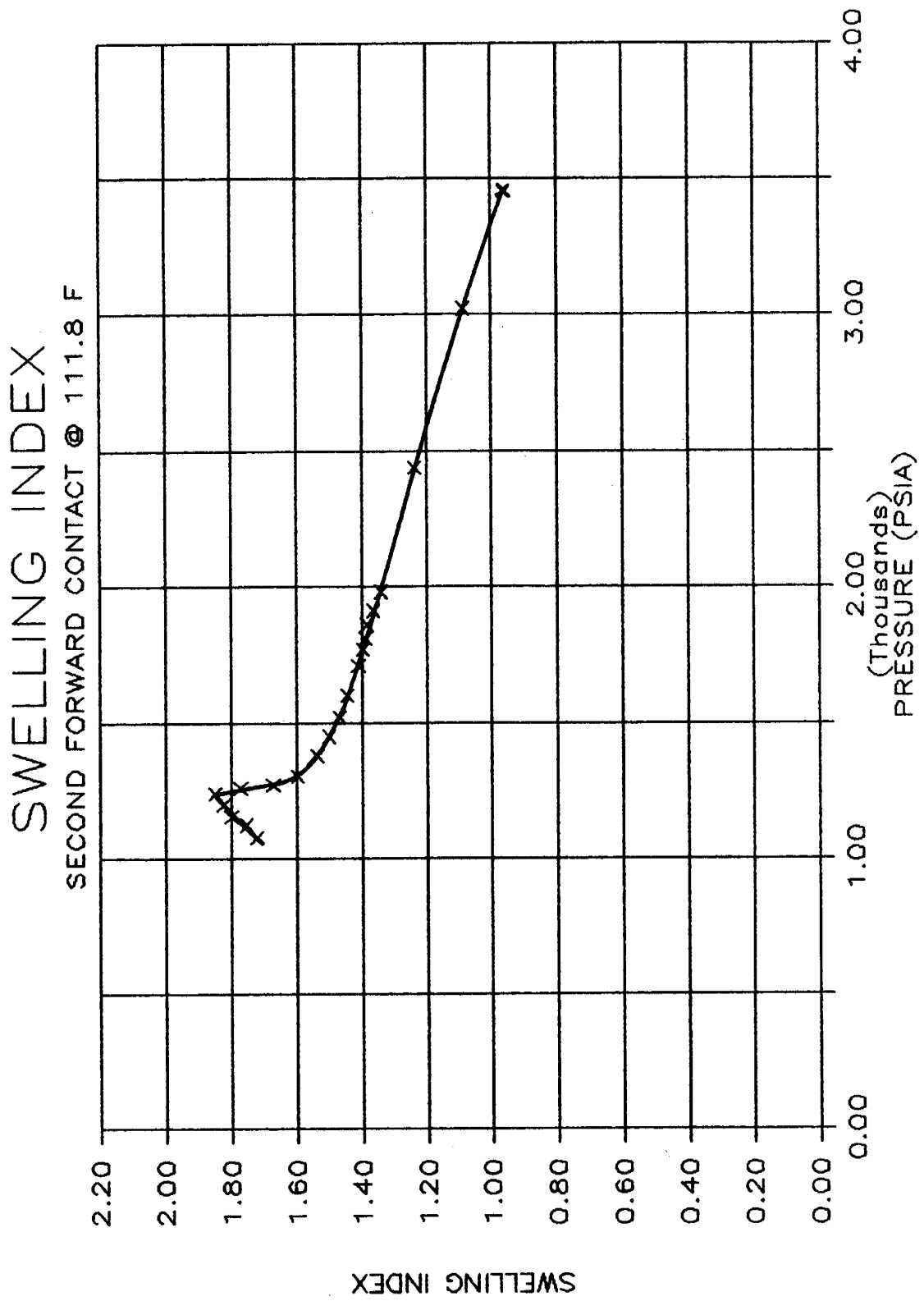


Figure 35.

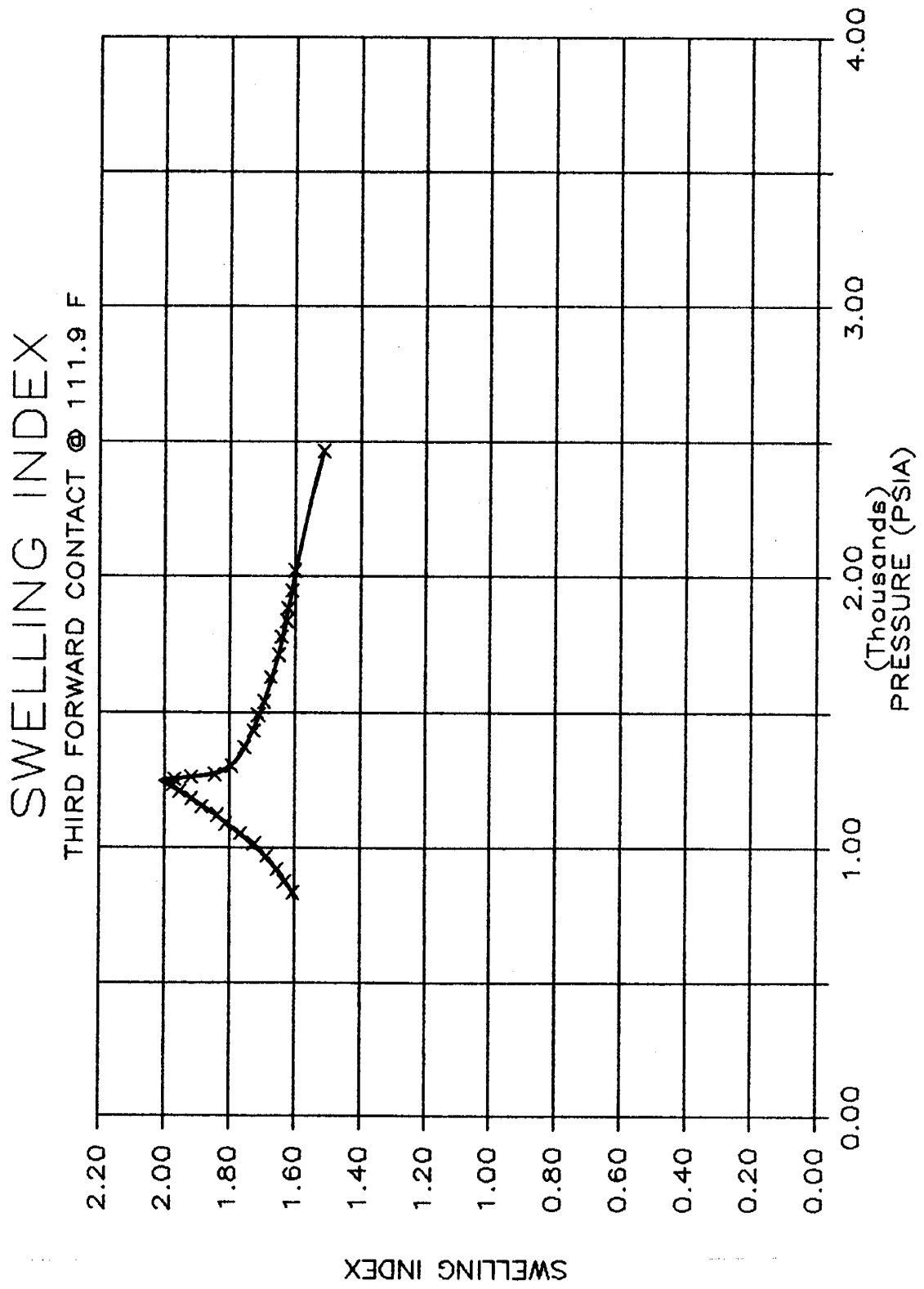


Figure 36.

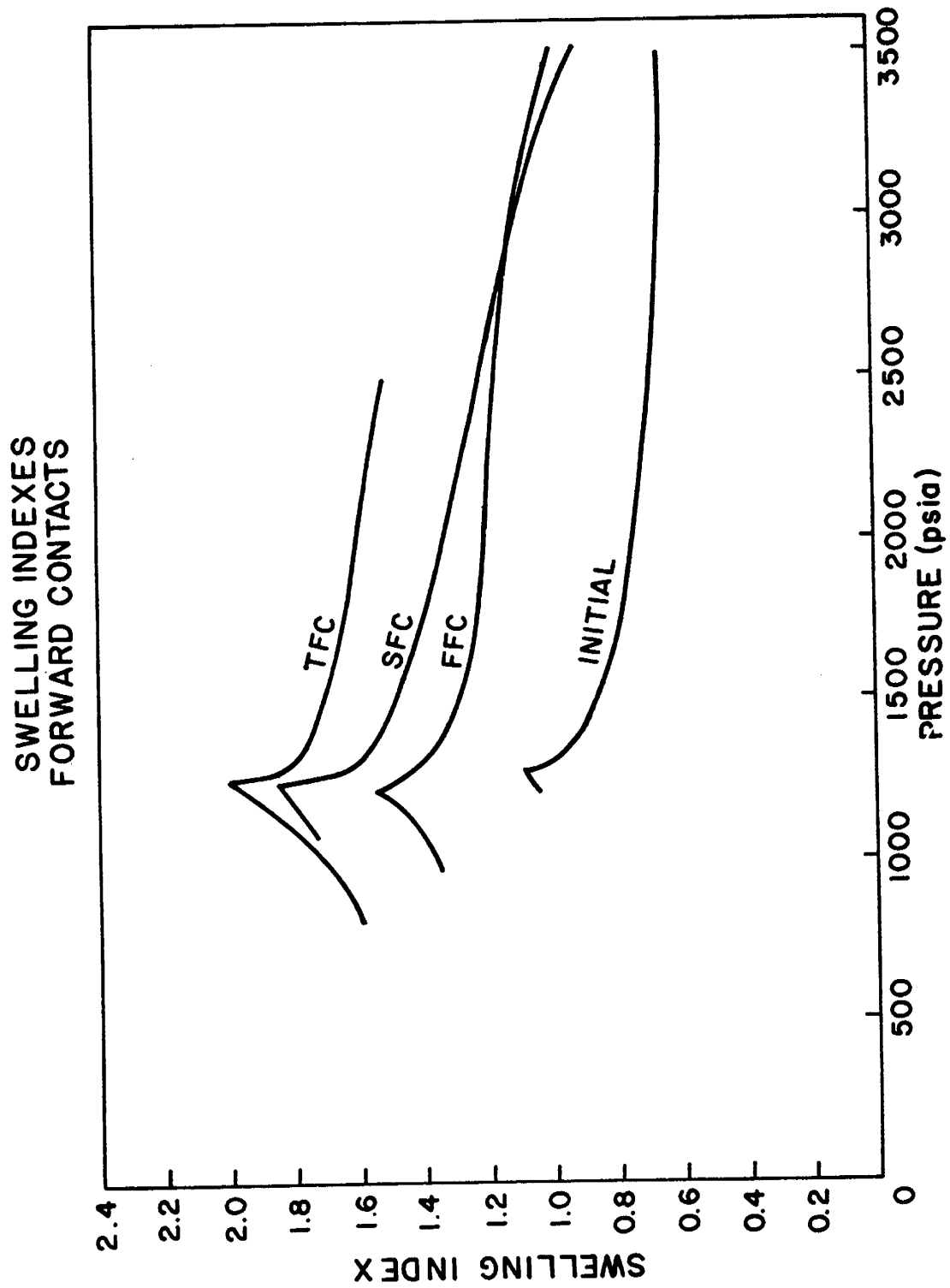


Figure 37.

Table 13: CO<sub>2</sub>-Rich Phase in the Forward Contacts - Physical Properties

Mixture	High Pressure/ Temperature Density <sup>a</sup> (g/cc)	Liquid From Flash Density <sup>b</sup> (g/cc)	GLR <sup>a</sup> (CF/BBL)	SF <sup>a</sup> (BBL/RB)
Initial	0.7350	0.794	39,734	0.0577
First Forward Contact	0.7522	-----	-----	-----
Second Forward Contact	0.7631	-----	-----	-----
Third Forward Contact	0.7720	0.800	8,908	0.1954

<sup>a</sup> Measured at approximately 1809 psia and 111.9°F.

<sup>b</sup> Measured at room conditions.

Table 14: Oil-Rich Phase in the Forward Contacts - Physical Properties

Mixture	High Pressure/ Temperature Density <sup>a</sup> (g/cc)	Liquid From Flash Density <sup>b</sup> (g/cc)	GLR <sup>a</sup> (CF/BBL)	SF <sup>a</sup> (BBL/RB)
Initial	0.8844	0.882	788	0.8476
First Forward Contact	0.8496	0.857	1,266	0.6861
Second Forward Contact	0.8458	0.851	1,548	0.6383
Third Forward Contact	0.8203	0.846	1,832	0.5956

<sup>a</sup> Measured at approximately 1809 psia and 111.9°F.

<sup>b</sup> Measured at room conditions.

The same trend of decreasing density with advancing contacts is seen for the flashed liquid densities. The GLR increases as the contacts advance and the SF decreases as the contacts advance. Both indicate increasing amounts of CO<sub>2</sub> and volatile hydrocarbons.

Table 15 shows the molecular weights calculated from high pressure/temperature and recombination of flash sample results for the CO<sub>2</sub>-rich phase in the forward contacts. The molecular weight increases as the contacts advance because the mole percent CO<sub>2</sub> is decreasing as the contacts advance. The agreement between the high pressure/temperature results and recombination of flash results are within experimental error. The chromatographic compositions of the CO<sub>2</sub>-rich phases in the forward contacts are given in Table 16 and shown in Figure 38. It can be seen that the CO<sub>2</sub> concentration decreases from contact to contact. The light hydrocarbons appear to be banking in the CO<sub>2</sub>-rich phase as the contacts advance because the relative concentrations of C<sub>4</sub> - C<sub>20</sub> are increasing from contact to contact. Examination of the composition of the liquid collected from flashing the CO<sub>2</sub>-rich phase in forward contacts (Table 17 and Figure 39) indicates that the C<sub>4</sub> - C<sub>9</sub> concentration is increasing while the C<sub>10+</sub> concentration is decreasing. This explains why the molecular weight of the flashed liquid from the CO<sub>2</sub>-rich phase decreases as the contacts advance (Tables 15 and 17). It seems likely that the C<sub>10+</sub> fraction is returning to the oil-rich phase because the overall mixture is approaching miscibility as the contacts advance.

Molecular weight calculations for the oil-rich phase in the forward contacts show that the molecular weight decreases as the contacts advance (Table 18). Comparing the high pressure/temperature results to the recombination of flash results, poor agreement is seen for the initial mixture with the agreement becoming better for the FFC, SFC, and TFC mixtures. The agreement is never better than about 7 g/g-mole, but does improve with increased formation of the solid phase. Perhaps the recombination of flash molecular weights are always greater than the high pressure/temperature molecular weights because the high pressure/temperature syringe restricts the flow of the very high molecular weight hydrocarbon components. The heavy molecular weight components are not as easily drawn into the syringe during sampling or expelled from the syringe when the sample is injected into the gas chromatograph. The recombination of flash results thus seem more representative of the true oil-rich phase composition. The fact that the recombination results map closer to the two phase envelope on a pseudoternary diagram confirms this choice.

Table 19 and Figure 40 show that for the oil-rich phase, the CO<sub>2</sub> and C<sub>2</sub> - C<sub>14</sub> concentrations increase as the contacts advance while the methane concentration remains approximately the same. The reason the C<sub>2</sub> - C<sub>14</sub> concentrations increase is that these components are condensing from the CO<sub>2</sub>-rich phase into the oil-rich phase as miscibility is approached. Since more of these CO<sub>2</sub> liked hydrocarbons are in the oil-rich phase, more CO<sub>2</sub> dissolves into the oil-rich phase. The mass transfer is working in both directions to make the two phase compositions identical, thus creating miscibility. The C<sub>36+</sub> concentration decreases from contact to contact because the heavy molecular weight hydrocarbons precipitate out of the oil-rich phase. The oil-rich phase enrichment in C<sub>4</sub> - C<sub>14</sub> components and the precipitation of C<sub>36+</sub> components are also evident in compositional results for the liquid obtained from flashing the oil-rich phase (Table 20 and Figure 41). This explains why the molecular weight of the liquid from flashing the oil-rich phase decreases from contact to contact (Tables 18 and 20).

Table 15: CO<sub>2</sub>-Rich Phase in the Forward Contacts - Molecular Weight

Mixture	Molecular Weight (g/g-mole)		
	High Pressure/ Temperature	Recombination of Flash	Liquid From Flash
Initial	46.4	46.2	161.5
First Forward Contact	47.3	----	-----
Second Forward Contact	50.0	----	-----
Third Forward Contact	55.6	52.8	147.4

Table 16: Composition of the CO<sub>2</sub>-Rich Phase in the Forward Contacts

COMPONENT	(Mole Percent)		SFC	TFC <sup>a</sup>
	Initial <sup>a</sup>	FFC		
C-1	0.516	0.984	1.495	1.585
CO2	96.155	92.059	87.272	81.724
C-2	0.207	1.413	1.038	1.384
C-3	0.194	0.690	1.027	1.475
C-4	0.394	0.937	1.628	2.328
C-5	0.202	0.442	0.862	1.132
C-6	0.286	0.461	0.895	1.228
C-7	0.344	0.474	1.170	1.660
C-8	0.369	0.646	1.234	1.711
C-9	0.274	0.456	0.774	1.300
C-10	0.232	0.323	0.645	0.943
C-11	0.181	0.265	0.490	0.760
C-12	0.140	0.176	0.372	0.590
C-13	0.122	0.139	0.309	0.501
C-14	0.096	0.101	0.220	0.397
C-15	0.075	0.068	0.162	0.296
C-16	0.056	0.049	0.125	0.246
C-17	0.052	0.050	0.113	0.230
C-18	0.030	0.043	0.063	0.148
C-19	0.020	0.028	0.038	0.069
C-20	0.017	0.033	0.027	0.051
C-21	0.012	0.022	0.016	0.061
C-22	0.007	0.021	0.010	0.049
C-23	0.007	0.016	0.006	0.050
C-24	0.004	0.013	0.003	0.022
C-25	0.002	0.016	0.002	0.016
C-26	0.001	0.016	0.001	0.013
C-27	0.001	0.014	0.001	0.010
C-28	0.001	0.016	0.001	0.009
C-29	0.001	0.017	0.001	0.007
C-30	0.001	0.015	0.001	0.005
C-31	0.001	0.000	0.001	0.002
Molecular Weight (g/g-mole)	46.3	47.3	50.0	54.3

<sup>a</sup> Composition calculated by combining the high pressure/temperature results with the recombination of flash liberation data results on an 1:1 basis.

# COMPOSITION OF THE CO<sub>2</sub>-RICH PHASE OF THE FORWARD CONTACTS

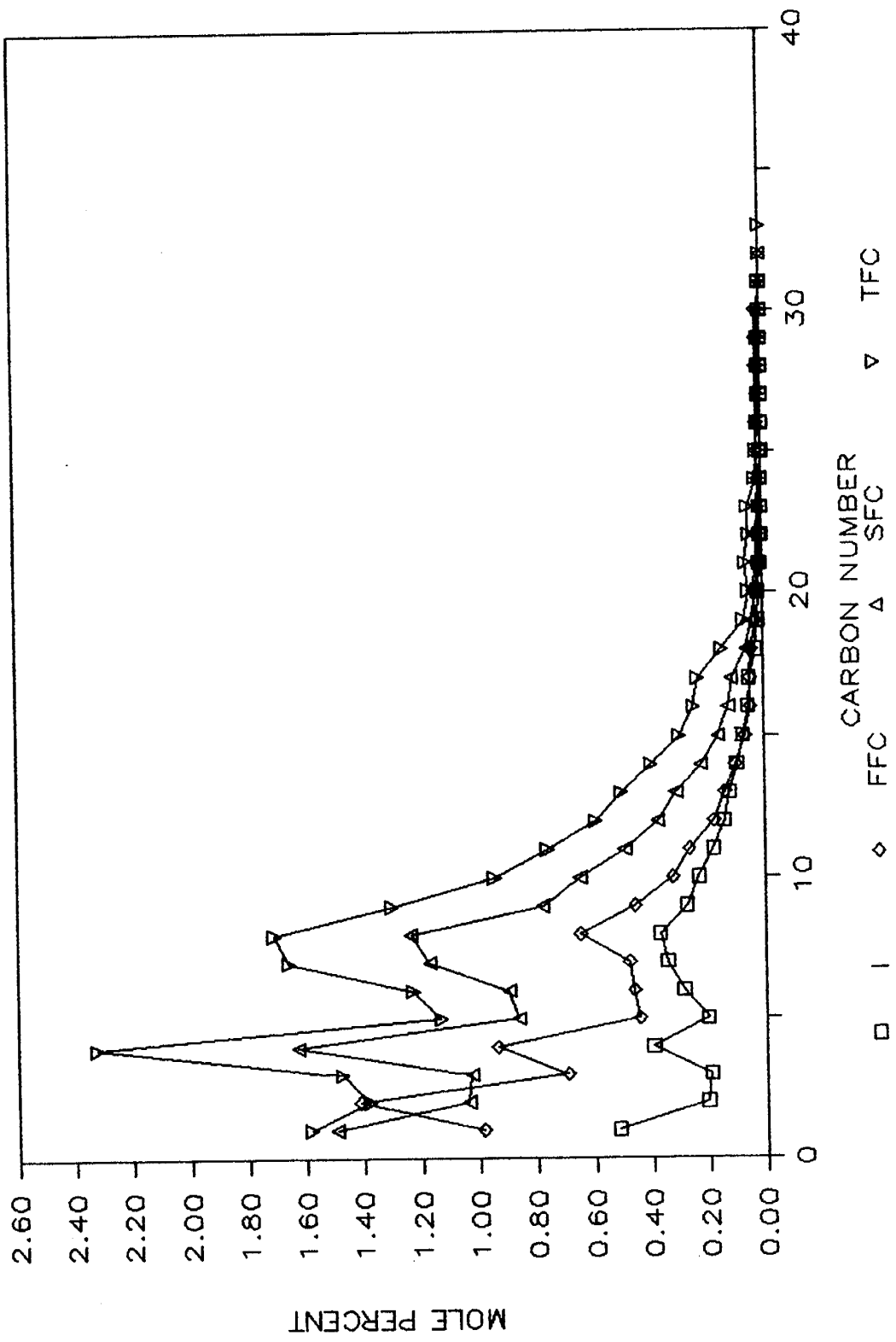


Figure 38.

Table 17: Composition of the Liquid Collected from Flashing the CO<sub>2</sub>-Rich Phase in the Forward Contacts

Component	(Mole Percent)	
	Initial	TFC
C-4	0.813	1.647
C-5	2.504	2.298
C-6	4.172	5.072
C-7	7.859	11.860
C-8	12.394	16.673
C-9	10.885	12.253
C-10	10.966	10.908
C-11	9.323	8.837
C-12	8.351	6.796
C-13	7.082	5.737
C-14	5.650	4.509
C-15	4.515	3.347
C-16	3.476	2.698
C-17	3.392	2.526
C-18	2.422	1.583
C-19	1.634	0.716
C-20	0.732	0.515
C-21	1.002	0.584
C-22	0.643	0.446
C-23	0.742	0.413
C-24	0.463	0.172
C-25	0.228	0.118
C-26	0.163	0.099
C-27	0.156	0.063
C-28	0.128	0.042
C-29	0.112	0.040
C-30	0.098	0.028
C-31	0.099	0.014
C-32	0.000	0.005
C-33	0.000	0.003
Molecular Weight (g/g-mole)	161.5	147.4

LIQUID COMPOSITION FROM FLASH OF CO<sub>2</sub>-RICH PHASE IN FORWARD CONTACTS

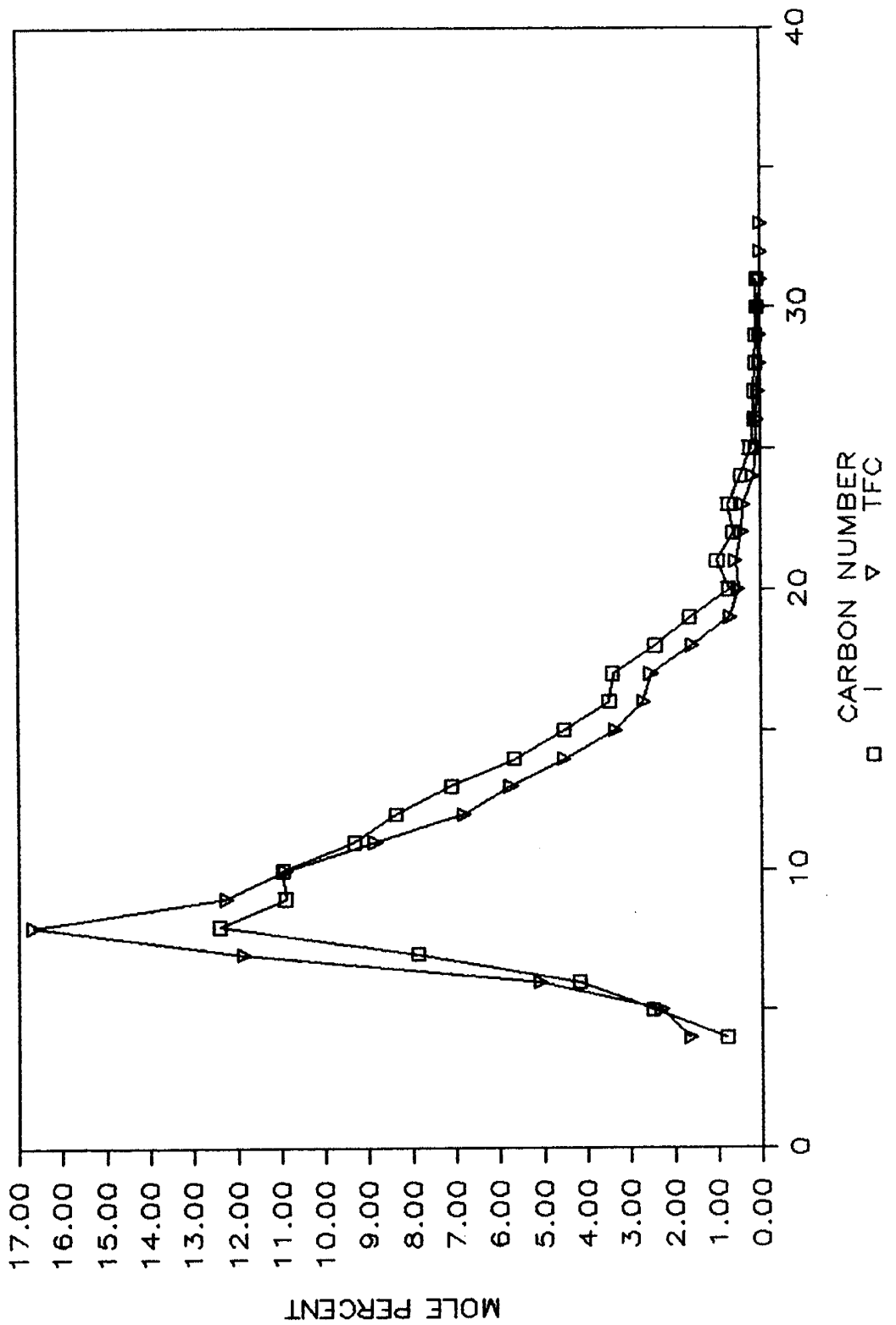


Figure 39.

Table 18: Oil-Rich Phase in the Forward Contacts - Molecular Weight

Mixture	Molecular Weight (g/g-mole)		
	High Pressure/ Temperature	Recombination of Flash	Liquid From Flash
Initial	78.0	127.8	291.7
First Forward Contact	89.8	96.4	218.0
Second Forward Contact	79.6	86.1	192.7
Third Forward Contact	70.4	78.8	175.5

Table 19: Composition of the Oil-Rich Phase  
in the Forward Contacts<sup>a</sup>

COMPONENT	(Mole Percent)		SFC	TFC
	Initial	FFC		
C-1	0.664	1.227	0.559	0.739
CO2	63.684	64.318	64.797	65.482
C-2	0.364	0.114	1.372	1.711
C-3	0.336	1.010	1.489	1.545
C-4	0.587	1.940	2.643	3.101
C-5	0.570	1.288	1.720	1.571
C-6	1.961	2.539	2.067	1.948
C-7	1.743	2.881	2.839	2.891
C-8	1.823	2.844	3.108	3.299
C-9	1.408	2.043	2.127	2.212
C-10	1.388	1.921	2.023	2.079
C-11	1.330	1.795	1.809	1.827
C-12	1.333	1.590	1.606	1.587
C-13	1.363	1.520	1.453	1.478
C-14	1.201	1.281	1.306	1.266
C-15	1.343	1.167	1.028	1.029
C-16	1.134	1.015	1.015	0.938
C-17	1.179	1.057	0.988	0.934
C-18	1.108	0.868	0.776	0.762
C-19	0.782	0.535	0.586	0.408
C-20	0.750	0.665	0.468	0.454
C-21	0.809	0.489	0.436	0.392
C-22	0.782	0.461	0.391	0.336
C-23	0.685	0.517	0.463	0.393
C-24	0.573	0.289	0.232	0.201
C-25	0.507	0.302	0.248	0.206
C-26	0.478	0.269	0.223	0.185
C-27	0.508	0.232	0.181	0.156
C-28	0.470	0.297	0.225	0.184
C-29	0.418	0.222	0.181	0.154
C-30	0.396	0.189	0.149	0.125
C-31	0.368	0.215	0.133	0.112
C-32	0.305	0.181	0.116	0.094
C-33	0.679	0.177	0.107	0.085
C-34	0.090	0.167	0.088	0.067
C-35	0.333	0.168	0.084	0.061
C-36+	6.548	2.206	0.969	0.000
Molecular Weight (g/g-mole)	172.8	96.4	86.1	78.8

<sup>a</sup> All values are calculated from recombination of flash liberation data.

# COMPOSITION OF THE OIL-RICH PHASE OF THE FORWARD CONTACTS

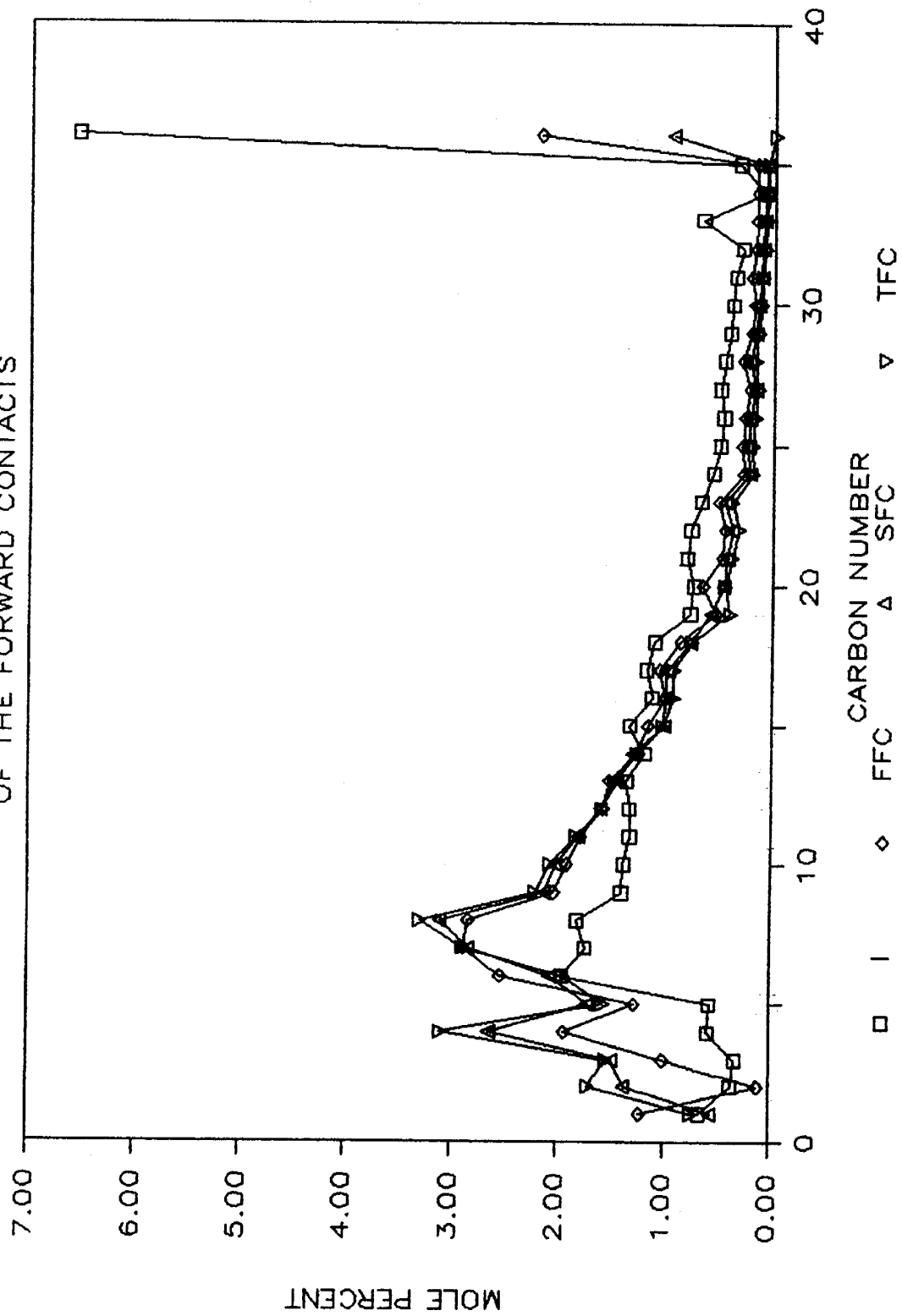


Figure 40.

Table 20: Composition of the Liquid Collected from Flashing the Oil-Rich Phase in the Forward Contacts

COMPONENT	(Mole Percent)		SFC	TFC
	Initial	FFC		
C-4	0.000	1.279	1.872	2.063
C-5	1.006	2.429	3.291	2.542
C-6	5.326	5.533	6.864	5.232
C-7	4.803	8.193	9.714	9.819
C-8	5.227	8.932	11.632	12.039
C-9	4.137	6.643	7.932	8.443
C-10	4.104	6.487	7.533	8.028
C-11	3.936	6.059	6.511	7.056
C-12	3.946	5.369	5.776	6.126
C-13	4.033	5.133	5.290	5.705
C-14	3.554	4.325	4.625	4.888
C-15	3.974	3.941	3.688	3.973
C-16	3.358	3.428	3.422	3.622
C-17	3.490	3.568	3.385	3.607
C-18	3.278	2.929	2.527	2.944
C-19	2.314	1.807	1.803	1.574
C-20	2.220	2.246	1.452	1.755
C-21	2.395	1.652	1.329	1.474
C-22	2.315	1.556	1.166	1.299
C-23	2.209	1.745	1.323	1.517
C-24	1.697	0.977	0.667	0.776
C-25	1.501	1.020	0.695	0.795
C-26	1.414	0.910	0.627	0.716
C-27	1.505	0.782	0.519	0.603
C-28	1.391	1.002	0.643	0.709
C-29	1.238	0.750	0.532	0.596
C-30	1.172	0.638	0.435	0.481
C-31	1.090	0.726	0.380	0.433
C-32	0.902	0.613	0.318	0.364
C-33	2.011	0.598	0.285	0.326
C-34	0.267	0.563	0.232	0.260
C-35	0.985	0.568	0.222	0.236
C-36+	19.383	7.448	3.313	0.000
Molecular Weight (g/g-mole)	291.7	218.0	192.7	175.5

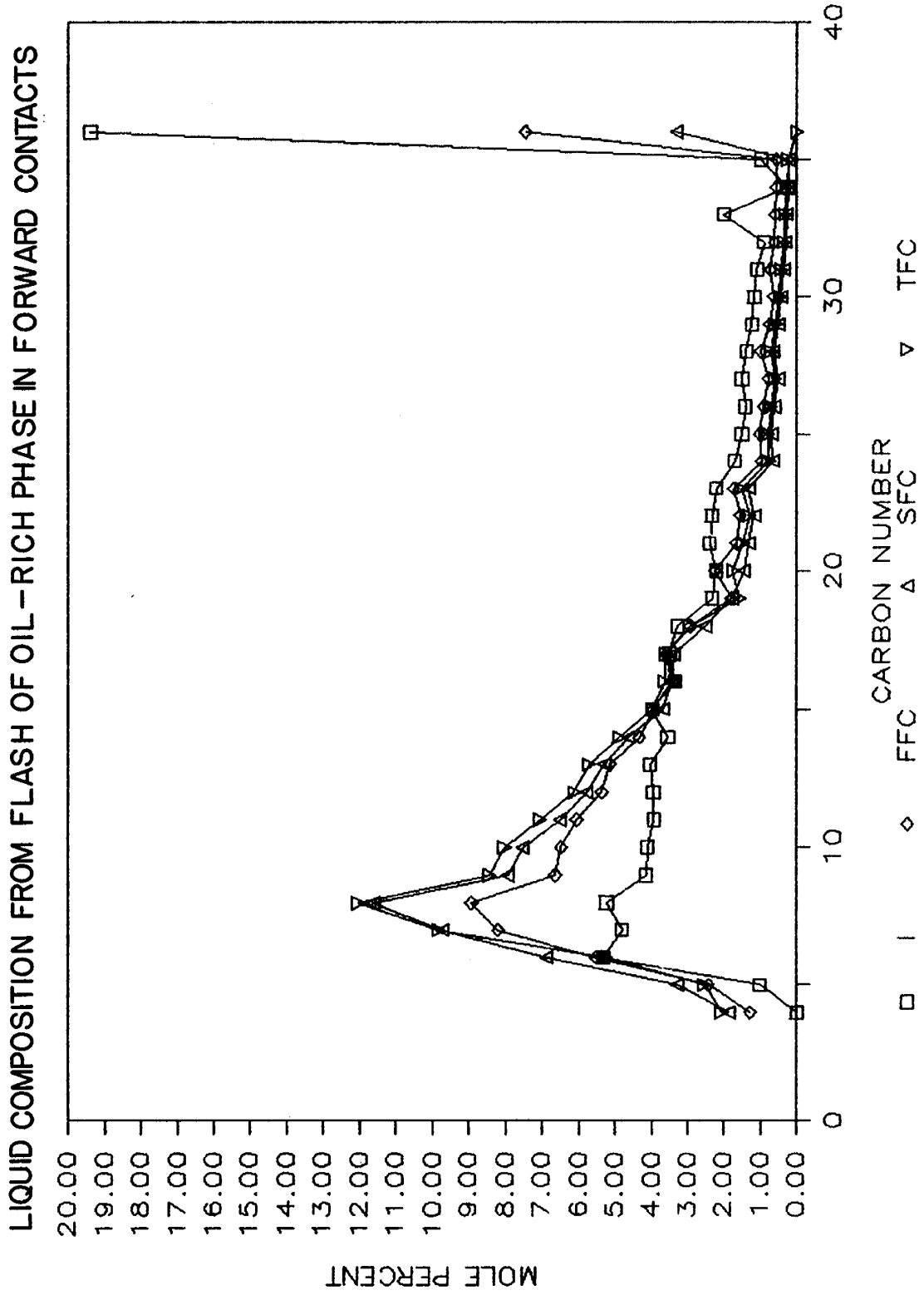


Figure 41.

Figure 42 shows a pseudoternary phase diagram constructed from the phase compositions in the forward contacts. The ternary diagram illustrates that the third forward contact is close to obtaining miscibility (Hutchinson and Braun, 1961). If a tangent is drawn to the two phase envelope of the same slope as the TFC tie line (commonly called a critical tie line), it is verified that the BF oil is multiple-contact miscible with carbon dioxide by the vaporizing-gas drive process at approximately 1809 psia and 111.9°F. The two phase envelope will get smaller as the pressure is increased if the temperature is held constant. With that in mind, miscibility may have been obtained at high pressure in the TFC as suggested by visual observations during that run. Figure 43 shows the same pseudoternary diagram, but the compositions of the initial and TFC CO<sub>2</sub>-rich phase were computed differently than the results shown in Figure 42. The values used in Figure 42 were computed by averaging the high pressure/temperature compositional results with the recombination of flash compositional results on an 1:1 basis and are deemed to be the best estimate of the true phase compositions. The values used in Figure 43 were computed from the high pressure/ temperature results only. The values used to construct Figures 42 and 43 are tabulated in Tables 21 and 22, respectively.

The results of the <sup>13</sup>C NMR analyses of the forward contact phases are shown in Table 23. The percent of aromatic carbon in the CO<sub>2</sub>-rich phase is higher for the initial mixture than for the other contacts. A likely explanation of this result is that the initial mixture extracts more of the higher molecular weight components (Figure 39). Aromatic carbons are associated more with high molecular weight hydrocarbons (Bunger and Li, 1981). The percent of aromatic carbon in the CO<sub>2</sub>-rich phase is lower for the FFC than for the other contacts. A likely explanation of this result is that hydrocarbon interactions in the oil-rich phase cause aromatics to selectively concentrate in the oil-rich phase (see below). This selective concentration is limited by solid phase precipitation in the SFC and TFC. The percent of aromatic carbon in the oil-rich phase decreases as the contacts advance as a result of solid phase precipitation. Aromatic carbon percent for the oil-rich phase in the TFC is somewhat higher than that for the SFC, although the difference may be within the ± 1% reproducibility of the measurements. A greater amount of precipitate was noted in the PVT cell for the TFC, and some of that solid phase may have been mobilized during flash liberation of the TFC oil-rich phase. This is not easily substantiated by the PVT program volumetric calculations, because the program's calculated total sample volume after the flash cannot account for the large amount of precipitate coating the inside of the cell.

Figure 44 shows the results of the aromatic carbon and STO mass balances. It is evident that the STO mass balance is within an experimental error of ±6% for all of the contacts. The aromatic carbon mass balance is within the same experimental error for the initial and FFC mixtures. Since the aromatic carbon mass balance depends upon the mass of STO, the <sup>13</sup>C NMR results for the initial and FFC seem very credible. Large amounts of precipitate were noted for the SFC and TFC. Figure 44 shows that the aromatic carbon percent errors for the SFC and TFC are very high. This suggests that the precipitate has a very high aromatic carbon content and agrees with the reported solid phase measurement of about 30% aromatic carbon content (Monger, 1984). It is believed that the aromatic carbons are largely present in very high molecular weight, multi-ring structures suspended in the crude oil (Bunger and Li, 1981). As the oil composition is altered during the development of miscibility so that high molecular weight hydrocarbons concentrate in the oil-rich phase, attractive molecular interactions between the multi-ring structures cause the more paraffinic hydrocarbons to be expelled. It has been proposed that

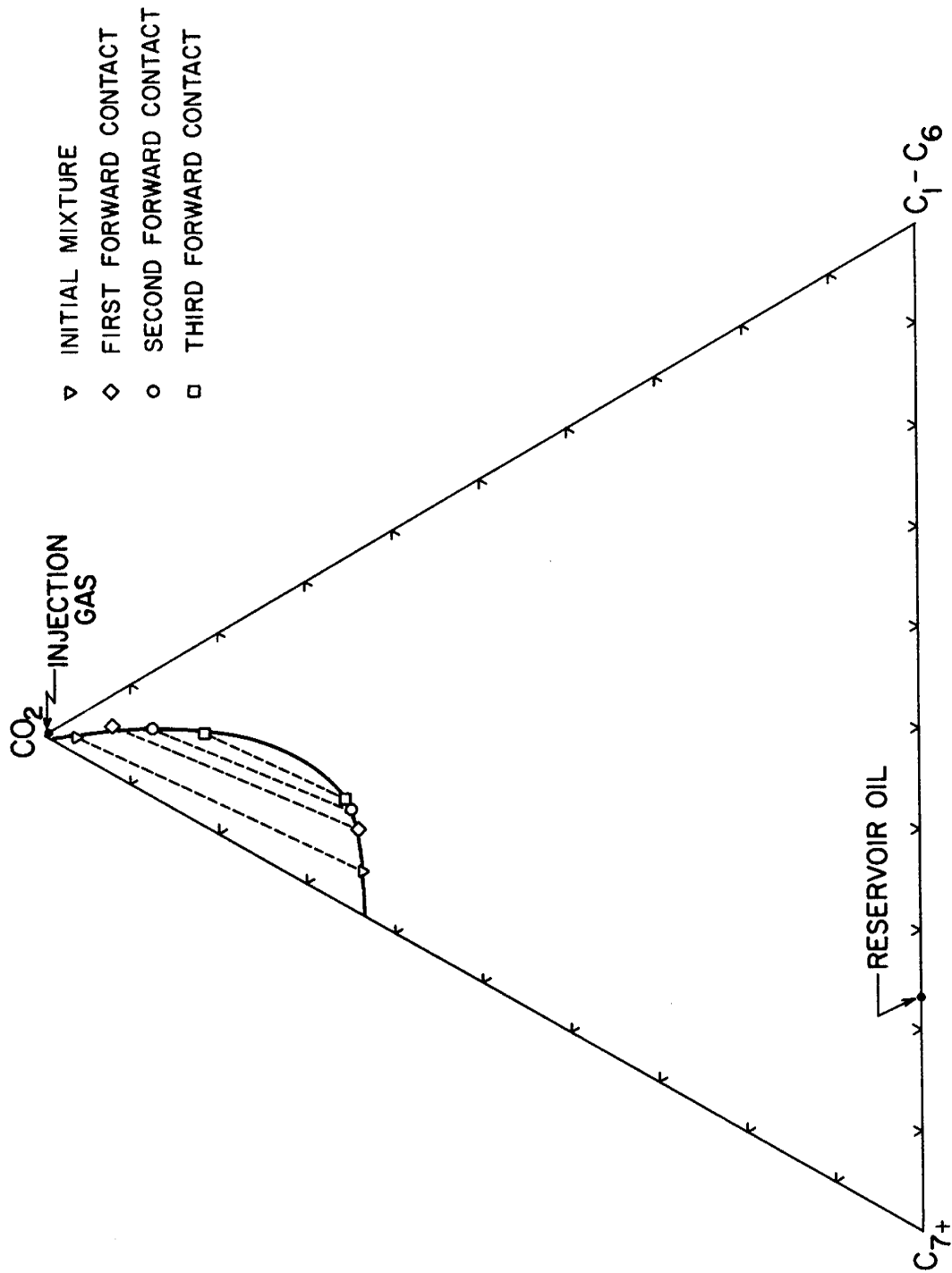


Figure 42. Best Estimate Pseudoternary Representation of the Mole Percent Composition of the CO<sub>2</sub>-Rich Phase in the Forward Contacts at @ 1809 psia and 111.9 °F

Table 21: Best Estimate of Phase Compositions in the Forward Contacts<sup>a</sup>

Mixture	Phase	Mole % CO <sub>2</sub>	Mole % C <sub>1</sub> -C <sub>6</sub>	Mole % C <sub>7+</sub>	MW (g/g-mole)
Initial	CO <sub>2</sub> -Rich <sup>b</sup>	96.155	1.798	2.047	46.3
	Oil-Rich	63.684	4.482	31.834	127.8
First Forward Contact	CO <sub>2</sub> -Rich <sup>c</sup>	92.059	4.926	3.015	47.3
	Oil-Rich	64.318	8.117	27.565	96.4
Second Forward Contact	CO <sub>2</sub> -Rich <sup>c</sup>	87.272	6.945	5.783	50.0
	Oil-Rich	64.797	9.849	25.354	86.1
Third Forward Contact	CO <sub>2</sub> -Rich <sup>b</sup>	81.723	9.131	9.146	54.3
	Oil-Rich	65.481	10.615	23.904	78.8

<sup>a</sup> Oil-rich phase composition calculated from recombination of flash data.

<sup>b</sup> Composition calculated from combination of high pressure/temperature and flash data.

<sup>c</sup> Composition calculated from high pressure/temperature data.

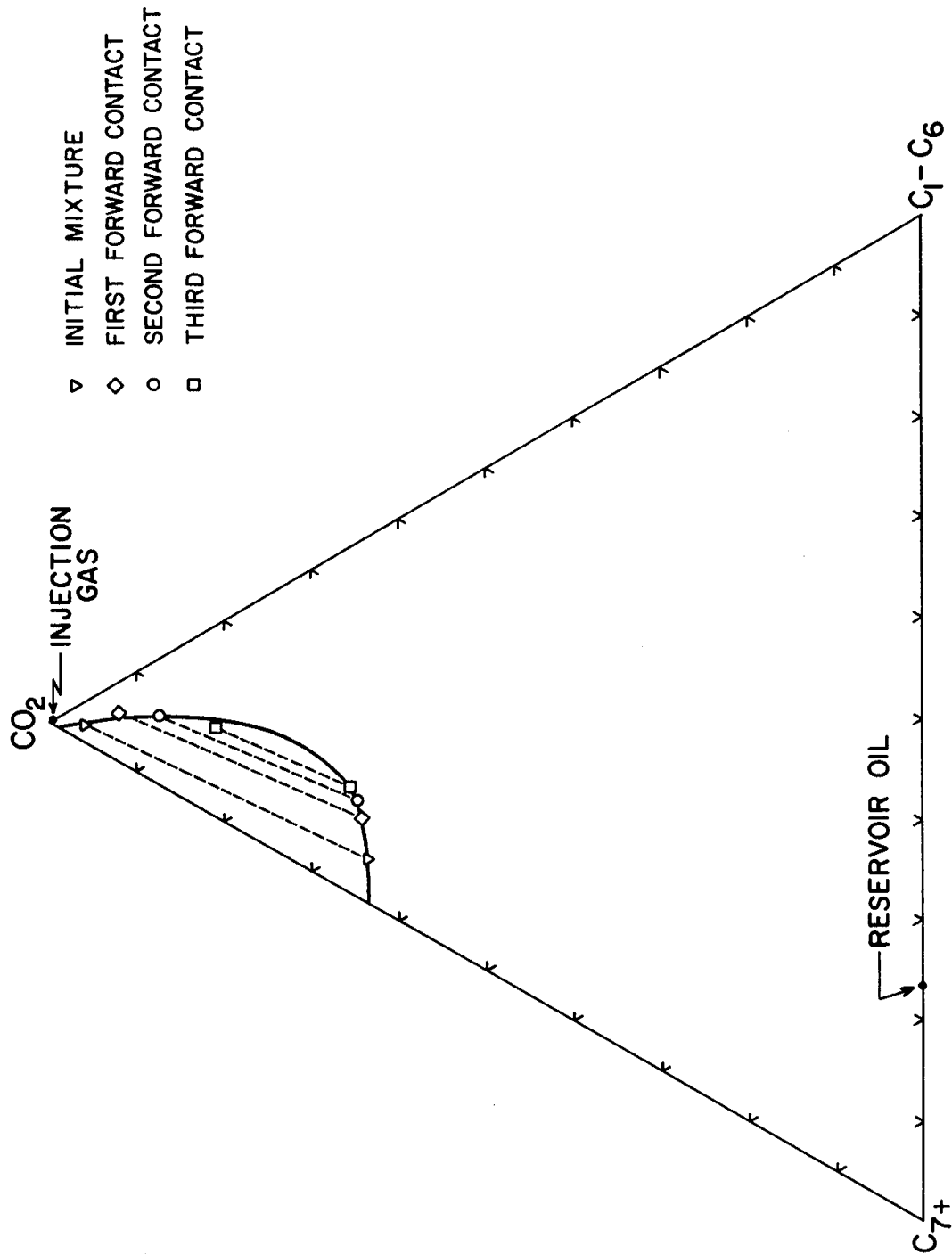


Figure 43. Pseudoternary Representation of the Mole Percent Compositions of the CO<sub>2</sub>-Rich and Oil-Rich Phases in the Forward Contacts at approximately 1809 psia and 111.9 °F

Table 22: Phase Compositions in the Forward Contacts<sup>a</sup>

Mixture	Phase	Mole % CO <sub>2</sub>	Mole % C <sub>1</sub> -C <sub>6</sub>	Mole % C <sub>7</sub> +	MW (g/g-mole)
Initial	CO <sub>2</sub> -Rich	95.928	1.750	2.323	46.4
	Oil-Rich	63.684	4.482	31.834	127.8
First Forward Contact	CO <sub>2</sub> -Rich	92.059	4.926	3.015	47.3
	Oil-Rich	64.318	8.117	27.565	96.4
Second Forward Contact	CO <sub>2</sub> -Rich	87.272	6.945	5.783	50.0
	Oil-Rich	64.797	9.849	25.354	86.1
Third Forward Contact	CO <sub>2</sub> -Rich	80.987	8.932	10.171	55.6
	Oil-Rich	65.481	10.615	23.904	78.8

<sup>a</sup> All oil-rich phase compositions were calculated from flash data. All CO<sub>2</sub>-rich phase compositions were calculated from high pressure/temperature data.

Table 23:  $^{13}\text{C}$  NMR Results in the Forward Contacts

Mixture	Percent of Aromatic Carbon	
	$\text{CO}_2$ -Rich Phase	Oil-Rich Phase
Initial	8.1	13.7
First Forward Contact	4.0	13.1
Second Forward Contact	6.9	7.3
Third Forward Contact	6.3	9.6

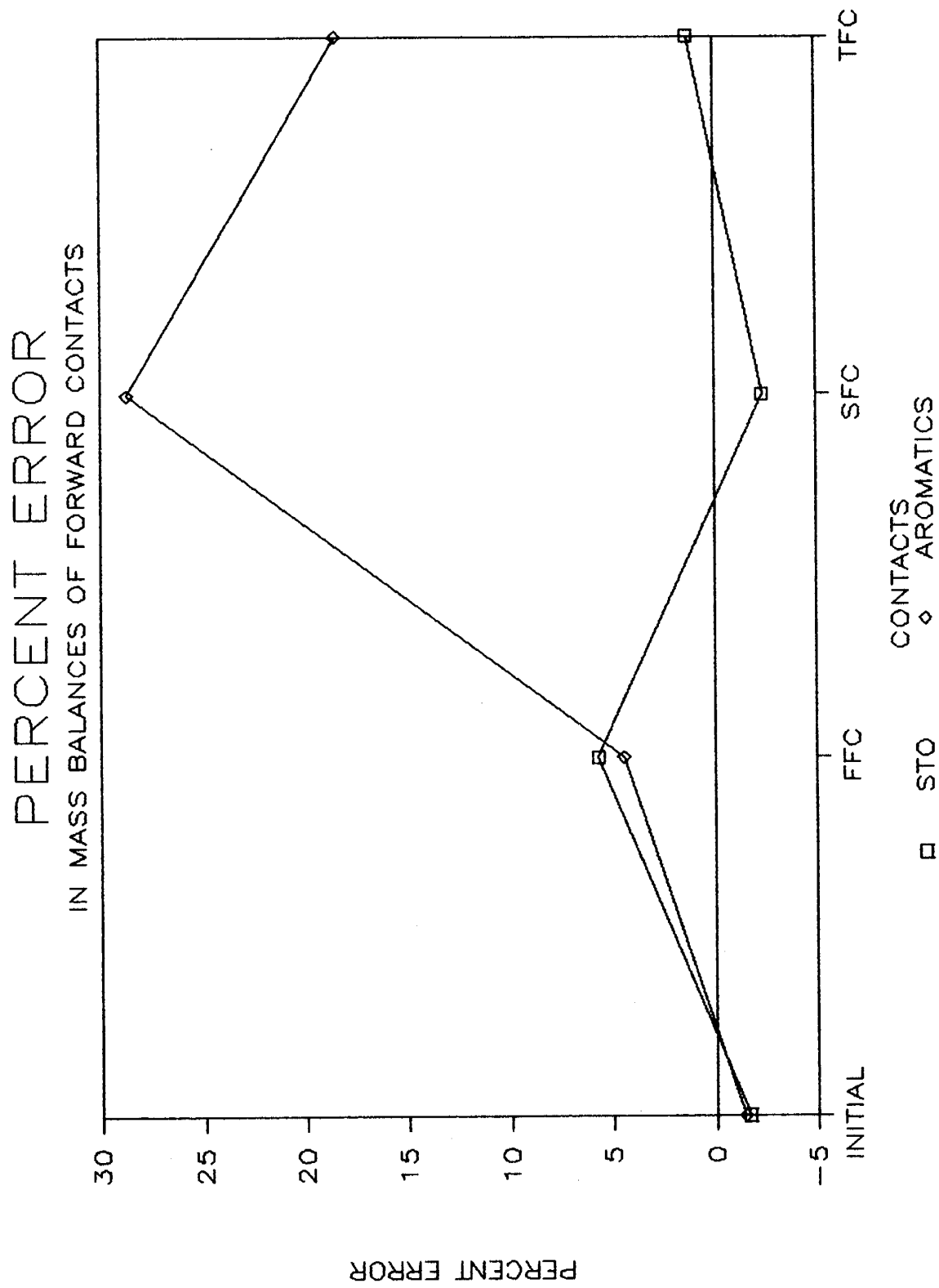


Figure 44.

this expulsion of paraffinic hydrocarbons enhances the development of miscibility (Monger, 1984).

### Results and Discussion of the Swept Zone Contacts

Starting with the initial mixture, Figure 45 illustrates the volume percent composition and resulting percent phase volumes at approximately 1821 psia and 111.5° F for the swept zone contacts.

Visual observations during the first swept zone contact (FSZC) revealed that a second liquid phase developed as mercury was injected into the cell to increase pressure, but disappeared upon cell equilibration. This non-equilibrium second liquid phase first formed at approximately 1350 psia and appeared to condense out of the CO<sub>2</sub>-rich phase. As the pressure increased, the amount of the non-equilibrium second liquid phase decreased. The oil-rich phase appeared very viscous because a dark film remained on the cell window during pressure and interface readings. The film was thin enough to transmit light, and the non-equilibrium second liquid phase washed it off the window above the interface. The film thus presented no problems in interface reading. At 2500 psia, bubbles appeared on top of the oil-rich phase next to the cell window indicating an increase in the surface tension. An increase in the interface's curvature was noted along with the bubbles. No precipitate of any type was observed on the cell windows during the FSZC.

Visual observations during the second swept zone contact (SSZC) were very similar to those in the FSZC; except that the appearance of the non-equilibrium second liquid phase stopped at 3000 psia. The film on the cell window appeared to be a little darker suggesting that the oil-rich phase in the SSZC was more viscous than the FSZC. The film did not hamper interface reading. The bubbles and the apparent increase in interface curvature were observed at approximately 2000 psia which is 500 psia lower than the FSZC. Again, no precipitate was observed on the cell windows. It thus appeared from visual observation that the system became more immiscible with successive swept zone contacts.

Figures 46 and 47 show the total sample volume versus pressure and percent phase volumes versus pressure graphs for the swept zone contacts. The graphs of percent phase volumes show a slight break in the curves at about 1400 psia for the FSZC and 1450 psia for the SSZC. At pressures below the break, the system exhibits liquid-gas compressibility as the CO<sub>2</sub>-rich phase is being compressed. The significant mechanism of mass transfer for most of this region is that CO<sub>2</sub> is forced to dissolve into the oil-rich phase. At pressures above the break, the system exhibits liquid-liquid compressibility and extraction of hydrocarbons into the CO<sub>2</sub>-rich phase becomes significant. Comparison of the FSZC and SSZC percent oil-rich phase volume curves shows that the two curves are identical to about 1400 psia because the compressibility of the CO<sub>2</sub>-rich phase remains about the same in successive contacts. At pressures greater than 1400 psia, the SSZC curve shows somewhat more swelling of the oil-rich phase because there are less extractable hydrocarbons carried over in the oil-rich phase from the previous contact. The rate at which the percent volume curves approach each other increases as the contacts advance. (The percent phase volume graphs for the initial 94.6% CO<sub>2</sub> - 5.4% BF oil mixture can be found in the Appendix.) This also indicates that there is less extraction of hydrocarbon and more swelling of the oil-rich phase as the contacts proceed. This explanation is confirmed by chromatographic compositional analysis of the oil-rich and CO<sub>2</sub>-rich phases.

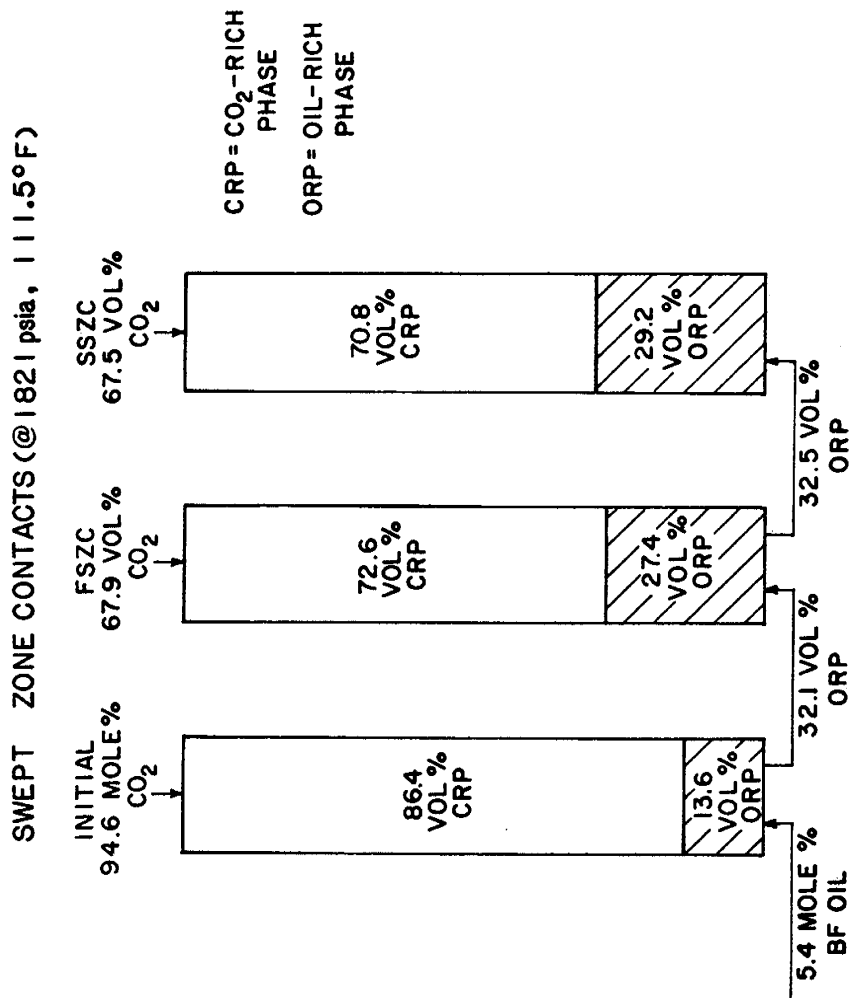


Figure 45. Summary of Swept Zone Contacts

# FIRST SWEEPED ZONE CONTACT 111.7F #2

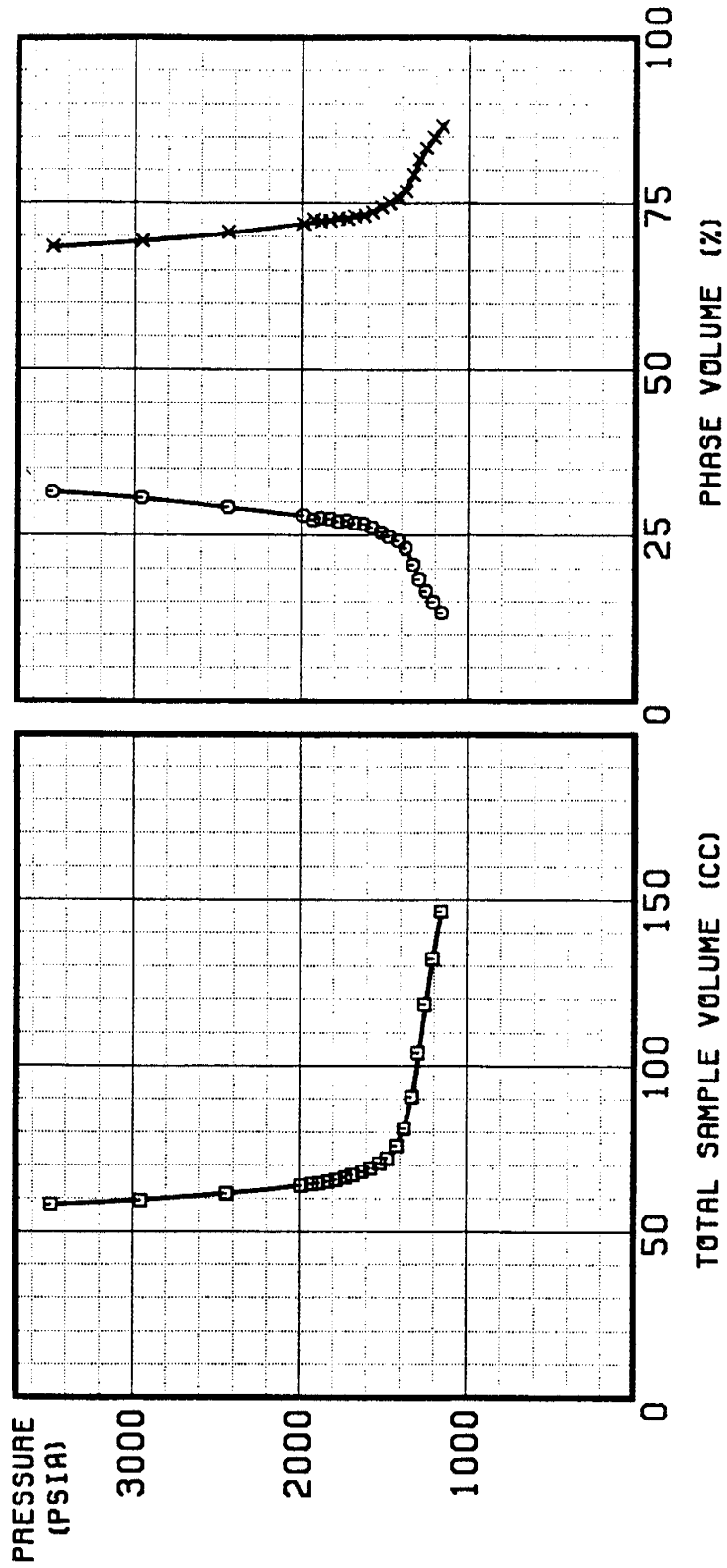


Figure 46. Pressure-Volume Isotherms (circles, oil-rich phase; x's, CO<sub>2</sub>-rich phase)

# SECOND SWEEP ZONE CONTACT 111.7F

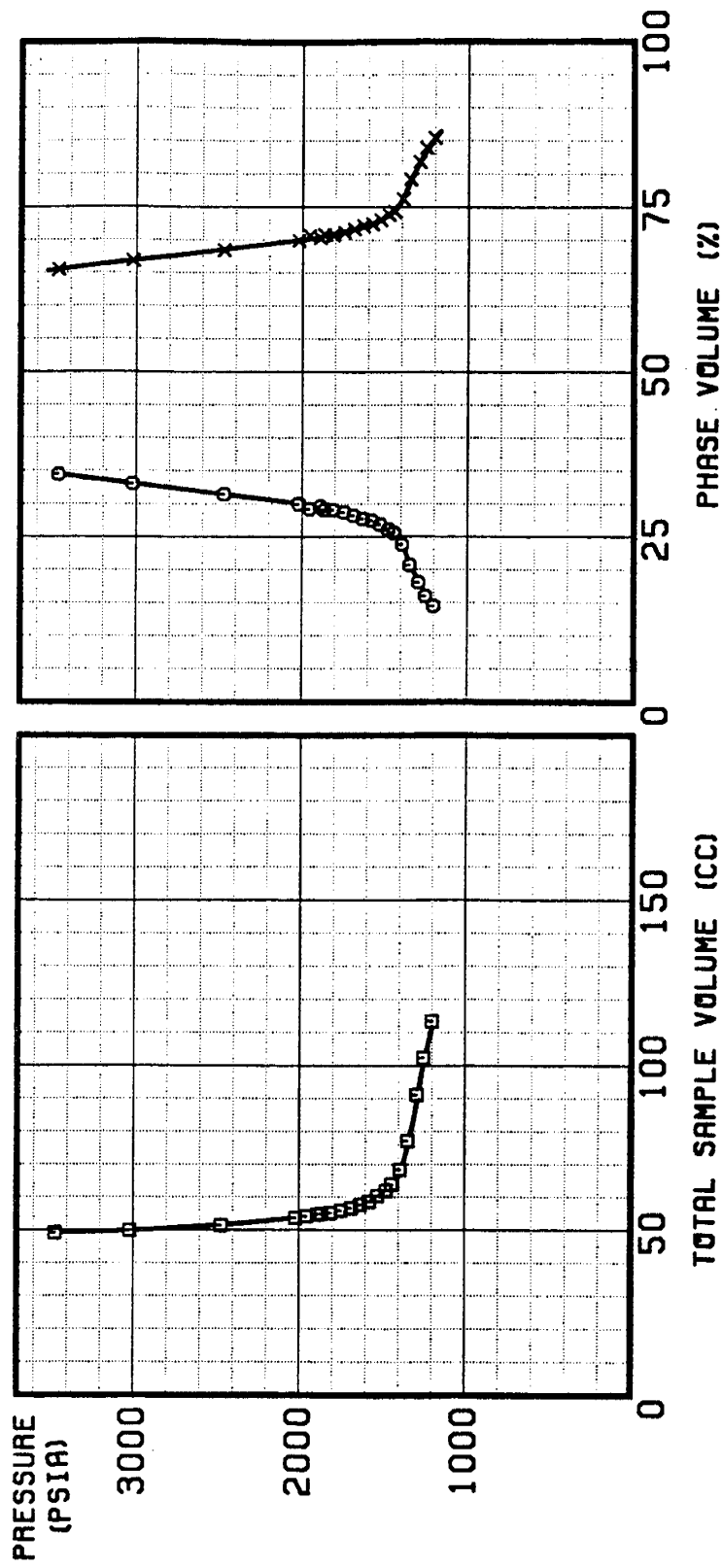


Figure 47. Pressure-Volume Isotherms (circles, oil-rich phase; x's, CO<sub>2</sub>-rich phase)

The swelling index curves for the swept zone contacts are shown in Figures 48 and 49. Figure 50 contrasts swelling observed for the FSZC, and SSZC, and the initial mixture. The swelling index curve for the SSZC is almost flat showing less competition between the CO<sub>2</sub> swelling and hydrocarbon extraction mass transfer mechanisms. (Difficulties encountered with the oil-rich phase volume calculations in the swept zone contacts may have somewhat exaggerated the difference between the FSZC and the SSZC curves.) Both the FSZC and the SSZC curves show a small but steady increase in the swelling index after a minimum value is reached at about 1800 psia; thus both swept zone contact curves approach, and the FSZC curve crosses the initial mixture curve. The above observations indicate that with successive swept zone contacts, hydrocarbon extraction becomes so insignificant that ultimately only minor swelling effects are produced by pressure changes.

Table 24 summarizes the physical properties of the CO<sub>2</sub>-rich phase in the swept zone contacts. The high pressure/temperature density, GLR, and SF were measured at approximately 1821 psia and 111.5°F. The density of the liquid obtained from a flash liberation was measured at room conditions. The high pressure/temperature density decreases as the contacts proceed because less hydrocarbons are extracted into the CO<sub>2</sub>-rich phase. The density of pure CO<sub>2</sub> at these conditions is 0.695 g/cc. The flashed liquid density increases as the contacts proceed because the small amounts of hydrocarbon that are extracted by the CO<sub>2</sub>-rich phase have increasingly higher molecular weights. The GLR increases and the SF decreases as the contacts proceed. Both indicate that less hydrocarbons are extracted.

The physical properties of the oil-rich phase from the swept zone contacts are summarized in Table 25. The high pressure/temperature density increases as the contacts proceed because the amount of CO<sub>2</sub> and light to intermediate hydrocarbons is decreasing. The same trend is seen in the flashed liquid densities. Both, the GLR and SF indicate that less CO<sub>2</sub> and volatile hydrocarbons are present in the oil-rich phase for each successive contact.

Table 26 shows the molecular weights calculated from the CO<sub>2</sub>-rich phase chromatographic data in the swept zone contacts. The agreement between the high pressure/temperature molecular weights and the recombination of flash molecular weights are well within experimental error. The trend illustrated by these results of decreasing molecular weight with successive contacts, again indicates that less hydrocarbons are extracted into the CO<sub>2</sub>-rich phase as the swept zone contacts proceed. The molecular weight of pure CO<sub>2</sub> is 44.0 g/g-mole. The chromatographic compositions for the CO<sub>2</sub>-rich phase in the swept zone contacts are given in Table 27 and shown in Figure 51. It is evident that the CO<sub>2</sub> content increases while the hydrocarbon content decreases as the contacts proceed because the hydrocarbons available for extraction decrease from contact to contact. The data also show that the initial mixture extracts mostly C<sub>1</sub> - C<sub>6</sub> hydrocarbons, while the FSZC extracts mostly C<sub>7</sub> - C<sub>12</sub> hydrocarbons. Thus the average molecular weight of the extracted hydrocarbons increases with successive contacts as confirmed by the flashed liquid molecular weight results shown in Table 26. Table 28 and Figure 52 show the chromatographic compositions of the liquids collected from flashing the CO<sub>2</sub>-rich phase in the swept zone contacts. It is again evident that the initial mixture extracts more C<sub>4</sub> - C<sub>10</sub> hydrocarbons while the FSZC and SSZC extract more C<sub>11</sub> - C<sub>28</sub> hydrocarbons. This again illustrates that there are less extractable hydrocarbons in each successive contact, and explains why the molecular weight of the flashed liquid increases from 161.5 g/g-mole for the initial mixture to 188.6 g/g-mole for the FSZC to 189.7 g/g-mole for the SSZC (Tables 26 and 28).

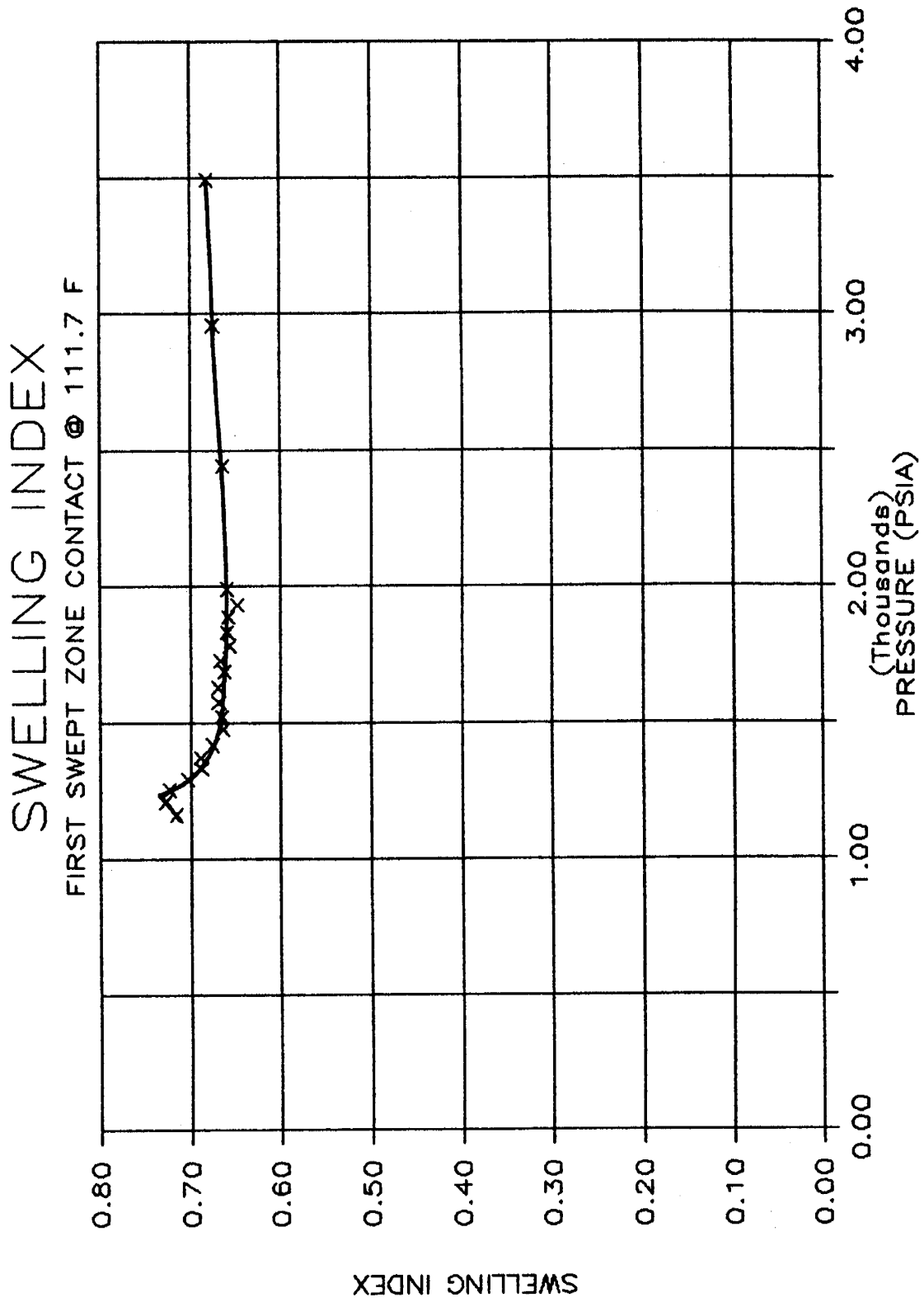


Figure 48.

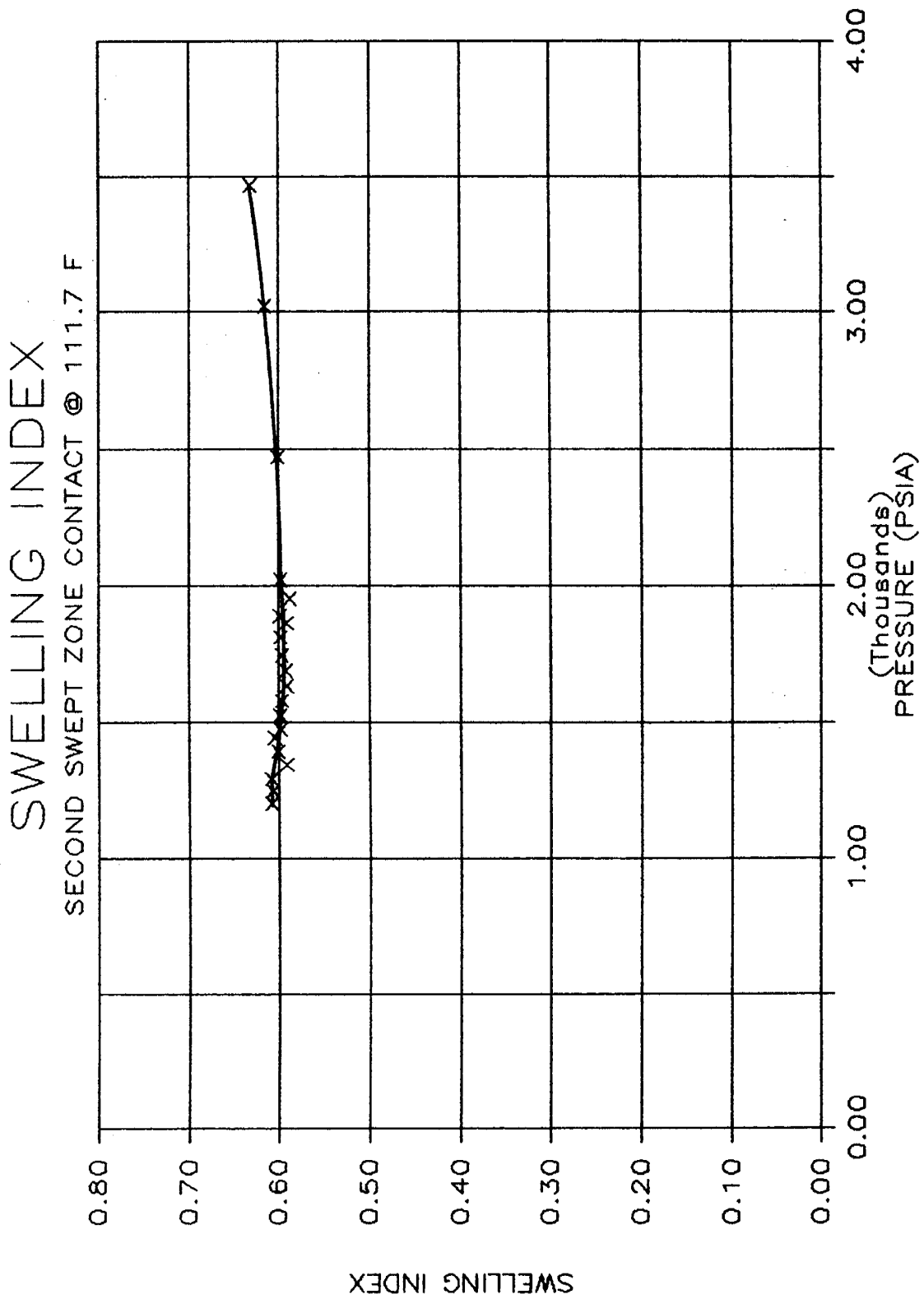


Figure 49.

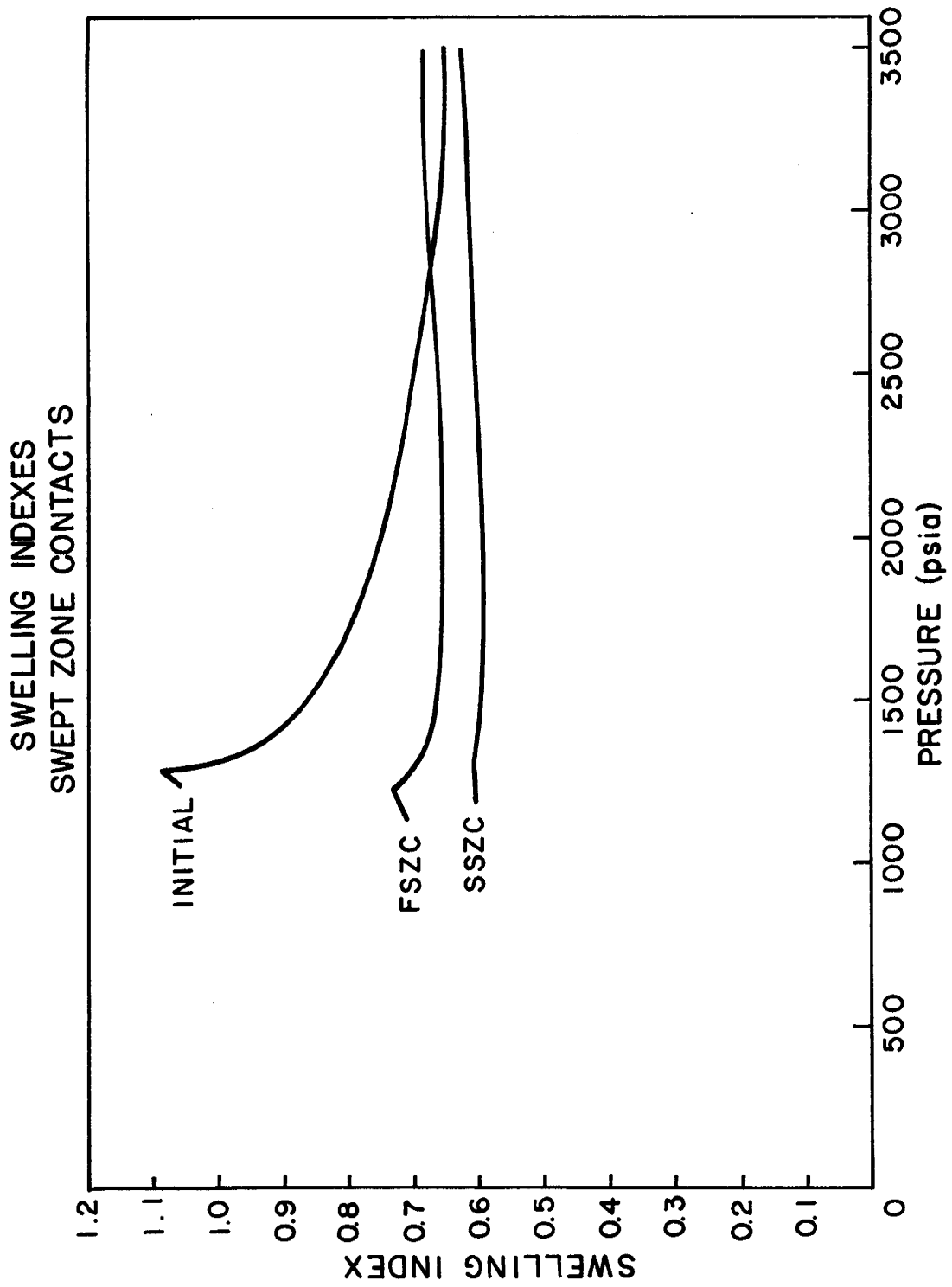


Figure 50.

Table 24: CO<sub>2</sub>-Rich Phase in the Swept Zone Contacts - Physical Properties

Mixture	High Pressure/ Temperature Density <sup>a</sup> (g/cc)	Liquid From Flash Density <sup>b</sup> (g/cc)	GLR <sup>a</sup> (CF/BBL)	SF <sup>a</sup> (BBL/RB)
Initial	0.7350	0.794	39,734	0.0577
First Swept Zone Contact	0.7303	0.819	63,230	0.0342
Second Swept Zone Contact	0.7208	0.828	179,849	0.0112

<sup>a</sup> Measured at approximately 1821 psia and 111.5°F.

<sup>b</sup> Measured at room conditions.

Table 25: Oil-Rich Phase in the Swept Zone Contacts - Physical Properties

Mixture	High Pressure/ Temperature Density <sup>a</sup> (g/cc)	Liquid From Flash Density <sup>b</sup> (g/cc)	GLR <sup>a</sup> (CF/BBL)	SF <sup>a</sup> (BBL/RB)
Initial	0.8844	0.882	788	0.8476
First Swept Zone Contact	0.8968	0.882	648	0.8599
Second Swept Zone Contact	0.9026	0.900	628	0.8815

<sup>a</sup> Measured at approximately 1821 psia and 111.5°F.

<sup>b</sup> Measured at room conditions.

Table 26: CO<sub>2</sub>-Rich Phase in the Swept Zone Contacts - Molecular Weight

Mixture	Molecular Weight (g/g-mole)		
	High Pressure/ Temperature	Recombination of Flash	Liquid From Flash
Initial	46.4	46.2	161.5
First Swept Zone Contact	45.1	45.7	188.6
Second Swept Zone Contact	44.4	45.5	189.7

Table 27: Composition of the CO<sub>2</sub>-Rich Phase  
in the Swept Zone Contacts<sup>a</sup>

Component	(Mole Percent)		
	Initial	FSZC	SSZC
C-1	0.516	0.187	0.145
CO2	96.155	97.905	99.301
C-2	0.207	0.103	0.022
C-3	0.194	0.067	0.020
C-4	0.394	0.129	0.039
C-5	0.202	0.123	0.023
C-6	0.286	0.117	0.027
C-7	0.344	0.302	0.050
C-8	0.369	0.311	0.070
C-9	0.274	0.226	0.052
C-10	0.232	0.156	0.051
C-11	0.181	0.076	0.041
C-12	0.140	0.048	0.036
C-13	0.122	0.053	0.030
C-14	0.096	0.035	0.022
C-15	0.075	0.035	0.020
C-16	0.056	0.026	0.012
C-17	0.052	0.028	0.012
C-18	0.030	0.019	0.009
C-19	0.020	0.012	0.005
C-20	0.017	0.011	0.004
C-21	0.012	0.008	0.003
C-22	0.007	0.007	0.002
C-23	0.007	0.004	0.001
C-24	0.004	0.003	0.001
C-25	0.002	0.003	0.001
C-26	0.001	0.002	0.001
C-27	0.001	0.002	0.001
C-28	0.001	0.001	0.000
C-29	0.001	0.001	0.000
C-30	0.001	0.000	0.000
C-31	0.001	0.000	0.000
Molecular Weight (g/g-mole)	46.3	45.4	44.5

<sup>a</sup> All values calculated by combining the high pressure/temperature results with the recombination of flash liberation data results on a 1:1 basis.

# COMPOSITION OF THE CO<sub>2</sub>-RICH PHASE OF THE SWEEPED ZONE CONTACTS

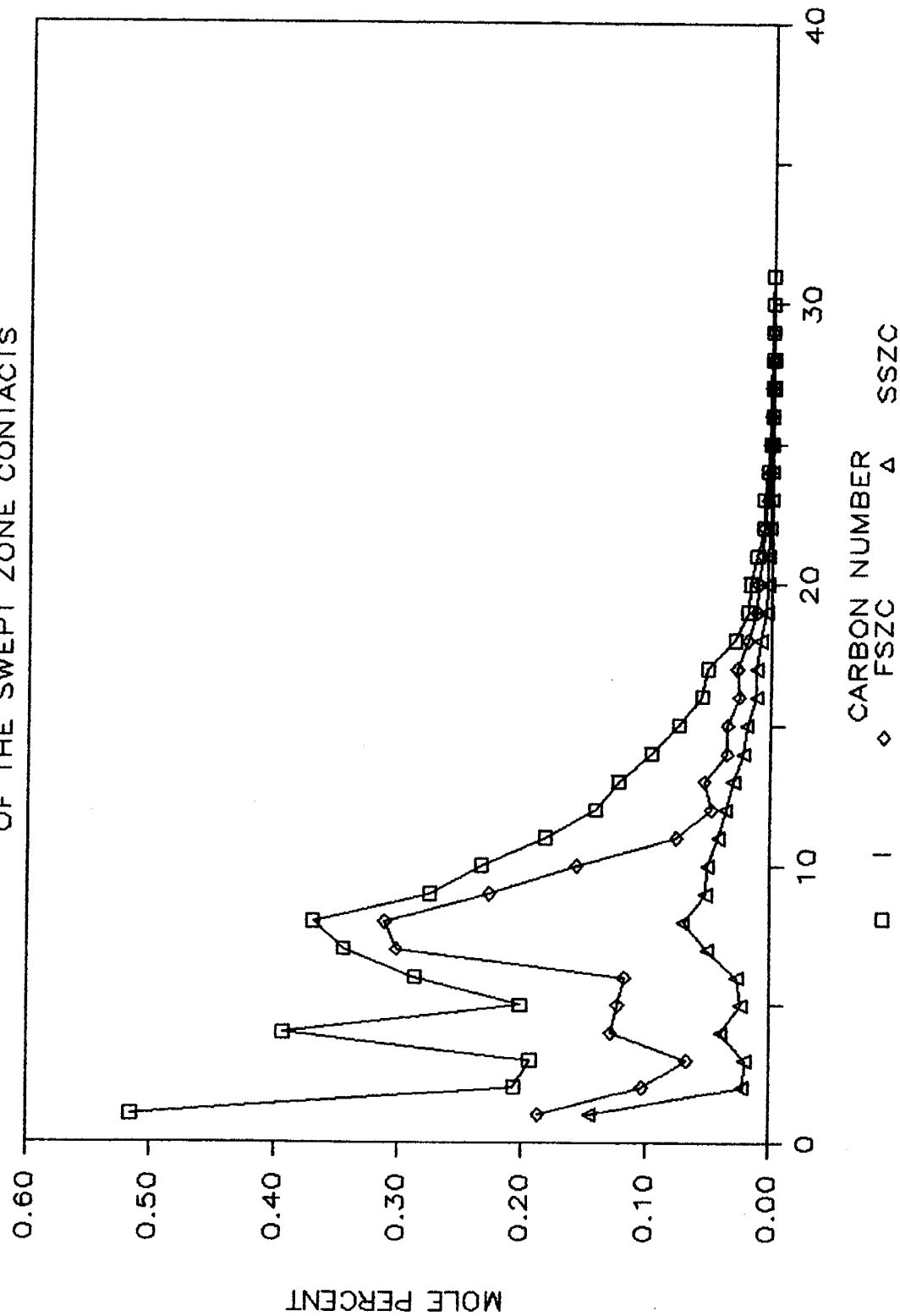


Figure 51.

Table 28: Composition of the Liquid Collected from Flashing the CO<sub>2</sub>-Rich Phase in the Swept Zone Contacts

Component	(Mole Percent)		
	Initial	FSZC	SSZC
C-4	0.813	0.000	0.013
C-5	2.504	0.009	0.215
C-6	4.172	0.894	1.463
C-7	7.859	3.054	3.847
C-8	12.394	7.366	4.851
C-9	10.885	8.204	6.380
C-10	10.966	10.104	9.307
C-11	9.323	10.266	10.287
C-12	8.351	9.596	10.160
C-13	7.082	9.366	9.802
C-14	5.650	7.251	8.027
C-15	4.515	7.206	7.826
C-16	3.476	5.369	6.015
C-17	3.392	5.624	6.310
C-18	2.422	3.831	4.825
C-19	1.634	2.382	2.522
C-20	0.732	2.444	1.967
C-21	1.002	1.723	2.028
C-22	0.643	1.521	1.268
C-23	0.742	0.947	0.883
C-24	0.463	0.674	0.650
C-25	0.228	0.595	0.470
C-26	0.163	0.507	0.363
C-27	0.156	0.496	0.326
C-28	0.128	0.309	0.196
C-29	0.112	0.263	0.000
C-30	0.098	0.000	0.000
C-31	0.099	0.000	0.000
Molecular Weight (g/g-mole)	161.5	188.6	189.7

LIQUID COMPOSITION FROM FLASH OF CO<sub>2</sub>-RICH PHASE IN SWEEP ZONE CONTACTS

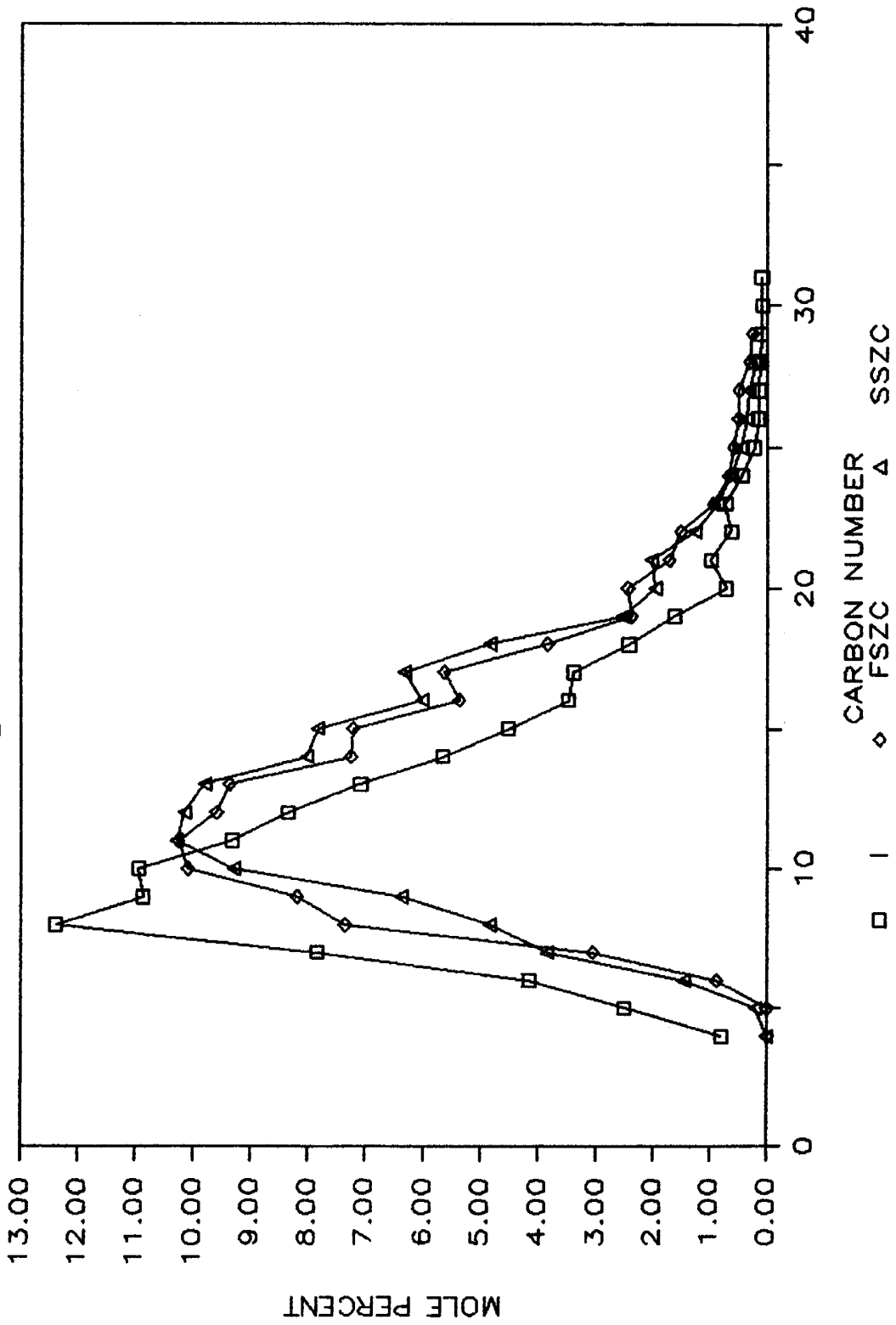


Figure 52.

The high pressure/temperature and recombination of flash molecular weights for the oil-rich phase in the swept zone contacts are shown in Table 29. Poor agreement is observed between the high pressure/temperature molecular weights and the recombination of flash molecular weights. The molecular weights calculated from the recombination of flash data are lower than those calculated from the high pressure/temperature data. Recalling similar results for the initial mixture and the forward contacts (Table 18), the agreement between high pressure/temperature and recombination of flash results was much improved, and the high pressure/temperature result were lower. Visual observations during runs and the appearance of the liquid collected from flash liberation of the oil-rich phase revealed that the oil-rich phase in the swept zone contacts was extremely viscous. It is believed that the high pressure/temperature sampling yoke and syringe lost CO<sub>2</sub> when flowing the oil-rich phase. The high pressure/temperature syringe thus collected samples somewhat depleted of CO<sub>2</sub>. This may have occurred because the viscous oil-rich phase interfered with the sealing of the packing in the high pressure/temperature syringe or yoke. Mass balance calculations of the CO<sub>2</sub> and hydrocarbon contents indicate that the recombination of flash data provide the best chromatographic composition for the oil-rich phase in the swept zone contacts. After a thorough examination of the chromatographic results from the high pressure/temperature syringe, the low pressure gas and liquid from flash liberation, as well as the GLR, it was concluded that the recombination of flash data are the best estimate of the true oil-rich phase composition in the swept zone contacts.

Table 30 and Figure 53 show the chromatographic compositional results for the oil-rich phase in the swept zone contacts. Table 30 indicates that the mole percent of CO<sub>2</sub> increases as the contacts proceed. The same trend is reported by Turek, et. al. (1984) for their CO<sub>2</sub> cycling (swept zone contacts) studies. Figure 53 shows that as the contacts proceed, the amount of C<sub>2</sub> - C<sub>14</sub> hydrocarbons decreases, with the C<sub>36+</sub> fraction representing a greater portion of the remaining hydrocarbons. These results illustrate CO<sub>2</sub>'s preference for intermediate molecular weight hydrocarbons. The C<sub>2</sub> - C<sub>14</sub> decrease and the C<sub>36+</sub> increase also explain why the calculated molecular weights increase as the contacts proceed (Tables 29 and 30). The same compositional trends are evident from the flashed liquid compositions (Table 31 and Figure 54). Figure 54 shows that nearly all of the C<sub>4</sub> - C<sub>10</sub> hydrocarbons are recovered by the SSZC, and that the C<sub>36+</sub> fraction increases as the contacts proceed. This again explains why the molecular weight of the flashed liquid from the oil-rich phase in the swept zone contacts increases as the contacts proceed (Table 29 and 31).

Table 32 summarizes the cumulative oil production in the swept zone contacts. The results of total hydrocarbon mass and liquid volume produced are presented as the percent of original oil in place (OOIP). Figure 55 is a graphical illustration of these results. Both mass and liquid volume cumulative productions show that CO<sub>2</sub>'s first contact with BF oil in the initial mixture recovers most of the extractable hydrocarbons, with each successive contact recovering significantly less. The curves in Figure 55 emphasize that maximum oil recovery is approached asymptotically with very little increase after the SSZC.

The results of the hydrocarbon type analyses for the swept zone contacts are shown in Table 33. The <sup>13</sup>C NMR results for the CO<sub>2</sub>-rich phase in the swept zone contacts indicate that about the same amount of aromatic carbon, which are associated with the heavy molecular weight hydrocarbons, are extracted into the CO<sub>2</sub>-rich phase in each contact. This is confirmed by the chromatographic compositional results (Table 28 and Figure 52). The <sup>13</sup>C NMR results for the oil-rich phase are difficult to interpret. They suggest that the percent of aromatic carbon increases from 13.7% for the initial mixture to 18.0% for the FSZC, and then decreases to

Table 29: Oil-Rich Phase in the Swept Zone Contacts - Molecular Weight

Mixture	Molecular Weight (g/g-mole)		
	High Pressure/ Temperature	Recombination of Flash	Liquid From Flash
Initial	78.0	127.8	291.7
First Swept Zone Contact	214.7	153.7	375.8
Second Swept Zone Contact	232.2	162.1	412.3

Table 30: Composition of the Oil-Rich Phase  
in the Swept Zone Contacts<sup>a</sup>

Component	(Mole Percent)		
	Initial	FSZC	SSZC
C-1	0.664	0.912	0.667
C02	63.684	64.032	66.732
C-2	0.364	0.285	0.036
C-3	0.336	0.089	0.022
C-4	0.587	0.291	0.075
C-5	0.570	0.504	0.226
C-6	1.961	0.998	0.019
C-7	1.743	1.364	0.058
C-8	1.823	0.782	0.270
C-9	1.408	0.520	0.328
C-10	1.388	0.509	0.391
C-11	1.330	0.574	0.435
C-12	1.333	0.761	0.687
C-13	1.363	1.003	0.949
C-14	1.201	1.127	0.821
C-15	1.343	1.056	1.141
C-16	1.134	1.201	0.989
C-17	1.179	1.311	1.220
C-18	1.108	1.048	0.930
C-19	0.782	0.943	0.896
C-20	0.750	0.882	0.924
C-21	0.809	0.810	0.765
C-22	0.782	0.761	0.877
C-23	0.685	0.936	0.631
C-24	0.573	0.506	0.573
C-25	0.507	0.508	0.620
C-26	0.478	0.504	0.602
C-27	0.508	0.420	0.649
C-28	0.470	0.525	0.507
C-29	0.418	0.442	0.475
C-30	0.396	0.361	0.401
C-31	0.368	0.310	0.345
C-32	0.305	0.270	0.274
C-33	0.679	0.223	0.234
C-34	0.090	0.174	0.172
C-35	0.333	0.138	0.152
C-36+	6.548	12.921	14.912
Molecular Weight (g/g-mole)	127.8	153.6	162.1

<sup>a</sup> All values are calculated from recombination of flash liberation data.

# COMPOSITION OF THE OIL-RICH PHASE OF THE SWEEP ZONE CONTACTS

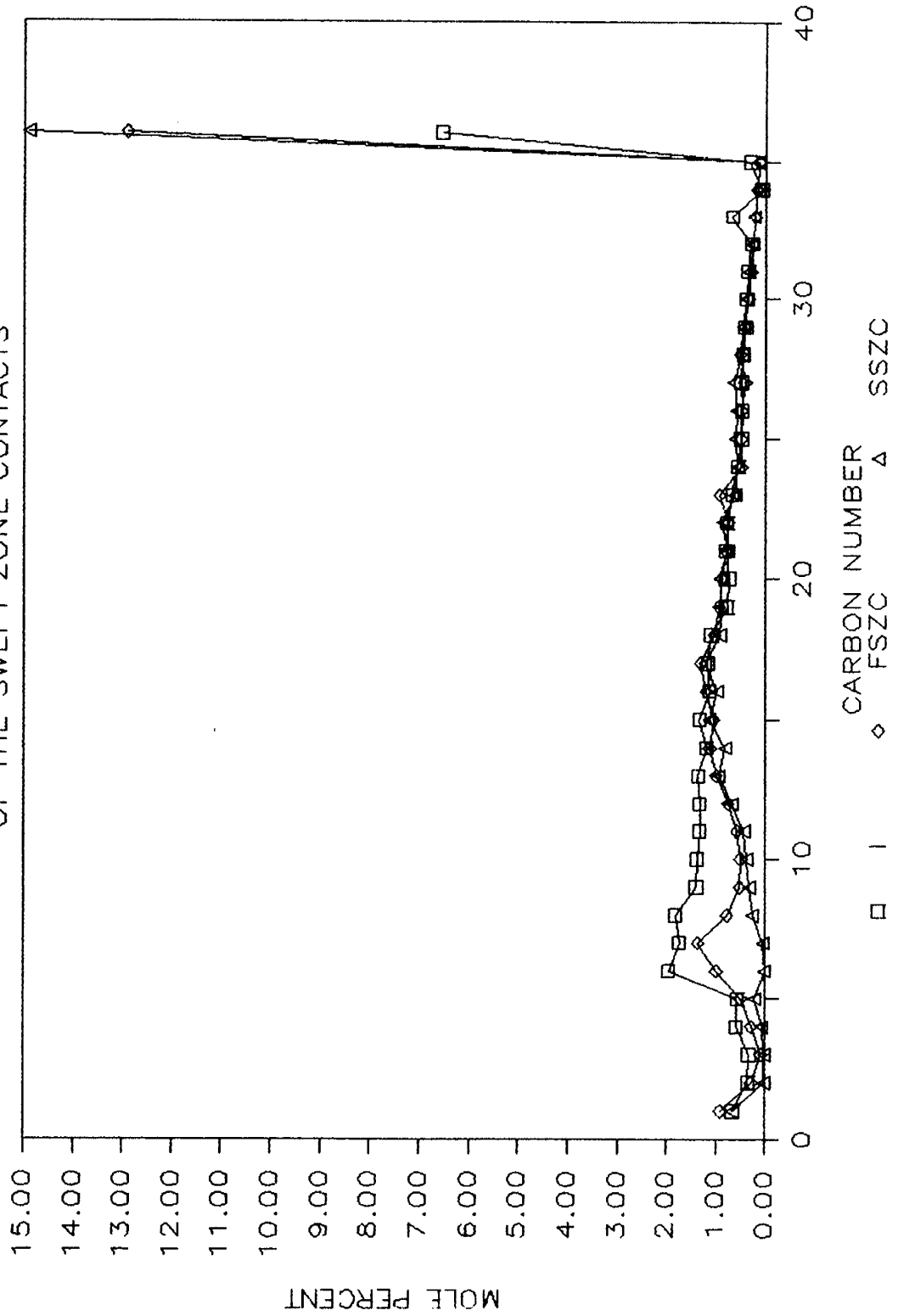


Figure 53.

Table 31: Composition of the Liquid Collected from Flashing the Oil-Rich Phase in the Swept Zone Contacts

Component	(Mole Percent)		
	Initial	FSZC	SSZC
C-5	1.006	0.000	0.000
C-6	5.326	0.125	0.000
C-7	4.803	4.141	0.019
C-8	5.227	2.374	0.605
C-9	4.137	1.580	0.961
C-10	4.104	1.546	1.218
C-11	3.936	1.743	1.355
C-12	3.946	2.311	2.143
C-13	4.033	3.045	2.957
C-14	3.554	3.422	2.560
C-15	3.974	3.207	3.556
C-16	3.358	3.647	3.082
C-17	3.490	3.980	3.803
C-18	3.278	3.181	2.898
C-19	2.314	2.863	2.793
C-20	2.220	2.678	2.881
C-21	2.395	2.461	2.384
C-22	2.315	2.312	2.733
C-23	2.029	2.843	1.968
C-24	1.697	1.537	1.787
C-25	1.501	1.542	1.932
C-26	1.414	1.529	1.876
C-27	1.505	1.275	2.022
C-28	1.391	1.594	1.580
C-29	1.238	1.342	1.482
C-30	1.172	1.096	1.249
C-31	1.090	0.942	1.075
C-32	0.902	0.820	0.853
C-33	2.011	0.678	0.729
C-34	0.267	0.529	0.536
C-35	0.985	0.420	0.474
C-36+	19.383	39.238	46.490
Molecular Weight (g/g-mole)	291.7	375.8	412.3

LIQUID COMPOSITION FROM FLASH OF OIL-RICH PHASE IN SWEEP ZONE CONTACTS

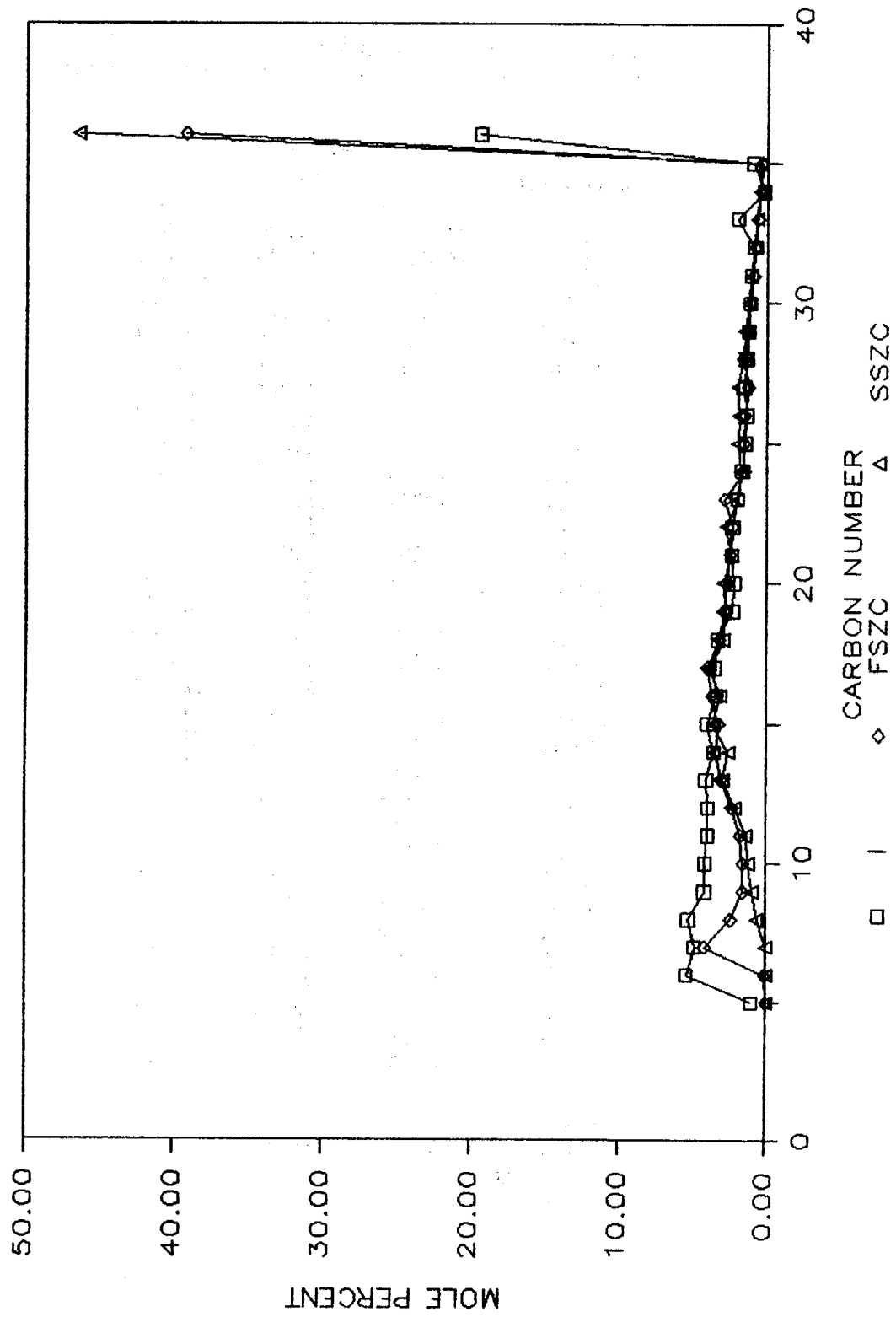


Figure 54.

Table 32: Cumulative Oil Production in the Swept Zone Contacts

Mixture	(Percent OOIP)	
	Mass	Liquid Volume
Initial	37.5	29.1
First Swept Zone Contact	45.3	35.1
Second Swept Zone Contact	47.4	36.8

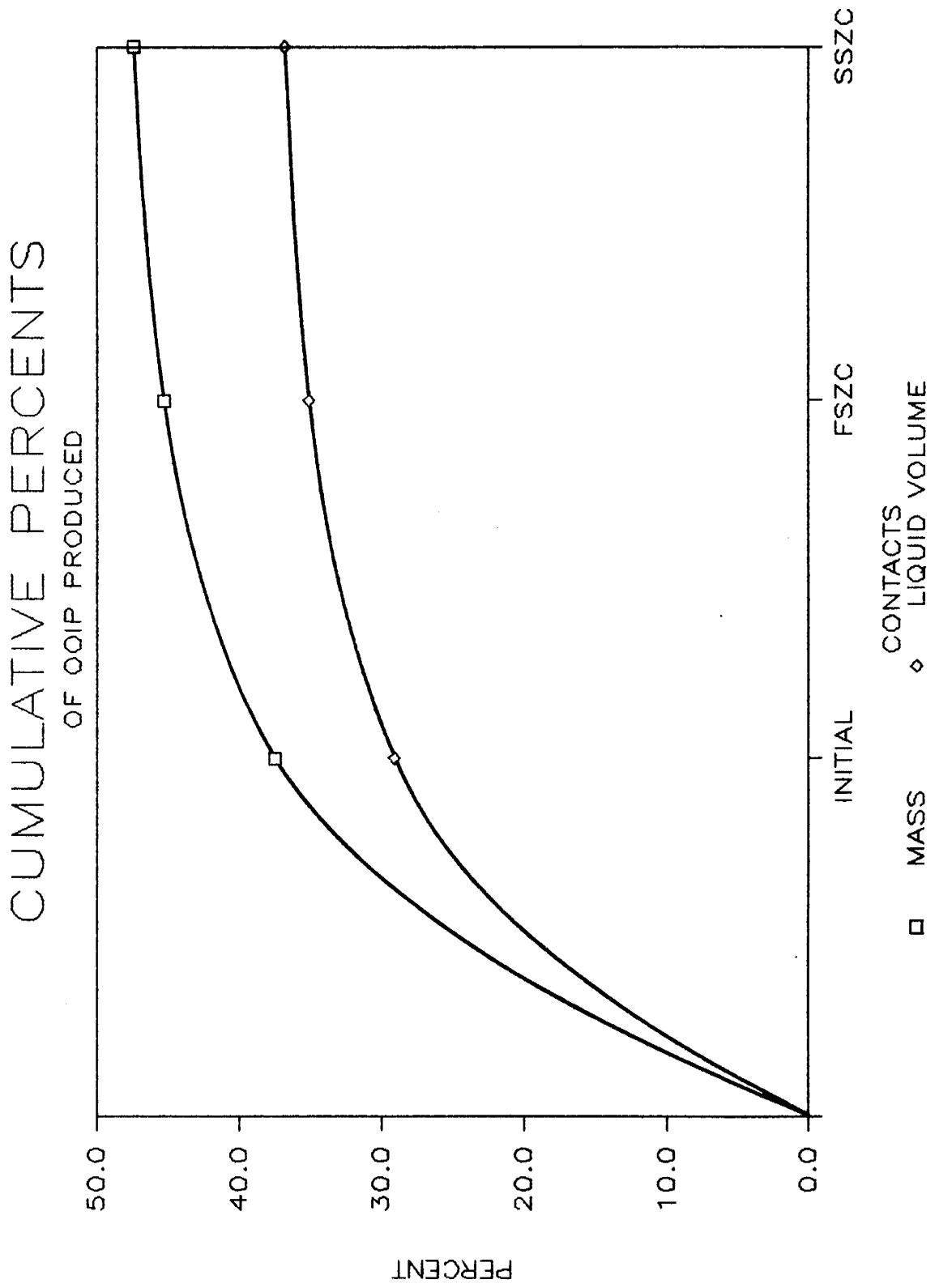


Figure 55.

Table 33: Results of Aromatic Carbon Mass Balance

Mixture	Percent of CO <sub>2</sub> -Rich Phase	Aromatic Carbons Oil-Rich Phase	% Error STO	% Error Aromatics
Initial	8.1	13.7	-0.90	-0.28
First Swept Zone Contact	7.5	18.0	-1.89	-25.46
Second Swept Zone Contact	8.8	13.8	5.46	28.46

13.8% for the SSZC. The STO and aromatic carbon mass balances are well within experimental error for the initial mixture and suggest that the results for the initial mixture are correct. The STO mass balance for the FSZC is within experimental error while the aromatic carbon mass balance is excessively high. If the assumptions made in performing the aromatic carbon mass balance are correct, then the negative percent error indicates that mass was generated. Since additional oil was not introduced into the cell, a more probable explanation is that the  $^{13}\text{C}$  NMR measurement for the FSZC was anomalous. It should be noted that this measurement was recorded two months before the additional swept zone results, and that the spectrometer underwent some probe repairs during the interim. Another possible explanation for the high value is that the test sample was made in a large container and transferred into a smaller container. Some of the lighter hydrocarbons which would have contained predominately non-aromatic carbon might have been lost upon transferal. The STO mass balance for the SSZC is within experimental error. The aromatic carbon mass balance is off, perhaps because the percent of aromatic carbon in the FSZC is incorrect. A back calculated value of the aromatic carbon percent for the FSZC indicates that the aromatic carbon percent for the SSZC is low. These calculations suggest that the FSZC should show about 14% aromatic carbon while the SSZC should show about 15% aromatic carbon. The likely explanation for why the aromatic carbon content is low in the SSZC is that the solvent did not dissolve all of the heavy hydrocarbons. It was difficult to visually ascertain whether all of the hydrocarbon material dissolved, because the samples were very dark, and some of the CrAcAc did not dissolve. Since no BF oil was added to the system after the initial mixture, no precipitate was observed during the runs, and this precipitate which is highly aromatic concentrates in the oil-rich phase, logic dictates that the aromatic carbon percent for the oil-rich phase should increase as the contacts proceed.

### General Discussion

A pseudoternary diagram constructed from the weight percent compositions of the phases from both the forward and swept zone contacts is shown in Figure 56. The pseudoternary diagram shows that multiple-contact miscibility will be developed by the vaporizing-gas drive mechanism. The first-contact miscible  $\text{CO}_2$ -rich phase composition is about 51 wt%  $\text{CO}_2$ , 10 wt%  $\text{C}_1 - \text{C}_6$ , and 39 wt%  $\text{C}_{7+}$ .

Figure 56 also illustrates that the limiting oil-rich phase composition after a few more swept zone contacts should be approximately 17 wt%  $\text{CO}_2$  and 83 wt%  $\text{C}_{7+}$ . Chromatographic compositional results of the oil-rich phase in the swept zone contacts indicate that the  $\text{C}_{7+}$  fraction will be composed of very high molecular weight hydrocarbons. The values used to construct Figure 56 are tabulated in Table 34. All compositional results determined from high pressure/temperature data, recombination of flash data, and an average of high pressure/temperature results and recombination of flash results are presented in the Appendix.

Visual observations and aromatic carbon mass balance calculations for the forward contacts show that as miscibility is generated the more aromatic hydrocarbons precipitate out of the oil-rich phase as a tar-like solid. Solid phase formation may cause miscibility by removing hydrocarbons which are not soluble in  $\text{CO}_2$ . It is possible that this precipitate reduces permeability or increases apparent displacing fluid viscosity in high permeability zones thus causing better flood conformance. It is also possible that this precipitate alters reservoir wettability to increase the amount of oil contacted by  $\text{CO}_2$  (Ehrlich, et. al., 1983). Using the  $^{13}\text{C}$  NMR results for the  $\text{CO}_2$ -rich phases, the STO fraction of BF

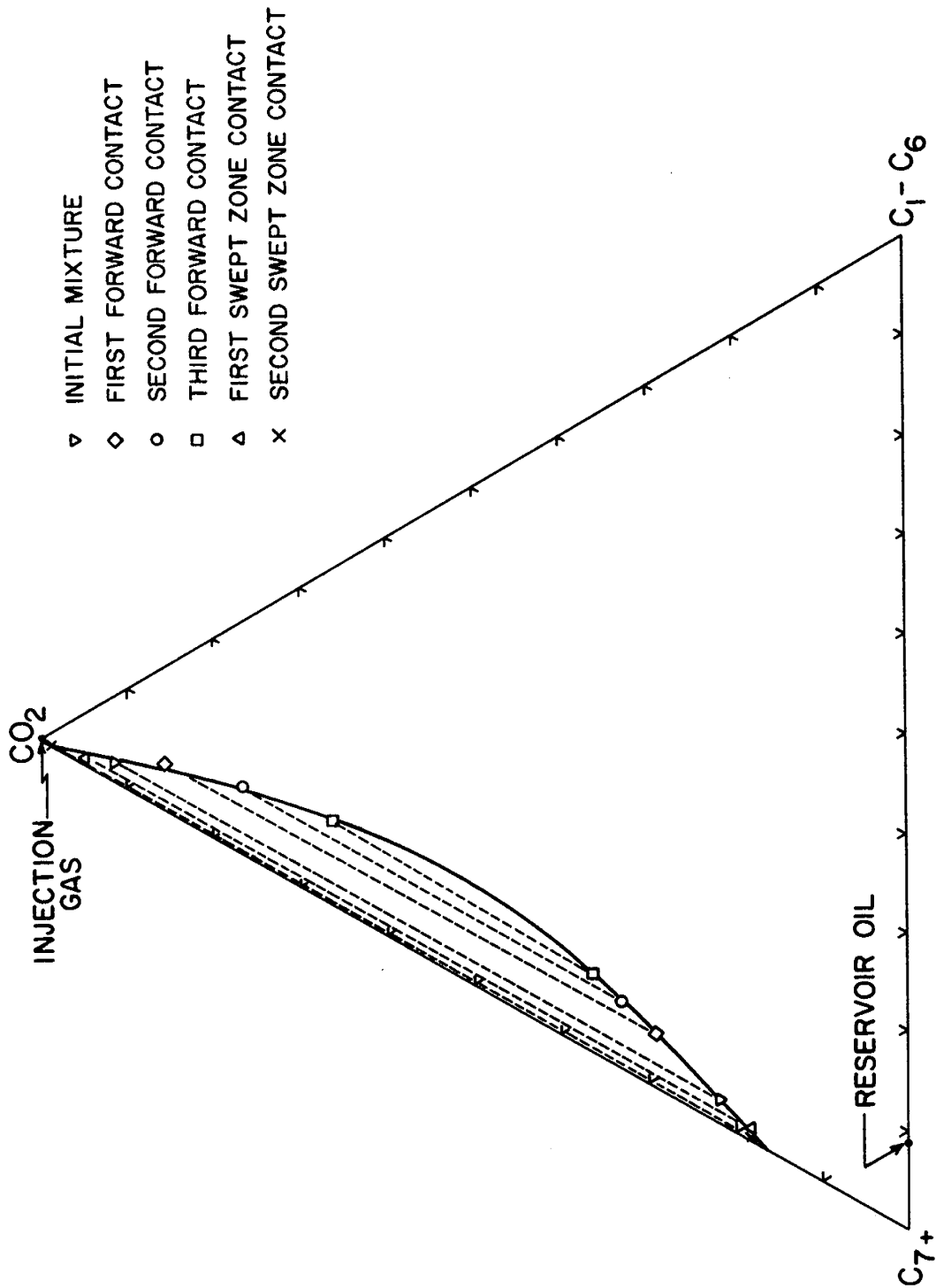


Figure 56. Pseudoternary Representation of the Weight Percent Compositions of the CO<sub>2</sub>-Rich and Oil-Rich Phases in the Multiple-Contact Experiments at approximately 1812 psia and 111.8 °F

Table 34: Weight Percent Compositions of All Multiple-Contact Phases

Mixture	Phase	wt % CO <sub>2</sub>	wt % C <sub>1</sub> -C <sub>6</sub>	wt % C <sub>7+</sub>	MW (g/g-mole)
Initial	CO <sub>2</sub> -Rich**	91.454	1.840	6.706	46.3
	Oil-Rich	21.934	2.196	75.870	127.8
First Forward Contact	CO <sub>2</sub> -Rich*	85.601	4.537	9.862	47.3
	Oil-Rich	29.365	5.105	65.530	96.4
Second Forward Contact	CO <sub>2</sub> -Rich*	76.781	6.686	16.533	50.0
	Oil-Rich	33.114	6.639	60.247	86.1
Third Forward Contact	CO <sub>2</sub> -Rich**	66.239	8.377	25.384	54.3
	Oil-Rich	36.561	7.522	55.917	78.8
First Swept Zone Contact	CO <sub>2</sub> -Rich**	94.908	0.782	4.310	45.4
	Oil-Rich	18.351	1.084	80.565	153.6
Second Swept Zone Contact	CO <sub>2</sub> -Rich**	98.266	0.227	1.507	44.5
	Oil-Rich	18.116	0.216	81.668	162.1

\*\* Values calculated from combining the high pressure/temperature and flash compositional results on an 1:1 basis.

\* Values calculated from high pressure/temperature compositional results all oil-rich values calculated from recombination of flash data.

oil, the oil-rich phase in the swept zone contacts, and the solid phase collected during sandpack displacements (Monger, 1984), the weight percent of solids in the BF oil is calculated to be approximately 20%.

In closing, the generality of the phase behavior data reported here for BF oil was tested using the effluent compositions determined for two repeat sandpack displacements as reported by Whitehead, et. al. (1981). Both sandpack displacements were performed at 1800 psia and 109°F with RR oil and 100% CO<sub>2</sub> as the injection fluid. Figure 57 shows the pseudoternary diagram which was constructed from forward contact results with BF oil (Figure 42). Plotted on the pseudoternary diagram are the sandpack effluent compositions, modified to exclude methane. In this modification, the methane fraction of the effluent was subtracted out, and the remaining fractions were renormalized. This was done because the pseudoternary diagram was generated using BF oil which is essentially methane free. The number beside each data point indicates the order and at what stage during the displacement the effluent samples were taken, with 1 indicating the start and 8 indicating the end of the displacement (Whitehead, et al., 1981). Figure 57 shows that the two phase envelope constructed from the BF oil phase behavior data can be used to predict the displacement compositional profile. As illustrated, the effluent compositions follow a compositional path which is to the right of the critical tie line until the plait point is reached. The effluent compositions then map along the dew-point curve of the two phase envelope. This is the compositional profile predicted by the vaporizing-gas drive mechanism of multiple-contact miscibility (Hutchinson and Braun, 1961). The scatter in the effluent compositions is due to problems associated with obtaining accurate compositional results using the high pressure/temperature syringe. The agreement between the sandpack effluent compositional results and the pseudoternary diagram is quite remarkable considering the different laboratory conditions; namely, different experimental setups, different experimenters, different gas chromatographs, different data analytical procedures, and the use of flash liberation versus a non-gravity stable displacement rate to expel methane.

#### CONCLUSIONS

1. No liquid-liquid-vapor three phase region was observed for CO<sub>2</sub> - BF oil mixtures at temperatures greater than 111°F. Carbon dioxide<sup>2</sup> - BF oil mixtures in the high CO<sub>2</sub> concentration range were capable of creating a liquid-liquid-vapor three phase region at room temperature.
2. No liquid-fluid (liquid-liquid) critical points were exhibited by CO<sub>2</sub> - BF oil mixtures at 111°F or 141.4°F over the pressure range tested.
3. Carbon dioxide is multiple-contact miscible with BF oil at approximately 1809 psia and 111.9°F by the vaporizing-gas drive mechanism.
4. Extensive precipitation of a tar-like solid phase is associated with the development of CO<sub>2</sub> - BF oil miscibility. How this affects CO<sub>2</sub> flood performance remains to be seen.
5. The BF oil precipitate appears to be highly aromatic and constitutes approximately 20 weight percent of the stock tank oil hydrocarbon.

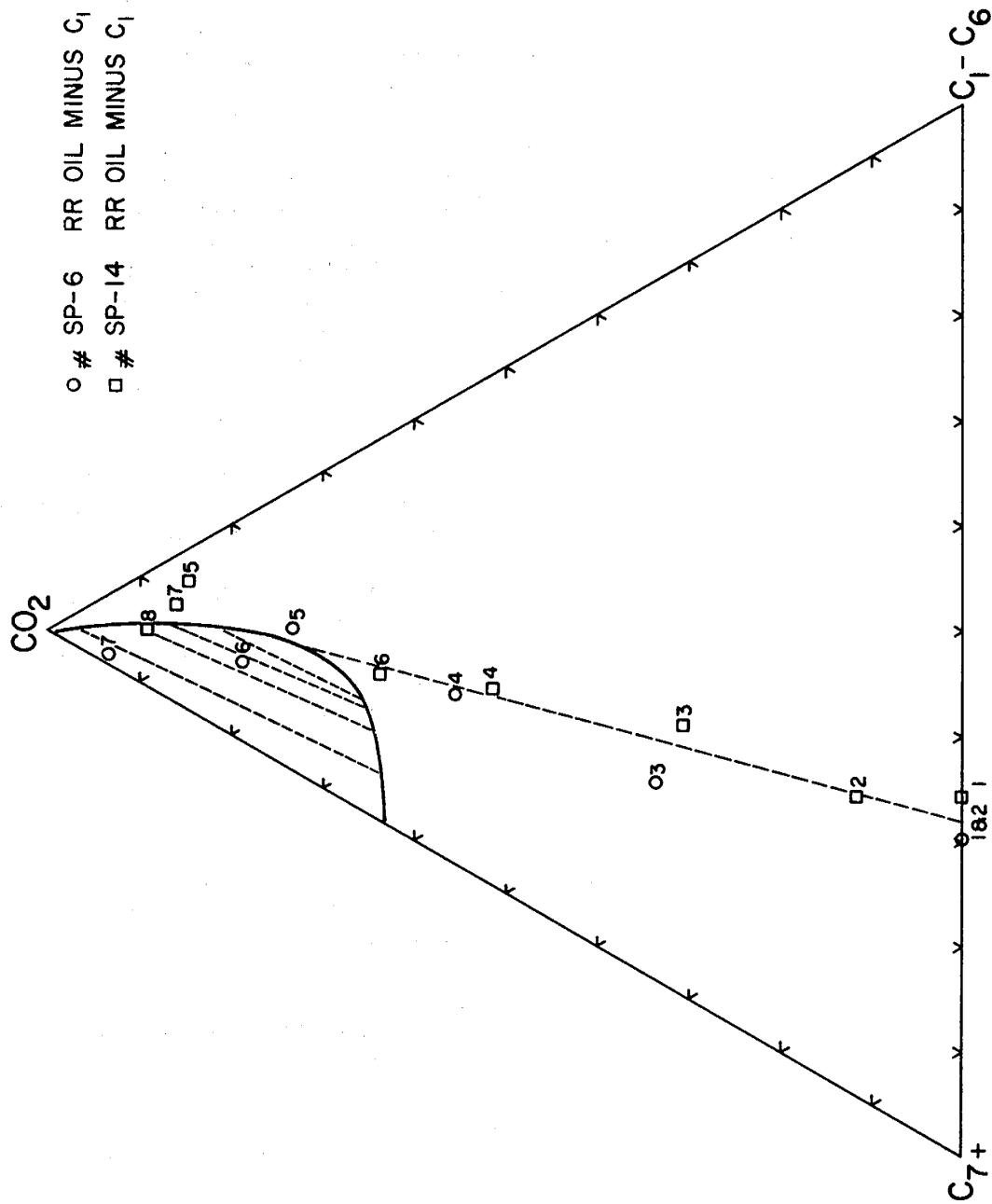


Figure 57. Pseudoternary Representation, Comparison of Forward Contacts Using BF Oil and of Sandpack Displacements of RR Oil on a Mole Percent Basis

6. The phase equilibria results presented provide multiple-contact phase compositions which are necessary to calibrate equations of state for reservoir simulation.
7. The results presented provide multiple-contact phase behavior data for a highly asphaltic (aromatic) crude which is lacking in the literature. The results thus provide a general model for predicting the phase behavior of other highly asphaltic crudes.
8. Very little oil recovery will be realized after the first swept zone contact (second CO<sub>2</sub> contact) in a hydrocarbon vaporization huf-n-puf process on the BF oil. The cumulative liquid volume recovered by two CO<sub>2</sub> contacts is approximately 35% of the original oil in place.
9. Aromatic hydrocarbons appear to concentrate in the oil-rich phase of CO<sub>2</sub> - BF oil mixtures. In the swept zone contacts these components constitute a large fraction of the unrecoverable oil. In the forward contacts these components are precipitated out as a solid phase. In both cases, potential problems associated with the refining or disposal of these toxic compounds are alleviated.

## BIBLIOGRAPHY

- ASTM Book of Standards, (1976) "Proposed Test Method for Boiling Range Distribution of Crude Petroleum By Gas Chromatography," American Society for Testing and Materials, Philadelphia (Nov., 1976) 716-723.
- Bunger, J. W. and Li, N. C. (1981) Chemistry of Asphaltenes. American Chemical Society, Washington, D.C.
- Coates, K. H., and Smart, G. T. (1982) "Application of a Regression-Based EOS PVT Program to Laboratory Data," SPE 11197, presented at the 57th annual Fall Technical Conference and Exhibition, New Orleans, Sept. 26-29, 1982.
- Ehrlich, J. H., et al. (1983) "Laboratory and Field Study of Effect of Mobile Water on CO<sub>2</sub> Flood Residual Oil Saturation," SPE 11957, presented at the 58th Annual Technical Conference and Exhibition, San Francisco, Oct. 5-8, 1983.
- Gardner, J. W., et al. (1979) "The Effect of Phase Behavior on CO<sub>2</sub> Flood Displacement Efficiency," SPE 8367, presented at the 54th Annual Fall Technical Conference and Exhibition, Las Vegas, Sept. 23-26, 1979; J. Pet. Tech. (Nov., 1981) 2067-2081.
- Holm, L. W., and Josendal, V. A. (1974) "Mechanisms of Oil Displacement by Carbon Dioxide," J. Pet. Tech. (Dec., 1974) 1427-1435.
- Holm, L. W., and Josendal, V. A. (1982) "Effect of Oil Composition on Miscible-Type Displacement by Carbon Dioxide," Soc. Pet. Eng. J. (Feb., 1982) 87-96.
- Holm, L. W. (1982) "CO<sub>2</sub> Flooding: Its Time Has Come," J. Pet. Tech. (Dec., 1982) 2739-2745.
- Hutchinson, C. A., Jr., and Braun, P. H. (1961) "Phase Relations of Miscible Displacement in Oil Recovery," A. I. Ch. E. Journal 7 (March 1961) 64-72.
- Leach, M. P., and Yellig, W. F. (1979) "Compositional Model Studies: CO<sub>2</sub>-Oil Displacement Mechanisms," SPE 8368, presented at the 54th Annual Fall Technical Conference and Exhibition, Las Vegas, Sept. 23-26, 1979.
- Menzie, D. E., and Nielsen, R. F. (1963) "A Study of Vaporization of Crude Oil by Carbon Dioxide Repressuring," J. Pet. Tech. (Nov., 1963).
- Monger, T. G. (1985) "Investigations of Enhanced Oil Recovery Through Use of Carbon Dioxide," Report DOE/BC/10344-15 Final Report for U.S. DOE Contract DE-AS19-80BC10344, Volume II.
- Monger, T. G. (1984) "The Impact of Oil Aromaticity on Carbon Dioxide Flooding," SPE/DOE 12708, presented at the SPE/DOE 4th Symposium on Enhanced Oil Recovery, Tulsa, April 15-18, 1984.

- Monger, T. G. and Khakoo, A. (1981) "The Phase Behavior of CO<sub>2</sub>-Appalachian Oil Systems," SPE 10269, presented at the 56th Annual Technical Conference and Exhibition, San Antonio, Oct. 5-7, 1981.
- Monger, T. G., and McMullan, J. H. (1983) "Investigations of Enhanced Oil Recovery Through Use of Carbon Dioxide," Report DOE/BC/10344-8 Second Annual Report for U.S. DOE Contract DE-AS19-80BC10344 (Aug., 1983).
- Newitt, D. M., et al. (1956) "Carbon Dioxide" in Thermodynamic Functions of Gases; Din, F., Ed.; Butterworths: London (1956) Volume I, 102-134.
- Orr, F. M., et al. (1981) "Liquid-Liquid Phase Behavior in CO<sub>2</sub>-Hydrocarbon Systems," presented at the American Chemical Society Symposium on Chemistry of Enhanced Oil Recovery, Atlanta, Mar. 29 - Apr. 3, 1981.
- Patton, J. T., and Coates, K. H. (1979) "A Parametric Study of the CO<sub>2</sub> Huff-n-Puff Process," SPE 9228, presented at the 54th Annual Fall Technical Conference and Exhibition, Las Vegas, Sept. 23-26, 1979.
- Reamer, H. H., and Sage, B. H. (1963) "Phase Equilibria in Hydrocarbon Systems. Volumetric and Phase Behavior of the n-Decane-CO<sub>2</sub> System," J. Chem. Eng. Data 8 (Oct., 1963) 508-513.
- Shelton, J. L., and Yarborough, L. (1976) "Multiple Phase Behavior in Porous Media During CO<sub>2</sub> or Rich Gas Flooding," SPE 5827, presented at the Improved Oil Recovery Symposium of Society of Petroleum Engineers of AIME, Tulsa, March 22-24, 1976.
- Schoolery, J. N., and Budde, W. L. (1976) "Natural Abundance Carbon-13 Nuclear Magnetic Resonance Spectrometry for Crude Oil and Petroleum Product Analyses," Anal. Chem. 48 (Sept., 1976).
- Stalkup, Fred I., Jr. (1983a) Miscible Displacement. SPE of AIME, New York (1983) 2-4, 17-22, and 137-147.
- Stalkup, Fred I., Jr. (1983b) "Status of Miscible Displacement," J. Pet. Tech. (April, 1983) 815-823.
- Tiffin, D. L., and Yellig, W. F. (1982) "Effects of Mobile Water on Multiple Contact Miscible Gas Displacements," SPE/DOE 10687, presented at the SPE/DOE 3rd Joint Symposium on Enhanced Oil Recovery, Tulsa, April 4-7, 1982.
- Turek, E. A., et al. (1984) "Phase Behavior of Several CO<sub>2</sub>-West Texas Reservoir Oil Systems," SPE 13117, presented at the 59th Annual Technical Conference and Exhibition, Houston, Sept. 16-19, 1984.
- Whitehead, W. R., et al. (1981) "Investigations of Enhanced Oil Recovery Through Use of Carbon Dioxide," Report DOE/BC/10344-4 First Annual Report for U.S. DOE Contract DE-AS19-80BC10344 (July, 1982).
- Williams, C. A., et al. (1980) "Use of the Peng-Robinson Equation of State to Predict Hydrocarbon Phase Behavior and Miscibility for Fluid Displacement," SPE 8817, presented at the SPE/DOE 1st Joint Symposium on Enhanced Oil Recovery, Tulsa, April 20-23, 1980.

- Yang, H. W., et al. (1976) "Phase Equilibria Behavior of the System Carbon Dioxide-n-Butylbenzene-2-Methylnaphthalene," J. Chem. Eng. Data (Vol. 21, No. 3, 1976) 330-335.
- Yellig, W. F., and Metcalfe, R. S. (1980) "Determination and Prediction of CO<sub>2</sub> Minimum Miscibility Pressure," J. Pet. Tech. (Jan., 1980) 160-168.
- Zarah, B. Y., et al. (1974) "Phase Equilibria Behavior of Carbon Dioxide in Binary and Ternary Systems with Several Hydrocarbon Components," AIChE Symp. Ser. (Vol. 140, 1974).

APPENDIX

TABLE A1

MEASURED VALUES OF PRESSURE-VOLUME ISOTHERMS  
 FOR CO<sub>2</sub>-BF OIL MIXTURES AT APPROXIMATELY 141.4 F

PRESSURE (psia)	TOTAL SAMPLE VOLUME (cc)	OIL-RICH PHASE (% volume)	CO <sub>2</sub> -RICH PHASE (% volume)
--------------------	-----------------------------	------------------------------	---

0 MOLE PERCENT CO<sub>2</sub>, 143.3 F

41	159.799	31.59	68.41
49	129.966	39.35	60.65
61	100.111	51.42	48.58
86	71.906	72.46	27.54
400	54.013	0.0	0.0
1145	53.636	0.0	0.0
1960	53.414	0.0	0.0
2788	53.153	0.0	0.0
3481	52.955	0.0	0.0

23.7 MOLE PERCENT CO<sub>2</sub>, 142.5 F

365	135.089	58.49	41.51
413	120.016	65.29	34.71
471	105.044	76.44	23.56
522	94.942	85.48	14.52
593	87.362	0.0	0.0

TABLE A1 (cont.)

713	83.966	0.0	0.0
1724	82.564	0.0	0.0
2759	81.835	0.0	0.0
3470	81.540	0.0	0.0

48.2 MOLE PERCENT CO<sub>2</sub>, 142.3 F

883	130.621	65.75	34.25
913	125.018	69.06	30.94
993	114.475	76.15	23.85
1088	104.665	84.79	15.21
1150	100.142	0.0	0.0
1219	96.141	0.0	0.0
1546	93.903	0.0	0.0
2236	92.819	0.0	0.0
2793	92.135	0.0	0.0
3492	91.779	0.0	0.0
3647	91.591	0.0	0.0

68.5 MOLE PERCENT CO<sub>2</sub>, 141.1 F

967	142.698	39.22	60.78
1093	122.632	46.39	53.61
1219	107.708	53.89	46.11
1441	89.602	61.57	38.43

TABLE A1 (cont.)

1793	75.305	83.64	16.36
1945	73.667	0.0	0.0
2410	72.179	0.0	0.0
2947	71.619	0.0	0.0
3453	71.162	0.0	0.0

78.8 MOLE PERCENT CO<sub>2</sub>, 140.0 F

1627	138.771	42.43	57.57
1715	128.774	45.09	54.91
1860	118.863	47.80	52.20
2264	109.218	50.23	49.77
3288	102.139	50.99	49.01

87.2 MOLE PERCENT CO<sub>2</sub>, 141.3 F

1356	168.676	20.91	79.09
1412	158.613	22.36	77.67
1465	148.446	24.09	75.91
1530	138.030	22.15	77.85
1594	127.834	28.76	71.24
1665	117.848	31.32	68.68
1762	106.885	33.74	66.26
1935	96.742	37.26	62.74
2342	88.040	36.95	63.05

TABLE A1 (cont.)

2723	84.595	36.93	63.07
3067	82.606	36.39	63.61
3383	81.321	35.48	64.52

TABLE A2  
 MEASURED VALUES OF PRESSURE-VOLUME ISOTHERMS  
 FOR CO<sub>2</sub>-BF OIL MIXTURES AT APPROXIMATELY 111.0 F

PRESSURE (psia)	TOTAL SAMPLE VOLUME (cc)	OIL-RICH PHASE (% volume)	CO <sub>2</sub> -RICH PHASE (% volume)
--------------------	-----------------------------	------------------------------	---

0 MOLE PERCENT CO<sub>2</sub> , 111.3 F

43	171.309	44.47	55.53
49	151.408	50.90	49.10
54	131.517	58.81	41.19
73	97.022	80.66	19.34
90	83.683	0.0	0.0
361	80.089	0.0	0.0
645	79.787	0.0	0.0
1164	79.568	0.0	0.0
2359	79.064	0.0	0.0
3465	78.643	0.0	0.0

23.7 MOLE PERCENT CO<sub>2</sub> , 111.3 F

320	133.885	57.41	42.59
341	123.787	62.46	37.54
370	113.852	67.99	32.01
425	97.833	80.04	19.96

TABLE A2 (cont.)

451	91.791	86.23	13.77
605	81.914	0.0	0.0
1091	80.806	0.0	0.0
1976	80.263	0.0	0.0
2540	79.985	0.0	0.0
3480	79.560	0.0	0.0

48.2 MOLE PERCENT CO<sub>2</sub> , 111.2 F

730	134.527	62.87	37.13
764	126.809	67.85	32.15
805	118.858	72.91	27.09
852	110.895	79.25	20.75
911	102.875	86.66	13.34
1022	94.273	0.0	0.0
1533	92.469	0.0	0.0
2210	91.923	0.0	0.0
2881	91.455	0.0	0.0
3400	91.113	0.0	0.0
3529	91.061	0.0	0.0

68.5 MOLE PERCENT CO<sub>2</sub> , 111.0 F

699	171.391	25.31	74.69
780	147.315	30.49	69.51

TABLE A2 (cont.)

869	126.558	36.42	63.58
971	106.819	44.02	55.98
1110	86.700	56.68	43.32
1183	76.618	66.11	33.89
1299	66.615	80.92	19.08
1490	62.045	0.0	0.0
1839	60.971	0.0	0.0
2517	60.263	0.0	0.0
3055	59.855	0.0	0.0
3519	59.546	0.0	0.0

78.8 MOLE PERCENT CO<sub>2</sub>, 110.6 F

1262	140.806	41.79	58.21
1276	135.772	43.09	56.91
1289	130.719	44.49	55.51
1300	125.694	45.92	54.08
1330	118.170	47.69	52.31
1427	110.897	49.34	50.66
1651	106.132	50.39	49.61
2009	103.004	50.68	49.32
2509	100.590	50.70	49.30
3519	97.771	50.68	49.32

TABLE A2 (cont.)

87.2 MOLE PERCENT CO<sub>2</sub>, 110.3 F

1090	191.810	18.13	81.87
1141	171.778	20.70	79.30
1202	151.777	23.90	76.10
1259	131.751	28.19	71.81
1305	111.732	32.71	67.29
1429	91.783	36.63	63.37
1729	84.484	37.42	62.58
2250	81.014	37.14	62.86
2630	79.397	36.74	63.26
3007	78.206	36.67	63.33
3500	76.986	36.28	63.72

89.3 MOLE PERCENT CO<sub>2</sub>, 111.5 F

733	185.350	6.49	93.51
772	172.534	7.22	92.78
822	157.573	8.23	91.77
856	148.383	8.98	91.02
895	138.426	9.63	90.37
940	127.735	10.36	89.64
974	120.171	11.42	88.58
1004	113.686	11.27	88.73
1046	105.089	13.18	86.82

TABLE A2 (cont.)

1080	98.368	14.06	85.94
1118	91.130	15.27	84.73
1158	83.494	16.55	83.45
1182	78.887	18.05	81.95
1229	69.554	20.14	79.86
1274	58.873	23.43	76.57
1312	49.328	27.08	72.92
1561	41.052	29.61	70.39
1880	39.128	29.73	70.27
2390	37.638	28.35	71.65
3515	36.009	27.96	72.04

94.6 MOLE PERCENT CO<sub>2</sub> (INITIAL MIXTURE)  
 FIRST MIXING, 111.6 F

1245	131.599	9.96	90.04
1269	122.494	10.89	89.11
1294	110.761	10.92	89.08
1326	96.256	12.34	87.66
1371	86.425	13.15	86.85
1431	80.920	13.44	86.56
1498	77.542	13.70	86.30
1685	72.930	13.08	86.92
2075	68.521	12.57	87.43
2652	65.270	11.88	88.12

TABLE A2 (cont.)

3496	62.531	12.94	87.06
------	--------	-------	-------

SECOND MIXING, 110.4 F

1290	183.232	13.10	86.90
1330	173.244	13.66	86.34
1397	163.287	13.97	86.03
1430	158.309	14.01	85.99
1495	150.700	14.03	85.97
1600	145.587	13.98	86.02
1860	138.653	13.85	86.15
2590	130.004	13.71	86.29
3146	126.249	12.99	87.01
3410	124.279	12.68	87.32

THIRD MIXING, 111.7 F

1408	171.911	11.44	88.56
1535	166.399	13.71	86.29
1610	162.849	13.52	86.48
1682	160.240	13.62	86.38
1728	158.801	13.37	86.63
1762	157.679	13.22	86.78
1788	156.948	13.49	86.51
1845	155.543	13.31	86.69
1880	154.744	13.13	86.87
1995	152.648	13.25	86.75
2460	145.914	12.74	87.26
3018	140.979	12.61	87.39

TABLE A2 (cont.)

3459	138.015	12.51	87.49
FOURTH MIXING, 111.4 F			
1355	188.189	14.20	85.80
1421	177.022	14.29	85.71
1471	171.796	14.15	85.85
1603	164.869	14.19	85.81
1709	161.330	14.14	85.86
1727	159.957	14.13	85.87
1766	158.110	14.13	85.87
1838	156.303	14.21	85.79
1897	154.883	13.83	86.17
1992	153.115	13.86	86.14
2203	149.646	13.53	86.47
2751	143.674	13.41	86.59
3461	138.733	13.27	86.73

TABLE A3  
 MEASURED VALUES OF PRESSURE-VOLUME ISOTHERMS  
 FOR CO<sub>2</sub>-BF OIL MULTIPLE-CONTACT MIXTURES  
 2

PRESSURE (psia)	TOTAL SAMPLE VOLUME (cc)	OIL-RICH PHASE (% volume)	CO <sub>2</sub> -RICH PHASE (% volume)
FIRST FORWARD CONTACT			
FIRST MIXING, 113.1 F			
990	176.633	17.50	82.50
1030	164.366	19.44	80.56
1067	153.300	21.03	78.97
1106	141.675	23.07	76.93
1138	132.893	24.90	75.10
1179	121.047	28.22	71.78
1225	107.612	33.30	66.70
1268	91.201	37.18	62.82
1286	82.957	39.85	60.15
1311	76.939	41.78	58.22
1346	74.164	42.42	57.58
1394	72.255	42.78	57.22
1456	70.793	42.93	57.07
1536	69.590	43.15	56.85
1966	66.332	42.77	57.23
2994	63.065	40.44	59.56
3498	62.083	37.56	62.44

TABLE A3 (cont.)

3670	61.964	38.64	61.36
SECOND MIXING, 112.6 F			
1236	185.852	31.21	68.79
1235	183.391	31.69	68.31
1251	172.114	33.87	66.13
1284	148.709	38.42	61.58
1308	136.315	40.62	59.38
1510	120.769	42.22	57.78
1602	118.587	42.31	57.69
1671	117.403	42.18	57.82
1727	116.618	42.15	57.85
1806	115.616	42.28	57.72
1860	115.130	42.22	57.78
1900	114.759	41.95	58.05
2434	110.029	40.98	59.02
3256	107.651	38.90	61.10
SECOND FORWARD CONTACT, 111.8 F			
1079	180.603	24.19	75.81
1125	165.461	26.87	73.13
1155	153.850	29.69	70.31
1200	137.322	33.69	66.31
1240	121.811	38.48	61.52
1260	106.765	42.08	57.92

TABLE A3 (cont.)

1270	97.105	43.65	56.35
1305	92.303	43.89	56.11
1380	89.520	43.53	56.47
1450	88.003	43.26	56.74
1520	86.958	42.80	57.20
1602	86.028	42.53	57.47
1709	85.140	41.90	58.10
1770	84.714	41.72	58.28
1810	84.474	41.55	58.45
1860	84.175	41.58	58.42
1912	83.869	41.10	58.90
1980	83.493	40.57	59.43
2437	81.713	38.13	61.87
3021	80.178	34.18	65.82
3455	79.243	30.39	69.61
3532	79.127	28.81	71.19
3619	78.943	27.56	72.44

## THIRD FORWARD CONTACT, 111.9 F

836	178.145	18.14	81.86
875	165.737	19.79	80.21
922	152.123	21.84	78.16
969	139.331	24.29	75.71
1017	127.143	27.22	72.78

TABLE A3 (cont.)

1054	118.423	29.96	70.04
1089	110.172	33.04	66.96
1120	103.262	35.73	64.27
1151	96.492	39.21	60.79
1181	90.082	42.75	57.25
1207	84.290	46.48	53.52
1231	78.917	50.10	49.90
1250	74.100	53.33	46.67
1259	70.337	54.68	45.32
1269	65.331	56.63	43.37
1302	62.626	57.43	42.57
1372	61.045	57.53	42.47
1432	60.286	57.35	42.65
1491	59.766	57.33	42.67
1539	59.405	57.08	42.92
1629	58.867	56.88	43.12
1711	58.471	56.42	43.58
1778	58.199	56.41	43.59
1836	57.989	56.08	43.92
1946	57.630	55.82	44.18
2021	57.416	55.67	44.33
2463	56.414	53.47	46.53
2760	55.832	0.0	0.0
3031	55.394	0.0	0.0
3502	54.756	0.0	0.0

TABLE A3 (cont.)  
 FIRST SWEEP ZONE CONTACT  
 FIRST MIXING, 110.3 F

1059	141.225	10.42	89.58
1090	133.204	11.16	88.84
1140	120.590	12.41	87.59
1185	108.903	13.12	86.88
1230	96.915	15.01	84.99
1275	84.524	17.54	82.46
1318	73.687	19.91	80.09
1340	66.749	21.94	78.06
1380	62.061	23.46	76.54
1412	59.322	24.68	75.32
1465	57.290	25.58	74.72
1510	55.922	25.50	74.50
1580	54.383	25.68	74.32
1680	53.053	26.74	73.26
1782	51.966	27.38	72.62
1903	51.013	27.83	72.17
2008	50.370	28.95	71.05
2491	48.379	28.63	71.37
3015	47.026	30.81	69.19
3500	46.156	32.02	67.98

SECOND MIXING, 111.7 F

1162	146.511	13.35	86.65
1209	132.367	14.98	85.02

TABLE A3 (cont.)

1254	118.379	16.66	83.34
1293	104.082	18.43	81.57
1332	90.747	20.64	79.36
1373	81.159	23.13	76.87
1418	75.982	24.22	75.78
1476	72.519	24.92	75.08
1521	70.753	25.55	74.45
1574	69.299	26.25	73.75
1626	68.195	26.73	73.27
1685	67.170	26.84	73.16
1726	66.552	27.25	72.75
1780	65.870	27.11	72.89
1830	65.315	27.44	72.56
1886	64.756	27.61	72.39
1931	64.394	27.35	72.65
1989	63.968	27.99	72.01
2441	61.413	29.28	70.72
2957	59.586	30.63	69.37
3492	58.348	31.48	68.52

## SECOND SWEEP ZONE CONTACT, 111.7 F

1202	113.417	14.54	85.46
1248	102.591	16.03	83.97
1291	91.229	18.08	81.92

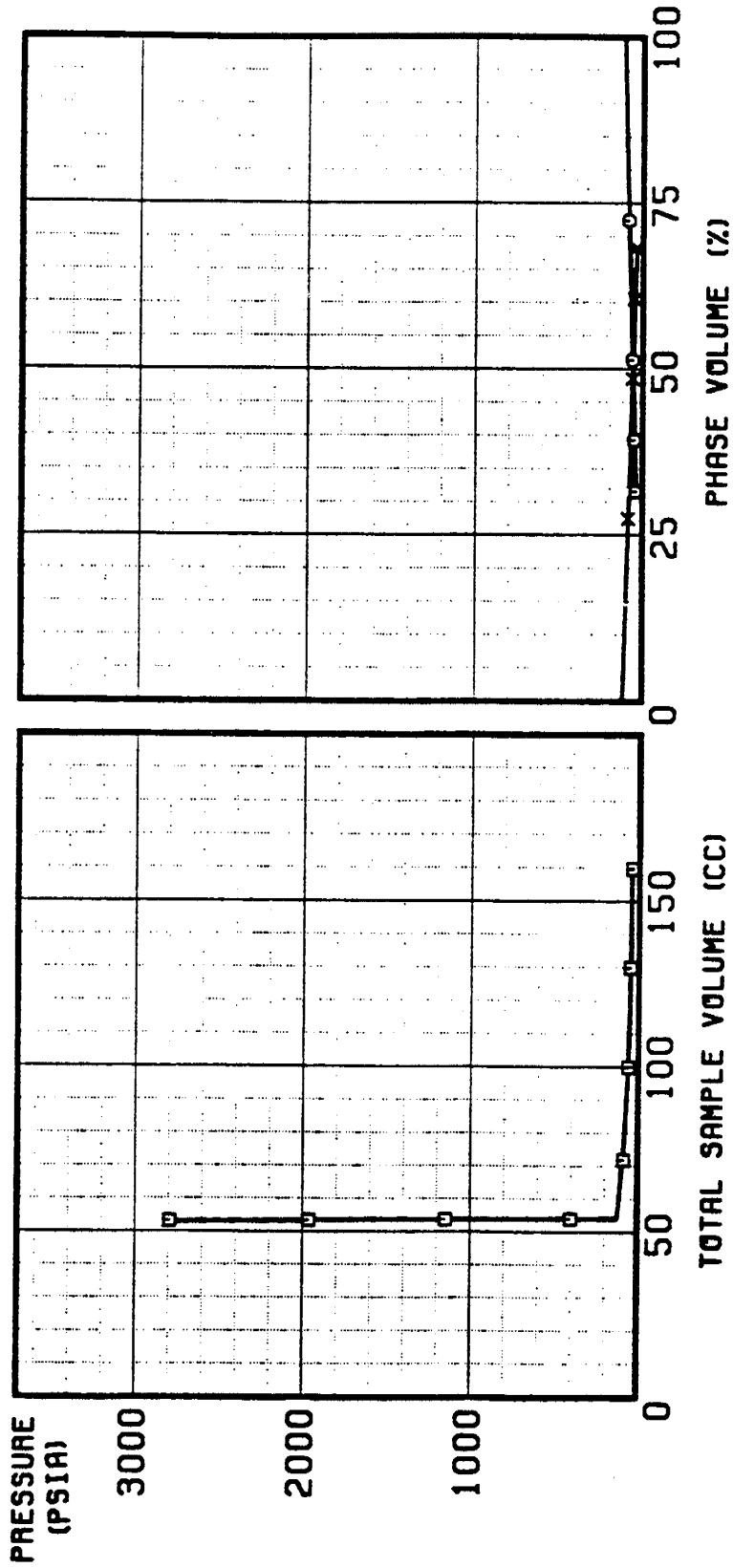
TABLE A3 (cont.)

1343	77.359	20.72	79.28
1392	68.413	23.81	76.19
1442	63.884	25.61	74.39
1473	62.020	26.07	73.93
1523	60.381	26.82	73.18
1577	58.778	27.48	72.52
1631	57.686	27.73	72.27
1687	56.778	28.21	71.79
1745	56.051	28.75	71.25
1811	55.357	29.16	70.84
1863	54.893	29.11	70.89
1889	54.667	29.58	70.42
1953	54.169	29.29	70.71
2022	53.718	30.04	69.96
2469	51.589	31.44	68.56
3022	50.044	33.08	66.92
3468	49.148	34.44	65.56

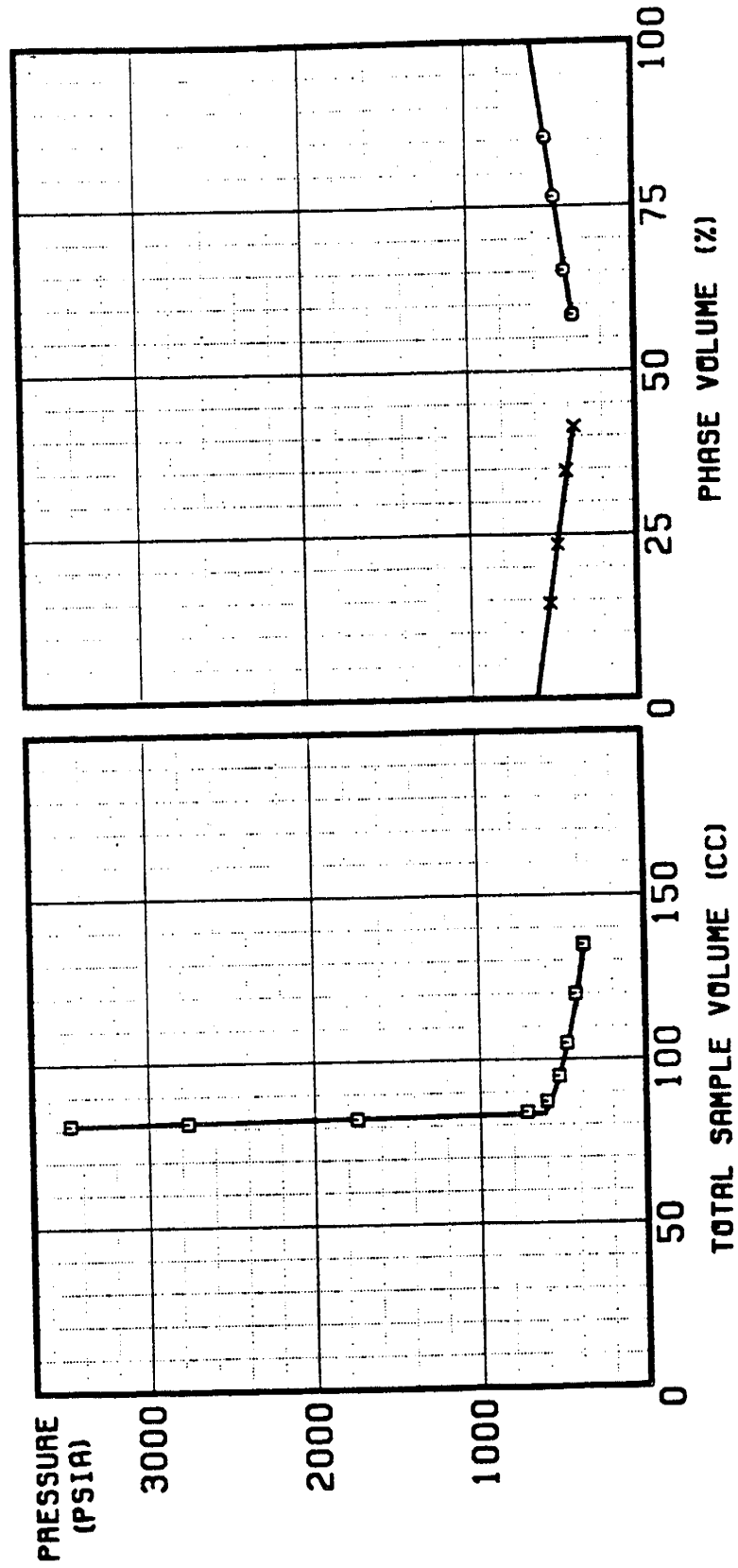
TABLE A4  
 MEASURED VALUES OF PRESSURE-VOLUME ISOTHERMS  
 FOR CO<sub>2</sub>-BF<sub>2</sub> OIL MIXTURE AT 79.8 F

PRESSURE (psia)	TOTAL SAMPLE VOLUME (cc)	OIL-RICH LIQUID (% volume)	CO <sub>2</sub> -RICH VAPOR (% volume)	CO <sub>2</sub> -RICH LIQUID (% volume)
89.3 MOLE PERCENT CO <sub>2</sub>				
769	132.776	10.44	89.56	0.0
796	124.957	11.37	88.63	0.0
824	116.469	11.92	88.08	0.0
864	101.673	15.06	84.94	0.0
883	84.748	15.77	76.07	8.16
892	79.758	16.54	72.95	10.51
899	74.765	17.55	69.13	13.32
905	69.769	18.40	64.48	17.12
912	64.776	19.39	58.77	21.84
917	59.781	20.37	52.47	27.16
927	49.788	25.00	34.38	40.62
934	44.794	27.17	23.01	49.82
1389	37.082	30.14	0.0	69.86
1845	36.056	-----	-----	-----
2306	35.403	-----	-----	-----
2852	34.828	-----	-----	-----
3415	34.294	-----	-----	-----

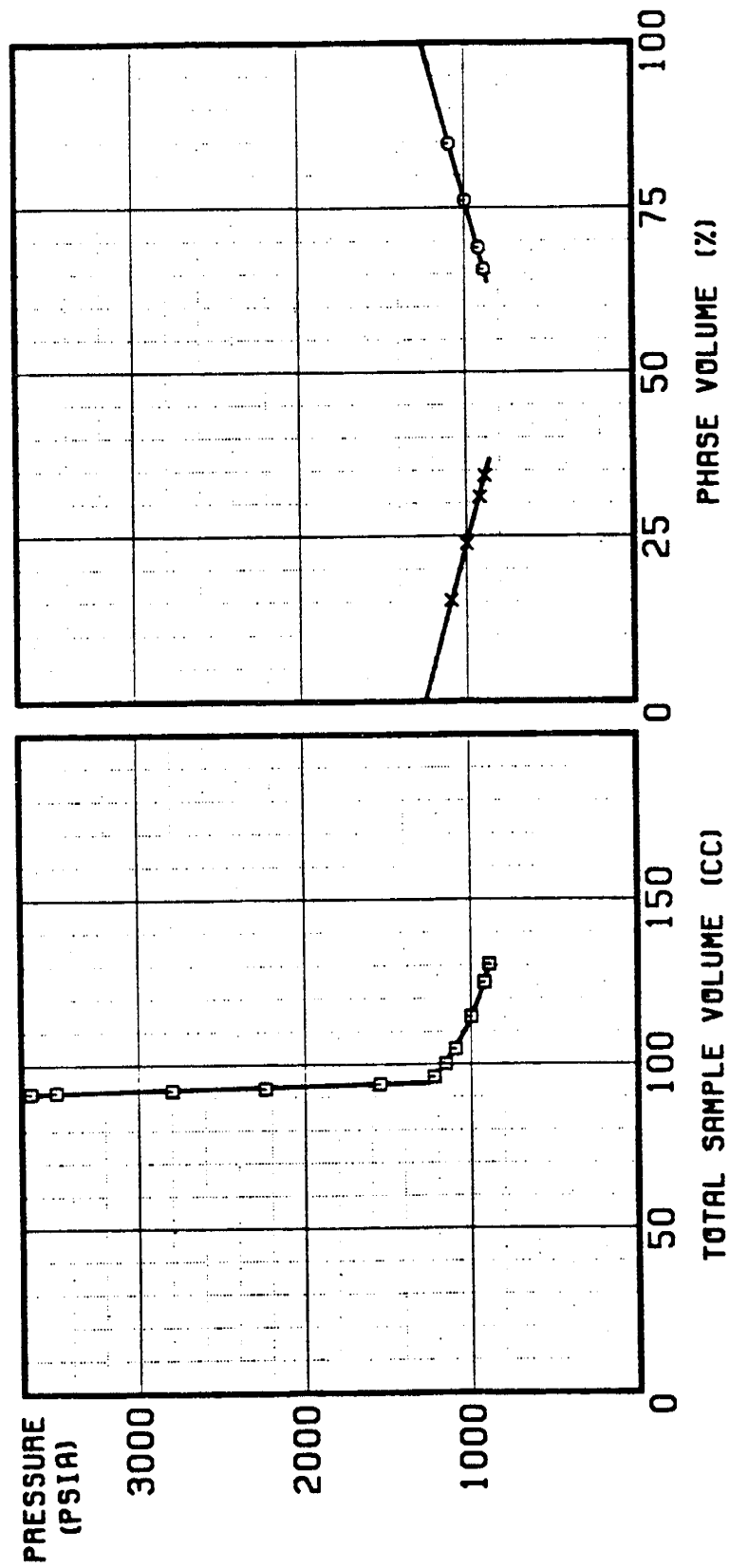
# 0% CO2 - 100% BF 143.3F



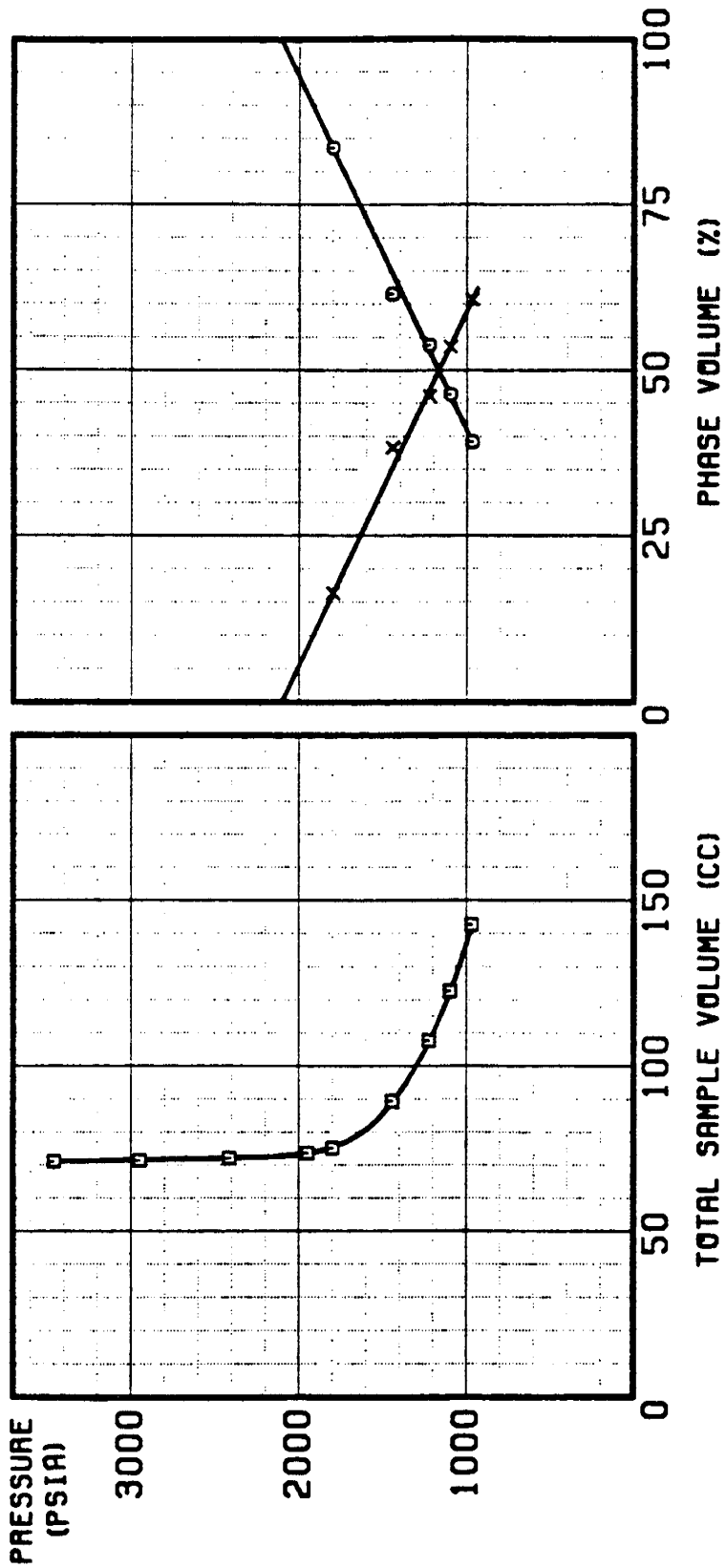
23.7% CO2 - 76.3% BF 143.0F



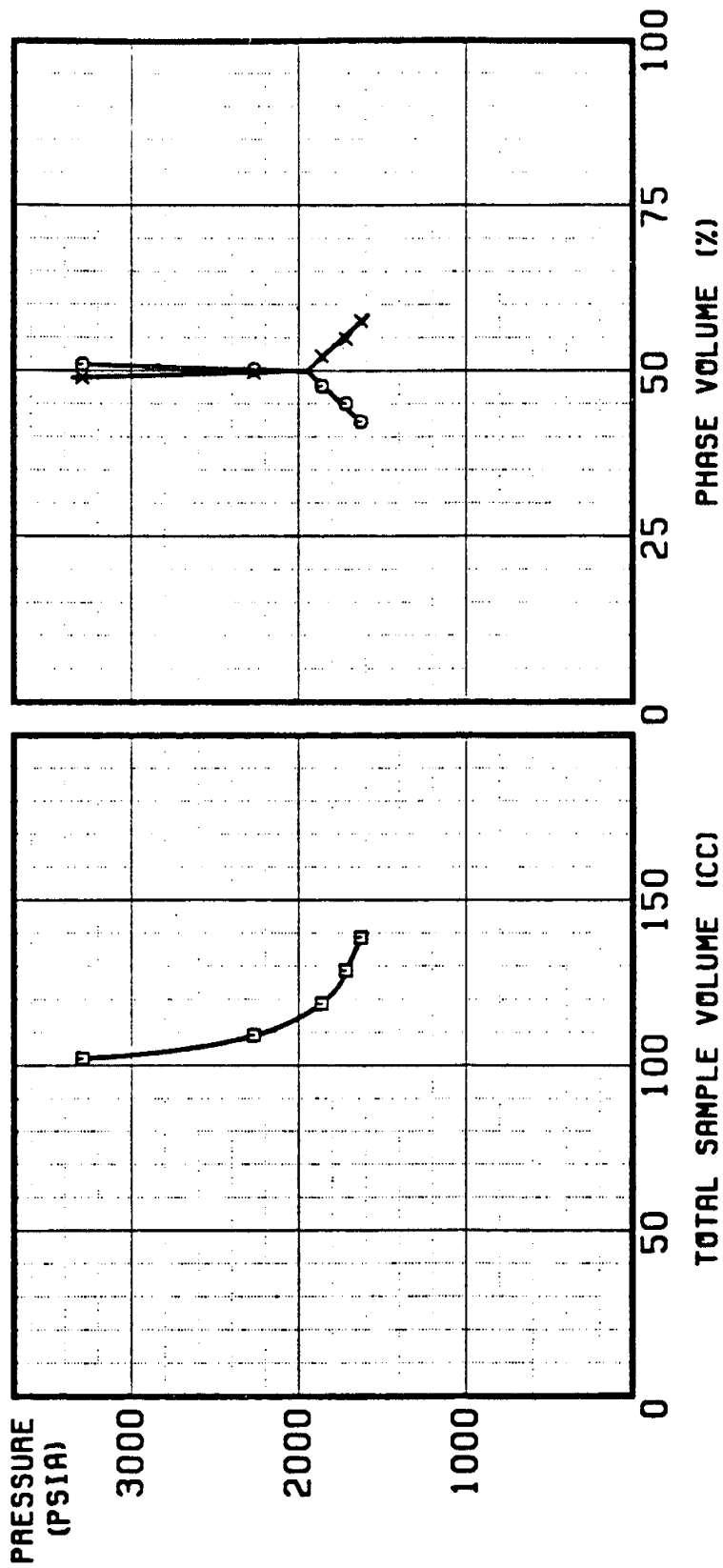
# 48.2% CO2 - 51.8% BF 142.3F



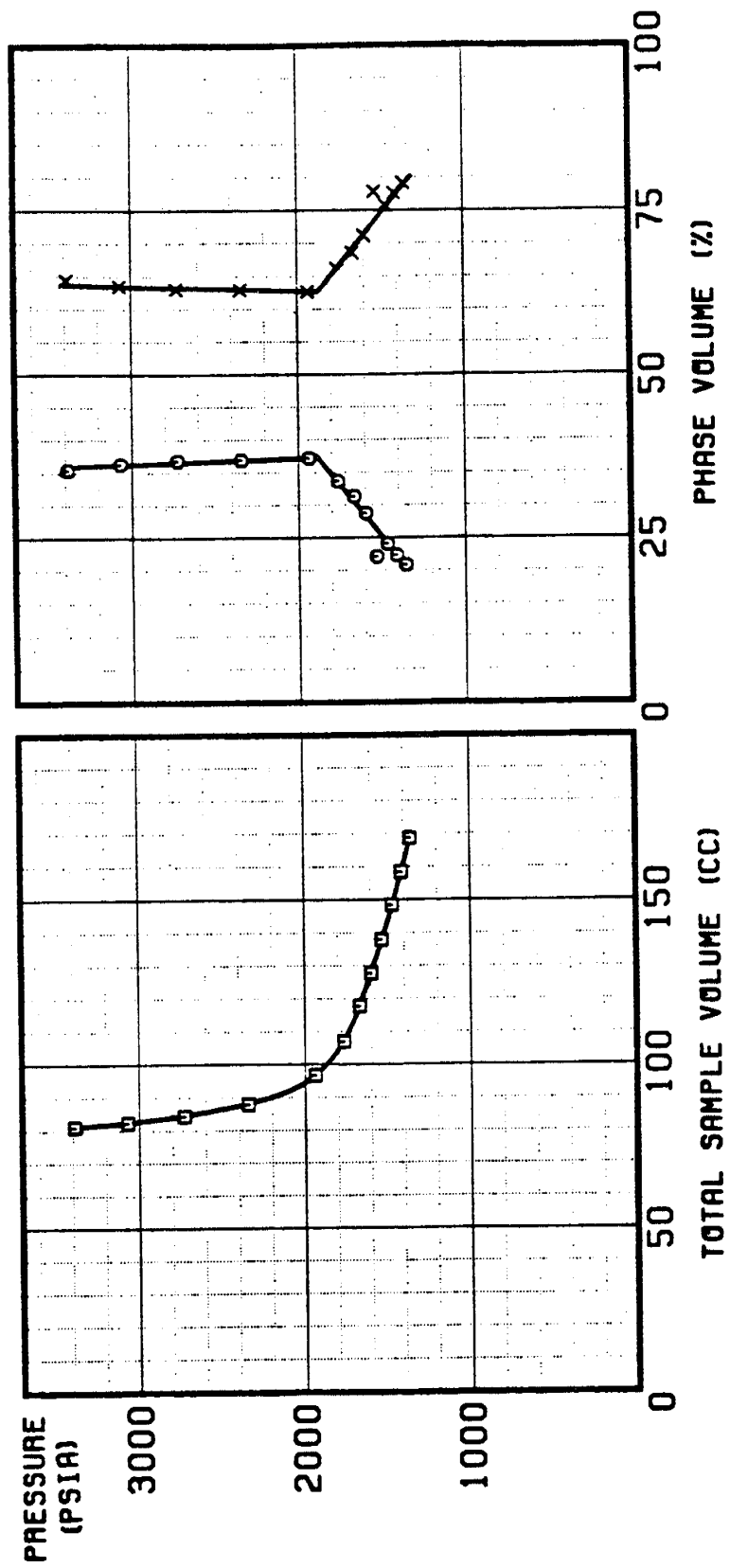
# 68.5% CO<sub>2</sub> - 31.5% BF 141.1F



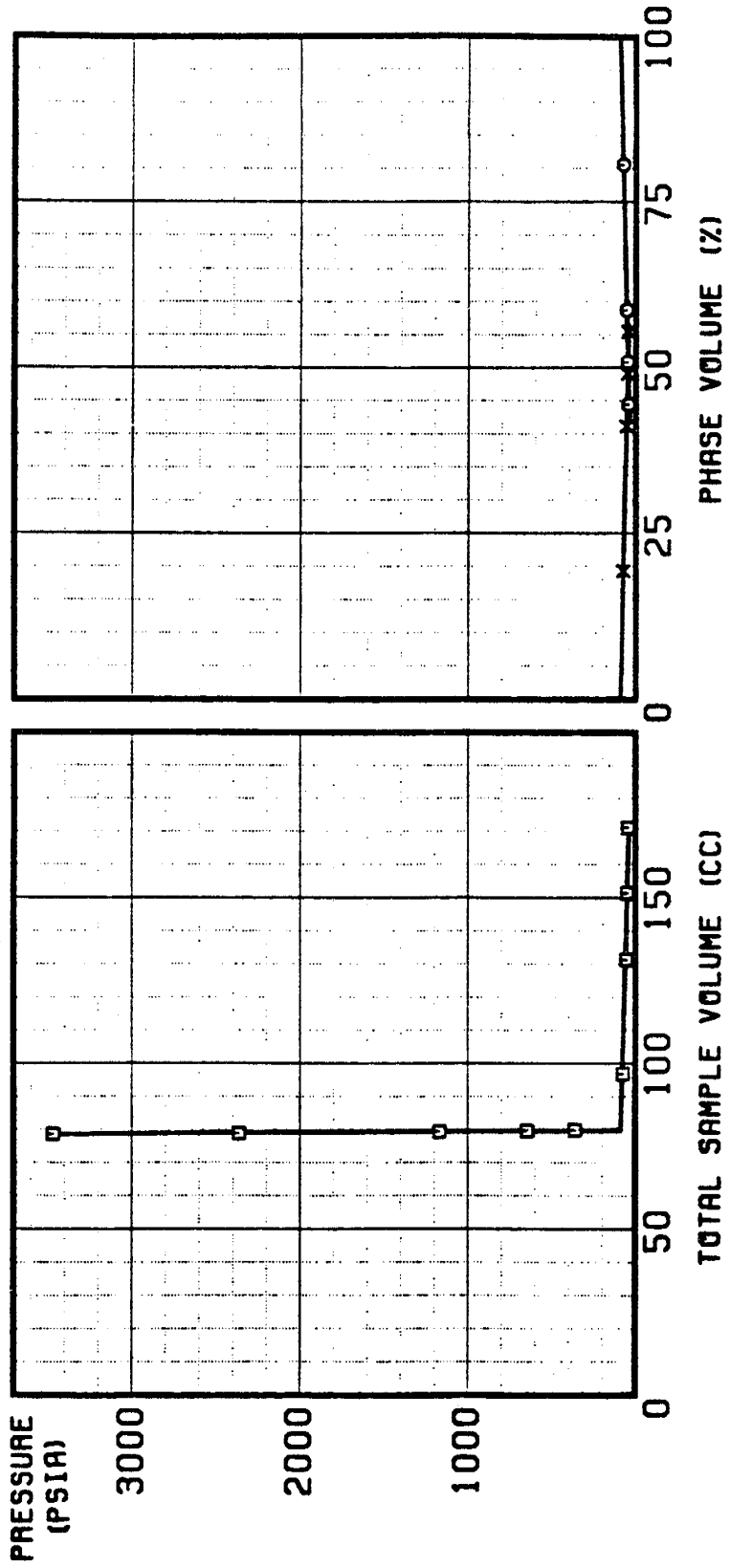
# 78.8% CO2 - 21.2% BF 140.0F



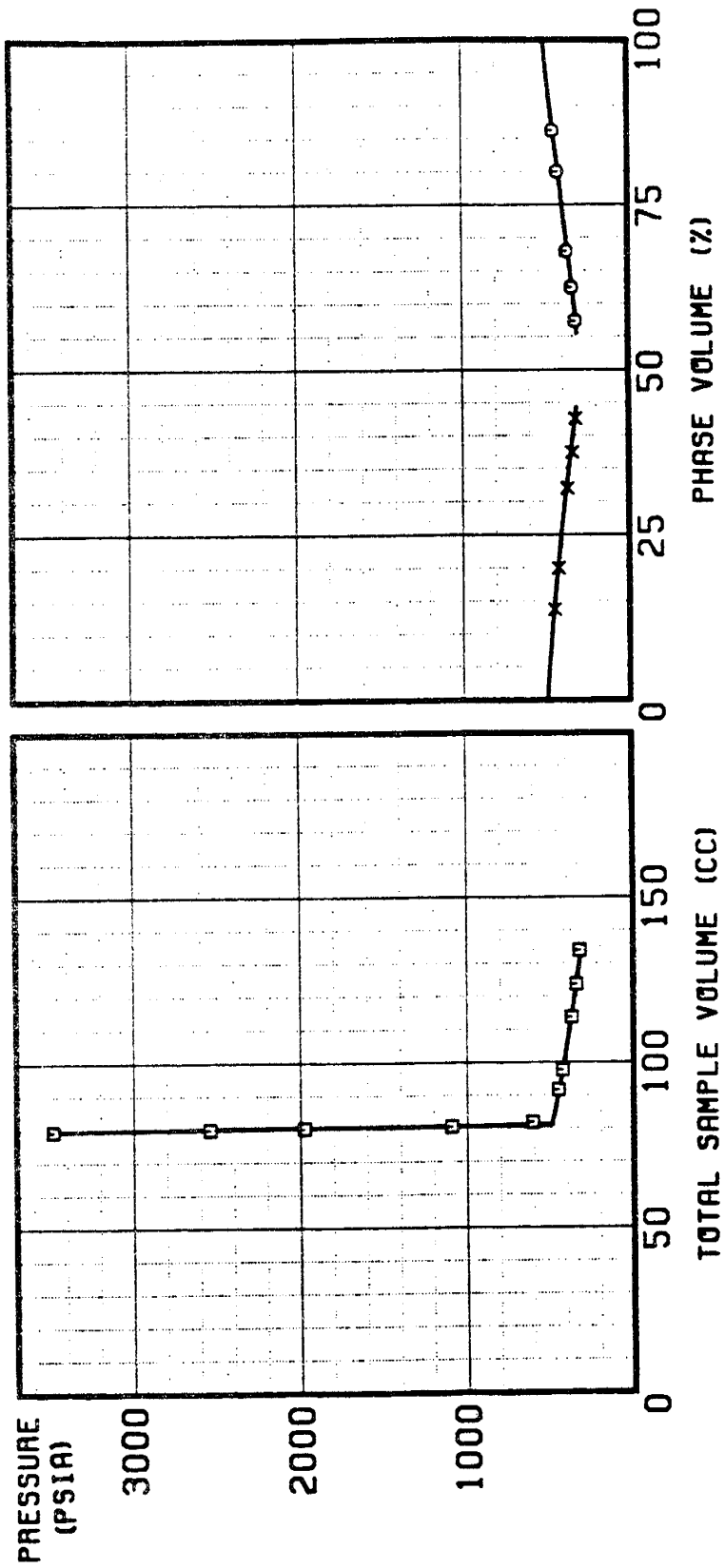
# 87.2% CO<sub>2</sub> - 12.8% BF 141.3F



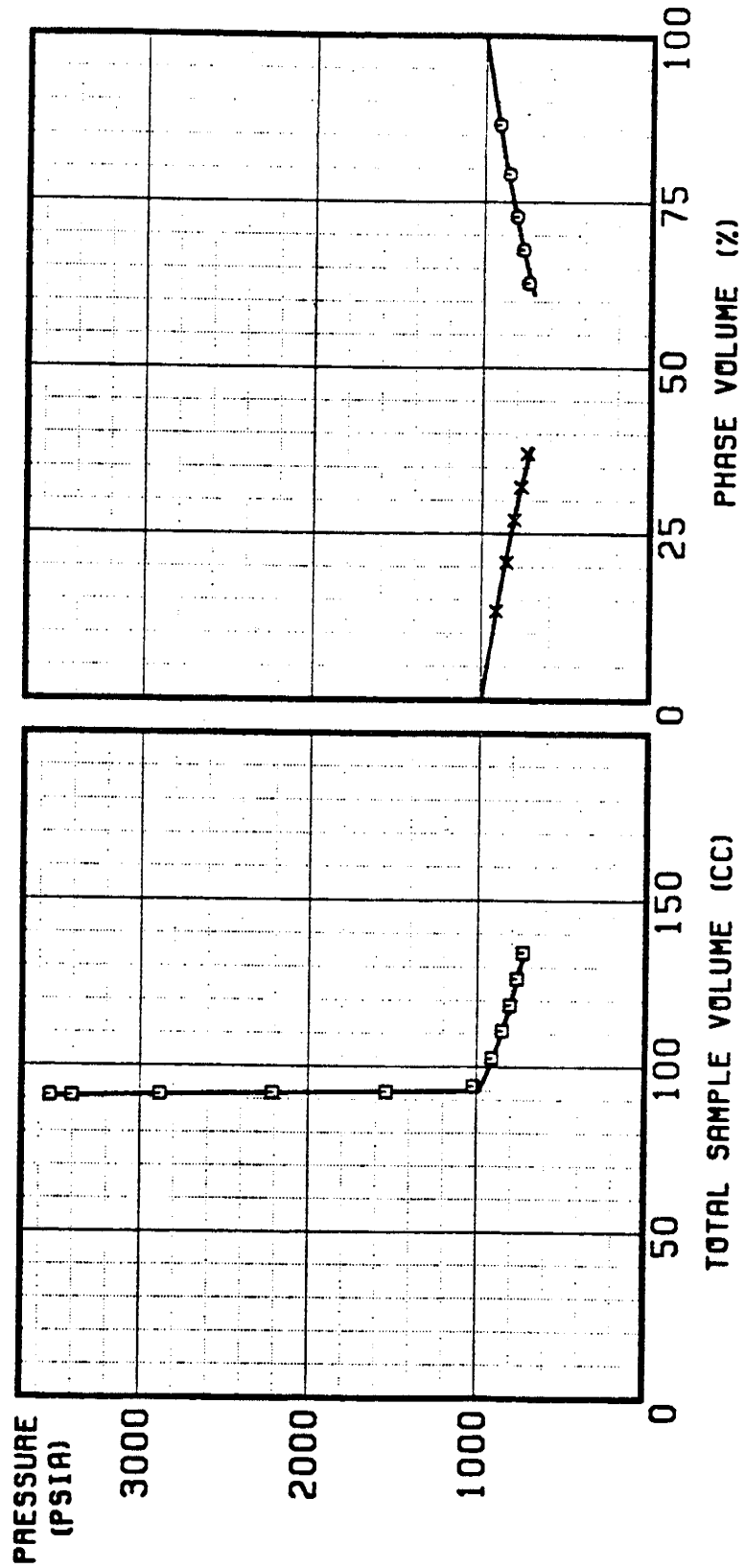
0% CO2 - 100% BF 111.4F



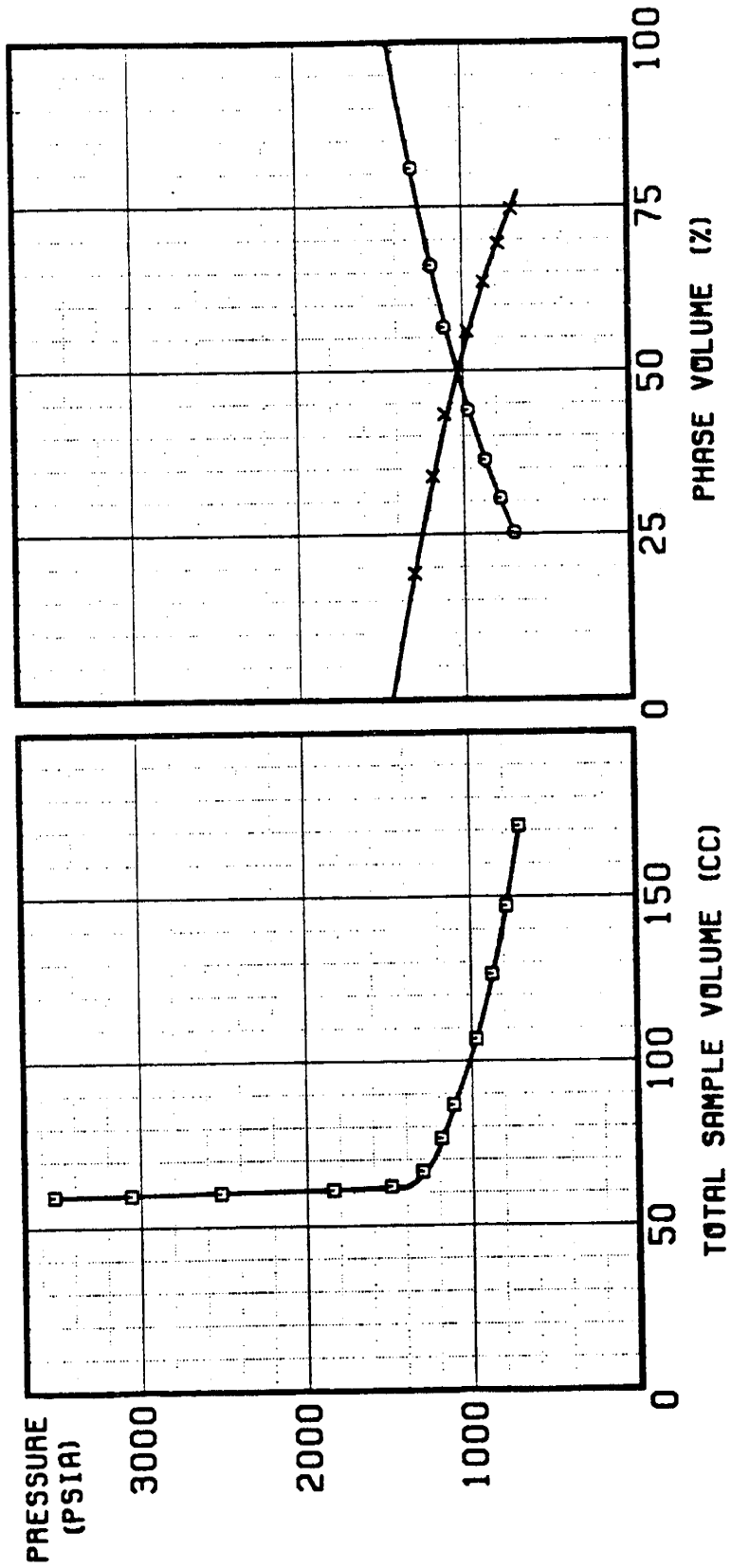
23.7% CO2 - 76.3% BF 111.3F



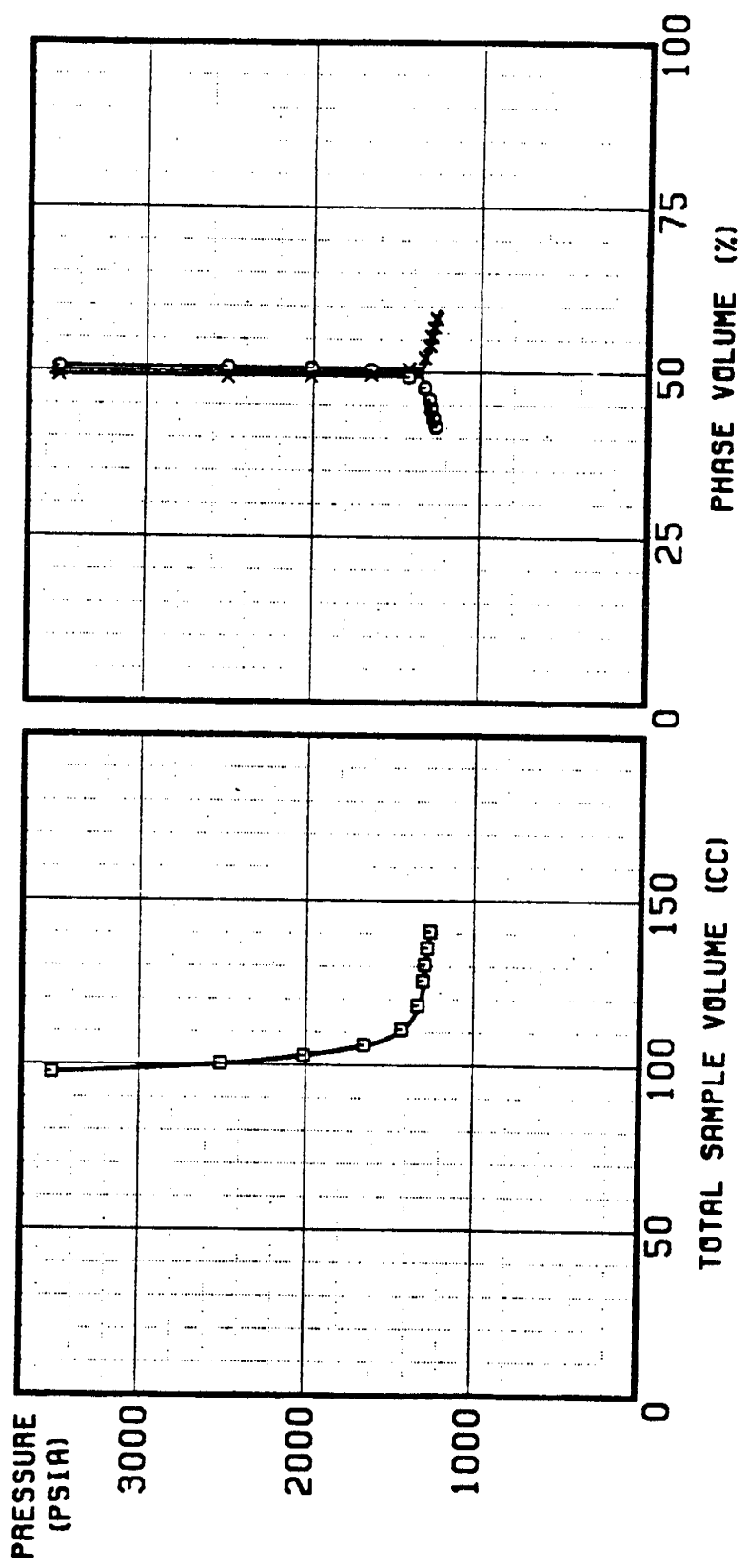
# 48.2% CO2 - 51.8% BF 111.2F



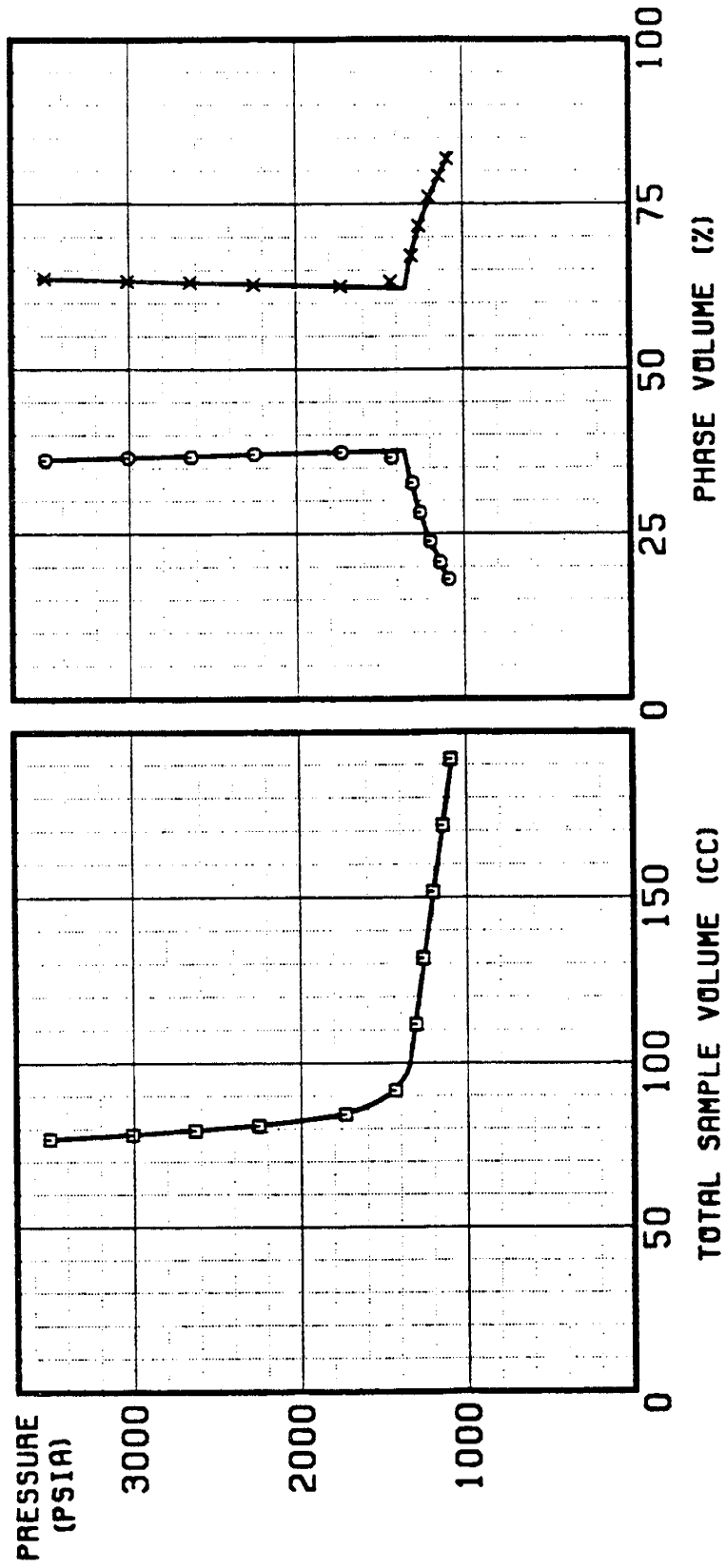
# 68.5% CO<sub>2</sub> - 31.5% BF 111.0F



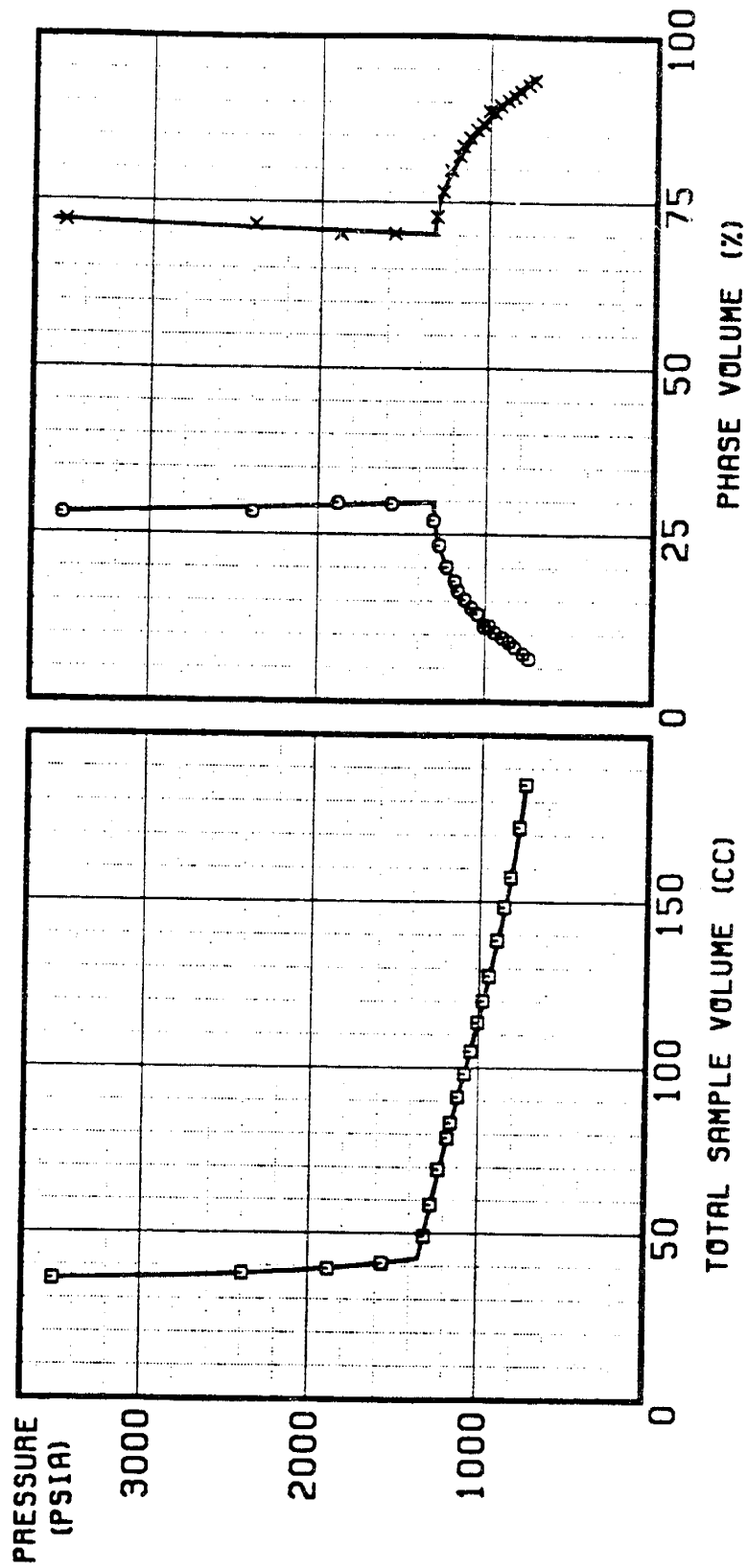
# 78.8% CO2 - 21.2% BF 110.6F



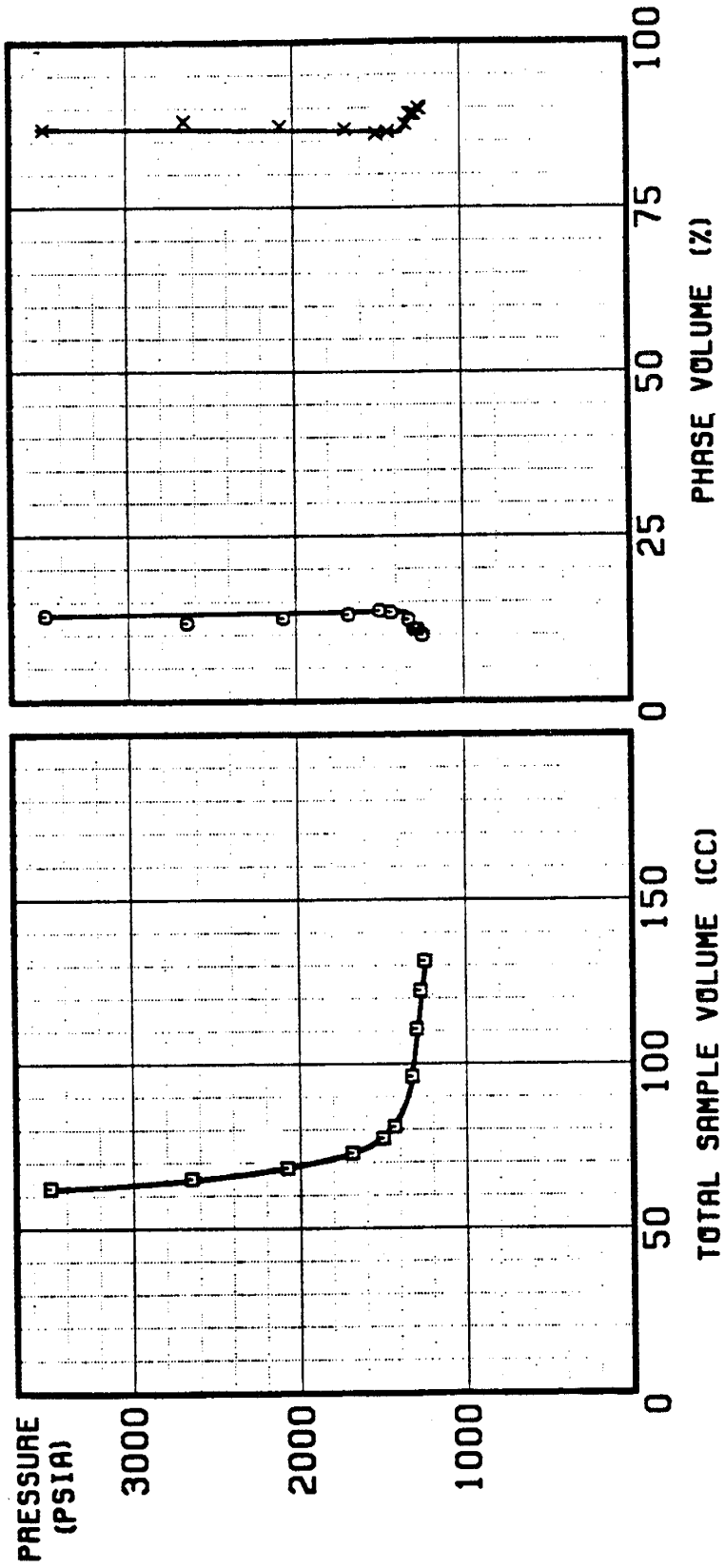
# 87.2% CO2 - 12.8% BF 110.3F



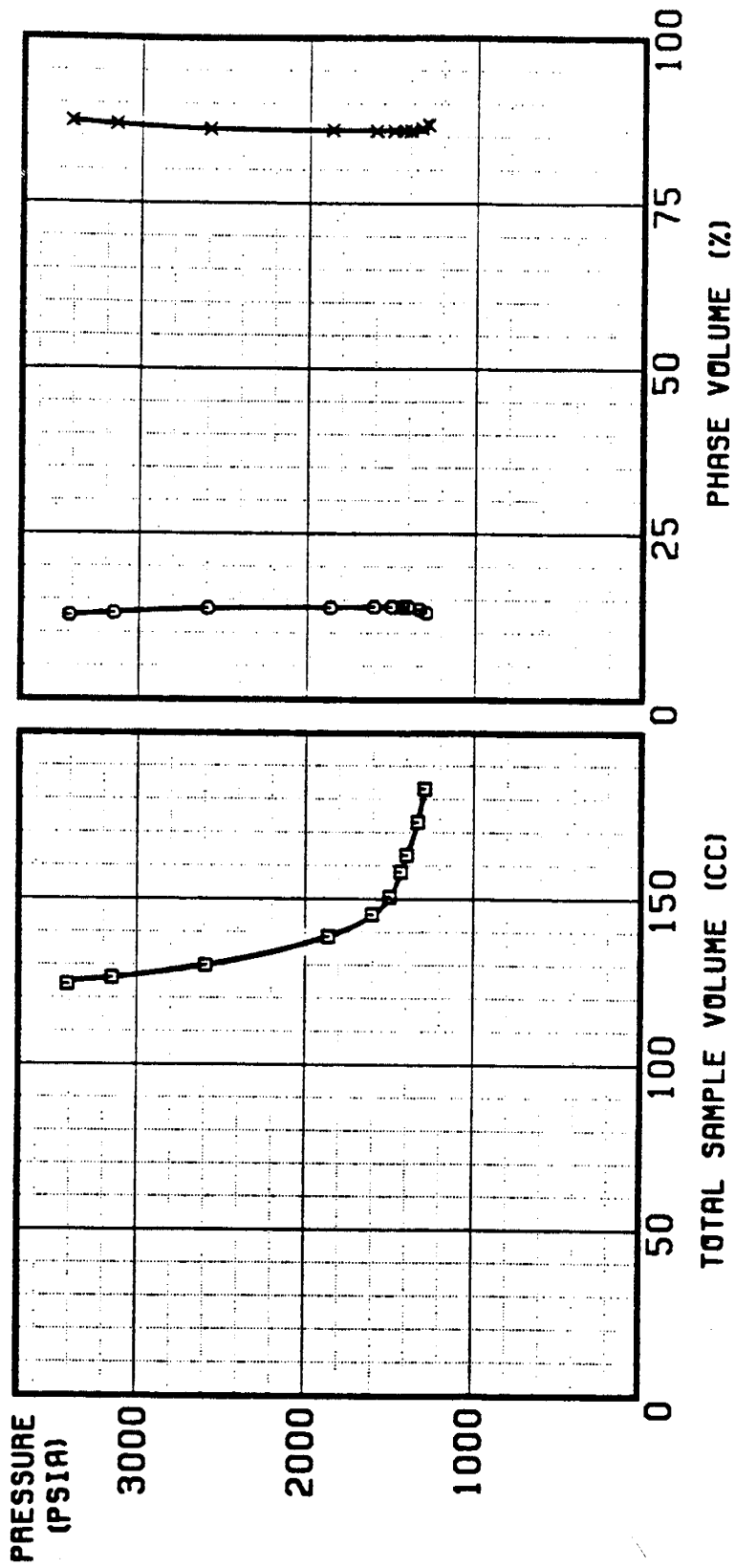
# 89.3% CO<sub>2</sub> - 10.7% BF 111.5F



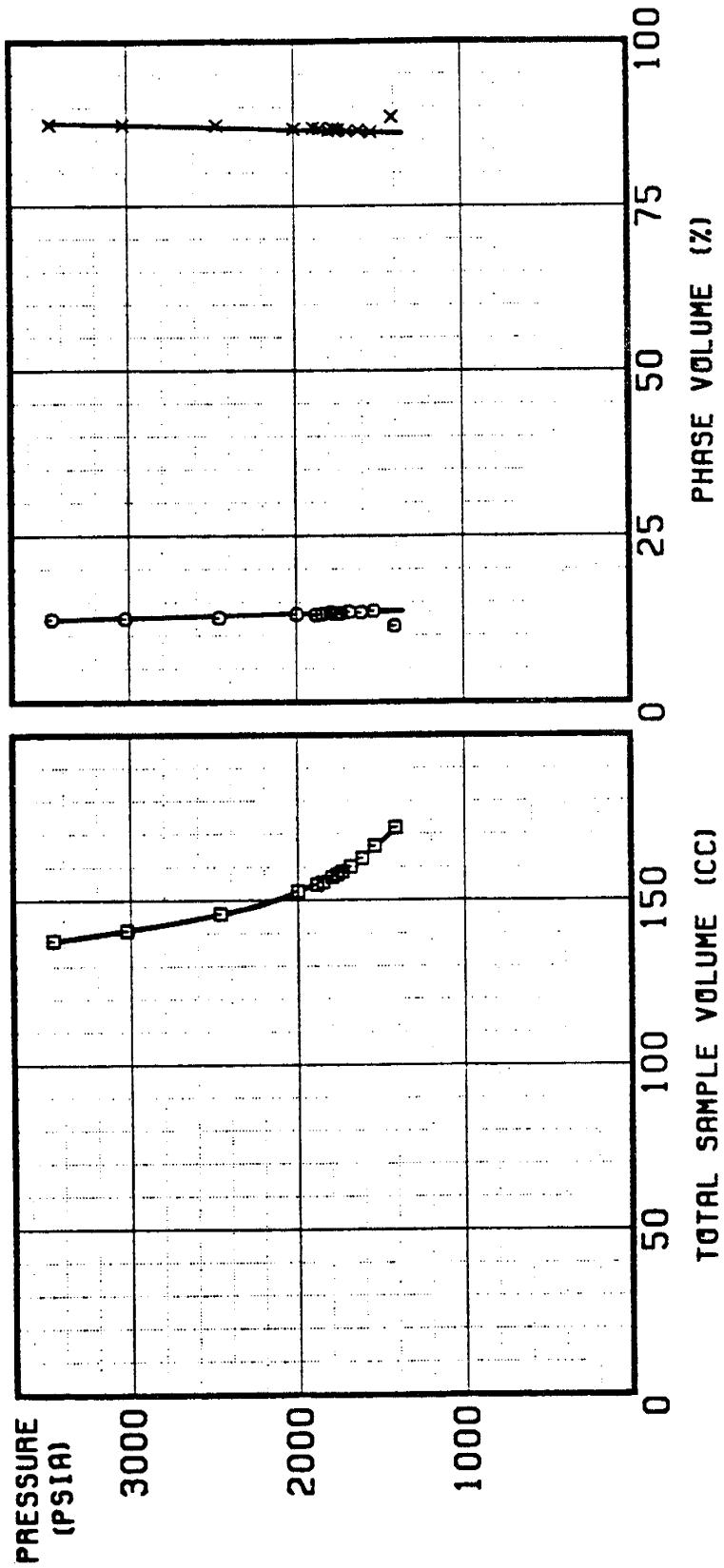
# 94.6% CO<sub>2</sub> - 5.4% BF 111.6F



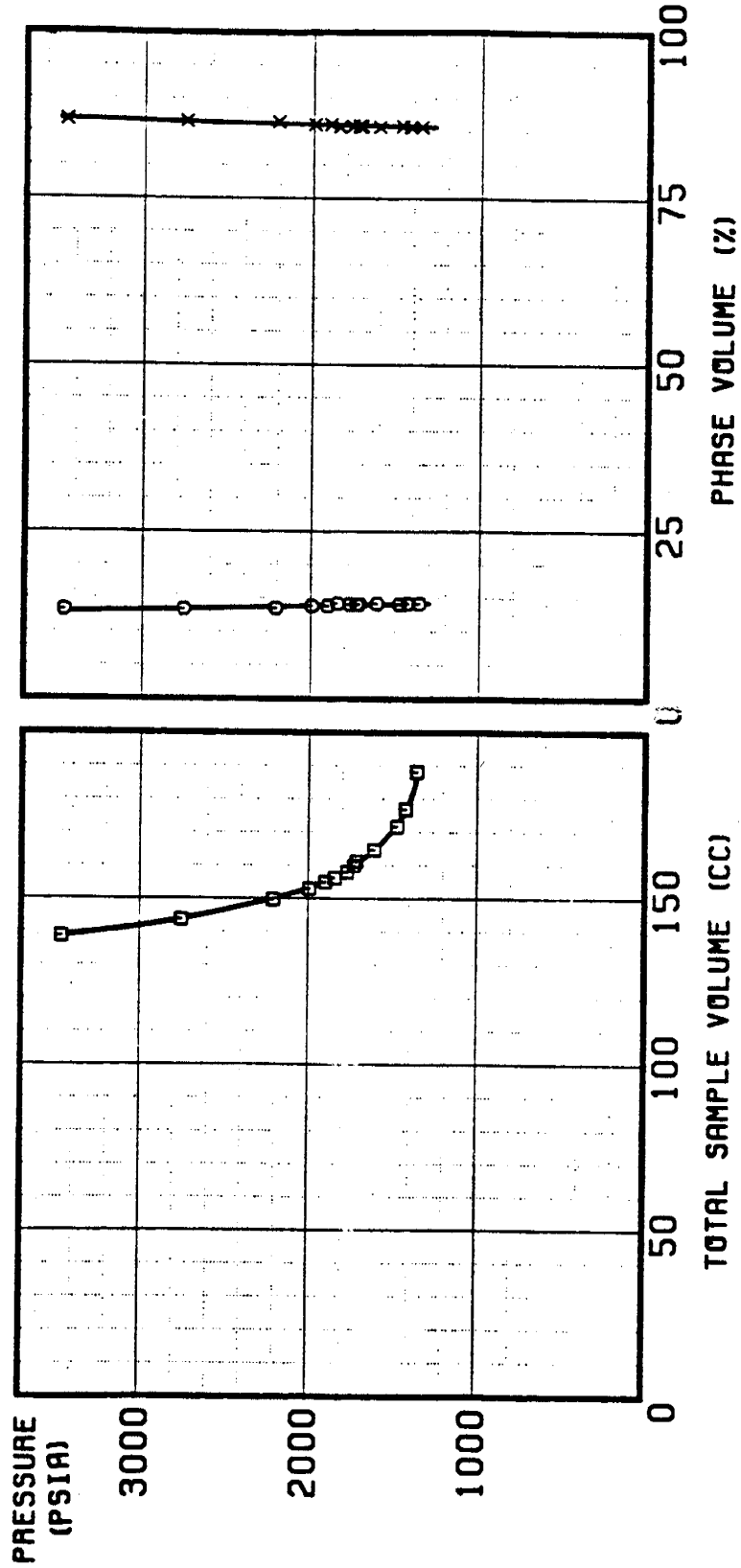
94.6% CO2 - 5.4% BF 110.4F #2



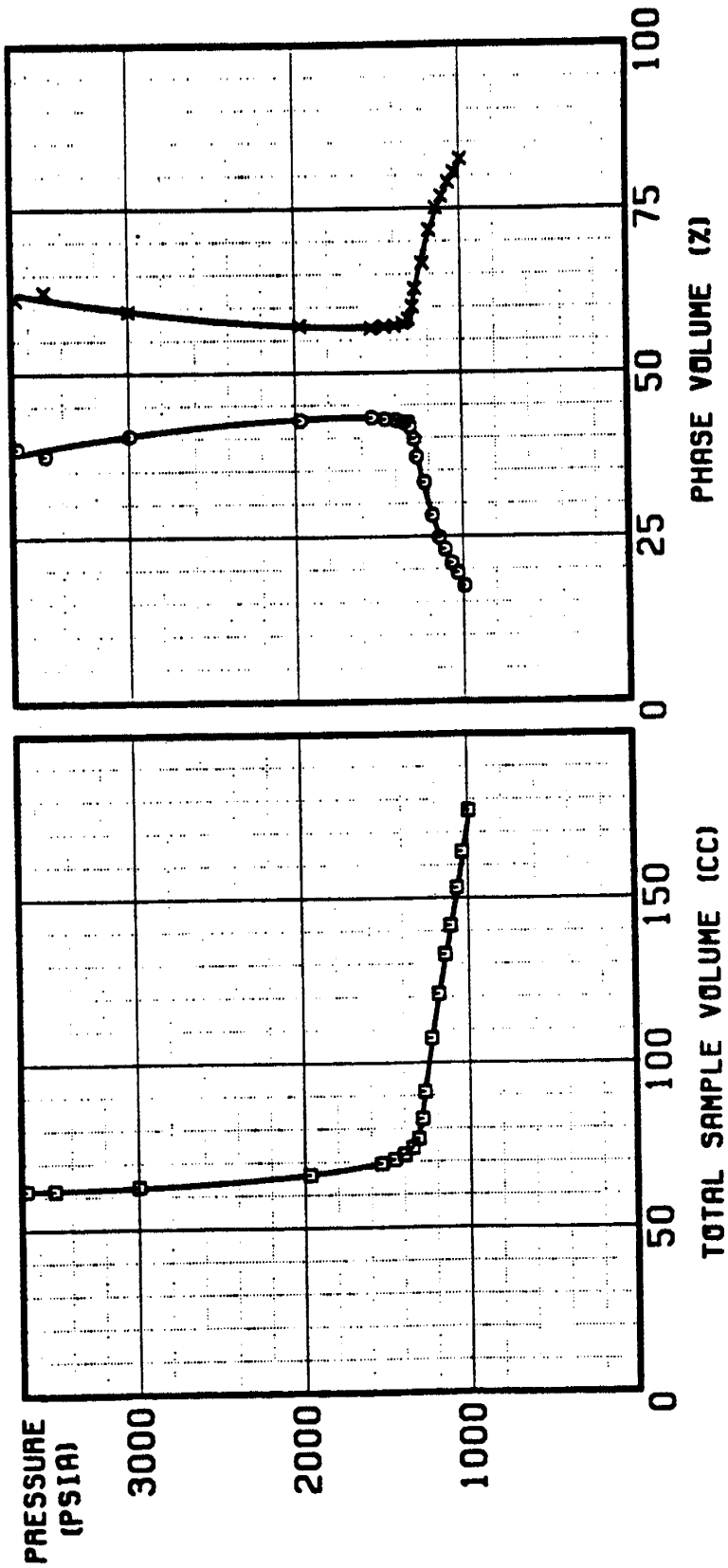
94.6% CO<sub>2</sub> - 5.4% BF 111.7F #3



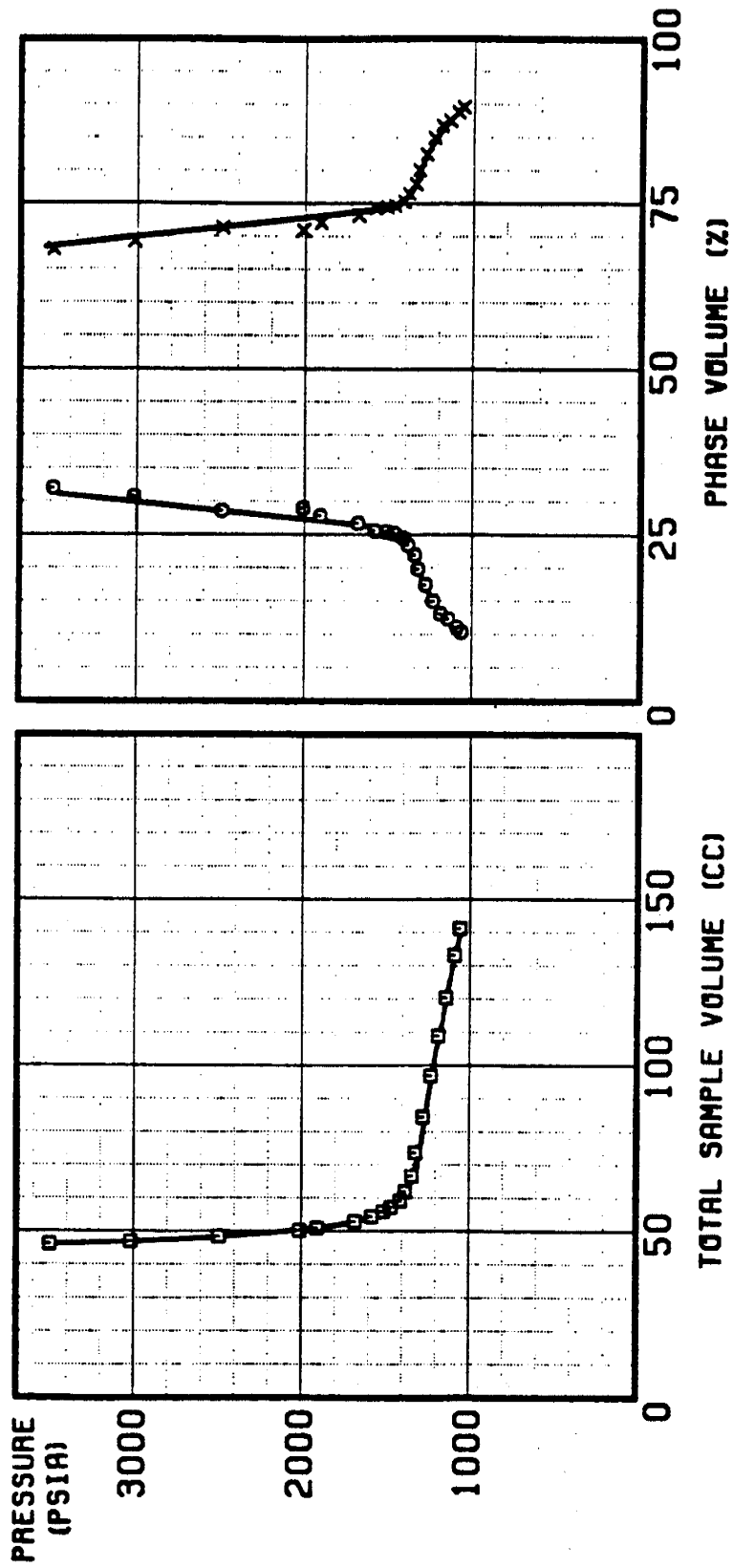
94.6% CO<sub>2</sub> - 5.4% BF 111.4F #4



# FIRST FORWARD CONTACT 113.5F



# FIRST SWEEP ZONE CONTACT 110.3F



PVT PROGRAM

```
INTEGER C6,C3
COMMON A1,A2,A3,A4,A5,A6,A7,A8,A9,B1,B2,B3,B4,B5,D1,D2,B3,D4,C2,
+C3,C4,C5,C7,V1,V2,V3,V4,TF
COMMON P,V,T,M,NT
DIMENSION B6(66),P(99),T(99),V(99),NT(5),VS(99),
&VCELL(99),VLIQC(99),DENS(99),Z(99),
&AC2(99),AC3(99),AC4(99),AC5(99),AC6(99),
&VLIQVP(99),VGASC(99),VGASVP(99),PAP(99),PAVS(99)
READ(5,*)A1,A2,A3,A4,A5,A6,A7
READ(5,*)A8,A9,B1,B2,B3,B4,B5
WRITE(6,100)
JCOM=0
M=0
ACUM=0
JPM=0
N=1
L=0
6 READ(5,1010) B6
  READ(5,*) B7,B8,B9,C1
1010 FORMAT(66A1)
  WRITE(6,101) B6
  WRITE(6,102) A4,A5,A6,A7
  WRITE(6,200)
  WRITE(6,103) A2,A3,A9,A8,B1
  WRITE(6,104) B7,B2,B3,B4,B5
  WRITE(6,105) B9,C1,B8
  IF(B1)1,2,3
2 B1=0.0
  D7=0.
  GO TO 7
1 TF=A9
  C4=A8
  CALL CELLV
  B1=V1
3 TF=A9
  C4=A8
  D1=B1
  CALL MERC
  D7=D2
7 READ(5,*,END=9) C2,C3,C4,C5,C6
  AC2(N)=C2
  AC3(N)=C3
```

```

AC4(N)=C4
AC5(N)=C5
AC6(N)=C6
8 GO TO(10,11,11,13),C6
10 CALL MANIC
   IF(JCOM)14,14,15
14 JCOM=1
   WRITE(6,107)
15 WRITE(6,108) C4,C5,C7
   GO TO 7
11 D1=0.0
   D2=A1
   TF=B7
   CALL MERC
   D4=D3-D1
   CALL COMAT
   D1=V2
   CALL MERC
   IF(C6-2)16,16,17
16 D5=D2
   GO TO 7
17 D6=D2
   D2=D5-D2
   D7=D7+D2
   D2=D7
   D5=D6
   TF=B8
   D1=0.
   CALL MERC
   V4=D1
   IF(A4)18,18,19
19 CALL CELLV
   VS(N)=V1-V4
   VCELL(N)=V1
   IC2=C2
   IF(IC2.NE.0) GO TO 21
   VLIQC(N)=0.
   VGASC(N)=0.
   VLIQVP(N)=0.
   VGASVP(N)=0.
   GO TO 20
21 CALL CATH (C2,C3,V4,VLIQ)
26 VLIQC(N)=VLIQ
   VGASC(N)=VS(N)-VLIQC(N)
   VLIQVP(N)=(VLIQC(N)/VS(N))*100.

```

```

      VGASVP(N)=(VGASC(N)/VS(N))*100.
20 DENS(N)=B9/VS(N)
      IF(C1.EQ.0.0) GO TO 18
      Z(N)=(1.4935E-3*C4*VS(N))/(C1*(BB+460.))
18 V(N)=V4
      P(N)=C4
      IF(JPM)22,22,23
22 WRITE(6,109)
23 WRITE(6,110) P(N),VCELL(N),V(N),VS(N),DENS(N),Z(N),VLIQC(N),VLIQVP
      &(N),VGASC(N),VGASVP(N)
      N=N+1
      JPM=1
      GO TO 7
13 M=M+1
      B1=V4
      A9=BB
      AB=C4
      JPM=0
      NT(M)=N-ACUM-1
      T(M)=BS
      ACUM=NT(M)+ACUM
      GO TO 6
9 IF(A4)24,24,25
24 M=M+1
      NT(M)=N-ACUM-1
      T(M)=BB
      CALL CALIBR
25 CONTINUE
100 FORMAT(/17X,'PROGRAM PVT MERCURY CALCULATIONS')
101 FORMAT(/17X,66A1/)
102 FORMAT(20X,'C E L L E Q U A T I O N'//16X,'CELL VOL.',4X,'TEM',
      + 'P-COEF',3X,'PRESS COEF-A',3X,'PRESS COEF-B'/12X,3E13.6,E15.6)
103 FORMAT(/14X,'PUMP COEF-A PUMP COEF-B START-TEMP START-PRESS ',
      + 'MERC-CELL'/12X,2E13.6,2(F10.3,2X),F9.3)
104 FORMAT(/14X,'RM.TEMP REF-PRESS REF-VOL MANIFL-500 MANIFL',
      + '8000'/12X,F9.3,1X,F10.4,1X,3F10.7)
105 FORMAT(/14X,'GRAMS IN CELL WCLS IN CELL CELL TEMP'/14X,3E13.6)
107 FORMAT(/26X,'MANIFOLD CALIBRATION'//23X,'PRESS. EXP-VOL',3X,
      + 'CAL.VOL')
108 FORMAT(17X,F10.0,2F10.4)
109 FORMAT(/8X,'PRESS. CELL-VOL CELL-HG SMPL-VOL DENSITY Z-FACTOR LIQ
      &-VOL Z-OIL-VOL GAS-VOL Z-GAS-VOL')
110 FORMAT(11H,5X,F7.0,3F9.3,2F9.5,4F8.2)
200 FORMAT(/26X,'I N I T I A L D A T A')
      WRITE(6,39)

```

```

39 FORMAT(///1H0,21X,'I N P U T   D A T A'/1H0,5X,'C2',10X,
&'C3',10X,'C4',10X,'C5',10X,'C6')
DD 1000 II=1,N
WRITE(6,40) AC2(II),AC3(II),AC4(II),AC5(II),AC6(II)
40 FORMAT(1H0,5F12.4)
1000 CONTINUE
59 STOP
END
SUBROUTINE CELLV
INTEGER C6,C3
COMMON A1,A2,A3,A4,A5,A6,A7,A8,A9,B1,B2,B3,B4,B5,
&D1,D2,D3,D4,C2,C3,C4,C5,C7,V1,V2,V3,V4,TF
V1=A4+A5*TF+(A6+A7*TF)*C4
RETURN
END
SUBROUTINE MANIC
INTEGER C6,C3
COMMON A1,A2,A3,A4,A5,A6,A7,A8,A9,B1,B2,B3,B4,B5,D1,D2,D3,D4,C2,
+C3,C4,C5,C7,V1,V2,V3,V4,TF
IF(B5-1.E-2)1,1,2
2 B5=(B3-B5)/(B2-3500)
B4=(B3-B4)/(B2-500.)
C7=0.
RETURN
1 C7=B3-((B5+((B4-B5)*1.E6)/(C4*B2))*(B2-C4))
RETURN
END
SUBROUTINE MERC
INTEGER C6,C3
COMMON A1,A2,A3,A4,A5,A6,A7,A8,A9,B1,B2,B3,B4,B5,D1,D2,D3,D4,C2,
+C3,C4,C5,C7,V1,V2,V3,V4,TF
HG1=(.2414+2.05E-4*TF)*1.E-6
HG2=0.5*(.214E-6+8.88E-9*TF)*1.E-6
HG3=HG1*C4-HG2*C4**2
HG4=1.0+1.0086E-4*(TF-60.)+2.4E-9*(TF-60.)**2
IF(ABS(D1)-0.00001)16,16,17
16 D3=D2*HG4
D1=D3*EXP(-HG3)
RETURN
17 D3=D1*EXP(HG3)
D2=D3/HG4
RETURN
END
SUBROUTINE COMAT
INTEGER C6,C3

```

```

COMMON A1,A2,A3,A4,A5,A6,A7,A8,A9,B1,B2,B3,B4,B5,D1,D2,D3,D4,C2,
+C3,C4,C5,C7,V1,V2,V3,V4,TF
CALL MANIC
V3=C7
V3=V3-D4
V2=A1-A2+C5-A3+C5**2+V3
RETURN
END
SUBROUTINE CATH(C2,C3,V4,VLIQ)
INTEGER C6,C3,C8
GOTO(1,2),C3
1 IF(C2.GT.250.0)GOTO11
VLIQ=(1.0418*C2+31.434)-V4
C8=2
GOTO8
11 VLIQ=(1.0478*C2-321.454)-V4
C8=1
GOTO8
2 IF(C2.GT.250.0)GOTO12
VLIQ=(1.0607*C2+1.550)-V4
C8=1
GOTO8
12 VLIQ=(1.0317*C2-345.053)-V4
C8=2
8 IF(VLIQ.GT.5.0)GOTO10
VLIQ=0.213*VLIQ
RETURN
10 GOTO(13,14),C8
13 VLIQ=VLIQ-3.679
RETURN
14 VLIQ=VLIQ-3.372
RETURN
END
SUBROUTINE CALIBR
INTEGER C6,C3
COMMON A1,A2,A3,A4,A5,A6,A7,A8,A9,B1,B2,B3,B4,B5,D1,D2,D3,D4,C2,
+C3,C4,C5,C7,V1,V2,V3,V4,TF
COMMON P,V,T,M,NT
DIMENSION B6(66),P(99),T(99),V(99),NT(5),VS(99),VCELL(99),VLIQC(99
+),DENS(99),Z(99)
DIMENSION SLOP(99),AINTER(99),AVRS(99),AVR(99),A(5),B(5),C(5),D(5)
+,AVRI(99)
N=0
KMAX=0
KNIN=1

```

```

L=0
K=0
DO 1 J=1,M
ASLOP=0.
ACINTR=0.
L=L+NT(J)-1
DO 10 I=KMIN,L
IF(P(I).NE.P(I+1)) GO TO 11
K=K+1
10 CONTINUE
11 KMIN=I
DO 12 I=KMIN,L
IF(P(I+1).EQ.P(KMIN)) GO TO 13
IF(I.NE.L) GO TO 12
WRITE(6,124)
RETURN
12 CONTINUE
13 KMAX=I-1
DO 2 I=KMIN,KMAX
SLOP(I)=(V(I+1)-V(I))/(P(I+1)-P(I))
ASLOP=ASLOP+SLOP(I)
AINTER(I)=V(I)-SLOP(I)*P(I)
ACINTR=ACINTR+AINTER(I)
2 CONTINUE
APOINT=NT(J)-K-2
AVRS(J)=ASLOP/APOINT
AVRI(J)=ACINTR/APOINT
K=0
KMIN=KMAX+3
L=L+1
1 CONTINUE
J=1
IF(N.EQ.2) GO TO 14
N=N-1
DO 3 J=1,N
14 D(J)=(AVRS(J)-AVRS(J+1))/(T(J)-T(J+1))
C(J)=AVRS(J)-D(J)*T(J)
B(J)=(AVRI(J)-AVRI(J+1))/(T(J)-T(J+1))
A(J)=AVRI(J)-B(J)*T(J)
A4=A4+A(J)
A5=A5+B(J)
A6=A6+C(J)
A7=A7+D(J)
3 CONTINUE
A4=A4/(M-1)

```

```

A5=A5/(M-1)
A6=A6/(M-1)
A7=A7/(M-1)
WRITE(6,120) A4,A5,A6,A7
120 FORMAT (/26X,'CELL CALIBRATION'//16X,'CELL VOL',4
+X,'TEMP-COEF',3X,'PRESS COEF-A',3X,'PRESS COEF-B',/12X,3E13.6,
+E15.6)
K=1
L=0
DO 4 J=1,M
WRITE(6,121) T(J)
WRITE(6,122)
L=L+NT(J)
DO 5 I=K,L
VHG=A4+A5*T(J)+(A6+A7*T(J))*P(I)
WRITE(6,123) P(I),V(I),VHG
5 CONTINUE
K=1+L
4 CONTINUE
121 FORMAT(//14X,'TEMPERATURE= ',F6.0)
122 FORMAT(/20X,'PRESS EXP-VOL CALC-VOL')
123 FORMAT(//18X,F7.0,F9.3,F10.3)
124 FORMAT(/20X,'MISTAKE IN INPUT DATA')
RETURN
END

```

TABLE A5: CO2-RICH PHASE

INITIAL MIXTURE (94.6% CO2 - 5.4% BF OIL)

COMPONENT	HIGH PRESSURE/ TEMPERATURE		RECOMBINATION OF FLASH		COMBINATION OF RESULTS	
	WEIGHT %	MOLE %	WEIGHT %	MOLE %	WEIGHT %	MOLE %
C-1	0.164	0.475	0.194	0.557	0.179	0.516
CO2	90.914	95.928	91.712	96.169	91.454	96.155
C-2	0.139	0.215	0.129	0.199	0.134	0.207
C-3	0.170	0.179	0.281	0.294	0.185	0.194
C-4	0.396	0.316	0.593	0.471	0.495	0.394
C-5	0.352	0.227	0.359	0.228	0.314	0.202
C-6	0.627	0.338	0.459	0.246	0.533	0.286
C-7	0.844	0.391	0.645	0.297	0.744	0.344
C-8	1.210	0.492	0.811	0.328	0.910	0.369
C-9	0.939	0.340	0.578	0.208	0.759	0.274
C-10	0.872	0.285	0.555	0.180	0.714	0.232
C-11	0.688	0.204	0.516	0.152	0.612	0.181
C-12	0.530	0.144	0.504	0.137	0.517	0.140
C-13	0.511	0.129	0.462	0.116	0.486	0.122
C-14	0.428	0.100	0.397	0.092	0.412	0.096
C-15	0.034	0.075	0.340	0.074	0.342	0.075
C-16	0.268	0.055	0.279	0.057	0.274	0.056
C-17	0.248	0.048	0.289	0.055	0.269	0.052
C-18	0.109	0.020	0.218	0.040	0.164	0.030
C-19	0.072	0.012	0.155	0.027	0.114	0.020
C-20	0.058	0.010	0.073	0.012	0.106	0.017
C-21	0.054	0.009	0.105	0.016	0.080	0.012
C-22	0.027	0.004	0.071	0.011	0.049	0.007
C-23	0.018	0.003	0.085	0.012	0.051	0.007
C-24	0.006	0.001	0.056	0.008	0.031	0.004
C-25	0.005	0.001	0.029	0.004	0.017	0.002
C-26	0.002	0.000	0.021	0.003	0.011	0.001
C-27	0.001	0.000	0.021	0.003	0.011	0.001
C-28	0.001	0.000	0.018	0.002	0.009	0.001
C-29	0.002	0.000	0.016	0.002	0.009	0.001
C-30	0.001	0.000	0.015	0.002	0.008	0.001
C-31	0.000	0.000	0.015	0.002	0.008	0.001
C-32	0.000	0.000	0.000	0.000	0.000	0.000
C-33	0.000	0.000	0.000	0.000	0.000	0.000
C-34	0.000	0.000	0.000	0.000	0.000	0.000
C-35	0.000	0.000	0.000	0.000	0.000	0.000
C-36	0.000	0.000	0.000	0.000	0.000	0.000
C-37+	0.000	0.000	0.000	0.000	0.000	0.000
TOTALS	100.000	100.000	100.000	100.000	100.000	100.000
MOLECULAR WEIGHT (g/g-mole)		46.44		46.15		46.27

TABLE A6: OIL-RICH PHASE

INITIAL MIXTURE (94.6% CO<sub>2</sub> - 5.4% BF OIL)

COMPONENT	HIGH PRESSURE/ TEMPERATURE		RECOMBINATION OF FLASH	
	WEIGHT %	MOLE %	WEIGHT %	MOLE %
C-1	0.100	0.484	0.083	0.664
CO <sub>2</sub>	44.553	78.933	21.934	63.684
C-2	0.420	1.090	0.086	0.364
C-3	0.242	0.428	0.116	0.336
C-4	0.917	1.230	0.267	0.587
C-5	0.822	0.888	0.322	0.570
C-6	1.310	1.186	1.323	1.961
C-7	1.850	1.440	1.367	1.743
C-8	2.480	1.692	1.630	1.823
C-9	1.951	1.186	1.414	1.408
C-10	1.961	1.075	1.545	1.388
C-11	1.617	0.807	1.627	1.330
C-12	1.663	0.761	1.777	1.333
C-13	1.884	0.797	1.966	1.363
C-14	1.768	0.695	1.864	1.201
C-15	2.038	0.748	2.232	1.343
C-16	1.699	0.585	2.010	1.134
C-17	2.091	0.678	2.219	1.179
C-18	1.544	0.473	2.206	1.108
C-19	0.975	0.283	1.643	0.782
C-20	0.843	0.233	1.659	0.750
C-21	0.731	0.192	1.878	0.809
C-22	0.525	0.132	1.901	0.782
C-23	0.376	0.090	1.741	0.685
C-24	0.585	0.135	1.520	0.573
C-25	0.617	0.137	1.400	0.507
C-26	0.677	0.144	1.371	0.478
C-27	0.752	0.154	1.515	0.508
C-28	0.972	0.192	1.452	0.470
C-29	0.642	0.122	1.338	0.418
C-30	0.486	0.090	1.311	0.396
C-31	0.336	0.060	1.259	0.368
C-32	0.265	0.046	1.075	0.305
C-33	0.101	0.017	2.471	0.679
C-34	0.050	0.008	0.338	0.090
C-35	0.037	0.006	1.284	0.333
C-36	0.000	0.000	0.000	0.000
C-37+	20.120	2.786	28.858	6.548
TOTALS	100.000	100.000	100.000	100.000
MOLECULAR WEIGHT (g/g-mole)		77.97		127.78

TABLE A7: CO2-RICH PHASE

FIRST FORWARD CONTACT

HIGH PRESSURE/  
TEMPERATURE

COMPONENT	WEIGHT %	MOLE %
C-1	0.334	0.984
CO2	85.601	92.059
C-2	0.898	1.413
C-3	0.643	0.690
C-4	1.150	0.937
C-5	0.674	0.442
C-6	0.839	0.461
C-7	1.004	0.474
C-8	1.559	0.646
C-9	1.234	0.456
C-10	0.972	0.323
C-11	0.874	0.265
C-12	0.635	0.176
C-13	0.540	0.139
C-14	0.422	0.101
C-15	0.306	0.068
C-16	0.233	0.049
C-17	0.255	0.050
C-18	0.230	0.043
C-19	0.157	0.028
C-20	0.199	0.033
C-21	0.136	0.022
C-22	0.137	0.021
C-23	0.111	0.016
C-24	0.089	0.013
C-25	0.120	0.016
C-26	0.123	0.016
C-27	0.112	0.014
C-28	0.130	0.016
C-29	0.147	0.017
C-30	0.138	0.015
C-31	0.000	0.000
C-32	0.000	0.000
C-33	0.000	0.000
C-34	0.000	0.000
C-35	0.000	0.000
C-36	0.000	0.000
C-37+	0.000	0.000
TOTALS	100.000	100.000

MOLECULAR  
WEIGHT 47.33  
(g/g-mole)

TABLE A8: OIL-RICH PHASE

## FIRST FORWARD CONTACT

COMPONENT	HIGH PRESSURE/ TEMPERATURE		RECOMBINATION OF FLASH	
	WEIGHT %	MOLE %	WEIGHT %	MOLE %
C-1	0.211	1.184	0.204	1.227
CO2	33.066	67.487	29.365	64.318
C-2	0.026	0.078	0.036	0.114
C-3	0.497	1.012	0.462	1.010
C-4	1.084	1.675	1.170	1.940
C-5	0.940	1.170	0.964	1.288
C-6	1.696	1.767	2.270	2.539
C-7	3.259	2.921	2.995	2.881
C-8	3.860	3.035	3.370	2.844
C-9	3.212	2.249	2.719	2.043
C-10	3.227	2.037	2.836	1.921
C-11	3.136	1.802	2.910	1.795
C-12	2.827	1.491	2.810	1.590
C-13	2.871	1.399	2.908	1.520
C-14	2.436	1.103	2.637	1.281
C-15	2.415	1.021	2.572	1.167
C-16	2.085	0.827	2.385	1.015
C-17	2.310	0.863	2.637	1.057
C-18	1.908	0.673	2.291	0.868
C-19	1.422	0.476	1.491	0.535
C-20	1.440	0.458	1.950	0.665
C-21	1.274	0.386	1.505	0.489
C-22	1.229	0.356	1.485	0.461
C-23	1.259	0.349	1.741	0.517
C-24	1.164	0.309	1.017	0.289
C-25	0.883	0.225	1.106	0.302
C-26	0.861	0.211	1.025	0.269
C-27	0.835	0.197	0.915	0.232
C-28	1.063	0.242	1.215	0.297
C-29	0.824	0.181	0.942	0.222
C-30	0.749	0.159	0.829	0.189
C-31	0.716	0.147	0.974	0.215
C-32	0.704	0.140	0.849	0.181
C-33	0.689	0.133	0.855	0.177
C-34	0.660	0.124	0.828	0.167
C-35	0.706	0.129	0.861	0.168
C-36	0.000	0.000	0.110	0.021
C-37+	12.457	1.987	12.765	2.185
TOTALS	100.000	100.000	100.000	100.000

MOLECULAR  
WEIGHT  
(g/g-mole)

89.82

96.39

TABLE A9: CO2-RICH PHASE

SECOND FORWARD CONTACT

HIGH PRESSURE/  
TEMPERATURE

COMPONENT WEIGHT % MOLE %

C-1	0.479	1.495
CO2	76.781	87.272
C-2	0.624	1.038
C-3	0.905	1.027
C-4	1.892	1.628
C-5	1.244	0.862
C-6	1.543	0.895
C-7	2.343	1.170
C-8	2.818	1.234
C-9	1.984	0.774
C-10	1.835	0.645
C-11	1.530	0.490
C-12	1.268	0.372
C-13	1.140	0.309
C-14	0.874	0.220
C-15	0.689	0.162
C-16	0.566	0.125
C-17	0.541	0.113
C-18	0.319	0.063
C-19	0.205	0.038
C-20	0.150	0.027
C-21	0.094	0.016
C-22	0.060	0.010
C-23	0.036	0.006
C-24	0.018	0.003
C-25	0.015	0.002
C-26	0.010	0.001
C-27	0.008	0.001
C-28	0.007	0.001
C-29	0.009	0.001
C-30	0.010	0.001
C-31	0.006	0.001
C-32	0.001	0.000
C-33	0.001	0.000
C-34	0.000	0.000
C-35	0.000	0.000
C-36	0.000	0.000
C-37+	0.000	0.000

TOTALS 100.000 100.000

MOLECULAR  
WEIGHT 50.02  
(g/g-mole)

TABLE A10: OIL-RICH PHASE

## SECOND FORWARD CONTACT

COMPONENT	HIGH PRESSURE/ TEMPERATURE		RECOMBINATION OF FLASH	
	WEIGHT %	MOLE %	WEIGHT %	MOLE %
C-1	0.121	0.599	0.104	0.559
C02	38.443	69.512	33.114	64.797
C-2	0.556	1.471	0.479	1.372
C-3	0.673	1.214	0.763	1.489
C-4	1.787	2.446	1.784	2.643
C-5	1.245	1.373	1.441	1.720
C-6	1.872	1.729	2.068	2.067
C-7	2.763	2.194	3.303	2.839
C-8	3.947	2.749	4.123	3.108
C-9	3.085	1.914	3.167	2.127
C-10	3.235	1.809	3.342	2.023
C-11	3.107	1.582	3.284	1.809
C-12	2.996	1.400	3.176	1.606
C-13	3.083	1.331	3.110	1.453
C-14	2.759	1.107	3.009	1.306
C-15	2.612	0.978	2.535	1.028
C-16	2.404	0.845	2.668	1.015
C-17	2.479	0.820	2.759	0.988
C-18	1.979	0.619	2.293	0.776
C-19	1.613	0.478	1.826	0.586
C-20	1.390	0.391	1.536	0.468
C-21	1.238	0.332	1.501	0.436
C-22	1.235	0.317	1.411	0.391
C-23	1.528	0.375	1.745	0.463
C-24	1.015	0.239	0.911	0.232
C-25	0.743	0.168	1.016	0.248
C-26	0.748	0.162	0.950	0.223
C-27	0.678	0.142	0.799	0.181
C-28	0.905	0.182	1.030	0.225
C-29	0.731	0.142	0.860	0.181
C-30	0.646	0.122	0.732	0.149
C-31	0.561	0.102	0.675	0.133
C-32	0.564	0.100	0.606	0.116
C-33	0.487	0.083	0.575	0.107
C-34	0.405	0.067	0.489	0.088
C-35	0.392	0.063	0.483	0.084
C-36	0.018	0.003	0.000	0.000
C-37+	5.959	0.842	6.334	0.969
TOTALS	100.000	100.000	100.000	100.000
MOLECULAR WEIGHT (g/g-mole)		79.58		86.12

TABLE A11: CO2-RICH PHASE

THIRD FORWARD CONTACT

COMPONENT	HIGH PRESSURE/ TEMPERATURE		RECOMBINATION OF FLASH		COMBINATION OF RESULTS	
	WEIGHT %	MOLE %	WEIGHT %	MOLE %	WEIGHT %	MOLE %
C-1	0.453	1.571	0.488	1.605	0.468	1.585
CO2	64.101	80.987	69.040	82.758	66.239	81.724
C-2	0.742	1.371	0.799	1.401	0.766	1.384
C-3	1.044	1.317	1.364	1.632	1.198	1.475
C-4	2.309	2.209	2.700	2.450	2.492	2.328
C-5	1.485	1.144	1.538	1.124	1.504	1.132
C-6	2.048	1.321	1.869	1.144	1.949	1.228
C-7	3.303	1.833	2.854	1.502	3.063	1.660
C-8	3.840	1.869	3.393	1.567	3.599	1.711
C-9	2.805	1.216	2.370	0.975	3.072	1.300
C-10	2.692	1.052	2.275	0.843	2.471	0.943
C-11	2.401	0.854	1.998	0.674	2.188	0.760
C-12	2.044	0.667	1.674	0.519	1.850	0.590
C-13	1.888	0.569	1.530	0.438	1.700	0.501
C-14	1.620	0.454	1.294	0.344	1.450	0.397
C-15	1.301	0.341	1.028	0.255	1.159	0.296
C-16	1.181	0.290	0.884	0.206	1.027	0.246
C-17	1.171	0.271	0.879	0.193	1.020	0.230
C-18	0.811	0.177	0.583	0.121	0.694	0.148
C-19	0.410	0.085	0.278	0.055	0.342	0.069
C-20	0.325	0.064	0.211	0.039	0.266	0.051
C-21	0.419	0.079	0.251	0.045	0.333	0.061
C-22	0.361	0.065	0.200	0.034	0.279	0.049
C-23	0.405	0.069	0.194	0.032	0.298	0.050
C-24	0.195	0.032	0.084	0.013	0.139	0.022
C-25	0.154	0.024	0.060	0.009	0.107	0.016
C-26	0.123	0.019	0.052	0.008	0.088	0.013
C-27	0.101	0.015	0.035	0.005	0.068	0.010
C-28	0.101	0.014	0.024	0.003	0.062	0.009
C-29	0.084	0.011	0.024	0.003	0.053	0.007
C-30	0.053	0.007	0.017	0.002	0.035	0.005
C-31	0.028	0.004	0.009	0.001	0.018	0.002
C-32	0.003	0.000	0.003	0.000	0.003	0.000
C-33	0.003	0.000	0.002	0.000	0.002	0.000
C-34	0.000	0.000	0.000	0.000	0.000	0.000
C-35	0.000	0.000	0.000	0.000	0.000	0.000
C-36	0.000	0.000	0.000	0.000	0.000	0.000
C-37+	0.000	0.000	0.000	0.000	0.000	0.000
TOTALS	100.000	100.000	100.000	100.000	100.000	100.000
MOLECULAR WEIGHT (g/g-mole)		55.60		52.76		54.30

TABLE A12: OIL-RICH PHASE

## THIRD FORWARD CONTACT

COMPONENT	HIGH PRESSURE/ TEMPERATURE		RECOMBINATION OF FLASH	
	WEIGHT %	MOLE %	WEIGHT %	MOLE %
C-1	0.180	0.788	0.150	0.739
C02	43.646	69.805	36.561	65.482
C-2	0.779	1.824	0.653	1.711
C-3	1.032	1.646	0.864	1.545
C-4	2.492	3.018	2.287	3.101
C-5	1.618	1.579	1.438	1.571
C-6	2.582	2.109	2.130	1.948
C-7	3.679	2.584	3.675	2.891
C-8	4.631	2.854	4.781	3.299
C-9	3.455	1.896	3.600	2.212
C-10	3.576	1.769	3.753	2.079
C-11	3.329	1.499	3.624	1.827
C-12	3.181	1.315	3.428	1.587
C-13	3.161	1.207	3.456	1.478
C-14	2.923	1.037	3.186	1.266
C-15	2.507	0.831	2.773	1.029
C-16	2.367	0.736	2.694	0.938
C-17	2.508	0.734	2.850	0.934
C-18	1.971	0.545	2.462	0.762
C-19	1.362	0.357	1.388	0.408
C-20	1.302	0.324	1.629	0.454
C-21	1.123	0.267	1.436	0.382
C-22	0.998	0.226	1.325	0.336
C-23	1.142	0.248	1.618	0.393
C-24	0.588	0.122	0.863	0.201
C-25	0.537	0.107	0.921	0.206
C-26	0.558	0.107	0.863	0.185
C-27	0.459	0.085	0.754	0.156
C-28	0.571	0.102	0.920	0.184
C-29	0.454	0.078	0.800	0.154
C-30	0.377	0.063	0.669	0.125
C-31	0.292	0.047	0.622	0.112
C-32	0.228	0.036	0.540	0.094
C-33	0.171	0.026	0.498	0.085
C-34	0.113	0.017	0.409	0.067
C-35	0.076	0.011	0.381	0.061
C-36	0.036	0.005	0.000	0.000
C-37+	0.000	0.000	0.000	0.000
TOTALS	100.000	100.000	100.000	100.000

MOLECULAR  
WEIGHT  
(g/g-mole)

70.39

78.82

TABLE A13: CO2-RICH PHASE

## FIRST SWEEPED ZONE CONTACT

COMPONENT	HIGH PRESSURE/ TEMPERATURE		RECOMBINATION OF FLASH		COMBINATION OF RESULTS	
	WEIGHT %	MOLE %	WEIGHT %	MOLE %	WEIGHT %	MOLE %
C-1	0.063	0.178	0.069	0.195	0.066	0.187
CO2	95.459	97.882	94.358	97.948	94.908	97.905
C-2	0.081	0.121	0.056	0.085	0.068	0.103
C-3	0.050	0.051	0.081	0.084	0.065	0.067
C-4	0.141	0.110	0.189	0.149	0.165	0.129
C-5	0.092	0.057	0.098	0.062	0.195	0.123
C-6	0.471	0.247	0.175	0.093	0.223	0.117
C-7	0.855	0.385	0.476	0.217	0.666	0.302
C-8	0.982	0.388	0.582	0.233	0.782	0.311
C-9	0.861	0.303	0.418	0.149	0.639	0.226
C-10	0.581	0.184	0.398	0.128	0.490	0.156
C-11	0.191	0.055	0.329	0.096	0.260	0.076
C-12	0.022	0.006	0.335	0.090	0.178	0.048
C-13	0.078	0.019	0.354	0.088	0.216	0.053
C-14	0.010	0.002	0.295	0.068	0.152	0.035
C-15	0.010	0.002	0.314	0.067	0.162	0.035
C-16	0.010	0.002	0.249	0.050	0.130	0.026
C-17	0.015	0.003	0.277	0.053	0.146	0.028
C-18	0.017	0.003	0.200	0.036	0.108	0.019
C-19	0.011	0.002	0.131	0.022	0.071	0.012
C-20	0.000	0.000	0.141	0.023	0.071	0.011
C-21	0.000	0.000	0.105	0.016	0.052	0.008
C-22	0.000	0.000	0.097	0.014	0.048	0.007
C-23	0.000	0.000	0.063	0.009	0.032	0.004
C-24	0.000	0.000	0.047	0.006	0.023	0.003
C-25	0.000	0.000	0.043	0.006	0.022	0.003
C-26	0.000	0.000	0.038	0.005	0.019	0.002
C-27	0.000	0.000	0.039	0.005	0.019	0.002
C-28	0.000	0.000	0.025	0.003	0.013	0.001
C-29	0.000	0.000	0.022	0.003	0.011	0.001
C-30	0.000	0.000	0.000	0.000	0.000	0.000
C-31	0.000	0.000	0.000	0.000	0.000	0.000
C-32	0.000	0.000	0.000	0.000	0.000	0.000
C-33	0.000	0.000	0.000	0.000	0.000	0.000
C-34	0.000	0.000	0.000	0.000	0.000	0.000
C-35	0.000	0.000	0.000	0.000	0.000	0.000
C-36	0.000	0.000	0.000	0.000	0.000	0.000
C-37+	0.000	0.000	0.000	0.000	0.000	0.000
TOTALS	100.000	100.000	100.000	100.000	100.000	100.000
MOLECULAR WEIGHT (g/g-mole)		45.13		45.68		45.40

TABLE A14: OIL-RICH PHASE

## FIRST SWEEPED ZONE CONTACT

COMPONENT	HIGH PRESSURE/ TEMPERATURE		RECOMBINATION OF FLASH	
	WEIGHT %	MOLE %	WEIGHT %	MOLE %
C-1	0.046	0.621	0.095	0.912
CO2	8.935	43.588	18.351	64.032
C-2	0.027	0.194	0.056	0.285
C-3	0.013	0.061	0.026	0.089
C-4	0.054	0.198	0.110	0.291
C-5	0.115	0.343	0.237	0.504
C-6	0.425	1.058	0.560	0.998
C-7	0.526	1.128	0.890	1.364
C-8	1.358	2.551	0.582	0.782
C-9	1.275	2.134	0.435	0.520
C-10	1.434	2.164	0.472	0.509
C-11	2.281	3.133	0.584	0.574
C-12	1.530	1.928	0.844	0.761
C-13	1.523	1.773	1.204	1.003
C-14	1.441	1.559	1.456	1.127
C-15	1.438	1.453	1.461	1.056
C-16	1.401	1.328	1.771	1.201
C-17	1.641	1.465	2.052	1.311
C-18	1.610	1.358	1.736	1.048
C-19	1.202	0.961	1.648	0.943
C-20	1.346	1.022	1.622	0.882
C-21	1.378	0.997	1.565	0.810
C-22	1.362	0.942	1.540	0.761
C-23	1.326	0.877	1.979	0.936
C-24	1.149	0.728	1.116	0.506
C-25	1.041	0.633	1.166	0.508
C-26	1.041	0.609	1.202	0.504
C-27	1.033	0.583	1.041	0.420
C-28	1.298	0.706	1.350	0.525
C-29	1.096	0.575	1.176	0.442
C-30	1.046	0.531	0.994	0.361
C-31	1.057	0.520	0.883	0.310
C-32	1.102	0.525	0.793	0.270
C-33	1.129	0.522	0.676	0.223
C-34	1.097	0.492	0.543	0.174
C-35	1.227	0.534	0.444	0.138
C-36	0.000	0.000	0.365	0.111
C-37+	53.000	20.207	46.975	12.810
TOTALS	100.000	100.000	100.000	100.000
MOLECULAR WEIGHT (g/g-mole)		214.69		153.56

TABLE A15: CO2-RICH PHASE

SECOND SWEEPED ZONE CONTACT

COMPONENT	HIGH PRESSURE/ TEMPERATURE		RECOMBINATION OF FLASH		COMBINATION OF RESULTS	
	WEIGHT %	MOLE %	WEIGHT %	MOLE %	WEIGHT %	MOLE %
C-1	0.040	0.112	0.065	0.179	0.052	0.145
CO2	98.388	99.342	98.143	99.260	98.266	99.301
C-2	0.010	0.015	0.019	0.028	0.015	0.022
C-3	0.012	0.012	0.028	0.028	0.020	0.020
C-4	0.039	0.029	0.064	0.049	0.051	0.039
C-5	0.034	0.021	0.041	0.025	0.038	0.023
C-6	0.054	0.028	0.049	0.025	0.052	0.027
C-7	0.133	0.059	0.093	0.041	0.113	0.050
C-8	0.228	0.089	0.131	0.051	0.180	0.070
C-9	0.193	0.067	0.107	0.037	0.150	0.052
C-10	0.204	0.064	0.119	0.037	0.162	0.051
C-11	0.174	0.049	0.117	0.033	0.145	0.041
C-12	0.149	0.039	0.126	0.033	0.137	0.036
C-13	0.119	0.029	0.131	0.032	0.125	0.030
C-14	0.079	0.018	0.116	0.026	0.097	0.022
C-15	0.068	0.014	0.121	0.025	0.094	0.020
C-16	0.026	0.005	0.099	0.019	0.063	0.012
C-17	0.021	0.004	0.110	0.020	0.066	0.012
C-18	0.015	0.003	0.089	0.016	0.052	0.009
C-19	0.007	0.001	0.049	0.008	0.028	0.005
C-20	0.007	0.001	0.040	0.006	0.024	0.004
C-21	0.000	0.000	0.044	0.007	0.022	0.003
C-22	0.000	0.000	0.029	0.004	0.014	0.002
C-23	0.000	0.000	0.021	0.003	0.010	0.001
C-24	0.000	0.000	0.016	0.002	0.008	0.001
C-25	0.000	0.000	0.012	0.002	0.006	0.001
C-26	0.000	0.000	0.010	0.001	0.005	0.001
C-27	0.000	0.000	0.009	0.001	0.005	0.001
C-28	0.000	0.000	0.006	0.001	0.003	0.000
C-29	0.000	0.000	0.000	0.000	0.000	0.000
C-30	0.000	0.000	0.000	0.000	0.000	0.000
C-31	0.000	0.000	0.000	0.000	0.000	0.000
C-32	0.000	0.000	0.000	0.000	0.000	0.000
C-33	0.000	0.000	0.000	0.000	0.000	0.000
C-34	0.000	0.000	0.000	0.000	0.000	0.000
C-35	0.000	0.000	0.000	0.000	0.000	0.000
C-36	0.000	0.000	0.000	0.000	0.000	0.000
C-37+	0.000	0.000	0.000	0.000	0.000	0.000
TOTALS	100.000	100.000	100.000	100.000	100.000	100.000
MOLECULAR WEIGHT (g/g-mole)	44.44		44.51		44.47	

TABLE A16: OIL-RICH PHASE

## SECOND SWEEPED ZONE CONTACT

COMPONENT	HIGH PRESSURE/ TEMPERATURE		RECOMBINATION OF FLASH	
	WEIGHT %	MOLE %	WEIGHT %	MOLE %
C-1	0.032	0.457	0.066	0.667
CO2	8.671	45.745	18.116	66.732
C-2	0.003	0.025	0.007	0.036
C-3	0.003	0.015	0.006	0.022
C-4	0.013	0.051	0.027	0.075
C-5	0.048	0.155	0.101	0.226
C-6	0.167	0.449	0.010	0.019
C-7	0.186	0.431	0.036	0.058
C-8	0.565	1.148	0.190	0.270
C-9	0.575	1.041	0.260	0.328
C-10	0.766	1.250	0.343	0.391
C-11	0.926	1.376	0.419	0.435
C-12	1.207	1.645	0.722	0.687
C-13	1.248	1.572	1.079	0.949
C-14	1.140	1.334	1.005	0.821
C-15	1.519	1.661	1.494	1.141
C-16	1.459	1.496	1.381	0.989
C-17	1.761	1.700	1.810	1.220
C-18	1.718	1.567	1.459	0.930
C-19	1.234	1.067	1.484	0.896
C-20	1.445	1.187	1.611	0.924
C-21	1.521	1.191	1.399	0.765
C-22	1.252	0.936	1.679	0.877
C-23	1.597	1.142	1.264	0.631
C-24	1.255	0.860	1.197	0.573
C-25	1.111	0.732	1.349	0.620
C-26	1.248	0.790	1.361	0.602
C-27	1.382	0.843	1.523	0.649
C-28	1.172	0.689	1.234	0.507
C-29	1.119	0.636	1.199	0.475
C-30	1.100	0.604	1.045	0.401
C-31	1.047	0.556	0.929	0.345
C-32	0.938	0.483	0.761	0.274
C-33	0.924	0.462	0.670	0.234
C-34	0.844	0.409	0.508	0.172
C-35	0.842	0.397	0.463	0.152
C-36	0.000	0.000	0.000	0.000
C-37+	57.962	23.899	51.795	14.912
TOTALS	100.000	100.000	100.000	100.000
MOLECULAR WEIGHT (g/g-mole)		232.18		162.12

PROGRAM 6CA

```

10 REM **THIS PROGRAM CALCULATES THE PHASE COMPOSITION
20 REM **FROM GAS CHROMATOGRAPHIC AREAS
30 DEFINT I-N
40 DEFDBL A,C,G,T,W,X,Y
50 DIM A(40),W(40),X(40),Y(40),DSN$(10)
60 REM **ENTERING KEYBOARD DATA
70 INPUT "RUN TITLE";RT$
80 INPUT "SAMPLE";S$
90 INPUT "FRACTION OF C5+ SEEN BY GC";FS
100 INPUT "NUMBER OF DATA SETS";ND
110 FOR NI=1 TO ND
120 REM **STARTING THE LOOP TO ENTER THE DATA SET NAMES
130 REM **INTO AN ARRAY
140 PRINT "ENTER FILE NAME OF DATA SET";NI
150 INPUT DSN$(NI)
160 NEXT NI
170 REM **SETTING THE TOTAL AREA EQUAL TO ZERO
180 GCS = 0
190 FOR NI=1 TO ND
200 J = 0
210 REM **READING THE DATA INTO THE PROGRAM
220 OPEN "I",#1,DSN$(NI)
230 IF EOF(1) THEN 310
240 INPUT#1,AA
250 REM **COMPUTING THE TOTAL AREA
260 GCS = GCS+AA
270 REM **COMPUTING THE TOTAL COMPONENT AREA
280 A(J) = A(J) + AA
290 J = J+1
300 GOTO 230
310 CLOSE #1
320 NEXT NI
330 REM **SETTING THE C5 - C36 AREA EQUAL TO ZERO
340 C5C36 = 0
350 REM **COMPUTING THE C5 - C36 AREA
360 FOR K=5 TO 36
370 C5C36 = C5C36+A(K)
380 NEXT K
390 REM **COMPUTING THE C37+ AREA
400 A(37) = C5C36/FS-C5C36

```

```

410 REM **COMPUTING THE TOTAL AREA THAT SHOULD HAVE BEEN
420 REM **SEEN BY THE GAS CHROMATOGRAPH
430 TA = GCS+A(37)
440 REM **SETTING THE TOTAL WEIGHT PERCENT AND MOLES TO ZERO
450 TMP = 0
460 TM = 0
470 REM **COMPUTING THE WEIGHT PERCENT AND MOLES
480 REM **FOR EACH COMPONENT
490 FOR I=0 TO 37
500 W(I) = A(I)/TA*100!
510 IF I>=2 THEN GOTO 550
520 IF I=0 THEN X(I) = W(I)/16.04303
530 IF I=1 THEN X(I) = W(I)/44.01
540 GOTO 570
550 X(I) = W(I)/(I*12.01115+1.00797*(2*I+2))
560 IF I =37 THEN X(I) = W(I)/563.09954#
570 TMP = TMP+W(I)
580 TM = TM+X(I)
590 NEXT I
600 REM **SETTING THE TOTAL MOLE PERCENT EQUAL TO ZERO
610 TMP = 0
620 REM **COMPUTING THE MOLE PERCENT FOR EACH COMPONENT
630 FOR J=0 TO 37
640 Y(J) = X(J)/TM*100!
650 TMP = TMP+Y(J)
660 NEXT J
670 REM **COMPUTING THE MOLECULAR WEIGHT OF THE PHASE
680 MM = 100!/TM
690 REM **OUTPUTTING THE RESULTS TO THE PRINTER AND CRT
700 LPRINT
710 LPRINT
720 LPRINT
730 LPRINT "   RUN TITLE: ";RT$
740 LPRINT
750 LPRINT "   SAMPLE: ";S$
760 LPRINT
770 LPRINT "   MOLECULAR WEIGHT =";USING"#####.##";MM
780 PRINT
790 PRINT "   MOLECULAR WEIGHT = ";USING"#####.##";MM
800 PRINT
810 PRINT
820 LPRINT
830 LPRINT
840 LPRINT "   COMPONENT      AREA      WEIGHT %      MOLE      MOLE %"
850 LPRINT "   C-1            ";USING"#####.####";A(0),M(0),X(0),Y(0)
860 LPRINT "   CO2            ";USING"#####.####";A(1),M(1),X(1),Y(1)

```

```

870 FOR I=2 TO 9
880 L = -1*I
890 LPRINT "      C";L;"      ";USING"#####.###";A(I),M(I),X(I),Y(I)
900 NEXT I
910 FOR M=10 TO 36
920 L = -1*M
930 LPRINT "      C";L;"      ";USING"#####.###";A(M),M(M),X(M),Y(M)
940 NEXT M
950 LPRINT "      C-37+      ";USING"#####.###";A(37),M(37),X(37),Y(37)
960 LPRINT
970 LPRINT "      TOTALS      ";USING"#####.###";TA,TMP,TM,TMP
980 LPRINT
990 LPRINT
1000 LPRINT "      AREA SEEN BY GC =";USING"#####.##";GCS
1010 LPRINT
1020 LPRINT "      C5 - C36 AREA =";USING"#####.##";C5C36
1030 LPRINT
1040 LPRINT "      FRACTION OF C5+ SEEN BY GC =";USING"#.###";FS
1050 LPRINT CHR$(12);
1060 INPUT "ENTER 1 FOR NEW RUN OR 0 TO STOP";NI
1070 IF NI=0 GOTO 1160
1080 REM **RESETTING THE PROGRAM FOR NEW DATA
1090 FOR I=0 TO 40
1100 A(I) = 0!
1110 M(I) = 0!
1120 X(I) = 0!
1130 Y(I) = 0!
1140 NEXT I
1150 GOTO 70
1160 END

```

PROGRAM GCC

```

10 REM **THIS PROGRAM CALCULATES THE PHASE COMPOSITION
20 REM **BY RECOMBINING THE CHROMATOGRAPHIC RESULTS
30 REM **OF THE FLASH LIBERATED GAS AND LIQUID
40 DEFINT I-L
50 DEFDBL A,B,M,R,T,V,W
60 DIM A(40),B(40),W(40),MO(40),MP(40),MP(40)
70 REM **ENTERING KEYBOARD INFORMATION
80 INPUT "RUN TITLE";DRT$
90 INPUT "FILE NAME OF DATA";DSN$
100 J=0
110 REM **READING THE DATA INTO THE PROGRAM
120 OPEN "I",#1,DSN$
130 IF EOF(1) THEN 170
140 INPUT#1,A(J),B(J)
150 J=J+1
160 GOTO 130
170 CLOSE #1
180 REM **ENTERING KEYBOARD DATA
190 INPUT "CONDITIONS";DC$
200 INPUT "DENSITY OF GAS (G/CC)";RHO1
210 INPUT "DENSITY OF LIQUID (G/CC)";RHO2
220 INPUT "VOLUME OF GAS (CC)";V1
230 INPUT "VOLUME OF LIQUID (CC)";V2
240 REM **COMPUTING THE MASS OF GAS AND LIQUID
250 M1=RHO1*V1
260 M2=RHO2*V2
270 REM **SETTING THE TOTAL WEIGHT AND MOLES EQUAL TO ZERO
280 TW=0!
290 TN=0!
300 REM **COMPUTING THE WEIGHT AND MOLES OF EACH COMPONENT
310 FOR I=0 TO J
320 W(I)=(A(I)*M1+B(I)*M2)/100!
330 TW=TW+W(I)
340 IF I>=2 THEN GOTO 380
350 IF I=0 THEN MO(I)=W(I)/16.04303
360 IF I=1 THEN MO(I)=W(I)/44.01
370 GOTO 400
380 MO(I)=W(I)/(I*12.01115+1.00797*(2*I+2))
390 IF I=37 THEN MO(I)=W(I)/563.09954#
400 TN=TN+MO(I)

```

```

410 NEXT I
420 REM **SETTING THE TOTAL WEIGHT AND MOLE PERCENTS EQUAL TO ZERO
430 TMP=0!
440 TWP=0!
450 REM **COMPUTING THE WEIGHT AND MOLE PERCENTS FOR EACH COMPONENT
460 FOR K=0 TO J
470 MP(K)=W(K)/TW*100!
480 MD(K)=MO(K)/TM*100!
490 TWP=TWP+MP(K)
500 TMP=TMP+MP(K)
510 NEXT K
520 REM **COMPUTING THE MOLECULAR WEIGHT OF THE PHASE
530 MW=TW/TM
540 REM **COMPUTING THE MOLE PERCENT OF C1 - C6
550 MPC6 = MP(0)+MP(2)+MP(3)+MP(4)+MP(5)+MP(6)
560 REM **COMPUTING THE MOLE PERCENT OF C7+
570 MPC7 = 100!-MPC6-MP(1)
580 PRINT
590 REM **OUTPUTTING THE RESULTS TO THE CRT
600 PRINT " MOLE% CO2 =";USING"###.###";MP(1)
610 PRINT " MOLE% C1-C6 =";USING"###.###";MPC6
620 PRINT " MOLE% C7+ =";USING"###.###";MPC7
630 LPRINT
640 REM **OUTPUTTING THE RESULTS TO THE PRINTER AND CRT
650 LPRINT
660 LPRINT
670 LPRINT " RUN TITLE: ";DRT$
680 LPRINT
690 LPRINT
700 LPRINT " MOLECULAR WEIGHT =";USING "###.##";MW
710 PRINT
720 PRINT " MOLECULAR WEIGHT =";USING "###.##";MW
730 LPRINT
740 LPRINT
750 LPRINT " COMPONENT WEIGHT WEIGHT % MOLES MOLE %"
760 LPRINT " C-1 ";USING"#####.###";W(0),MP(0),MO(0),MP(0)
770 LPRINT " CO2 ";USING"#####.###";W(1),MP(1),MO(1),MP(1)
780 FOR I=2 TO 9
790 L = -1+I
800 LPRINT " C";L;" ";USING"#####.###";W(I),MP(I),MO(I),MP(I)
810 NEXT I
820 FOR K=10 TO 36
830 L = -1+K
840 LPRINT " C";L;" ";USING"#####.###";W(K),MP(K),MO(K),MP(K)
850 NEXT K
860 LPRINT " C-37+ ";USING"#####.###";W(37),MP(37),MO(37),MP(37)

```

```

870 LPRINT
880 LPRINT "      TOTALS  "; USING "#####.###"; TM, TMP, TH, TNP
890 LPRINT
900 LPRINT
910 LPRINT "  GAS DENSITY @ CONDITIONS ="; RHO1 "(G/CC)"
920 LPRINT "  LIQUID DENSITY @ CONDITIONS ="; RHO2 "(G/CC)"
930 LPRINT "  GAS VOLUME @ CONDITIONS ="; V1 "(CC)"
940 LPRINT "  LIQUID VOLUME @ CONDITIONS ="; V2 "(CC)"
950 LPRINT "  CONDITIONS = "; DC$
960 LPRINT
970 LPRINT "  MOLE% CO2 ="; USING "###.###"; MP(1)
980 LPRINT "  MOLE% C1-C6 ="; USING "###.###"; MPC6
990 LPRINT "  MOLE% C7+ ="; USING "###.###"; MPC7
1000 PRINT
1010 LPRINT CHR$(12);
1020 INPUT "ENTER 1 FOR NEW DENSITY OR 0 TO STOP"; IC
1030 PRINT
1040 IF IC=1 THEN GOTO 200
1050 END

```

